2003

Heat transfer in outdoor aquaculture ponds

Jonathan Lamoureux
Louisiana State University and Agricultural and Mechanical College, jlamou1@lsu.edu

HEAT TRANSFER IN OUTDOOR AQUACULTURE PONDS

A Thesis

Submitted to the Graduate Faculty
of Louisiana State University and
Agricultural and Mechanical College
in partial fulfilment of the
requirements for the degree of
Master of Science in
Biological and Agricultural
Engineering

in

The Department of Biological and Agricultural Engineering

by
Jonathan Lamoureux
B.S. (Ag. Eng.) McGill University, 2001
August 2003

ACKNOWLEDGMENTS

The presented research was supported in part by funding from the USDA, the Louisiana Catfish Promotion and Research Board, the Louisiana College Sea Grant Program, and the LSU Agricultural Center.

I would like to thank all the people at the farm (Fernando, Daisy, Christie, Akos, Tyler, Roberto, Brian, Amogh, Jamie, Patricio, Mike, Jay, Vernon, Dr. Romaire, Dr. Hargreaves) for being such gracious hosts, for helping me either with my work, or in keeping my spirits up. I would especially like to thank Patrice, who was a great partner and a good friend, for standing by me throughout my struggles with wells, automated valves, fiberglass and other demons.

I would like to thank all the grad students from BAE (Mr. Sandeep, Matt, Erika and Patrick, Brendan, Paresh, Sireesha, Niconor, Dan, Daniel, Lakiesha, Giri, Rohit, Zhu, Shufang, Na Hua) for their support and friendship during the past 18 months. It helps a lot to know you're not alone working late at night or on the weekends. Special thanks are in order to James who's been a great help in bouncing of ideas, both professional and satirical. Special thanks are also warranted to Praveen, who's relentless (and sometimes sickening) optimism has been the perfect counter-balance to my cynicism.

I would like to thank the staff and faculty from BAE (Stephanie, Zack, Jeremy, Mindy, Mr Thomas, Mr Tom McClure, Ben, Miss Danielle, Miss Angela, Miss Rhonda, Dr. Bengston) for helping me out in their respective fields. Anybody can do their job. Not everyone does it cheerfully. Special thanks are given to [Sensei] Mr. Tom Bride, to whom I feel fortunate for keeping a special eye on me.

I would like to thank my friends (all the international students whom I've had the privilege to know, especially Annett, Alexander and Ingebørg) for enriching my Louisiana experience with great friendships.

I would like to thank my family and friends back home for supporting me in my decision to move to Louisiana, despite the painful problem of geography which separated us for two years.

I would like to thank my committee members Dr. Drapcho and Dr.Tiersch. Dr. Drapcho gave me a different perspective on heat transfer and science in general while Dr. Tiersch initiated me to technical writing.

Finally, I would like to thank Steve (and his "grande" and "petite" boss) for bringing me down to Louisiana. I think it was the best decision I've ever taken and I'll always be grateful for his hospitality, generosity, patience, support and encouragement.

TABLE OF CONTENTS

ABSTRACT

An energy balance was developed for heated and unheated earthen aquaculture ponds to 1) determine the relative importance of energy transfer mechanism affecting pond temperature; 2) predict pond temperatures; 3) estimate the energy required to control pond temperatures, and 4) recommend efficient heating and cooling methods. PHATR (Pond Heating and Temperature Regulation), a computer program using 4^{th} order Runge-Kutta numerical method was developed to solve the energy balance using weather, flow rate and pond temperature data.

By comparing measured and modeled pond temperatures, the average difference (the average bias) was 0.5°C for unheated ponds and 2.4°C for heated ponds. The error in warm water flow measurements explained the elevated average bias for heated ponds.

The dominant energy transfer mechanisms for unheated ponds were solar radiation (maximum: 55%), pond radiation (average: 35% to 42%) and longwave sky radiation (average: 28% to 34%). The dominant energy transfer mechanisms for heated ponds were solar radiation (maximum: 50%), pond radiation (average: 25%), longwave sky radiation (average: 19%) and the 36°C water used to heat the ponds (maximum: 60%).

The difference in biases when comparing three empirical evaporation equations ranged from 0.2°C to 1.9°C. The difference in biases when comparing two empirical convection equations ranged from 0.0°C to 2.1°C.

The average light extinction coefficient for the ponds was 0.013 mm^{-1}.

The sensitivity analysis, used to determine how variations in input data affected the model results, showed that output varied linearly with changes in average air temperature and solar radiation. The output decayed exponentially to changes in wind speed and flow rate.

Using PHATR and 40 years of weather data, the pond temperature for a 400-m^3 pond was calculated for cold, hot and average years. The average pond temperature for an average year was 21.8°C. The net energy required to maintain the pond temperature at 25°C was 3.24×10^9 J/m^3. Warming a 400-m^3 pond 2°C/day during a typical mid-January week would require 7.64×10^{10} J over 9 days.

CHAPTER 1 - JUSTIFYING THE NEED FOR AN ENERGY BALANCE FOR AQUACULTURE PONDS

Water temperature is a critical water quality parameter in aquaculture. Because fish are ectothermic animals, temperature affects their biology in many ways:

- Survival. Certain species are sensitive to water temperature. *Oreochromis mossambicus* died at 13°C and *Oreochromis niloticus* died at 7°C (Avault and Shell, 1968). In one study, shrimp (*Penaeus vannamei*) were successfully overwintered in ponds benefitting from warm water power plant effluent (6.9°C warmer than the ambient water temperature). The survival rate for shrimp raised in warm water was as high as 82% while the survival rate for shrimp in ambient temperature water was 0% (Chamberlain et al., 1980).

- Growth rate. The growth rate of aquatic species is normally a function of temperature. There are many examples of species which grow fastest within an optimum temperature range. For instance, although rainbow trout (*Oncorhynchus mykiss*) can be grown at temperatures between 16 and 18˚C, it is preferable to grow this specie at 13-15˚C (Davis, 1961). The eastern oysters (*Crassostrea virginica*), an other example, grows to market size within 2 years in the warm waters of the Gulf of Mexico. Conversely, the same species can take 5 years to grow off the Eastern Seaboard. (Galtsoff, 1964).

- Spawning. In many temperate and polar fish species, water temperature plays a role in triggering spawning (Bye, 1984). Rainbow trout, for example, spawned in December (the normal spawning season is between March and April) because they were kept in 10°C water instead of 2°C water. Red drum (*Sciaenops ocellatus*) spawn in the fall when the water is between 24 and 28˚C (Arnold, 1988).

- Fish health. The health of aquatic species is linked to environmental stress. Extreme water temperature is one factor which can weaken fish, making them susceptible to infectious diseases (Avault, 1996). Furthermore, pathogens may thrive within a given temperature range. White spot disease, also known as Ich (*Ichthyophthiris multifiliis*), is a protozoan finfish disease which can spread when temperatures are between 21 and 24˚C. The disease, however, resolves in warmer waters (Avault, 1996).

Water temperature can also affect management practices. Oxygen is less soluble in warm water than it is in cool water (Lawson, 1995). Consequently, aquaculturists pay special attention to dissolved oxygen concentrations during warm summer nights. The efficient use chemicals such as herbicides is also dependent on the water temperature (Avault, 1996). Applications should be made in the spring when the water temperatures are between 21 and 26˚C for two reasons: bacterial decomposition is moderately fast in this temperature range and there is enough dissolved oxygen to support the decomposition of the weeds (Masser et al., 2001).

There are many more examples of how water temperature plays a pivotal role in the development of aquatic crops. From a commercial perspective, lengthening the growing season and controlling breeding cycles are reasons justifying the control of water temperature. However, the amount of energy required to heat an outdoor pond can be as expensive as $33 000.

Consider a hypothetical pond 5 ha in area and 1.5 m deep. To increase the pond temperature from 15°C to 27°C by 2°C/day, as was done by Hall et al. (2002), the energy required can be calculated:

$$E = mc_p\left(T_2 - T_1\right)$$

$$E = \left(50000m^2\right)(1.5m)\left(1000kg/m^3\right)\left(4.2kJ/kg^\circ C\right)(27 - 15^\circ C)$$

$$E = 3780000MJ = 1.36 \times 10^{10}\ MWhr$$

where E is the internal energy of the pond,
m is the mass of water in the pond,
c_p is the specific heat of water and
T is the temperature at times 1 and 2.

As can be seen, the amount of energy required to heat just one pond is large, especially considering heat losses have yet to be considered. The rate of delivery is also challenging. To deliver this quantity of energy in 6 days, as done by Hall et al. (2002), would require a 7.29 MW heater. Thus, using conventional means to heat water is not likely to be feasible.

Two main sources of inexpensive energy are used in aquaculture today: thermal effluents from power plants and factories, and warm water from geothermal wells. Warm water effluent (11.1˚C warmer than ambient water) from a local power station was used to successfully overwinter *Penaeus vannamei* in Corpus Christi, Texas (Chamberlain et al., 1980). Similarly, a viable shellfish hatchery was operated within the discharge lagoon of a Long Island Power Station (Kildow and Huguenin, 1974). The hatchery commercially grews oysters, clams, scallops and shrimp, at the time producing profits of 5$ million/year (Kildow and Huguenin,1974).

The use of geothermal water has been documented by Ray (1981), Lang (2001) and Hall et al. (2002). Channel catfish were grown-out for 6 years in Idaho using a blend of cool spring water and 32°C geothermal water to produce 26-27°C water (Ray, 1981). Without the use of geothermal water, it would have been impossible to commercially grow channel catfish. With geothermal water, the commercial growing season for channel catfish lasted the entire year (Ray, 1981). Similar experiments were successful in Louisiana, where channel catfish were spawned as early as March, instead of May, by using geothermal warm water (36°C) to keep the ponds at 27°C (Lang, 2001; Hall et al., 2002) These results suggest that a farmer could avoid dependency on natural weather cycles, allowing farming for potentially 365 days a year.

Not all farmers have access to an inexpensive source of warm water. If the advantages of warm water are to be used by aquaculturists, an affordable and generic method of heating and cooling

water must be developed. The first step involves determining the energy load; how much energy must be supplied or removed from a pond to control its temperature? To do this, an energy balance must be performed.

Energy balances for bodies of water have been done before. Three cases in particular (solar ponds, cooling ponds and winter waterways) are especially interesting because of the similarities between these ponds and aquaculture ponds.

- Solar ponds. Solar ponds are salt water ponds (salinity of 35%) which capture and store solar energy. These ponds can be used for low temperature (90˚C) heat applications (ex: heating water). (An excellent and extensive solar pond literature review with cross-references has been published (Kamal, 1991) Energy balances are done in these studies to determine the pond performance with respect to varying amounts of solar radiation. However, the water in solar ponds does not move, whereas aquaculture pond water is often mixed by aerators. Nonetheless, studies about these ponds have useful insights about energy balances in general.

- Cooling ponds. Cooling ponds are of interest to power plants which must return water to the environment without added energy. Cooling ponds are also used in agriculture to cool livestock to relieve stress. Heat balances have been done for industrial cooling ponds (Pawlina et al., 1977; Cheih and Verma,1978) and for agricultural cooling ponds (Husser, 2001) to see how quickly heat is dissipated. Collectively, these models provide a wealth of information, especially concerning pond surface heat transfer phenomena.

- Winter waterways. Energy balances have been used to predict winter fog and ice breaks on waterways in the winter (Miles and Carlson ,1984; Andres,1984). By applying an energy balance, these studies were able to determine a heat transfer coefficient for the water/ice surface.

Despite the numerous listed advantages of water temperature control, and despite all the research done on energy balances in other areas, an energy balance performed for aquaculture ponds was not found. Such an energy balance, as argued before, would identify dominant energy transfer mechanisms and allow engineers to properly design temperature control systems for outdoor aquaculture ponds. The same energy balance could be used as a management tool in maintaining desired pond temperatures.

Such an energy balance was done for the warm water ponds at the Louisiana State University Aquaculture Research Station (see Chapter 2 for a description of the warm water ponds).

A review of the theory pertaining to energy transfer mechanisms allowed for the development of a differential equation describing energy transfer and temperature changes in aquaculture ponds. To solve this non-linear first order differential equation, a FORTRAN computer model called PHATR (Pond Heat And Temperature Regulation), which used the forth order Runge-Kutta numerical method, was written and developed. Initial model runs for both heated and unheated

ponds revealed the model's ability to predict pond temperature changes. The appropriate time step was also determined. The model was refined by examining how different equations predicting evaporation and surface convection affected the output data. The extinction coefficient for certain warm-water ponds was determined experimentally while the albedo for these ponds was determined empirically.

The model's sensitivity to errors in the input data was studied by running the model several times, using hypothetical weather data, while varying one of the parameters of interest. The parameters of interest were average air temperature, solar radiation, wind speed and warm-water flow rate.

Finally, management and design questions about the warm-water aquaculture ponds at the ARS were addressed. PHATR was used to calculate the pond temperature throughout an average weather year, the amount of energy needed to maintain the pond temperature constant at 15, 20, 25, 30 and 35°C, the time it took to cool a 27°C pond on a cold winter night and the amount of energy required to warm a pond from 10 to 27°C during a typical January. Based on the research done for this document, improvements for the current ARS warm-water pond setup were then suggested.

CHAPTER 2: DESCRIPTION OF THE WARM-WATER PONDS AND ITS INSTRUMENTATION

2.1 The Ponds

The geothermal warm water ponds, located at the LSU Agricultural Center Aquaculture Research Station (ARS) in Baton Rouge, Louisiana, were used as a reference for comparing calculated results from energy balances with measured pond data. These ponds were also used to experimentally obtain certain parameters for calculations.

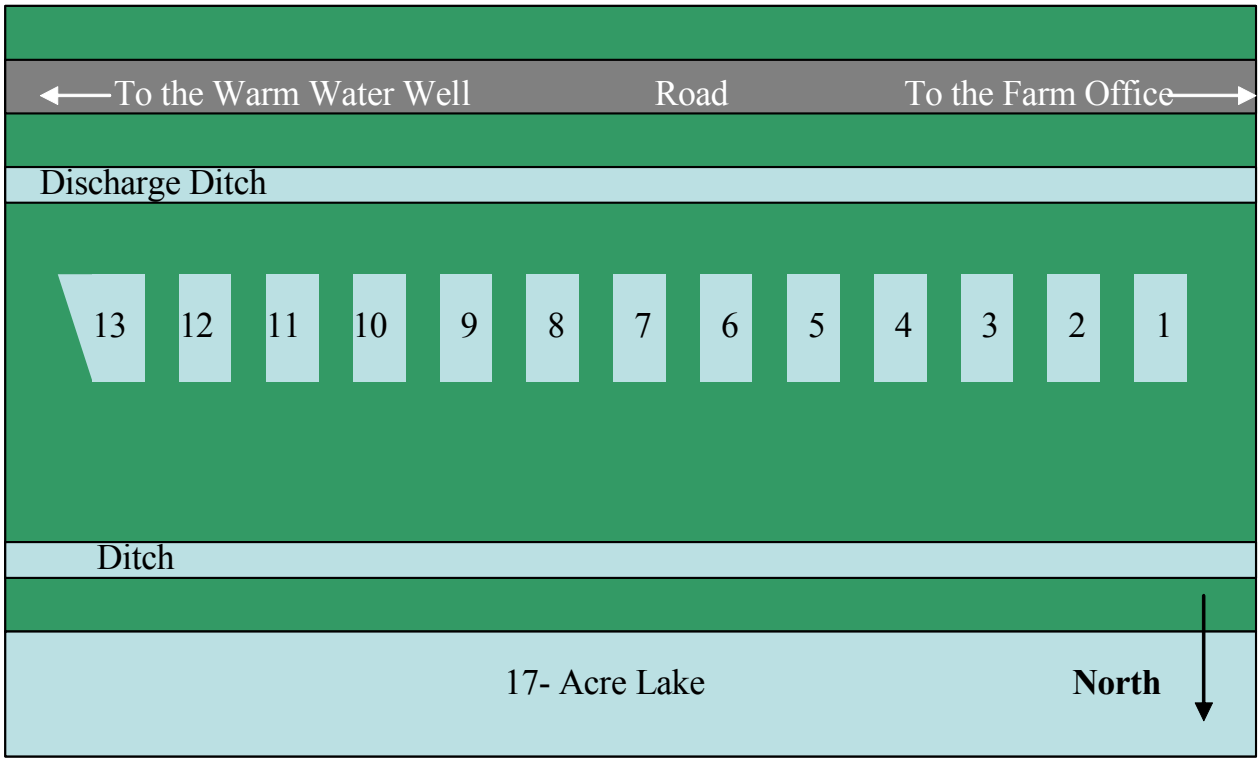

Figure 2.1: There were twelve rectangular and one trapezoidal warm water ponds at the LSU Aquaculture Research Station. Each pond had access to cool (21°C) and warm (36°C) water. Each rectangular pond was approximately 10 m by 30 m. The pond discharge pipes were at the South end where excess water was sent to the discharge ditch between the ponds and the road.

There were 13 clay earthen ponds (Figure 2.1). Twelve ponds were roughly 10 meters by 30 meters (Figure 2.2) and a 13th pond was a trapezoid (the dimensions of the ponds, as of September**,** 2002, are listed in Table 2.1). The pond bottom soil was classified as a Sharkey Dundee clay.

Each pond had access to warm geothermal water (36°C) and cold well water (21°C). Each pond had a discharge pipe which maintained the pond depth at 1.22 m. An aerator (Power House, 3/4 hp) was

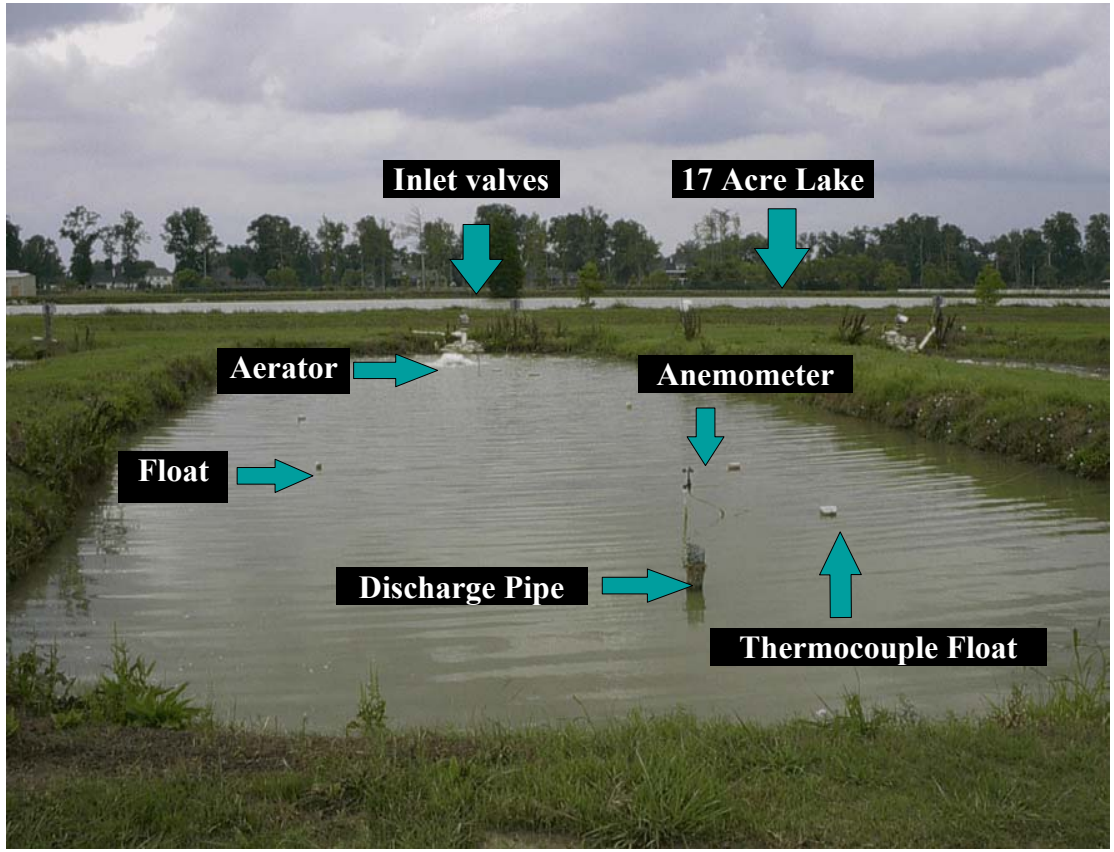

Figure 2.2: Pond 6, shown here, faced North towards the 17-Acre Lake (shown in back). The pond was equipped with an aerator and inlet valves for cold and warm water. The discharge pipe was at the South end of the pond. Floats marked the location of spawning cans on the pond bottom. An anemometer was installed to measure wind speed. Also present were thermocouples, measuring the pond temperature at 0, 2.5, 5 and 10 cm below the water surface.

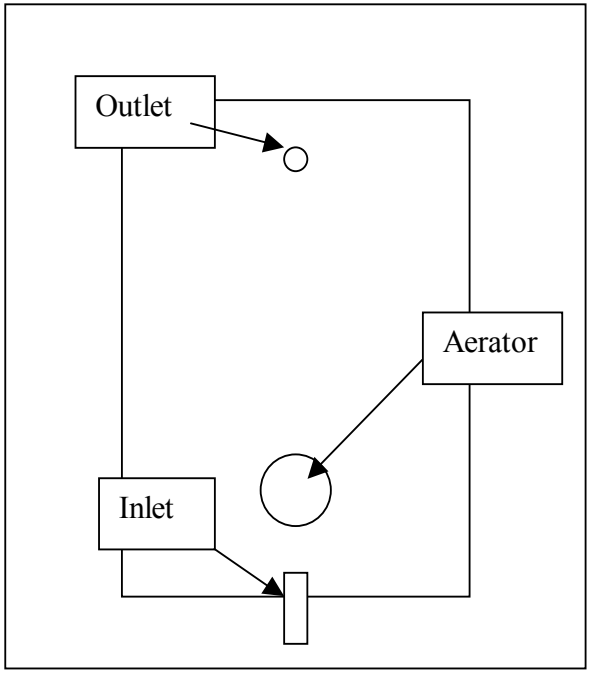

Figure 2.3: The general layout of a warm water pond consisted of an aerator, approximately 2 m from the inlet, and a discharge pipe, approximately 28 m from the inlet. The pond dimensions were roughly 30 m x 10 m. The water column was maintained at 1.22 m..

located in each pond approximately 2 m from the inlets, both of which were at the North end of the pond (Figures 2.2 and 2.3).

Table 2.1: These were the dimensions for the warm water ponds. The average pond area was 329 m^2 and the average pond volume was 400 m^3. The water depth was assumed to be 1.22 m.

Pond	Length (m)	Width (m)	Perimeter (m)	Area (m^2)	Volume (m^3)
1	32	8	83	281	342
2	34	11	90	367	345
3	34	10	88	333	406
4	33	11	88	358	436
5	34	9	88	325	397
6	34	11	90	375	457
7	34	9	88	325	397
8	33	11	89	361	440
9	32	10	85	318	388
10	32	9	85	305	372
11	33	9	85	314	383
12	31	8	81	280	342
Average	33	10	87	329	401
Standard Deviation	0.9	0.8	3	32	39
13	---	---	87	394	480

The cold water came from a 91-m deep well. The pump, a Detroit Diesel 3-71 rated at 84 kW (113 hp), 2100 rpm, delivered 4536 lpm (1200 gpm) of flow (Figure 2.5). The warm water was drawn from a 700-m deep geothermal well. The pump, rated at 30 kW (40 hp) delivered a flow rate of 2400 lpm (Figure 2.6).

Figure 2.4: This Detroit Diesel well, rated at 113 hp, supplied cold 21°C water to the warm water ponds. The well was 91 m deep.

Figure 2.5: This pump, rated at 30 kW, supplied warm water (36°C) to the warm water ponds. The well was 700 m deep.

2.2 The Instrumentation

The pond temperature was regulated with the use of a solenoid ball valve connected to a Campbell Scientific CR 23X data logger (Campbell Scientific Inc., North Logan, UT). In response to low temperatures automatically measured with a type T (copper-constantan) thermocouple, a signal, sent from the data logger, opened the solenoid valve, allowing warm water to flow into the pond. Once the desired temperature was attained, the valve was closed until the pond cooled to the minimum set temperature. Below this point, the valve was again opened. Hall et al. (2002) described in greater detail the control system. When inducing spawning in channel catfish, the pond temperature was maintained between 26°C and 27°C.

Campbell Scientific 21X data loggers (Campbell Scientific Inc., North Logan, UT) measured the pond temperature in locations described in Table 2.2.

(a) (b)

Figure 2.6: The data logger (a) was used to automatically open and close a ball valve (b) with the use of an actuator. The ball valve controls the flow of warm geothermal water. Submerged thermocouples located roughly 20 m from the inlet sent signals to the data logger. The data logger processed the signals: if the pond temperature was too cold, the automatic valve opened. If the pond was too warm, the valve closed.

Using these ponds and this instrumentation as a reference, calculated results from a theoretical energy balance were validated.

Table 2.2: This is the location log for all the Campbell Scientific 21X data loggers used. Each data logger was assigned a letter for identification purposes. Two data loggers, Ca and D, were replaced over an 18 month period. Each data logger had 8 channels (Channels 1 through 9) devoted to measuring temperature. Thermocouples (TC) were located either within a meter of the aerator, a meter from the discharge pipe, or approximately in the middle of the pond. Different configurations were used to measure different temperature profile with respect to depth (see Table 2.3 for more details about the configuration).

Dates	Pond	Data logger	Channels	Location of TC	Configuration
2/19/02 to 03/20/02	9	A	6, 7, 8, 9	Aerator	1
2/19/02 to 03/20/02	9	B	6, 7, 8, 9	Middle	1
2/19/02 to 03/20/02	9	C	6, 7, 8, 9	Discharge	1
2/19/02 to 03/20/02	10	A	2, 3, 4, 5	Aerator	1
2/19/02 to 03/20/02	10	B	2, 3, 4, 5	Middle	1
2/19/02 to 03/20/02	10	C	2, 3, 4, 5	Discharge	1
2/19/02 to 03/20/02	11	D	6, 7, 8, 9	Aerator	1
2/19/02 to 03/20/02	11	E	6, 7, 8, 9	Middle	1
2/19/02 to 03/20/02	11	F	6, 7, 8, 9	Discharge	1
2/19/02 to 03/20/02	12	D	2, 3, 4, 5	Aerator	1
2/19/02 to 03/20/02	12	E	2, 3, 4, 5	Middle	1
2/19/02 to 03/20/02	12	F	2, 3, 4, 5	Discharge	1
4/02/02 to 05/11/02	5	A	6, 7, 8, 9	Aerator	1
4/02/02 to 05/11/02	5	B	6, 7, 8, 9	Middle	1
4/02/02 to 05/11/02	5	C	6, 7, 8, 9	Discharge	1
4/02/02 to 05/11/02	6	A	2, 3, 4, 5	Aerator	1
4/02/02 to 05/11/02	6	B	2, 3, 4, 5	Middle	1
4/02/02 to 05/11/02	6	C	2, 3, 4, 5	Discharge	1
4/02/02 to 05/11/02	7	D	6, 7, 8, 9	Aerator	1
4/02/02 to 05/11/02	7	E	6, 7, 8, 9	Middle	1
4/02/02 to 05/11/02	7	F	6, 7, 8, 9	Discharge	1

Table 2.2 Continued

Dates	Pond	Data logger	Channels	Location of TC	Configuration
4/02/02 to 05/11/02	8	D	2, 3, 4, 5	Aerator	1
4/02/02 to 05/11/02	8	E	2, 3, 4, 5	Middle	1
4/02/02 to 05/11/02	8	F	2, 3, 4, 5	Discharge	1
05/11/02 to 06/25/02	1	D	6, 7, 8, 9	Aerator	1
05/11/02 to 06/25/02	1	B	6, 7, 8, 9	Middle	1
05/11/02 to 06/25/02	1	A	6, 7, 8, 9	Discharge	1
05/11/02 to 06/25/02	2	D	2, 3, 4, 5	Aerator	1
05/11/02 to 06/25/02	2	B	2, 3, 4, 5	Middle	1
05/11/02 to 06/25/02	2	A	2, 3, 4, 5	Discharge	1
05/11/02 to 06/25/02	3	E	6, 7, 8, 9	Aerator	1
05/11/02 to 06/25/02	3	H	6, 7, 8, 9	Middle	1
05/11/02 to 06/25/02	3	F	6, 7, 8, 9	Discharge	1
05/11/02 to 06/25/02	4	E	2, 3, 4, 5	Aerator	1
05/11/02 to 06/25/02	4	H	2, 3, 4, 5	Middle	1
05/11/02 to 06/25/02	4	F	2, 3, 4, 5	Discharge	1
10/07/02 to 11/02/02	7	A	all	Aerator	2
10/07/02 to 11/02/02	7	D	all	Middle	2
10/07/02 to 11/02/02	7	H	all	Discharge	2
10/07/02 to 01/24/03	13	E	all	Aerator	2
10/07/02 to 01/24/03	13	F	all	Middle	2
10/07/02 to 01/24/03	13	B	all	Discharge	2
11/08/02 to 01/24/03	13	H	all	Aerator	3
11/08/02 to 01/24/03	13	A	all	Middle	3
11/08/02 to 01/24/03	13	G	all	Discharge	3

Table 2.2 Continued

Dates	Pond	Data logger	Channels	Location of TC	Configuration
02/12/03 to 03/28/03	9	E	all	Aerator	4
02/12/03 to 03/28/03	9	F	all	Discharge	4
02/12/03 to 03/28/03	12	H	all	Aerator	4
02/12/03 to 03/28/03	12	A	all	Discharge	4
02/12/03 to 03/28/03	3	G	all	Aerator	4
02/12/03 to 03/28/03	3	B	all	Discharge	4

Table 2.3: These thermocouple configurations were used to measure the temperature profile within the water column. The channel refers to the data logger space where the information was stored. Location refers to the thermocouple location within the water column. The "reference" location refers to the reference thermocouple inside the data logger. The "voltage" location refers to the channel which recorded the data logger voltage. The thermocouple locations in Configuration 1 were not measured. All measurements in Configuration 2 were below the pond bottom - soil surface. All measurements in Configuration 3 were below the water surface.

Configuration	Channel	Location	Configuration	Channel	Location
1	1	Reference	3	1	Reference
1	2	Soil	3	2	0 cm
1	3	Bottom	3	3	2.5 cm
1	4	Top	3	4	5 cm
1	5	Surface	3	5	7.5 cm
1	6	Soil	3	6	10 cm
1	7	Bottom	3	7	12.5 cm
1	8	Top	3	8	15 cm
1	9	Surface	3	9	20 cm
1	10	Voltage	3	10	Voltage
2	1	0 cm	4	1	Reference

Table 2.3 Continued

Configuration	Channel	Location	Configuration	Channel	Location
2	2	2.5 cm	4	2	Water surface
2	3	5 cm	4	3	2.5 cm below
2	4	7.5 cm	4	4	7.5 cm below
2	5	7.5 cm	4	5	10 cm below
2	6	10 cm	4	6	60 cm above soil
2	7	15 cm	4	7	30 cm above soil
2	8	20 cm	4	8	soil surface
2	9	25 cm	4	9	30 cm below soil surface
2	10	Voltage	4	10	Voltage

CHAPTER 3: THEORY

The theory used to develop an energy balance for outdoor aquaculture ponds is presented in this chapter.

3.1 Definitions

3.1.1 Energy and Heat

Although the terms energy and heat may be used interchangeably in everyday language, both terms are thermodynamically different. Obert (1949) gave the following definition of energy:

> "Energy is broadly defined as the ability to produce a change from the existing conditions."

Energy exists in various forms: kinetic, potential, internal, etc. Because one can consider a pond to have no kinetic or potential energy, a pond simply has internal energy, which was defined by American Society of Heating, Refrigerating and Air-conditioning (ASHRAE) (Anonymous, 1985) as:

> "The energy possessed by a system caused by the motion of the molecules and/or intermolecular forces."

Heat, on the other hand, should be considered as energy in transit. ASHRAE (1985) defined heat as:

> "the mechanism that transfers energy across the boundary of systems with differing temperatures, always in the direction of the lower temperature."

to which Obert (1949) would have added:

> "Heat is technically a term reserved for transfers of energy where the driving factor (potential) is a temperature difference across a system boundary. It is wrong under this definition to speak of heat contained in a body; the correct term is internal energy."

Therefore, for the purposes of this study, a pond has **internal energy** and heat is the energy being exchanged between the pond and the surroundings.

3.1.2 The Principle Behind the Heat Balance

The conventional method of performing a heat balance requires the definition of a control

volume. Therefore, for this study, all liquid water in the pond was defined as the control volume and E_{pond} was the amount of energy within its boundaries. The amount of internal energy inside the control volume can be calculated at any time as:

$$E_{pond} = \rho \forall c_p T \tag{3.1}$$

where ρ is the density of the water (kg/m^3),
$\forall$ is the volume of water in the pond,
c_p is the specific heat of water (kJ/kg˚C) and
T is the temperature (˚C).

It is assumed that the pond is sufficiently mixed so that the temperature throughout the pond is approximately the same (see Appendix 1). In the event where this is not the case (for instance, when thermal layering occurs), the total energy in the pond is the sum of the energy in the two layers, or:

$$E_{pond} = E_{top} + E_{bottom} = \left(\rho \forall c_p T\right)_{top} + \left(\rho \forall c_p T\right)_{bottom} \tag{3.2}$$

Because the temperature and occasionally the volume of the water changes over time, the amount of energy within the control volume also changes, as described by the following equation:

$$\left(\frac{\partial E}{\partial t}\right)_{pond} = \left(\frac{\partial\left(\rho c_p \forall T\right)}{\partial t}\right)_{pond} = \rho c_p \left[T \frac{\partial \forall}{\partial t} + \forall \frac{\partial T}{\partial t}\right]_{pond} \tag{3.3}$$

These changes are caused in part by:

- the absorbtion of solar radiation by the water,
- the exchange of heat with the soil, primarily due to conduction,
- heat exchanges with the air, due to convection, evaporation and back radiation,
- the bulk movement of water (and thus the bulk transport of energy) across the control system boundary.

All these vectors of heat movement can be quantified and balanced with the rate at which the energy within the system is changing. (This is the principle behind the heat balance.) Figure 3.1 schematically represents the following mathematical expression:

$$\left(\frac{dE}{dt}\right)_{pond} = q_{solar} - q_{back} + q_{sky} - q_{evap} \pm q_{conv} \pm q_{soil} - q_{seep} + q_{rain} + q_{well} - q_{out} \pm q_{other} \tag{3.4}$$

where E is the total energy at any given time (t) in the pond,
q_{solar} is the rate of energy gained by the pond by radiation

q_{back} is the rate of heat exchanged due to back radiation
q_{sky} is the long wave radiation from the sky,
q_{evap} is the rate of heat lost through the evaporation of water
q_{conv} is the rate of heat exchanged with the air by convection
q_{soil} is the rate of heat exchanged with the soil
q_{seep} is the rate of bulk energy lost through seepage
q_{rain} is the rate of bulk energy gained due to rainfall
q_{well} is the rate of bulk energy gained from the warm water well
q_{out} is the rate of bulk energy lost to the overflow of water
q_{other} is the rate of energy transfer from or to other sources.

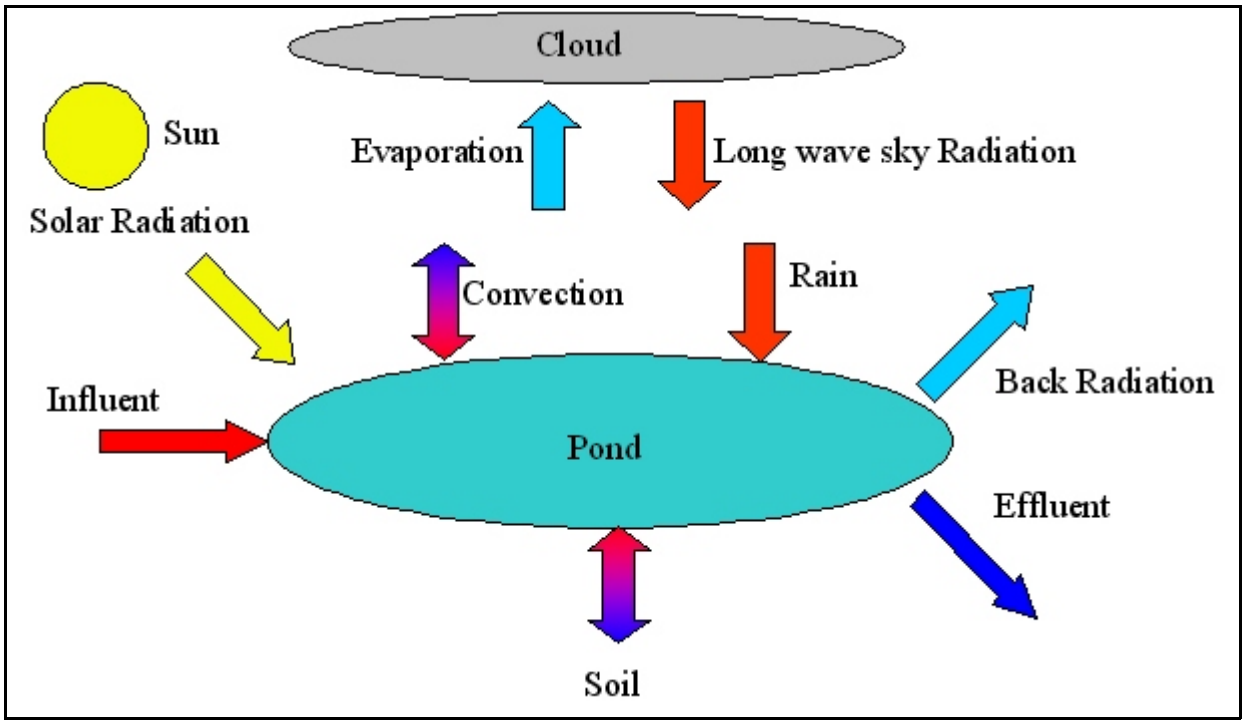

Figure 3.1: Each arrow in this schematic of an energy balance centered around a pond represents an energy transfer mechanism (energy vector) which must be accounted for when determining the rate at which energy is stored in the pond. Vectors considered minor and not shown in this diagram are the absorption of light by chlorophyll, energy losses through seepage and light reflected by the suspended particles in the pond.

Note that individual heat transfer components can be either positive or negative, depending on whether energy is entering or leaving the system. In order to avoid confusion, energy entering the system will be considered positive (heat gain) while energy exiting the system will be treated as negative (heat loss).

3.2 Heat Transfer through Radiation (q_{solar}, $q_{backrad}$,q_{sky})

3.2.1. Definition of Thermal Radiation

Radiation, in general, can be viewed as the propagation of energy in the form of electromagnetic waves (classical approach) or discrete photons (quantum-mechanics approach). No medium is required in its propagation (Holman, 1997). Although there are many different kinds of radiation, for the purposes of this study, only thermal radiation (with wavelengths ranging from λ=0.2 to 1000 μm) will be considered and all usage of the term radiation will refer to thermal radiation.

For black and grey bodies, the amount of energy being propagated by radiation is dependant on the absolute temperature of the emitter. The general relationship quantifying heat transferred due to radiation, for a grey body, is:

$$q = \varepsilon A \sigma T^4 \tag{3.5}$$

where q is the heat transfer rate (W),
ε is the emissivity of the grey body (fraction)
σ is the Stefan-Boltzmann constant (5.67 x 10^{-8} W/m^2/K^4)
T is the temperature of the grey body (K)

For outdoor aquaculture ponds, two types of radiation must be considered: short wave and long wave radiation. Short wave radiation has more energy than long wave radiation, due to the following relationship:

$$E_{quantum} = h_{Planck} \nu = \frac{h_{Planck} C}{\lambda} \tag{3.6}$$

where $E_{quantum}$ is the energy within a quantum
h_{Planck} is Planck's constant (6.625 x 10^{-34} J s)
ν is the radiation frequency (s^{-1})
c is the speed of light (~3 x 10^{-8} m/s in a vacuum)
λ is the radiation wavelength (m)

This becomes important when considering the transmittance of radiation through media like the atmosphere or water.

3.2.2 Shortwave Radiation

3.2.2.1 Laws of Reflection and Refraction

When a beam goes from one medium to an other, as is shown in Figure 3.2, two phenomena occur: either the beam is reflected or refracted. Consider a beam striking a surface with an angle

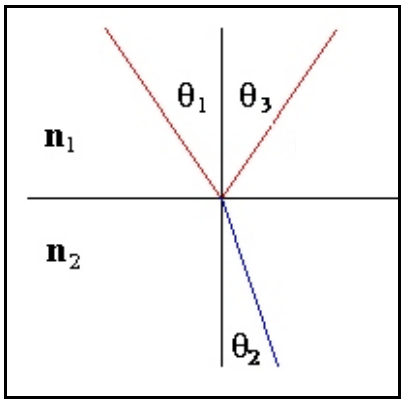

Figure 3.2: When light goes from one medium (n_1) to an other (n_2), part of the incident beam is reflected at an angle θ_3 while the rest is transmitted into the 2nd medium at an angle θ_2.

of incidence θ_1 to the normal. Part of the beam will be reflected with an angle of reflection θ_1 while the remainder of the beam will bend as it enters the new medium with an angle of

refraction θ_2. Snell's Law relates the angles of incidence (θ_1) and refraction (θ_2) to the index of refraction of the medium (n):

$$n_1 \sin\theta_1 = n_2 \sin\theta_2 \tag{3.7}$$

The amount of radiation reflected is a function of these angles of incidence and refraction, as well as the indices of refraction of the media. If R is the fraction of radiation reflected from the surface (albedo), then, for unpolarized light, by Fresnel's Law:

$$R = \frac{I_{reflected}}{I_{incident}} = \frac{1}{2}\left(\frac{\sin^2(\theta_2 - \theta_1)}{\sin^2(\theta_2 + \theta_1)} + \frac{\tan^2(\theta_2 - \theta_1)}{\tan^2(\theta_2 + \theta_1)}\right) \tag{3.8}$$

where I is the intensity of either the incident or reflected radiation (W).

In accordance with the law of conservation of energy, whatever energy from the incident beam is not reflected must be transmitted to the second medium, or:

$$R + \Gamma = 1 \tag{3.9}$$

where Γ is the fraction of incident radiation initially transmitted to the second medium.

3.2.2.2 Bouger-Beer Law

The attenuation of radiation through a pure medium is described by the Bouger-Beer Law:

$$dI(\lambda,z) = -\beta(\lambda,z)I(\lambda,z)dz \tag{3.10}$$

where I is the intensity of the radiation (W)
λ is the radiation wavelength (m)
β is the extinction coefficient (m^{-1})
z is the path length travelled by the radiation (m)

The extinction coefficient can be considered the sum of the absorption coefficient (a) and the scattering coefficient (s). Here, absorption is the phenomenon where the medium removes

energy from the radiation beam, causing the medium to gain more energy while reducing the intensity of the beam. Scattering, on the other hand, is the reflection of radiation by suspended

particles. For particles sizes with diameters much greater than the radiation wavelength, the scattering coefficient is (Siegel, 1981):

$$s = 2(\pi r^2)N \tag{3.11}$$

where r is the mean radius of the particle
N is the number of particles per unit volume

Both the absorption and scattering coefficients are dependant on the wavelength and the path traveled by the radiation.

3.2.2.3. Solar Radiation (q_{solar})

Radiation emitted by the Sun travels through the vacuum of space unaltered. Table 3.2 lists the percentage of energy associated with certain bandwidths of solar radiation emitted from a blackbody at 5800K (the temperature of the sun - Holman, 1997).

Table 3.2: Assuming the sun was a black body with a surface temperature of 5800 K, the total emitted energy for given bandwidths were calculated. 38.5% of all emitted energy is associated with the visible spectrum.

Bandwidth (nm)	Percentage of total emitted energy
under 0.2	0.1%
0.2-0.3	3.5%
0.3-0.4	6.9%
0.4-0.5	14.3%
0.5-0.6	12.2%
0.6-0.7	12.0%
0.7-0.8	9.0%
0.8-0.9	8.0%
0.9-1.0	6.0%
1.0 -1.2	9.0%
1.2 - 1.6	9.0%
1.6 - 2.2	5.0%
2.2 - 2.8	2.0%
above 2.8	3.0%

To determine the amount of incoming extraterrestrial radiation, the following equations can be used:

$$\tau = \frac{2\pi(n-1)}{365} \tag{3.15}$$

$$\left(\frac{R}{R_0}\right)^2 = 1.000110 + 0.034221\cos\tau + 0.001280\sin\tau \tag{3.16}$$

$$+ 0.000719\cos(2\tau) + 0.000077\sin(2\tau) \tag{3.17}$$

$$D_x = D_0\left(R/R_0\right)^2 \tag{3.18}$$

$$q_{solar} = \psi D_x \cos\theta_z \tag{3.19}$$

where τ is an angle (radians)
n is the day of the year (on January 1st , n = 1)
R is the distance from the Earth to the sun (km)
R_0 is the mean distance from the Earth ot the sun, 1.496×10^8 km
D_0 is the solar constant (1353 W/m^2)
D_x is the extra-terrestrial radiation
ψ is a "clearness" factor (1 on clear days, 0.2 on cloudy days)

Upon entering the Earth's atmosphere, the properties of this radiation change. Direct beam radiation, defined as solar radiation whose path has been unaltered by atmospheric scattering, changes intensity as atmospheric gases, such as ozone, water vapor and CO_2, absorb specific wavelength bands of radiation. For instance, it is well known that the ozone layer absorbs UV light. Water vapor and CO_2 absorb infra-red radiation (Kondratyev, 1969). Solar radiation which has changed direction due to scattering is called diffuse radiation. Needless to say, diffuse radiation is also absorbed by atmospheric gases (probably more so due to its increased traveling distance). Diffuse radiation, although it comes from all directions, can be considered like beam radiation incident to the Earth's surface at 60˚ (Duffie and Beckman, 1980). The solar radiation spectrum was measured by Threlkeld and Jordan (1958) and is shown in Figure 3.3.

The solar zenith (θ_z) is the angle formed by the pond normal and direct incident beam radiation (the angle of incidence in Figure 3.2), and this angle varies with the time of day, the time of year

and the geographical position of the pond. The solar zenith is given by the following equations (Anderson, 1983):

$$\cos\theta_z = \sin\phi\sin\delta + \cos\phi\cos\delta\cos\omega \tag{3.12}$$

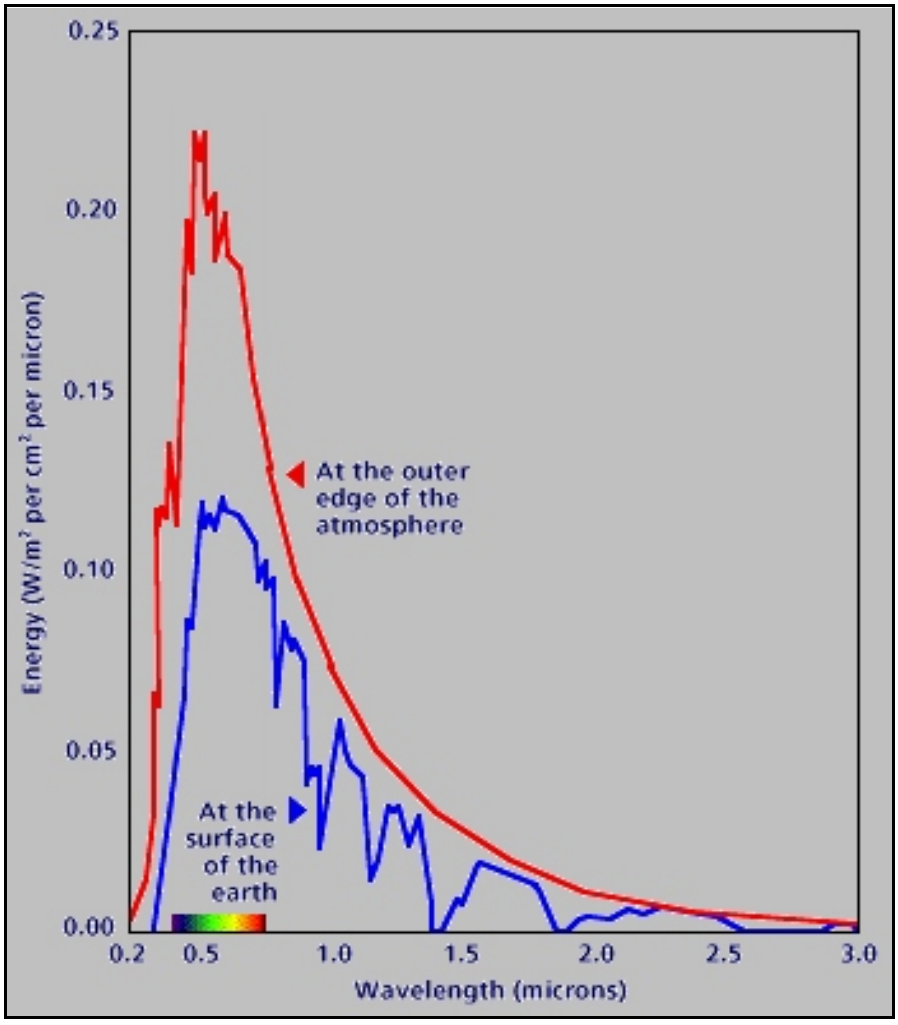

Figure 3.3: This is the solar spectrum. There is more energy in the visible spectrum because the frequency of the radiation waves is higher than waves in the infra-red spectrum. (Threlkeld and Jordan, 1958).

$$\delta = 23.45 \sin\left[\frac{360}{365}(284 + n)\right] \tag{3.13}$$

$$\omega = \left(12 - \omega_{time}\right) \times 15° \tag{3.14}$$

$$\omega_{time} = \text{LST} + (\text{Lnt} - \text{Lng}) \div 15 \tag{3.15}$$

where ϕ is the pond's latitude (positive for North) (degrees),
δ is the solar declination (the angle formed by the line from the center of the Earth to the center of the Sun and the Earth's equator) (degrees)
ω is the hour angle (degrees)
ω_{time} is the solar time (degrees)
LST is local standard time
Lnt is the longitude of the standard time meridian (degrees)
Lng is the longitude of the pond (degrees)

A numerical example showing how to calculate the solar zenith is shown in Appendix 2.

Using Fresnel's Law, and assuming the water surface is smooth, the fraction of reflected radiation R is:

$$R = \frac{I_{reflected}}{I_{incident}} = \frac{1}{2}\left(\frac{\sin^2(\theta_{water} - \theta_z)}{\sin^2(\theta_{water} + \theta_z)} + \frac{\tan^2(\theta_{water} - \theta_z)}{\tan^2(\theta_{water} + \theta_z)}\right) \tag{3.20}$$

where θ_z is the zenith angle and
θ_{water} is the refracted angle of the beam

Using Snell's Law, one can determine refraction angle.

$$n_{air} \sin\theta_z = n_{water} \sin\theta_{water} \tag{3.21}$$

where n_{air} is the index of refraction of air ($\approx$ 1) and
n_{water} is the index of refraction of water (1.33 in the visible spectrum).

Table 3.3 lists values of R for given zenith angles. As can be seen, reflection only becomes important when the sun's elevation is below 30˚ from the horizon (θ_{zenith}>60°).

Once radiation penetrates the water surface, it is either absorbed or scattered, according to the Bouger-Beer Law:

$$dI(\lambda, z) = -\beta(\lambda, z) I(\lambda, z) dz \tag{3.22}$$

In pure water, the path length (z) is:

$$z = \frac{z_{pond}}{\cos\theta_{water}} \tag{3.23}$$

Table 3.3: The amount of light reflected at the water surface is dependant on the angle of incidence (the zenith angle). Using Fresnel's Law, the following table was generated.

Zenith Angle (°)	Reflection (%)
10	2.0
20	2.0
30	2.1
40	2.4
50	3.3
60	5.9
70	13.3
80	34.7
89	89.6

The absorption of light in pure water has been reviewed (Irvine and Pollack, 1968; Kondratyev, 1969; Hale and Querry, 1973;Rabl and Nielsen, 1975; Tsilingiris, 1991). For shortwave radiation, water is not a grey body and, as a result, its absorbance varies with the wavelength of the incident radiation. Results from the literature have been compiled to produce tables describing the absoprtion coefficient of pure water as a function of the radiation wavelength (see Table 3.4 and Figure 3.4) (Irvine and Pollack, 1968; Hale and Querry, 1973). Water poorly absorbs radiation in the ultra-violet and visible spectrums while being an excellent absorber of infra-red radiation, especially above 1200 nm. Kondratyev (1969) has tabulated the penetration depth of solar radiation through various thicknesses of water and his results are shown in Table 3.5. Most of the solar radiation in the near infra-red spectrum is absorbed within the first centimeter of depth. Rabl and Nielsen (1975) determined that the radiation associated with wavelengths greater than 1200 nm represented 22.4% of the total incident radiation and this radiation was totally absorbed in this upper water boundary layer. For radiation with $\lambda < 1200$ nm, Rabl and Nielsen (1975) have developed the following approximation (to within 3%) to determine the amount of radiation absorbed by water (q_{rad-1}).

$$q_{rad} = (1 - R) q_{inc} \sum_{n=1}^{4} \eta_n e^{-a_n s} \tag{3.24}$$

where q_{inc} is the incident radiation upon the pond (W/m^2)
a_n is the absorption coefficient (cm^{-1})

s is the path length of the radiation (cm)
η is the fraction of radiation for the n^{th} spectral band
$\eta_1 = 0.237$ and $a_1 = 0.32 \times 10^{-3}$ cm^{-1} for λ = 200 to 600 nm
$\eta_2 = 0.193$ and $a_2 = 4.5 \times 10^{-3}$ cm^{-1} for λ = 600 to 750 nm
$\eta_3 = 0.167$ and $a_3 = 0.03$ cm^{-1} for λ = 750 to 900 nm
$\eta_4 = 0.179$ and $a_4 = 0.35$ cm^{-1} for λ = 900 to 1200 nm

Light entering the pond is also scattered by the various suspended particles. The scattering particles, however, are assumed not to absorb energy (Tsilingiris, 1991). Rather, they redirect radiation throughout the water, lengthening the path length of the radiation, allowing for further absorption. Because clay particles, with a maximum diameter of 2 μm (Kadlec and Knight, 1996), may be suspended in the pond, and because these particles are larger than the radiation wavelength (λ< 1.0 μm), a combination of both macroscopic (described previously) and Mie scattering occurs (Siegel, 1981). Mie scattering is difficult to predict so approximating all scattering as macroscopic scattering is necessary, although not totally accurate (Yaggobi, 1994; Guo and Kleis, 1997). Although these relations are more straight forward to use, these relations are specifically formulated for the researcher's pond. Applying such equations to other ponds could lead to large discrepancies between predicted and actual values.

Additionally, light is absorbed mainly by chlorophyll a (see Figure 3.6) present in algae and other photo-autotrophic organisms (Romaire, 2002). Light absorbed by chlorophyll is converted into chemical energy (carbon bonds in sugar) and will not be absorbed by the water. Consequently, this energy should not be accounted for in the heat balance.

The absorption coefficient of natural water bodies has been studied by Kirk (1980) in the visible spectrum. For the specific bodies of water he studied, the absorption coefficient (for light with λ = 440 nm) per unit of suspended solid particle density ranged from 0.93 X 10^{-4} m^2 mg^{-1} to 1.07 X 10^{-4} m^2 mg^{-1}.

Table 3.5: Fractions of solar radiation spectrum transmitted through various thicknesses of water have been tabulated (Kondratyev, 1969)

Spectral interval	Incident solar energy distribution	Transmitted energy distribution for water-layer thickness (cm)							
		0.001	0.01	0.1	1	10	100	1000	10000
0.3 - 0.6	0.237	0.237	0.237	0.237	0.237	0.236	0.229	0.173	0.014
0.6 - 0.9	0.36	0.36	0.36	0.359	0.353	0.305	0.129	0.01	
0.9 - 1.2	0.179	0.179	0.178	0.172	0.123	0.008			
1.2 - 1.5	0.087	0.087	0.082	0.063	0.017				
1.5 - 1.8	0.08	0.08	0.064	0.027					
1.8 - 2.1	0.025	0.025	0.011						

2.1 - 2.4	0.025	0.025	0.019	0.001
2.4 - 2.7	0.007	0.006	0.002	

Non-attenuated light will strike the pond floor, made up of organic material, mud and clay. Part of the light will be absorbed while the remainder of the light will be reflected. The albedo (the ratio of reflected to incident light) for moist gray soil is 0.10-0.12 and for moist black soil, 0.08 (Holman, 1997). Therefore, very little light will be reflected back into the pond. A summary of how solar radiation behaves as it enters water is presented in Figure 3.4.

3.2.3. Longwave Radiation (q_{back}, q_{sky})

3.2.3.1. Pond Backradiation (q_{back})

The range of wavelengths emitted from a pond at 27°C spans from about 4.8 to 74 μm (see Appendix 3 for calculations). As can be seen from Table 3.4, water, for this range, is opaque. This leads to three conclusions:

- There is no exchange of radiation within the body of water (Rabl and Nielsen, 1975).
- Pond backradiation is a surface phenomenon.
- The pond can be treated as a grey body.

Noting that the emissivity of water is 0.96 (Siegel and Howell, 1981; Kondratyev, 1969), the rate of heat loss due to pond backradiation is:

$$q_{back} = 0.96 A_{pond} \sigma \left(T_{air} + 273 \right)^4 \tag{3.25}$$

where q_{back} is the backradiation of the pond (W)
A_{pond} is the pond area (m^2)
T_{pond} is the temperature of the pond (K)

3.2.3.2. Longwave Sky Radiation (q_{sky})

Longwave sky radiation can be seen as the emission of radiation from two atmospheric gases: water vapour and carbon dioxide, both of which are generally opaque to the longwave radiation emitted by the Earth (Bliss, 1961, Kondratyev, 1969). The apparent emissivity of these gases from the Earth's surface is strongly related to the total precipitable water in the atmosphere (i.e. the more water vapour in the air, the greater the absorbance and emittance power of this gas). Figure 3.7 illustrates how the intensity of the emitted radiation at certain wavelengths increases as the air's water content (m_w) increases. As m_w increases (for instance, on cloudy days), the sky resembles more and more a black body.

For a cloudless sky, the apparent emissivity can be estimated with the following equation (compiled from Bliss, 1961):

$$\varepsilon_{sky} = \frac{1}{c_1 - c_2 T_{dew} + c_3 T_{dew}^2} \tag{3.26}$$

where $c_1 = 1.2488219$
$c_2 = -0.0060896701$
$c_3 = 4.8502935 \times 10^{-5}$
T_{dew} is the dew temperature (°C)

The dew temperature can be calculated from the following equation:

$$T_{dew} = \frac{1}{\frac{1}{T_{air} + 273} - (1.846 \times 10^{-4}) \ln(rh)} - 273 \tag{3.27}$$

where T_{air} is the air temperature (°C)
rh is the relative humidity (decimal)

Using the apparent emissivity, the longwave sky radiation is, in Watts (Bliss, 1961):

$$q_{sky} = \varepsilon_{sky} A_{pond} \sigma (T_{air} + 273)^4 \tag{3.28}$$

where T_{air} is the air temperature (K).

3.3 Heat Transfer through Conduction (q_{soil})

3.3.1 Thermal Soil Properties

In practice, soil properties can vary tremendously in any given soil because of the local changes in soil composition and temperature.

Two soil properties are of interest here: the thermal conductivity (k_{soil}) and the volumetric specific heat (C_v) of the soil. Both can be determined from correlations found in the literature. The correlations relate these thermal properties to the physical properties of the soil, such as porosity, bulk density, soil texture, soil moisture content and soil type.

Farouki (1986) reviewed 11 methods to predict the thermal conductivity, determining which method fared best under given circumstances. For the case of unfrozen saturated soils, the Johansen method, with its correlation shown below, proved to be the most accurate:

$$k = k_{solid}^{(1-n)} k_{water}^{n} \tag{3.29}$$

where k_{solid} is the thermal conductivity of the soil solids, k_{water} is the thermal conductivity of soil water and n is the porosity of the soil (decimal). Changes in temperature could alter k_{water} (ranging from 0.569 W/mK at 0˚C to 0.598 W/mK at 27˚C to 0.620 W/mK at 42˚C), which would in turn affect the thermal conductivity of the soil. An average value for k_{solid} for Healy clay has been determined by De Vries (1966) to be 2.5 W/mK.

The volumetric specific heat of soil (C_v) can be computed with the following relation (De Vries, 1966):

$$C_v = C_{solid}x_{solid} + C_{org}x_{org} + C_{water}x_{water} \tag{3.30}$$

$$C_v = 1.92x_{solid} + 2.51x_{org} + 4.18x_{water}\left(MJ/m^3K\right) \tag{3.31}$$

where x is the soil fraction and
C is the volumetric specific heat of each of the soil's components: solids (s), water (w) and organic matter (org).

Table 3.7 is a list of values describing the thermal parameters of heavy soils in the literature.

Table 3.7 Presented here are thermal soil properties of interest found in the literature.

Soil	k (W/m K)	C_v (MJ/m^3K)	Source	Note
Clay minerals	2.92	2	De Vries (1966)	Property evaluated at 10˚C
Organic matter	0.25	2.51	De Vries (1966)	Property evaluated at 10˚C
Silty clay loam	1.45-2.07	1.6-2.05	Sikora et al.(1990)	Severely compacted soil
Saturated clay	1.6	2.9	Kimball (1983)	Soil has a porosity of 0.4.

Because the pond is lined with compacted heavy clay, in order to prevent leaks, these properties should be fairly uniform. According to data presented by Sikora et al. (1990), compacted soils tend to have less variable thermal properties probably because less water and air is present in the soil. Despite the fact that the upper layer of the soil is composed mainly of organic mud, the liner was assumed to be uniform. Furthermore, the pond liner can be assumed to be saturated with water, which removes the complications of gas-water mixtures in the soil. However, because the thermal properties of water change with temperature, the soil's properties too may be influenced by temperature variations.

3.3.2 Heat Conduction in Soil

For soils, conduction was experimentally verified to be the predominant mode of heat transfer (Kimball et al, 1976). Consequently, the rate at which heat is exchanged with the soil (q_{soil}) can be described by Fourier's Law of heat conduction:

$$q_{soil} = -k_{soil} A \left.\frac{\partial T}{\partial z}\right|_{z=0} \tag{3.32}$$

where k is the soil's thermal conductivity (W/m K)
A is the pond floor area (m^2)
T is the temperature of the soil (°C)
z is the soil depth (m)
$(\partial T/\partial z)|_{z=0}$ is the temperature gradient at the pond floor

The temperature gradient, in turn, can be determined from solutions to the heat diffusion equation:

$$\frac{\partial T}{\partial t} = \alpha \nabla^2 T \tag{3.33}$$

If the propagation of heat is in the z direction only, then Equation 3.33 can be simplified to:

$$\frac{\partial T}{\partial t} = \alpha \frac{\partial^2 T}{\partial z^2} \tag{3.34}$$

where t is time (s)
α is the soil's thermal diffussivity (m^2/s).

If assumed constant, the thermal diffusivity can be calculated from other soil parameters:

$$\alpha = \frac{k_{soil}}{\rho_{soil} c_{p-soil}} = \frac{k_{soil}}{C_v} \tag{3.35}$$

where k_{soil} is the soil's thermal conductivity (W/m/K)
ρ_{soil} is the soil's bulk density (kg/m^3)
$c_{p\text{-}soil}$ is the soil's specific heat (J/kg/K)
C_v is the soil's volumetric specific heat ($J/m^3/K$).

To solve the heat diffusion equation, one initial and two boundary conditions are required. For the initial condition, it was assumed that the temperature throughout the entire soil was initially the same at all depths.

$$T_{soil}(z,t) = T_{initial} \tag{3.36}$$

Since the liner can be treated as a semi-infinite solid (Van Wijk and De Vries,1966; Horton and Wierenga,1983; Horton et al., 1983), the first boundary condition is

$$\lim_{z \to \infty} T_{soil}(z,t) = T_{z=\infty} \tag{3.37}$$

that is, at a very large depth, the soil's temperature will not change. The other boundary condition is dependent on the soil surface temperature. For the case where the water temperature varies diurnally, the second boundary condition is (Van Wijk and De Vries, 1966):

$$T(z=0,t) = T_{avg} + T_{amp-dqv} \sin\left(\omega_{dqv} t\right) + T_{amp-yr} \sin\left(\omega_{yr} t\right) \tag{3.38}$$

where T_{avg} is the average soil surface temperature for the period $1/\omega$ (°C)
T_{amp} is half the total variation of the average temperature(°C)
ω is the frequency of the period being considered (s^{-1})

The resulting solution to the heat equation is (Van Wijk and De Vries, 1966):

$$T(z,t) = T_{\substack{avg \\ yr}} + T_{\substack{amp \\ z=0 \\ yr}} e^{\left(-z/D_{yr}\right)} \sin\left(\omega_{yr} t + \phi_{\substack{z=0 \\ yr}} - z/D_{yr}\right) + T_{\substack{amp \\ z=0 \\ dqv}} e^{\left(-z/D_{dqv}\right)} \sin\left(\omega_{dqv} t + \phi_{\substack{z=0 \\ dqv}} - z/D_{dqv}\right) \tag{3.39}$$

where ϕ is the phase constant for temperature variations at z = 0 m
D is the dampening depth (m).

The dampening depth (D) is the depth where the variations in soil temperature are 1/e = 0.368 times the temperature variations at the soil surface (example: if the daytime variation in temperature is 10˚C at the surface, then at depth D, the temperature variation is 3.68˚C). The dampening depth is a function of the soil's thermal properties as well as the period of variation considered (Van Wijk and De Vries, 1966):

$$D = \sqrt{\frac{2k}{C_v \omega}} \tag{3.40}$$

where k is the thermal conductivity (W/m K),
C_v is the soil's volumetric specific heat (MJ/m^3 K) and
ω is the period of the variation being considered (s).

Note that the dampening depth is $\sqrt{365} \approx 19$ times greater for annual variations than it is for daily variations. The daily dampening depth, according to Van Wijk and De Vries (1966) for saturated clay is 12.2 cm and for an annual dampening depth, 233 cm.

The partial derivative of Equation 3.39, with respect to z, yields the temperature gradient for all depths:

$$\frac{\partial T(z,t)}{\partial z} = -T_{\underset{z=0}{amp}_{yr}} \frac{e^{\left(-z/D_{yr}\right)}}{D_{yr}} \left[\sin\left(\omega_{yr} t + \phi_{\underset{z=0}{\ }_{yr}} - z/D_{yr} \right) + \cos\left(\omega_{yr} t + \phi_{\underset{z=0}{\ }_{yr}} - z/D_{yr} \right) \right] - T_{\underset{z=0}{amp}_{day}} \frac{e^{\left(-z/D_{day}\right)}}{D_{day}} \left[\sin\left(\omega_{day} t + \phi_{\underset{z=0}{\ }_{day}} - z/D_{day} \right) + \cos\left(\omega_{day} t + \phi_{\underset{z=0}{\ }_{day}} - z/D_{day} \right) \right] \tag{3.41}$$

The temperature gradient at the soil surface (z = 0) is

$$\left.\frac{\partial T(z,t)}{\partial z}\right|_{z=0} = -T_{\underset{z=0}{amp}_{yr}} \frac{1}{D_{yr}} \left[\sin\left(\omega_{yr} t + \phi_{\underset{z=0}{\ }_{yr}} \right) + \cos\left(\omega_{yr} t + \phi_{\underset{z=0}{\ }_{yr}} \right) \right] - T_{\underset{z=0}{amp}_{day}} \frac{1}{D_{day}} \left[\sin\left(\omega_{day} t + \phi_{\underset{z=0}{\ }_{day}} \right) + \cos\left(\omega_{day} t + \phi_{\underset{z=0}{\ }_{day}} \right) \right] \tag{3.42}$$

This temperature gradient at the surface can be substituted into Fourier's Law of heat conduction to finally determine the rate of heat transfer in the soil (q_{soil}):

$$q_{soil} = -kA \left.\frac{\partial T}{\partial z}\right|_{z=0} \tag{3.43}$$

For the case where the water temperature and the flow characteristics along the soil surface remain constant, the second boundary condition is:

$$-k_{soil} A \left.\frac{\partial T}{\partial z}\right|_{z=0} = -hA\left(T_{soil} - T_{pond} \right) \tag{3.44}$$

where h is the heat transfer coefficient ($W/m^2/K$).

Finding the heat transfer coefficient may prove difficult. An alternate second boundary condition could be:

$$T(z = 0, t) \approx T_{pond} \tag{3.45}$$

The solution to the heat diffusion equation, with Equations 3.37 and 3.45 as boundary conditions, is (Holman, 1997):

$$\frac{T(z,t) - T_{pond}}{T_{initial} - T_{pond}} = erf\,\frac{z}{2\sqrt{\alpha t}} \tag{3.46}$$

where erf is the Gauss error function.

Taking the derivative with respect to z and substituting it into Fourier's Law of heat conduction, the rate of heat exchange, at the surface (z=0), is:

$$q_{soil} = kA\frac{\left(T(z=0,t) - T(z,t=0)\right)}{\sqrt{\pi\alpha t}} \tag{3.47}$$

3.4 Heat Transfer by Convection (q_{conv})

3.4.1 Newton's Law of Cooling

Convection can be viewed as the combining heat transfer effects of conduction and advection in fluids. Heat transferred through convection can be calculated using Newton's Law of cooling:

$$q_{conv} = hA\left(T_{surface} - T_{fluid}\right) \tag{3.48}$$

where q_{conv} is the heat transferred by convection (W)
h is the heat transfer coefficient (W/m^2 K)
A is the area of heat transfer (m^2)
$T_{surface}$ is the temperature of the surface (˚C or K)
T_{fluid} is the temperature of the cooling (or heating) fluid (˚C or K).

For ponds, convection occurs in two places, the soil-water interface and the water-air interface. As already discussed in section 3.3.2, the rate of energy exchanged between the liner and the pond can be estimated by either Equation 3.43, 3.47 or 3.48 . For the water-air interface, convection is the only mode of heat transfer.

3.4.2 Determination of a Heat Transfer Coefficient - Nusselt Number Correlations

Nusselt number (Nu) correlations are traditionally used to predict a heat transfer coefficient, depending on:

- the geometry of the surface
- the properties of the cooling fluid
- the velocity at which the cooling fluid is moving

However, there seems to be no Nusselt number correlations in the literature for bodies of water

cooled or heated by the ambient air.

For the case when there is no wind (i.e. free convection), the flat plate Nusselt number correlations might be valid. This is because there are no waves on the water surface, and

therefore, the approximation that the water surface is a flat plate might not be too far from the truth.

The Nusselt number, a dimensionless number, is the ratio between the rate of convection to the rate of conduction in a fluid. Numerically, the Nusselt number (Nu) is related to the heat transfer coefficient by:

$$Nu = \frac{hL_c}{k_{air}} \tag{3.49}$$

where L_c is the characteristic length of the surface (m)
h is the heat transfer coefficient (W/m^2 K)
k_{air} is the thermal conductivity of the air

$$L_c = \frac{Area}{Perimeter} \tag{3.50}$$

For the case of free convective surfaces, the Nusselt number is related to an other dimensionless number, the Rayleigh number (Ra), through empirical correlations. The Rayleigh number is:

$$Ra = \frac{g\beta\left(T_{water} - T_{air}\right)L_c^3}{\alpha_{air}\nu} \tag{3.51}$$

where g is the gravitational acceleration (9.81 m/s^2)
β is the coefficient of thermal expansion (K^{-1})
T is the temperature (K)
α is the thermal diffusivity of the air (m^2/s)
ν is the kinematic viscosity of the air (m^2/s)

Estimates for the case of a flat horizontal plate where the plate (in this case, the water) is warmer than the cooling fluid (in this case, the air), the following empirical correlations apply (Holman, 1997):

$Nu = 0.54\,Ra_L^{0.25}$ if Ra_{Lc} is between 10^4 and 10^7. (3.52)

$Nu = 0.15\,Ra_L^{1/3}$ if Ra_{Lc} is between 10^7 and 10^{11} (3.53)

If the plate is cooler than the fluid, and Ra is between 10^5 and 10^{10}, then

$$Nu = 0.27\,Ra_L^{1/4} \tag{3.54}$$

For cases where wind is present (i.e. forced convection), different flat plate correlations could be used but run the risk of not being appropriate. Under windy conditions, the pond surface is no longer flat because of waves. However, in the absence of any other relationship, the following Nusselt number correlation for mixed laminar and turbulent flow regions (for $5 \times 10^5 < Re < 10^8$) can be used (Holman, 1997):

$$\overline{Nu}_x = \left(0.037\,\mathrm{Re}_x^{4/5} - 871\right)\mathrm{Pr}^{1/3} \tag{3.55}$$

where x is the length in the direction of wind flow
Re is the Reynold's number
Pr is the Prandtl number

The previous equation is valid for Prandtl numbers between 0.6 to 60. The Reynold's number, Re, is a dimensionless number representing the ratio of inertial to viscous forces in the boundary layer of the fluid. It can be calculated as follows:

$$\mathrm{Re} = \frac{\rho_{air} V x}{\mu_{air}} \tag{3.56}$$

where ρ_{air} is the density of the air(kg/m^3)
V is the velocity of the air (m/s)
μ_{air} is the dynamic viscosity of the air (kg/m s).

The Prandtl number, Pr, is a dimensionless number representing the ratio of the ability of a fluid to diffuse momentum to that of heat. It can be calculated as follows:

$$\mathrm{Pr} = \frac{\nu}{\alpha} \tag{3.57}$$

where ν is the kinematic viscosity of the fluid (m^2/s).

3.4.3 Determination of a Heat Transfer Coefficient - Direct Correlations

Other empirical equations have been used in the literature to estimate the heat transfer coefficient for solar ponds, relating the heat transfer coefficient to wind speed (Duffie and Beckman, 1980,

Sodha et al., 1982; Subhakar and Murthy, 1993; Al-Nimir, 1998; Kurt et al., 2000). The most widely used equation is a corrected version of an equation referenced by McAdams (1954). It was originally intended for estimating the heat transfer coefficient for a 0.152 m^2 vertical copper plate exposed to air. The corrected version excludes the effects of surface radiation which are present in the original equation (Watmuff et al., 1977). The corrected equation used is:

$$h = 2.8 + 3.0V \tag{3.58}$$

where V is the wind velocity (m/s).

The equation is only valid for wind speeds between 0 and 7 m/s (0 to 25.2 km/hr). The original equation is presented with a table and is reproduced here, for imperial and metric units (McAdams, 1954).

$$h = a + b(V)^c \text{ (imperial units)} \tag{3.59a}$$

$$h = 5.677 \times \left(a + b(3.2808 \times V)^c\right) \text{ (metric units)} \tag{3.59b}$$

The units for V in Equations 3.59a are ft/s. The units for V in Equations 3.59b are m/s. The units for the heat transfer coefficient in Equation 3.59a are Btu/hr/ft^2/°F. For Equation 3.59b, the units for the heat transfer coefficient are W/m^2/°C.

Table 3.8: Presented are the convection coefficient factors a, b and c for Equations 3.59a and 3.59b (Source: McAdams, 1954).

Surface	Velocity less than 16 ft/s			Velocity between 16 100 ft/s		
	a	b	c	a	b	c
Smooth	0.99	0.21	1	0	0.5	0.78
Rough	1.09	0.23	1	0	0.53	0.78

Alternately, the heat transfer coefficient can be assumed constant, as was done by Singh et al. (1994). The heat transfer coefficient was fixed at 17.5 W/m^2/°C

3.5 Energy Associated with Movements of Water (q_{in}, q_{drain}, q_{rain}, $q_{seepage}$, $q_{evaporation}$)

3.5.1 Bulk Energy Transport in Liquid Water (q_{in}, q_{drain}, q_{rain}, $q_{seepage}$)

Because the liquid water entering or leaving the control volume also has internal energy,

movements of liquid water across the system boundary represent gains or losses of energy. The rate of bulk energy moved across the system boundary can be calculated with the following equation:

$$q = \dot{m} c_p T \tag{3.60}$$

where m' is the mass flow rate of water into (or out of) the system,
c_p is the specific heat of water and
T is the temperature of the water.

When considering seepage, energy losses may be assumed small with respect to other heat transfer mechanisms because of the small infiltration flow rate. To validate this assumption, consider Darcy's Equation, which states that the rate of seepage ($m'_{seepage}$) is:

$$\dot{m}_{seepage} = k_{hyd} i A \tag{3.61}$$

where k_{hyd} is the hydraulic conductivity (m/s),
i is the hydraulic gradient (dimensionless)
A is the pond floor area (m^2).

For saturated clays, k_{hyd} can vary from 10^{-11} to 10^{-6} cm/s (Carbeneau, 2000) and i = 0.01 (Cedergren, 1966). Therefore, for every square meter of pond area, 10^{-15} to 10^{-10} $m^3/s/m^2$ (or 10^{-9} to 10^{-4} $mL/s/m^2$ = 8.64 x 10^{-5} to 8.64 $mL/day/m^2$) of water are lost. As a result, it was assumed that water infiltration, being so small, is negligible in the transport of energy (i.e. $q_{seepage} = 0$) for ideal conditions. This may not necessarily be true in the case of ponds where various animals (ex: crawfish, nutria, muskrats) dig tunnels through the levees. In such cases, water losses through leaks may be considerable (even dangerous for the levee in some cases). Unfortunately, it is impossible to predict how much water (or energy) will flow through an animal's tunnel system.

3.5.2 Latent Heat Loss (q_{evap})

The process of evaporation requires a lot of energy. Evaporation heat losses (q_{evap}) are calculated with the following set of equations (Anonymous, 1992):

$$q_{evap} = \dot{m}_{evap} h_{fg} = E_0 \rho_{water} h_{fg} \tag{3.62}$$

$$h_{fg} = 2{,}502{,}535{,}259 - 212{,}563{,}84T \tag{3.63}$$

where m'_{evap} is the rate of evaporation (kg/s)

h_{fg} is the latent heat of vaporization (J/kg)
E_0 is the volumetric rate of evaporation (m^3/s)
ρ_{water} is the density of water (kg/m^3)
T is the water temperature (°C).

The difference in water vapor pressure between the water surface and the air vapor pressure is the driving force behind evaporation (Penman, 1948). The following equation is Dalton's Law and many equations used to predict evaporation have the same form:

$$\dot{m} = f(x)\left(p_{water} - p_{air}\right) \tag{3.64}$$

where f(x) is an experimentally determined function, based on external parameters
p_{water} is the saturated liquid vapor pressure of the liquid water
p_{air} is the partial pressure of water vapor in the air.

The diffusion of water vapor from the pond can be determined with the use of Fick's Law, which uses the same concept of vapor pressure differences as the driving force behind evaporation:

$$\dot{m} = -DA\left(\frac{\partial C_{water}}{\partial z}\right) \tag{3.65}$$

where D is the diffusion coefficient (m^2/s)
(for water diffusing into air at 25°C, D = 0.28 X 10^{-4} m^2/s)
A is the area of the pond (m^2)
C_{water} is the water vapour concentration in the air (kg/m^3)
z is the distance above the water surface (m)
$\partial C_{water}/\partial z$ is the concentration gradient of water vapor in the z direction (above the water surface).

Water vapor can be considered an ideal gas, and because of this, Fick's Law can be rewritten as a function of partial pressures, rather than concentration.

$$\dot{m} = -DA\frac{MM}{R_0 T}\left(\frac{\partial p_{vp}}{\partial z}\right) \tag{3.66}$$

where MM is the molar mass of water vapor (18 kg/mol)
R_0 is the universal gas constant (8314 J/mol K)
T is the temperature of the water vapor (K)
p_{vp} is the vapor pressure (Pa).

Although all the values in Fick's Law are known, the diffusion coefficient (D) might not be totally accurate when considering ponds exposed to wind (Holman, 1997). Whenever possible, experimental correlations should be developed and used (Holman, 1997; Pierahita, 1991).

Empirical equations specifically developed for bodies of water have been developed. One such equation is (Penman, 1948):

$$E_0 = \frac{0.35A(10^{-3})}{86400}(1 + 9.8 \times 10^{-3}V_2)(p_{sat-ws} - p_{vp})\left(\frac{760mmHg}{101300Pa}\right) \quad (3.67)$$

where E_o is the evaporation rate (m^3/s)
V_2 is the wind velocity at two meters above the surface (miles per day)
p_{sat-ws} is the saturated vapor pressure of the water surface, evaluated at the surface water temperature (Pa)
p_{vp} is the vapor pressure of the air (Pa).

The vapor pressure (p_{vp}), (Anonymous, 1985), is:

$$p_{vp} = p_{vp-sat}\phi \quad (3.68)$$

where p_{vp-sat} is the saturated vapor pressure of the air (Pa)
ϕ is the relative humidity (decimal)

The saturated vapor pressure of the water surface or the water vapor can be calculated using the following equations from (Anonymous, 1985).

$$\ln p_{sat} = \frac{C_1}{T} + C_2 + C_3T + C_4T^2 + C_5T^3 + C_6 \ln T \quad (3.69)$$

where T is the temperature of the water surface (K)
C_1 = -5800.2206
C_2=1.3914993
C_3= -0.04860239
C_4= $0.41764768 \times 10^{-4}$
C_5 = $-0.14452093 \times 10^{-7}$
C_6 = 6.5459673

When determining the vapor pressure of the air, the saturated vapor pressure is evaluated for the current air temperature.

Alternately, the following equation can be used to estimate the rate of evaporation (Piedrahita,

1991):

$$E_0 = \frac{2.241}{3600} A \times 10^{-6} \times V_2 \times (p_{sat-ws} - p_{vp}) \left(\frac{760 mmHg}{101300 Pa} \right) \tag{3.70}$$

where E_0 is the rate of evaporation (m^3/s)
A is the pond area (m^2),
V_2 is the wind velocity 2 meters above the pond surface (km/h)
p_{sat-ws} is the saturated vapor pressure (Pa)
p_{vp} is the air vapor pressure (Pa)

The Lake Hefner Equation is yet another equation which predicts evaporation (Anonymous, 1952):

$$E_o = \left(0.068 + 0.059 V_{13ft}\right)\left(p_{sat-wv} - p_{vp}\right) \tag{3.71}$$

where E_0 is the evaporation rate (in/day)
V_{13ft} is the wind speed recorded at 13 feet (mph)
p_{sat-ws} is the saturated vapor pressure (in Hg)
p_{vp} is the air vapor pressure (in Hg)

A metric version of Equation 3.71

$$E_o = \left(0.068 + 0.13 u_{4m}\right)\left(p_{sat-wv} - p_{vp}\right)\left(1.344 \times 10^{-7}\right) \tag{3.72}$$

where E_0 is the evaporation rate (m/s)
u_{4m} is the wind speed recorded at 4 meters (m/s)
p_{sat-ws} is the saturated vapor pressure (Pa)
p_{vp} is the air vapor pressure (Pa)

In order to determine the wind speed at any height, the following equation can be used:

$$\frac{u_y}{u_x} = \frac{\ln y}{\ln x} \tag{3.73}$$

where u is the wind speed at either height x or y (feet)

As can be seen from Equation 3.71, the Lake Hefner Equation was designed for estimating daily evaporation rates.

3.6 Other Sources of Energy

3.6.1 Pond Mud Respiration

Decomposition in pond muds may be a source of energy in aquaculture ponds. The energy released in pond muds is a byproduct of decomposer respiration (Boyd, 1995). Chemically, the aerobic respiration of glucose can be described with the following equation:

$$C_6H_{12}O_6 + 6O_2 \rightarrow 6CO_2 + 6H_20 + \Delta H_c$$

where ΔH_c is heat of combustion for glucose = 15.58 kJ/mol of glucose (Doran, 1995)

Semi-intensive aquaculture pond soils consume 1 to 2 $gO_2/m^2/day$ (or 0.03125 to 0.0625 $molO_2/m^2/day$) while intensive aquaculture pond soils use 4 $gO_2/m^2/day$ (or 0.125 $molO_2/m^2/day$) (Boyd, 1995). Assuming that most of the generated energy does come from the combustion of glucose, the total energy produced by decomposers in semi-intensive aquaculture pond soils is 81.25 to 162.5 $J/m^2/day$ and in intensive aquaculture pond soils is 325 $J/m^2/day$.

Factors which may cause variations in the rate of pond mud respiration include temperature, oxygen availability, pH and nutrient availability (Boyd, 1995).

3.6.2 Work Done by the Aerator

The aerators used for the warm water ponds are brand name Power House Aerators, rated at 3/4 hp (746 Watts). The work done by the aerator on the pond represents an input of energy.

The presented theory was reviewed in order to develop an energy balance for an outdoor earthen aquaculture pond. The development of the energy balance will be presented in Chapter 4.

CHAPTER 4: THE CREATION OF A THEORETICAL COMPUTER MODEL

4.1 Introduction

Two models describing the rate of energy change in an aquaculture pond have been presented in Chapter 3. The conceptual model (Figure 4.1) qualitatively describes how energy moves into and out of a pond.

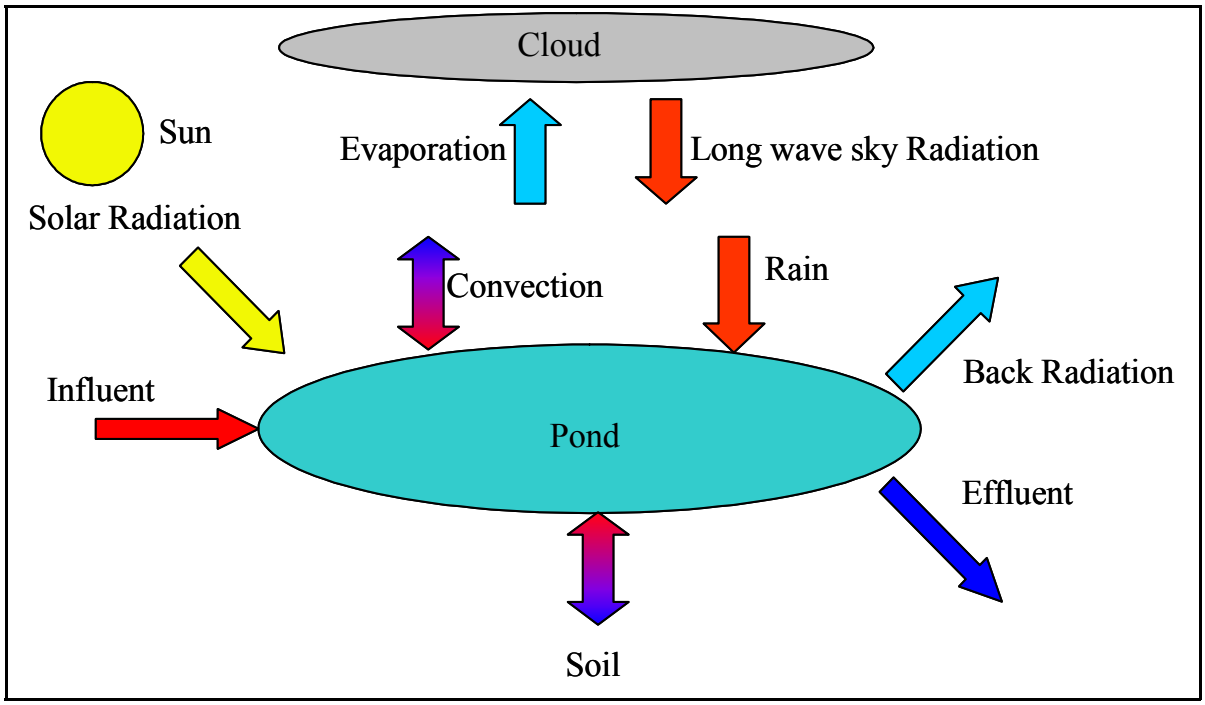

Figure 4.1: This figure (taken from Figure 3.1) is a conceptual representation of an energy balance for an aquaculture pond. Each arrow represents an energy vector (a term in Equation 3.4). Two-headed arrows represent transport phenomena which either move energy into the pond (when the surroundings are warmer than the pond) or out of the pond (when the surroundings are cooler than the pond). By taking the sum of all vectors, the rate of change for both the pond's internal energy and the pond temperature can be determined.

A second model, Equation 3.4, is the mathematical representation of Figure 4.1. This 1st order non-linear differential equation describes and quantifies each vector of energy transfer. Two different solutions to Equation 3.4 are required for different types of circumstances:

- a steady state solution ($dE/dt = 0$): This solution quantifies energy vectors when the pond water temperature, volume, specific heat and water density are constant. This includes the case where the water temperature is held artificially high in the winter or artificially low in the summer.

- a transient solution ($dE/dt \neq 0$): This solution is applicable when the water temperature changes either naturally or artificially.

Although the steady state solution will yield the "answer" to the initial problem (i.e. how much energy is required to heat or cool a pond), the transient solution is insightful because it:

- identifies when there is a surplus or deficit of internal energy in the pond
- quantifies these surpluses and deficits, and
- estimates the required power necessary to artificially change or maintain the water temperature.

An analytical solution to Equation 3.4 is mathematically difficult to find, especially when the system is transient. For this reason, numerical methods have been used. The following chapter is a detailed description of PHATR (Pond Heating And Temperature Regulation), version 1.0, a computer program used to numerically solve Equation 3.4.

4.2 Description of PHATR

PHATR was developed in FORTRAN, using the Essential Layhey FORTRAN 90 (ELF 90) compiler. It determines:

- the amount of energy being transferred through various transport mechanisms (i.e. the size of each arrow - energy vector - in Figure 4.1)
- the predicted pond temperature

4.2.1 Equations Used to Solve Equation 3.4

Table 4.1 lists the equations for each of the terms in Equation 3.4 used by PHATR. Solar radiation, q_{solar}, is measured directly from field observations and is available to PHATR in a data file.

4.2.2 Assumptions

These assumptions were used to simplify the solution of Equation 3.4.

- The water density and specific heat remained constant, despite changes in water temperature. This was a reasonable assumption because at 0°C, the density 999.8 kg/m^3 and at 43.3 °C, the density is 990.6 kg/m^3 (less than 1% change). At 0°C, the specific heat is 4225 J/kg°C and at 43.3°C, the specific heat is 4174 J/kg˚C (a relative change of 1.2%) (Holman, 1997).

Table 4.1: This is a list of all the equations used by PHATR. Each vector, a term in Equation 3.4, requires one or several equations before it can be used to determine the pond's internal energy.

Vector (term in Equation 3.4)	Reference equation(s)
Pond back radiation (q_{back})	3.25
Longwave sky radiation (q_{sky})	3.26, 3.27, 3.28
Soil heat conduction - natural (q_{soil})	3.41, 3.43
Soil heat conduction - forced steady-state (q_{soil})	3.47
Air convection (q_{conv})	3.48, 3.58
Evaporation (q_{evap})	3.62, 3.63, 3.71
Bulk water movements (q_{in}, q_{drain})	3.60

- The pond volume was constant. This was not totally true, because losses due to leaks and evaporation were present. However, this assumption held when the water flushed the ponds, because water was continuously being discharged at the standpipe.

- The pond was ideally mixed and the temperature was the same throughout the pond, including at the surface. This assumption was verified within the bulk of the fluid (not at the surface) with manual thermometer measurements at various locations in aerated 400 m^3 ponds (see Appendix 1 for a description of the ponds or Lang, 2001).

- The sky was cloudless (for the purposes of calculating the emitted atmospheric longwave radiation). For Louisiana, this was not a good assumption. However, longwave radiation from a cloudless sky was the "worst case" scenario because a cloudy sky has more moisture emitting longwave radiation to the ground. Using the worst-case scenario ensured that the model did not under predict the amount of energy required to heat a pond during the winter.

- The soil properties of the pond were uniformly distributed. This assumption was supported by the fact that the soil at the pond floor was compacted and fully saturated with water.

- The following equation describing the heat transfer for semi-infinite solids with constant temperature at the soil surface was accurate in describing the heat transfer between the soil and the pond.

$$q_0 = \frac{kA\left(T_{pond} - T_{initial}\right)}{\sqrt{\pi \alpha t}} \tag{4.1}$$

(Holman, 1997)

This assumption was reasonable if the following two conditions were satisfied:

- the considered time period (i.e. the time step) was small, which guaranteed that the soil could be considered as a semi-infinite solid.
- the Biot number was large. This assumption allowed for the use of a simpler boundary condition, as described in Appendix 4.

- There was no evaporation when the relative humidity of the air is at or above 100%.

- The Lake Hefner Equation (Equation 3.70) was accurate in predicting instantaneous evaporation .

- All incident solar radiation was absorbed by the water. This assumption was reasonable for the following two reasons:
  - very little light was reflected at the pond surface (as shown in Table 3.3).
  - the water was turbid, preventing the escape of scattered solar radiation.

- All energy absorbed by the phytoplankton was transferred to the water, thus ignoring the amount of energy converted into sugars by chlorophyll.

- The decomposing microorganisms in the pond mud generated negligible amounts of heat.

- The aerators did negligible amounts of thermodynamic work. The amount of energy converted from the work done by the mixing of the aerator to the internal energy of the pond was considered negligible.

4.2.3 Logic

PHATR followed these steps to determine the pond temperature:

1. Data input. PHATR initially acquired data from files. Such files contained information about the weather (weather.dat), environmental constants and step sizes (information.dat) and the rate of water flow into the pond (flow.dat). For the special case where no warm water was flowing into the pond (i.e. natural unforced pond water temperature), no file with information about the flow of warm water was required. The data were converted into the proper units.

2. Determination of coefficients. With the acquired data, PHATR proceeded to determine the coefficients which did not depend on time or water temperature. Each mode of energy transfer had a coefficient term. Table 4.2 listed these coefficients.

Table 4.2: PHATR Version 1.0 used two arrays: coefficients and vectors. The each coefficient array was multiplied to a specific temperature term to get the vector array. The sum of the vector array is equal to the rate of change of internal energy in a pond.

Number	Description	Coefficient (κ)	Vector (v)
1	Pond longwave radiation	$\kappa_1 = \varepsilon_{water} A_{pond} \sigma$	$v_1 = \kappa_1 \left(T_{pond} + 273 \right)^4$
2	Atmospheric longwave radiation	$\kappa_2 = \varepsilon_{sky} A_{pond} \sigma$	$v_2 = \kappa_2 \left(T_{air} + 273 \right)^4$
3	Soil heat exchange (steady-state)	$\kappa_3 = 1$	$v_3 = equation\_3.42$
3	Soil heat exchange (transient)	$\kappa_3 = \frac{k A_{pond}}{\sqrt{\pi \alpha}}$	$v_3 = \kappa_3 \frac{\left(T_{pond} - T_{initial} \right)}{\sqrt{t}}$
4	Surface evaporation	$\kappa_4 = B_{conv} \left(0.068 + 0.059 u_{13} \left(p_{ws} - p_{vp} \right) \right) A_{pond} \rho h_{fg}$	$v_4 = \kappa_4$
5	Surface convection	$\kappa_5 = \left(2.8 + 3.0 u_0 \right) A_{pond}$	$v_5 = \kappa_5 \left(T_{air} - T_{pond} \right)$
6	Penetrated solar radiation	$\kappa_6 = \left(solar\_radiation \right) A_{pond}$	$v_6 = \kappa_6$

3. Determination of vectors. The coefficients were then multiplied to the appropriate time or water temperature term, the product being the vector term. The vector terms were "q"s in Equation 3.4 and arrows in Figure 4.1. Again, the formula for each vector term is given in Table 4.2.

4. Determination of the "thermal mass". The thermal mass is defined here as the energy required to raise the temperature of a given quantity of water by 1˚C. The "thermal inertia" of the pond is:

$$\rho \forall_{pond} c_p \tag{4.2}$$

where ρ is the density of water
$\forall_{pond}$ is the pond volume
c_p is the specific heat of water

5. Solving Equation 3.4 - performing the energy balance. By substituting the vectors and the thermal mass into Equation 3.4, the rate of change of pond temperature is:

$$\left(\frac{dT}{dt}\right)_{pond} = \frac{\sum q}{\rho \forall_{pond} c_p} = f(t,T) \tag{4.3}$$

where T is the temperature
t is time
q is an energy vector in Equation 3.4

To solve this differential equation, the 4th order Runge-Kutta numerical technique is used. The 4th order Runge-Kutta numerical technique is recognized as an accurate method in evaluating ordinary differential equations. With the use of initial conditions, the Runge-Kutta technique evaluates the pond temperature with the following set of equations:

$$T(t+\Delta t) = T(t) + \frac{F_1 + 2F_2 + 2F_3 + F_4}{6} \tag{4.4}$$

$$F_1 = (\Delta t) f(t,T) \tag{4.5}$$

$$F_2 = (\Delta t) f\left(t + \frac{\Delta t}{2}, T + \frac{F_1}{2}\right) \tag{4.6}$$

$$F_3 = (\Delta t) f\left(t + \frac{\Delta t}{2}, T + \frac{F_2}{2}\right) \tag{4.7}$$

$$F_4 = (\Delta t) f(t + \Delta t, T + F_3) \tag{4.8}$$

6. Data output. The time, the vectors and the pond temperature were all recorded in an output file (output.dat). Steps 1 through 5 were repeated for the desired time period. Once the model run was completed, the output was analyzed with a spreadsheet program. An example of the output is in Figure 4.2.

4.3 Performance Tests for PHATR Version 1.0.

Tests were done to determine PHATR's accuracy and stability for heated and unheated ponds. Model runs were compared to pond temperature data collected at the LSU Agriculture Center Aquaculture Research Station (ARS) warm water ponds (see Chapter 2). Each pond had one aerator running continuously, access to warm water from the geothermal well (36°C) and cool well water (21°C). The temperature was automatically controlled with an automated valve, actuated with a data logger (Campbell Scientific CR23X, Campbell Scientific Inc., North Logan, UT). The pond temperature was measured with a type T thermocouple 10 cm below the water surface near the pond's discharge and recorded with another data logger (Campbell Scientific CR23X, Campbell Scientific Inc., North Logan, UT).

Table 4.3 lists the dates and ponds chosen for performance tests.

Weather data used for the model runs were taken from the Louisiana Agriclimatic Information Web Site (www.lsuagcenter.com/weather) for the Ben Hur Weather Station, located less than a kilometer away from the warm water ponds. Parameters of interest were air temperature, solar radiation, wind speed and relative humidity. The flow rate for each combination of open and closed valves was measured by measuring the time it took to fill at 120 liter bucket. By knowing which combination of valves were open and closed, the flow rate at any time to any pond was known. The Campbell CR23X recorded when valves opened or closed.

By comparing the modeled data to the measured data, the model's accuracy was measured with three statistical parameters:

- the average bias: the bias is a measurement of how close the model is at estimating the actual pond temperature (i.e. the modeled temperature minus the measured temperature). The average bias is the average of all the biases at every time step.

- the standard deviation of the average bias: the standard deviation measures variations in the bias. It is a good indicator of the model's consistency (was the bias constant?) and its ability to predict changes in pond temperature.

- the correlation coefficient: the linear correlation coefficient - r- between the measured and modeled temperatures is an other indicator of the model's ability to predict changes in water temperature.

The time step for accuracy tests was 1 hour.

Time (seconds)	Pond Radiation (Watts)	Sky Radiation (Watts)	Soil Conduction (Watts)	Evaporation (Watts)	Convection (Watts)	Solar Radiation (Watts)	Pond Temperature (? C)
31104000	-141134.256	102730.3863	27196.6768	-9104.060549	-15206.08307	0	11.82
31107600	-141007.1272	102584.9839	19712.36689	-8880.972184	-15437.50172	0	11.75583932
31111200	-140853.229	102697.6145	10997.06019	-8990.033619	-14972.95103	0	11.67811036
31114800	-140670.5473	101974.0129	1644.622574	-8367.494577	-16197.67802	0	11.58576104
31118400	-140450.5958	102213.4047	-7707.660745	-8670.231252	-15298.18691	0	11.47445165
31122000	-140201.3417	103100.8852	-16422.51511	-8589.589696	-14067.51148	0	11.34815519
31125600	-139930.1224	103635.1791	-23906.10567	-24428.78718	-27609.71635	394	11.21053757
31129200	-139533.3166	104149.6273	-29648.50621	-8143.501163	-12495.80442	17730.00079	11.00883595
31132800	-139292.2733	105663.5437	-33258.44981	-7474.269247	-11259.5179	49644.00079	10.88610036

Figure 4.2: This is an example fo the output file generated by PHATR Version 1.0. For every time step, the time, the calculated value for each energy vector and the pond temperature were printed to an output file.

Table 4.3: Model runs were compared to the temperature data collected in these ponds at these times.

Dates	Pond	Temperature Regime	Performance Test
04/03/02 to 04/07/02	5, 6, 7, 8	Unheated	Accuracy of PHATR's transient mode
11/09/02 to 12/16/02	13	Unheated	Accuracy and stability of PHATR's transient mode
12/25/02 to 1/24/03	13	Unheated	Accuracy of PHATR's transient mode
02/13/03 to 03/23/03	3	Unheated	Accuracy of PHATR's transient mode
02/13/03 to 03/23/03	9, 12	Heated (pond temperature constant)	Accuracy and stability of PHATR's steady-state mode

Stability tests consisted of varying the time step used for a model run. Model runs with time steps of 10 minutes, 30 minutes, 1 hour, 2 hours, 4 hours, 6 hours, 12 hours and 24 hours were studied. Again the average bias, its standard deviation and the correlation coefficient were used to compare model runs with the measured pond temperature.

4.4 Results of Performance Tests

4.4.1 Accuracy - Unheated Ponds

Measured and modeled pond temperatures for Pond 13 between November 9th and December 16th, 2002, are compared in Figure 4.3. The difference between the two curves is the bias. How the bias changes is measured with the standard deviation. A plot of the modeled pond temperature versus the measured pond temperature is shown in Figure 4.4. The closer the correlation coefficient is to 1, the more precise the model is at predicting change. The average bias, the standard deviation and the correlation coefficient for all the model runs for unheated ponds are presented in Table 4.4. An average and weighted average for each parameter was then determined, the weighted averages reflecting the greater importance given to longer model runs.

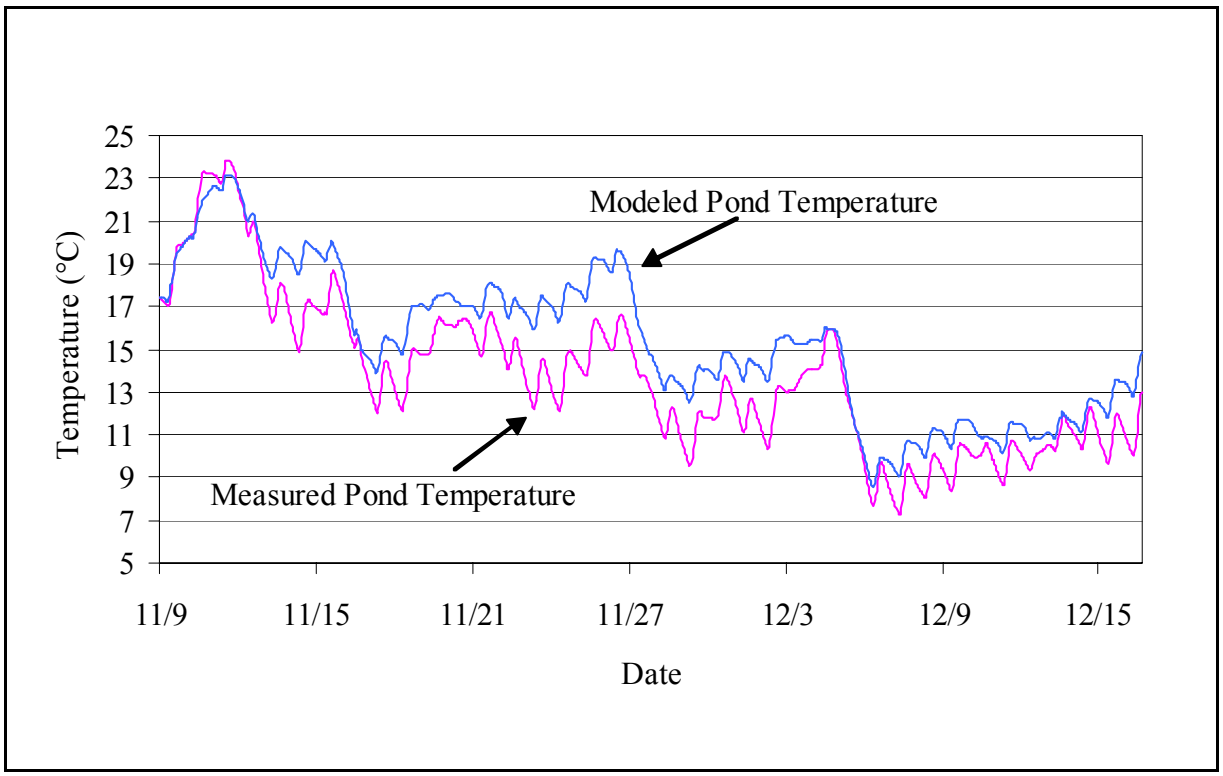

Figure 4.3: The modeled and measured pond temperatures, for Pond 13, were plotted against time. The model had a tendency of over-predicting the pond temperature (average bias of 1.6°C) but the shape of the two curves is similar (correlation coefficient = 0.95).

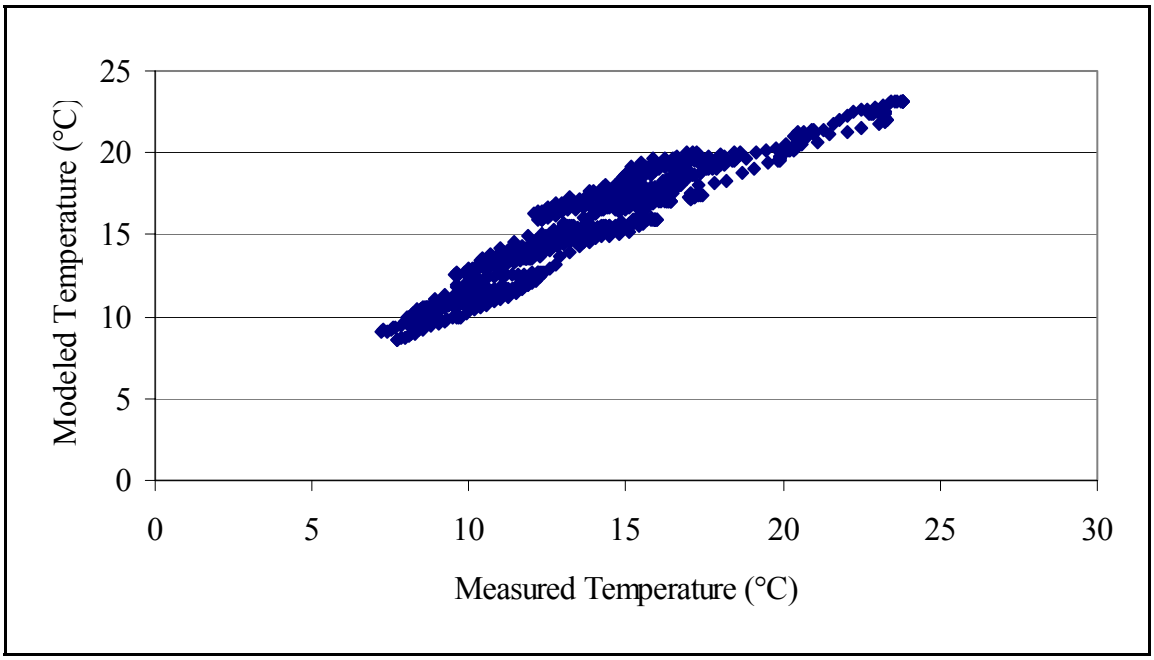

Figure 4.4: The above scatter plot is one way of measuring PHATR's accuracy. A model capable of perfectly predicting changes would have a linear correlation coefficient r = 1.0. For the Pond 13 model run (11/09 to 12/16, 2002), r = 0.95.

Table 4.4: Presented here are the statistical parameters evaluating PHATR's ability to predict the temperature in unheated ponds

Pond	Average Bias (°C)	Standard Deviation (°C)	Correlation Coefficient
5	0.2	0.9	0.96
6	0.5	0.9	0.97
7	0.7	0.6	0.99
8	0.6	0.7	0.97
13 (1st run)	1.6	1.1	0.95
13 (2nd run)	-0.9	1.0	0.90
3	0.2	2.0	0.94
Average	0.5	0.86	0.96
Weighted average	0.5	0.99	0.94

The maximum, minimum and average relative importance of each energy vector was also determined and results are shown in Figures 4.5, 4.6, 4.7 and 4.8. Because different model runs examined the effects of heat transfer over different lengths of time, weighted averages for each vector were calculated, giving more importance to runs with longer time spans.

4.4.2 Accuracy - Heated Ponds

There was less measured data to compare the model's output for heated ponds. Nonetheless, the average bias, its standard deviation and the correlation coefficient were calculated and are shown in Table 4.5. The measured and modeled pond temperature for pond 12, between the 13th of February and the 22nd of March, 2003, is shown in Figure 4.9. Modeled and measured temperatures for the same model run are also plotted against each other in Figure 4.10. The maximum, minimum and average relative importance of each energy vector was also determined and results are shown in Figure 4.11.

Table 4.5: These are statistical parameters describing PHATR's accuracy when predicting the temperature in heated ponds.

Pond	Average Bias (˚C)	Standard Deviation (˚C)	Correlation coefficient
Pond 9	2.2	1.1	0.83
Pond 12	2.6	1.6	0.92
Average	2.4	1.25	0.875

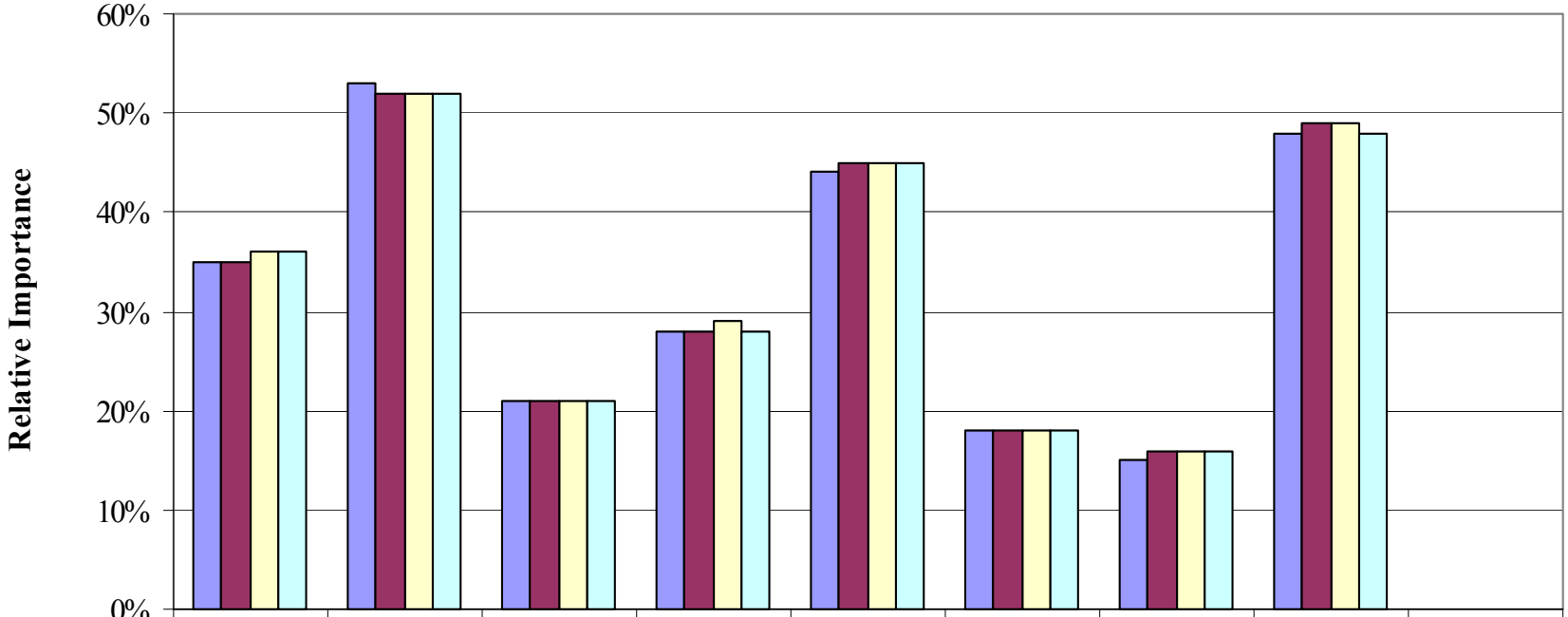

	Average qpond	Maximum qpond	Minimum qpond	Average qsky	Maximum qsky	Minimum qsky	Average qsolar	Maximum qsolar	Minimum qsolar
Pond 5	35%	53%	21%	28%	44%	18%	15%	48%	0%
Pond 6	35%	52%	21%	28%	45%	18%	16%	49%	0%
Pond 7	36%	52%	21%	29%	45%	18%	16%	49%	0%
Pond 8	36%	52%	21%	28%	45%	18%	16%	48%	0%

Figure 4.5: The maximum, minimum and average relative importance of each radiation vector is presented for Ponds 5, 6, 7 and 8. The ponds were unheated and the model run was for the time period between March 3rd and March 7th, 2002. q_{pond} is long wave pond radiation, q_{sky} is long wave sky radiation and q_{solar} is solar radiation.

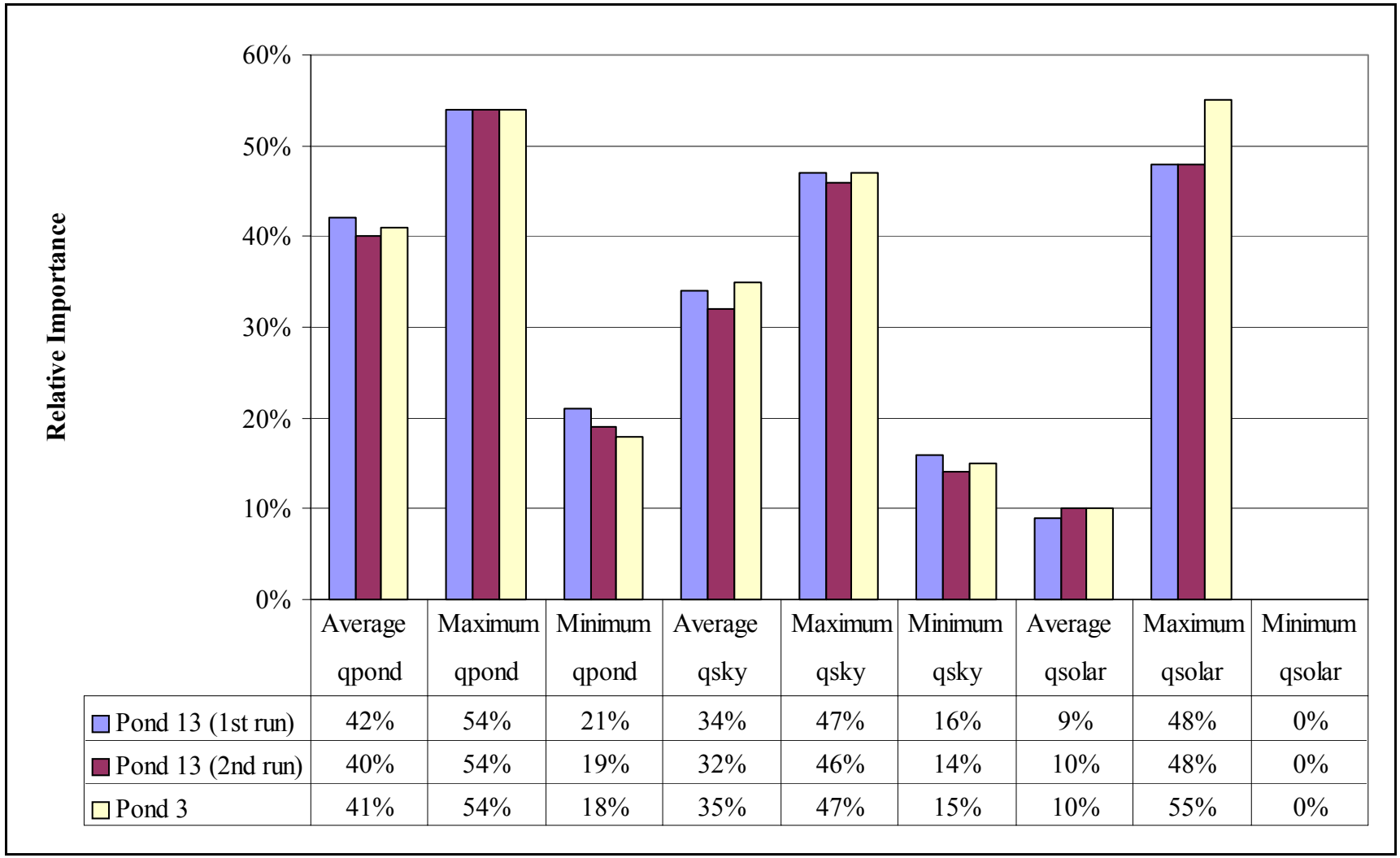

	Average qpond	Maximum qpond	Minimum qpond	Average qsky	Maximum qsky	Minimum qsky	Average qsolar	Maximum qsolar	Minimum qsolar
Pond 13 (1st run)	42%	54%	21%	34%	47%	16%	9%	48%	0%
Pond 13 (2nd run)	40%	54%	19%	32%	46%	14%	10%	48%	0%
Pond 3	41%	54%	18%	35%	47%	15%	10%	55%	0%

Figure 4.6: The maximum, minimum and average relative importance of each radiation vector is presented fro both Pond 13 model runs and Pond 3. The ponds were unheated. The first model run for Pond 13 was between November 9 and December 16, 2002. The second Pond 13 model run was for the time between December 25, 2002 and January 24, 2003. The period for the Pond 3 model run was between February 13 and March 23, 2003. q_{pond} is long wave pond radiation, q_{sky} is long wave sky radiation and q_{solar} is solar radiation.

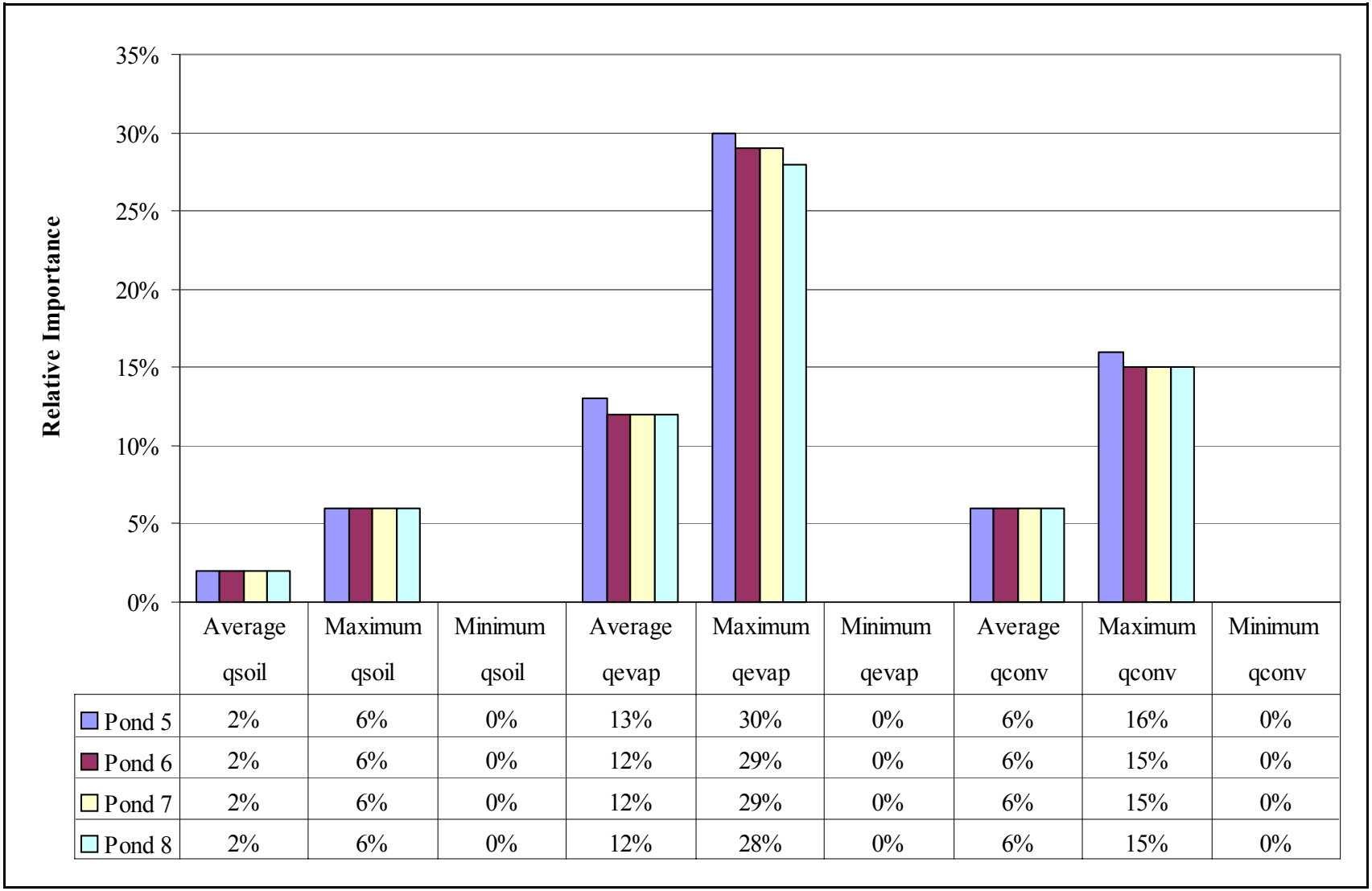

	Average qsoil	Maximum qsoil	Minimum qsoil	Average qevap	Maximum qevap	Minimum qevap	Average qconv	Maximum qconv	Minimum qconv
Pond 5	2%	6%	0%	13%	30%	0%	6%	16%	0%
Pond 6	2%	6%	0%	12%	29%	0%	6%	15%	0%
Pond 7	2%	6%	0%	12%	29%	0%	6%	15%	0%
Pond 8	2%	6%	0%	12%	28%	0%	6%	15%	0%

Figure 4.7: The maximum, minimum and average relative importance for soil conduction (q_{soil}), evaporation (q_{evap}) and surface convection (q_{conv}) are presented for Ponds 5, 6, 7 and 8. The ponds were unheated and the model run was for the time period between April 3 and April 7, 2002.

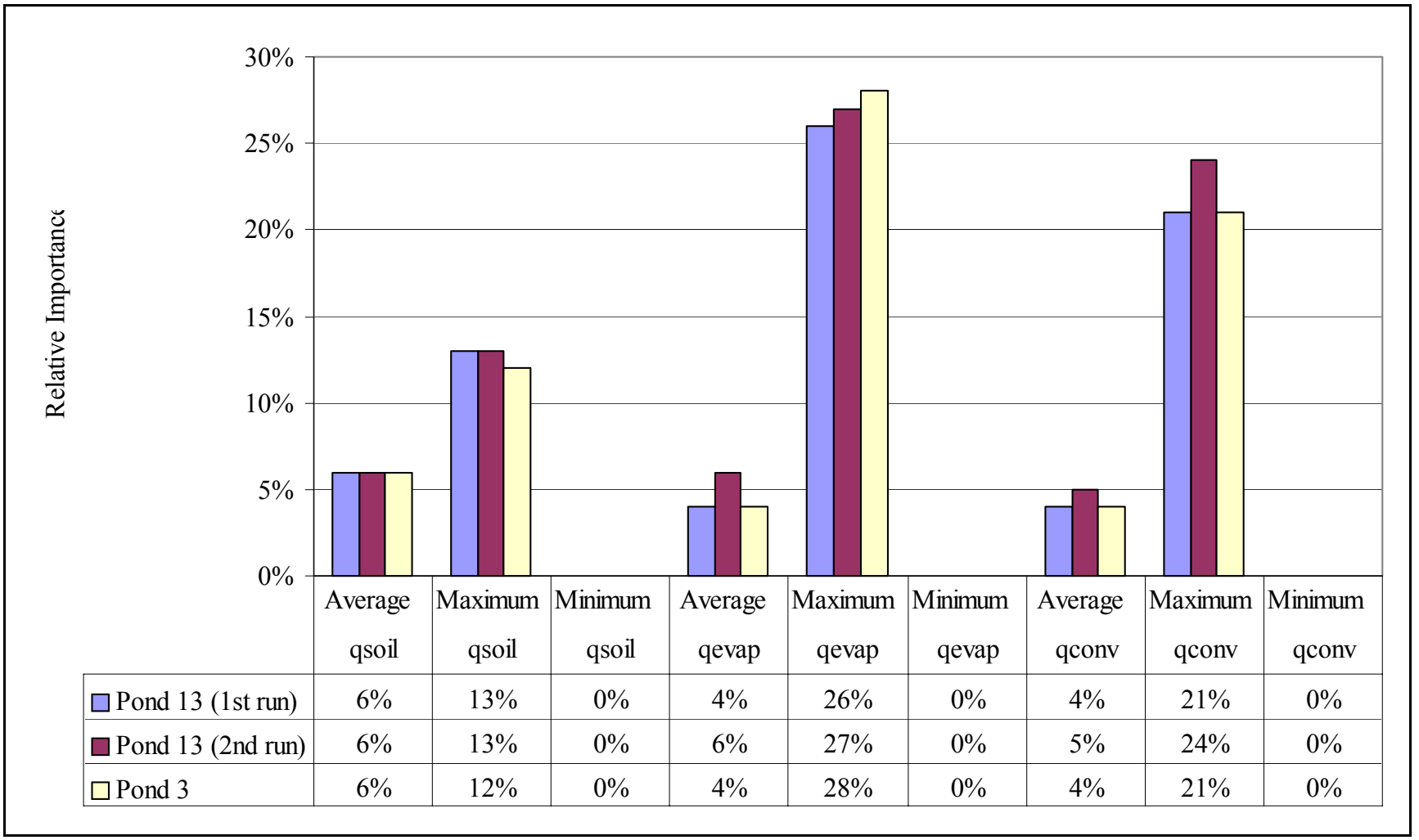

	Average qsoil	Maximum qsoil	Minimum qsoil	Average qevap	Maximum qevap	Minimum qevap	Average qconv	Maximum qconv	Minimum qconv
Pond 13 (1st run)	6%	13%	0%	4%	26%	0%	4%	21%	0%
Pond 13 (2nd run)	6%	13%	0%	6%	27%	0%	5%	24%	0%
Pond 3	6%	12%	0%	4%	28%	0%	4%	21%	0%

Figure 4.8: The maximum, minimum and average relative importance of soil conduction (q_{soil}), evaporation (q_{evap} and surface convection (q_{conv}) are presented for both Pond 13 model runs and Pond 3. The ponds were unheated. The first model run for Pond 13 was between Nomber 9 and December 16, 2002. The second Pond 13 model run was for the time between December 25, 2002 and January 24, 2003. The period for the Pond 3 model run was between February 13 and March 23, 2003.

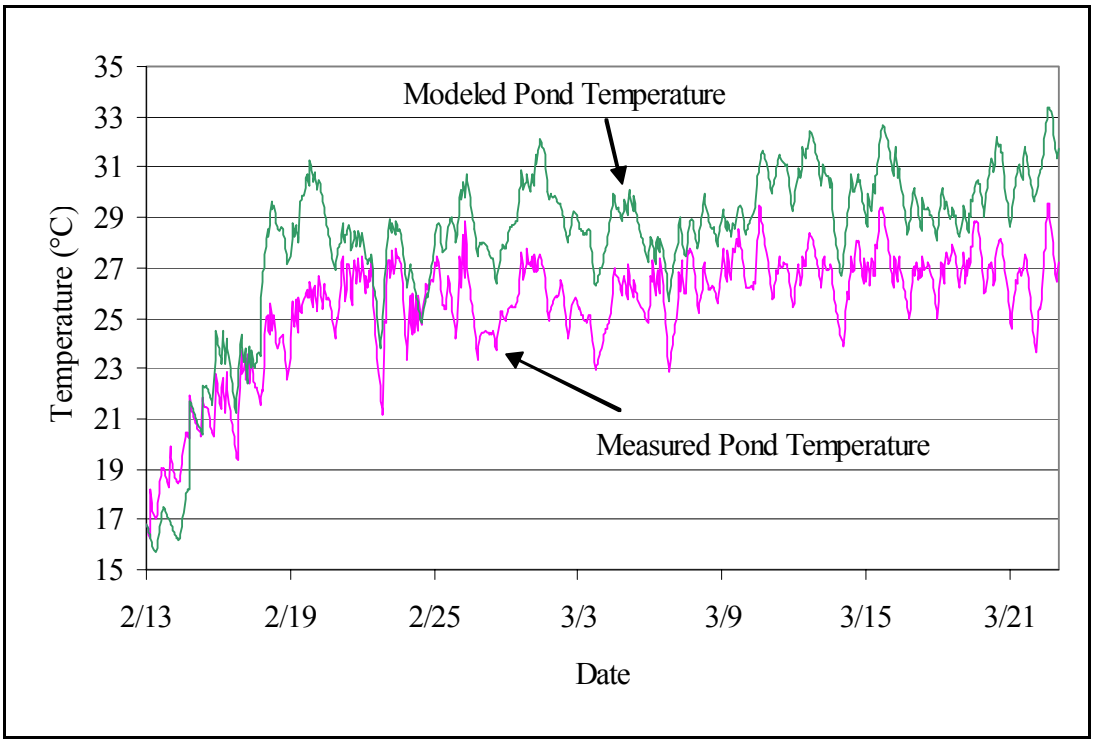

Figure 4.9: The modeled and measured temperatures for Pond 12 were plotted against time. The model had a tendency of over-predicting the pond temperature (average bias of 2.6°C) but the shape of the curves is similar (correlation coefficient = 0.92).

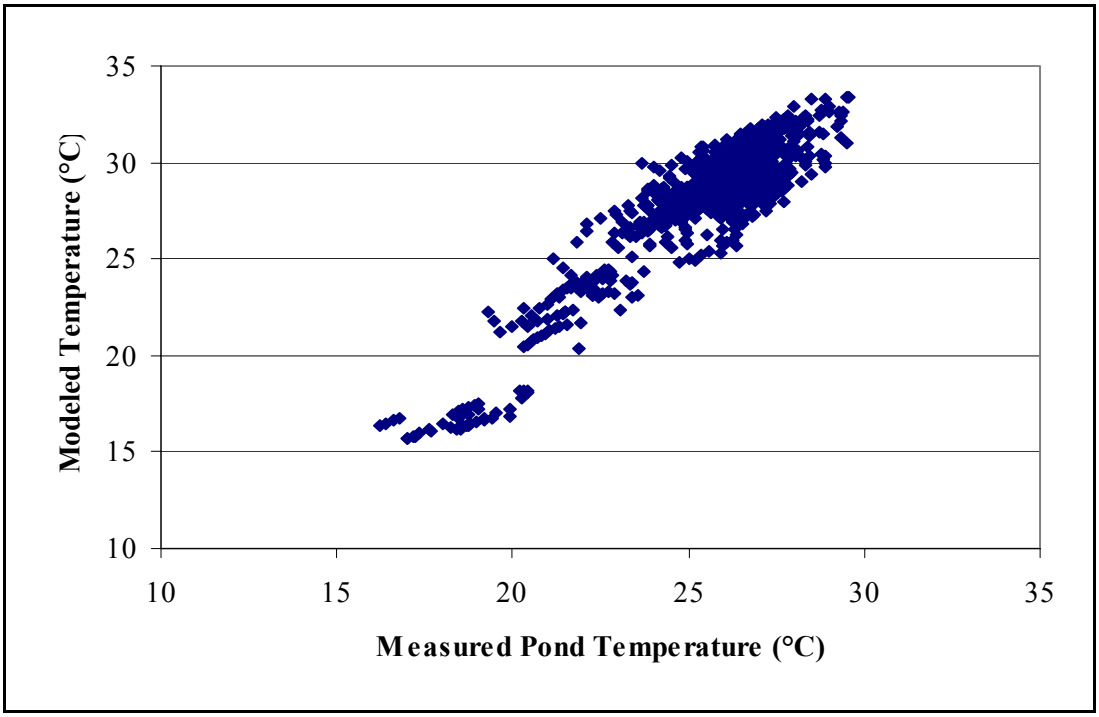

Figure 4.10: For Pond 12, from 02/13 to 03/22, 2003, the correlation coefficient was 0.92.

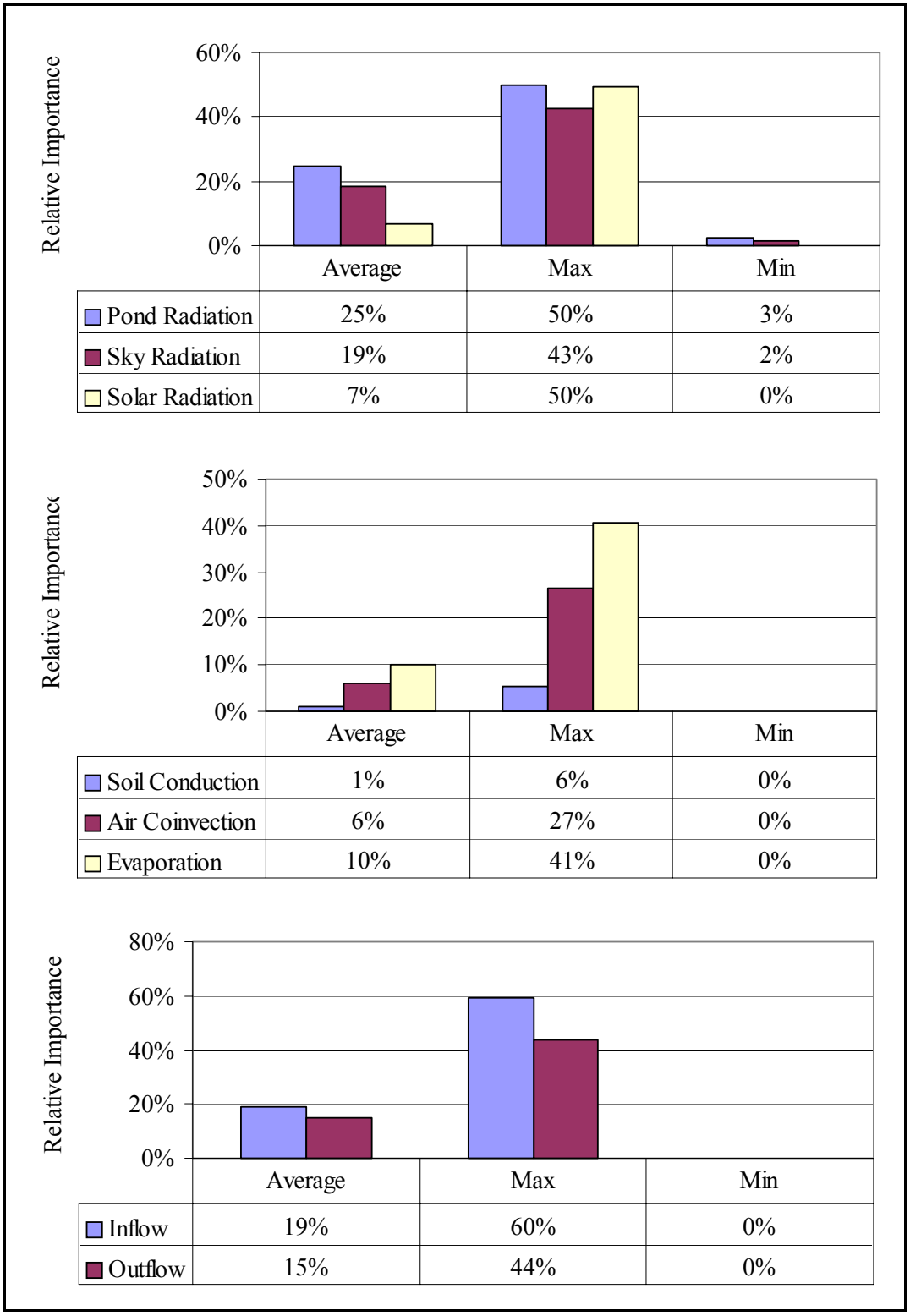

Figure 4.11: The relative importance of each vector for heated Ponds 9 and 12 are presented. The model runs were for February 13 to March 22, 2003.

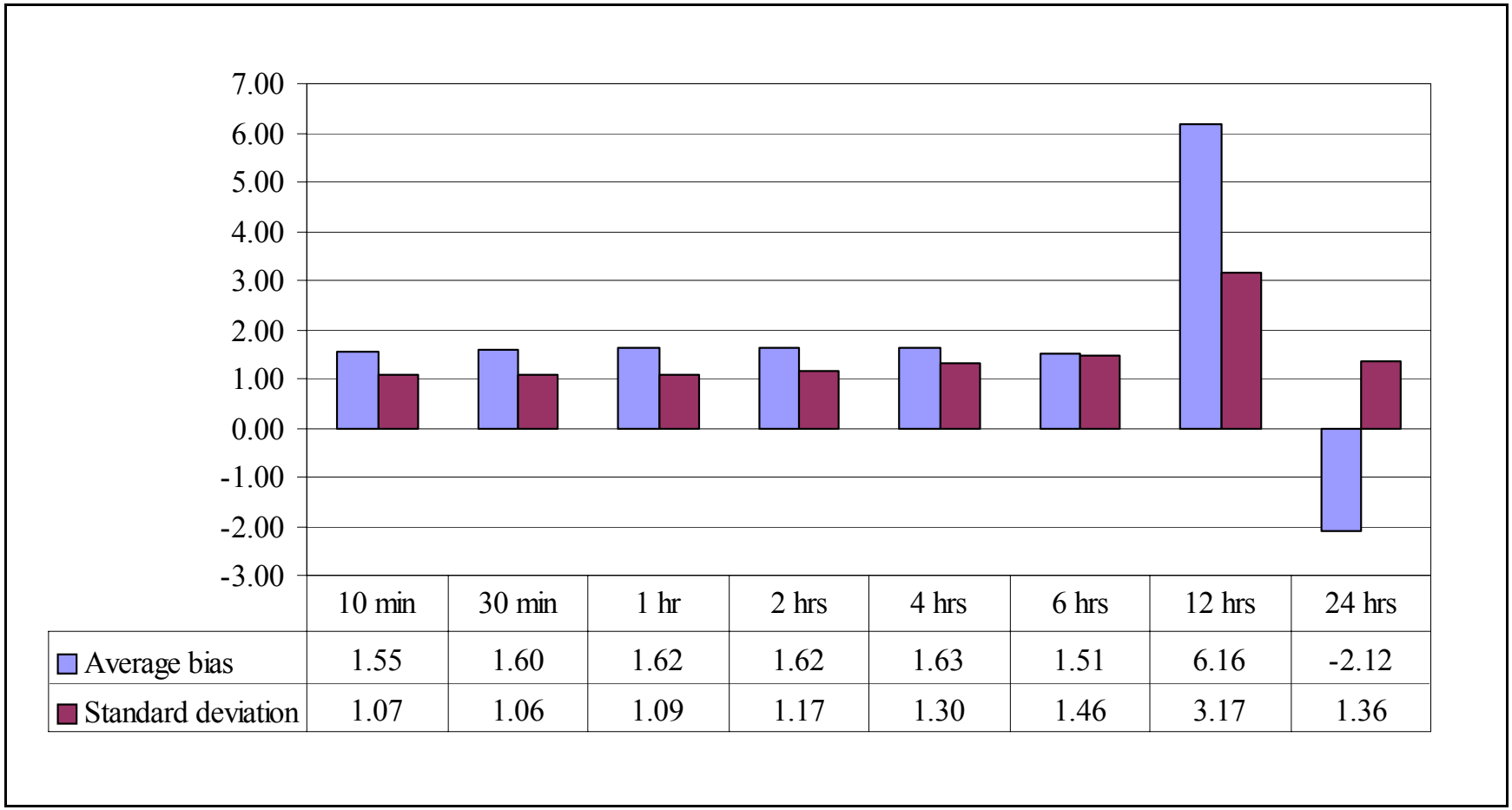

	10 min	30 min	1 hr	2 hrs	4 hrs	6 hrs	12 hrs	24 hrs
Average bias	1.55	1.60	1.62	1.62	1.63	1.51	6.16	-2.12
Standard deviation	1.07	1.06	1.09	1.17	1.30	1.46	3.17	1.36

Figure 4.12: Stability analysis for an unheated pond (Pond 13, between November 13 and Decmber 16, 2002) was done for the shown time steps. The average bias and the standard deviation are in degrees Celcius.

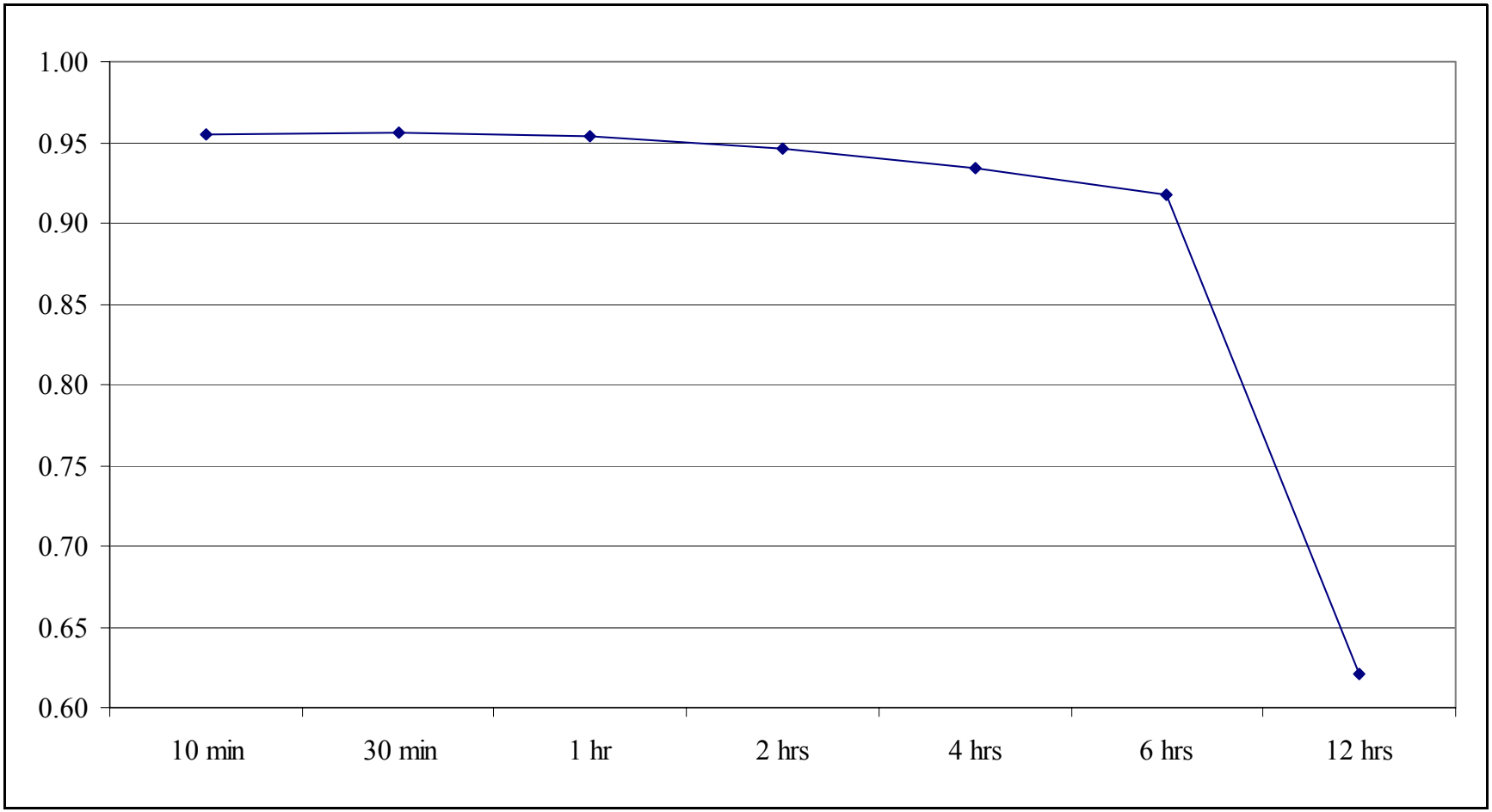

Figure 4.13: Correlation coefficients for the stability analysis for an unheated pond (Pond 13, between November 13 and December 16, 2002) were done for the shown time steps. Correlation coefficients were done between the measured and modeled pond temperature runs.

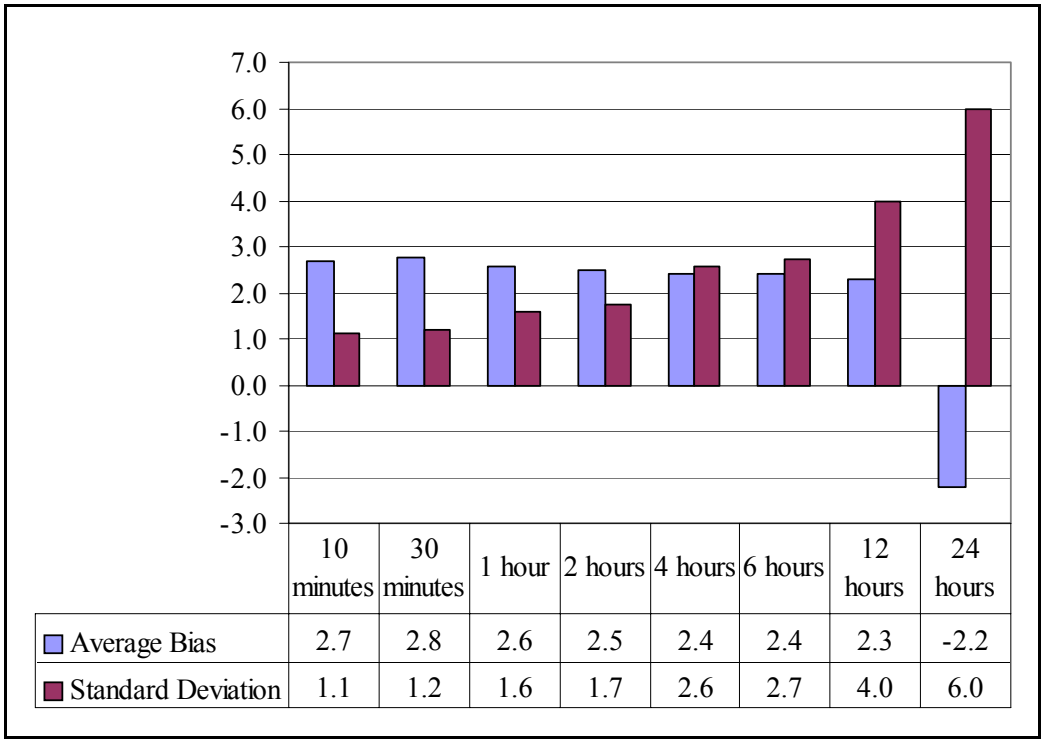

	10 minutes	30 minutes	1 hour	2 hours	4 hours	6 hours	12 hours	24 hours
Average Bias	2.7	2.8	2.6	2.5	2.4	2.4	2.3	-2.2
Standard Deviation	1.1	1.2	1.6	1.7	2.6	2.7	4.0	6.0

Figure 4.14: These are the results from the stability analysis for a heated Pond 12 between February 13 and March 23, 2003. The average bias and the standard deviation are in degrees Celsius.

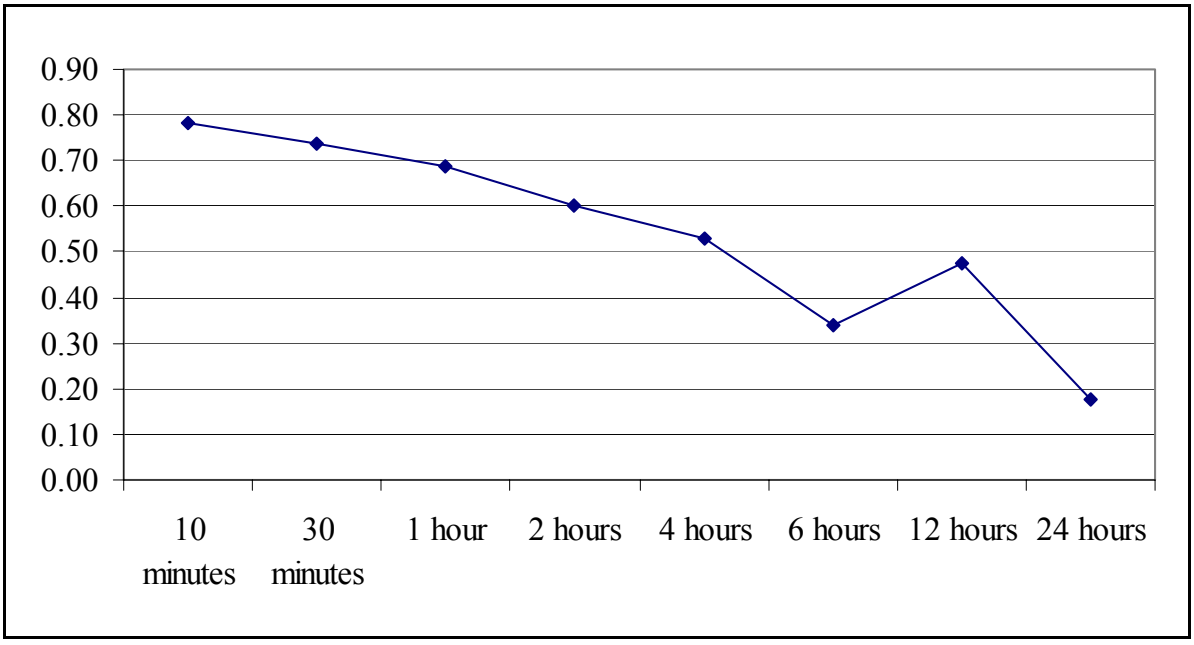

Figure 4.15: These are the correlation coefficients for the model runs in the stability analysis for heated ponds. (Pond 12, between the February 13 and March 23).

4.4.3 Stability tests

A stability test for an unheated pond was compared with data from Pond 13 (11/13 to 12/16, 2003) since the period during which data for this pond was collected is the longest. Pond 12 was chosen for the stability test for heated ponds. Results from each stability test are shown in Figures 4.12, 4.13, 4.14 and 4.15.

4.5 Analysis

4.5.1 Accuracy - Unheated Ponds

Results in Table 4.4 indicated that, in general, the model had a tendency to over-estimate the temperature of unheated ponds by 0.5°C (standard deviation = 1.0°C), despite the fact that the model underestimated the pond temperature for the run between December 26th, 2002 and January 24, 2003 (bias = -0.86°C, standard deviation = 0.98°C). Furthermore, the model could not predict the pond temperature with the same average bias. The average bias for 1st Pond 13 model run (Pond 13, 11/13/2002 to 12/16/2002) was 1.6°C (standard deviation = 1.1°C). The average bias for the 2nd Pond 13 model run (Pond 13, 12/25/02 to 01/24/2003) was -0.9°C (standard deviation = 1.0˚C). The average bias for the Pond 3 model run (Pond 3, 02/13/03 to 03/23/03) was 0.2°C (standard deviation = 2.0°C).

The discrepancy in the results can be explained in part by poor input weather data. The relative humidity measurements at the Ben Hur weather station, between December 31st, 2002 and

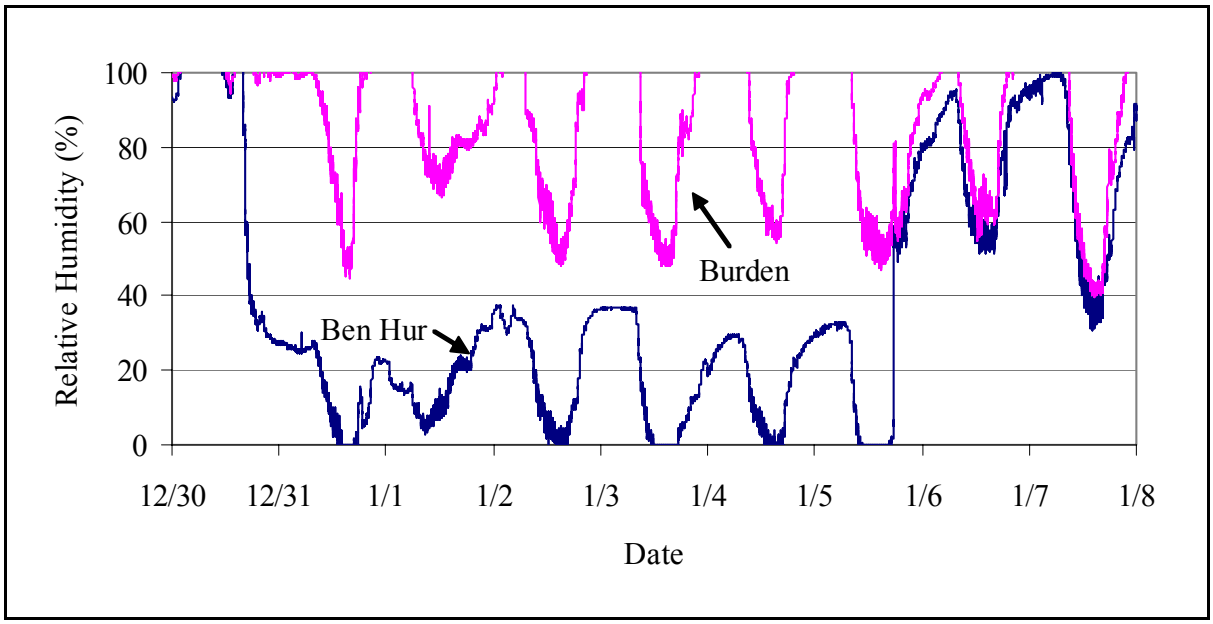

Figure 4.16: The relative humidity measurements from the Ben Hur Weather Station and the Burden Weather Station, both in the Baton Rouge area, give different results between December 31, 2002 and January 6, 2003. Using the Ben Hur data caused the average bias to be -0.9°C. Using the Burden data caused the average bias to be 1.0°C.

January 6th, 2003, did not agree with the relative humidity measurements recorded at the Burden Weather Station, also located in Baton Rouge. Ben Hur Weather Station data had relative humidity readings below 40% and in some cases as low as 0%. For the same time period, the Burden Weather Station recorded relative humidity readings in the 90%-100% range (see Figure 4.16). Using low relative humidity data caused PHATR to over-estimate evaporative energy losses (which explains the negative bias for this model run). Running PHATR again for the time period between December 26th, 2002 and January 24th, 2003 using weather data from the Burden Station yielded an average bias of 1.0°C (standard deviation = 1.2˚C, r = 0.85). The graphical output of both model runs, one using Ben Hur relative humidity data, the other using Burden relative humidity, and the actual measured pond temperature are presented in Figure 4.17.

The general tendency to over-predict may be explained in three ways:

- PHATR was sometimes overestimating energy vectors coming into the pond. Such energy vectors included solar radiation and longwave sky radiation. By over-estimating the amount of energy entering the pond, the pond's internal energy and temperature were also over-estimated.

  As with the relative humidity readings, the radiation readings at the Ben Hur station were

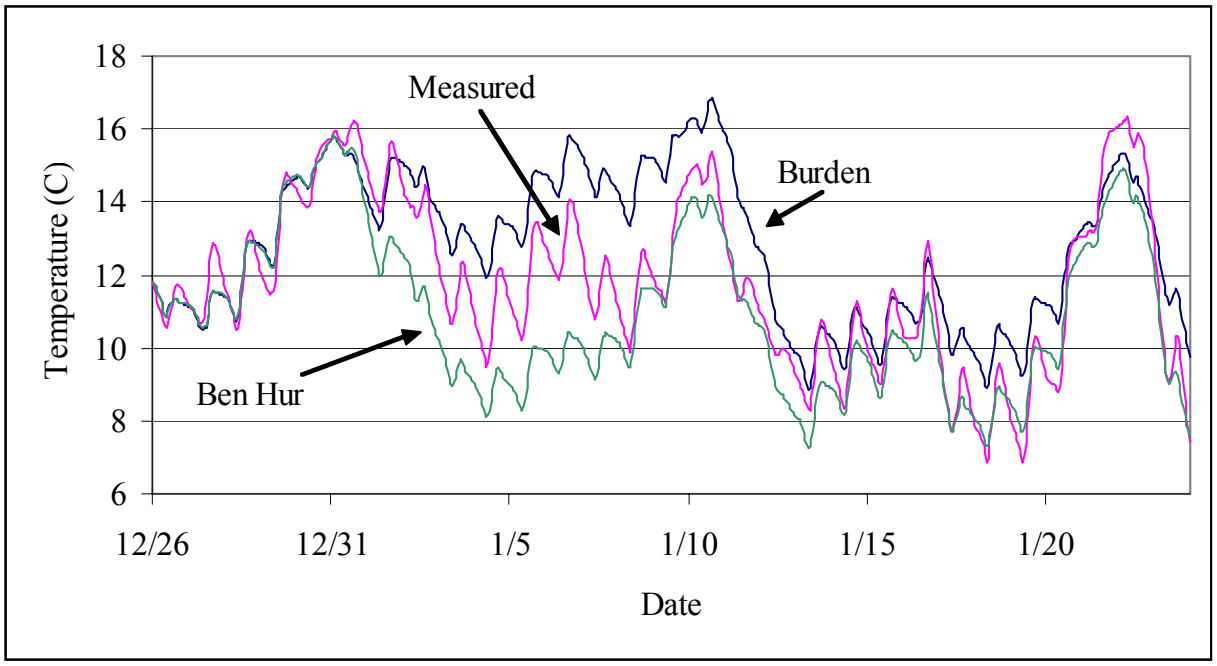

Figure 4.17: These are the results for the model runs for Pond 13 between December 25th, 2002 and January 24th, 2003. The Ben Hur curve shows how the model under predicted the pond temperature with data from the Ben Hur Weather Station. The Burden curve, generated with the relative humidity data from the Burden Weather Station, over -predicts the measured pond temperature.

suspect. Radiation readings at the Burden Station were lower than those at Ben Hur. For instance, for the month of January, 2003, Ben Hur Station radiation measurements were 20W greater than Burden Station radiation measurements (standard deviation = 53W). Running PHATR for the first Pond 13 model run (11/09/02 to 12/16/02) using Burden Station weather data yielded an average bias of 1.6°C (standard deviation =1.06°C) as opposed to an average bias of 1.6°C obtained for Ben Hur weather data. For the second Pond 13 model run (12/26/02 to 01/24/03), the average bias was 0.1°C (standard deviation 1.1°C) as opposed to an average bias of 1.0°C using Ben Hur weather data. These results suggest that input data did have an effect on how well PHATR predicted pond temperature.

The equation used by PHATR to estimate longwave sky radiation assumes that the sky is cloudless and the atmosphere can be considered as stratified layers of different gas mixtures. If this was not the case (because of turbulence from a weather front), then the underlying assumptions used by Bliss (1961) to develop Equation 3.26 (the equation used to determine the sky's emissivity) were no longer valid. For the present case, Equation 3.26 was not necessarily accurate. A pyrgeometer would have to be used to directly measure long wave sky radiation.

- PHATR was underestimating energy losses, probably because the evaporation rate was being underestimated. Evaporation, on average, accounted for 12% of all energy in transit for the spring model runs and 5% of all energy in transit in the fall. However, evaporation's importance was as high as 30% (see Figure 4.7). Equation 3.71, the Lake Hefner Equation, was designed to predict the daily evaporation over a lake using the daily average wind speed (actually, the units for wind speed used in the original reference by Anonymous, 1952, are miles per day). This same equation might not have been as accurate when predicting instantaneous or hourly evaporation rates.

  For natural systems, the importance of air convection and soil conduction was between 2 and 6% (see Figures 4.7 and 4.8). Because the temperature gradient between the pond and its environment, the driving force behind both heat transfer mechanisms, was small, these vectors were not as important as radiation energy transfer mechanisms (for instance, the average importance for long wave sky radiation ranged from 28% to 35%; see Figures 4.5 and 4.6). Therefore, even if both these vectors were not properly estimated, the weight of their errors was small and should not be used to explain PHATR's tendency to over-predict pond temperature.

- PHATR might not have been taking into account other energy transfer mechanisms. Such mechanisms could have been scattered solar radiation which was reflected out of the pond. Light, usually greenish light, was poorly absorbed by phytoplankton and water. Green light (average wavelength at 550 nm, Smith and Cooper, 1957) represented 12% of the total solar radiation (see Table 3.2) or 6% of all energy fluxes into and out of the pond when the importance of solar radiation was at its peak (49% Pond 6 and 7; see

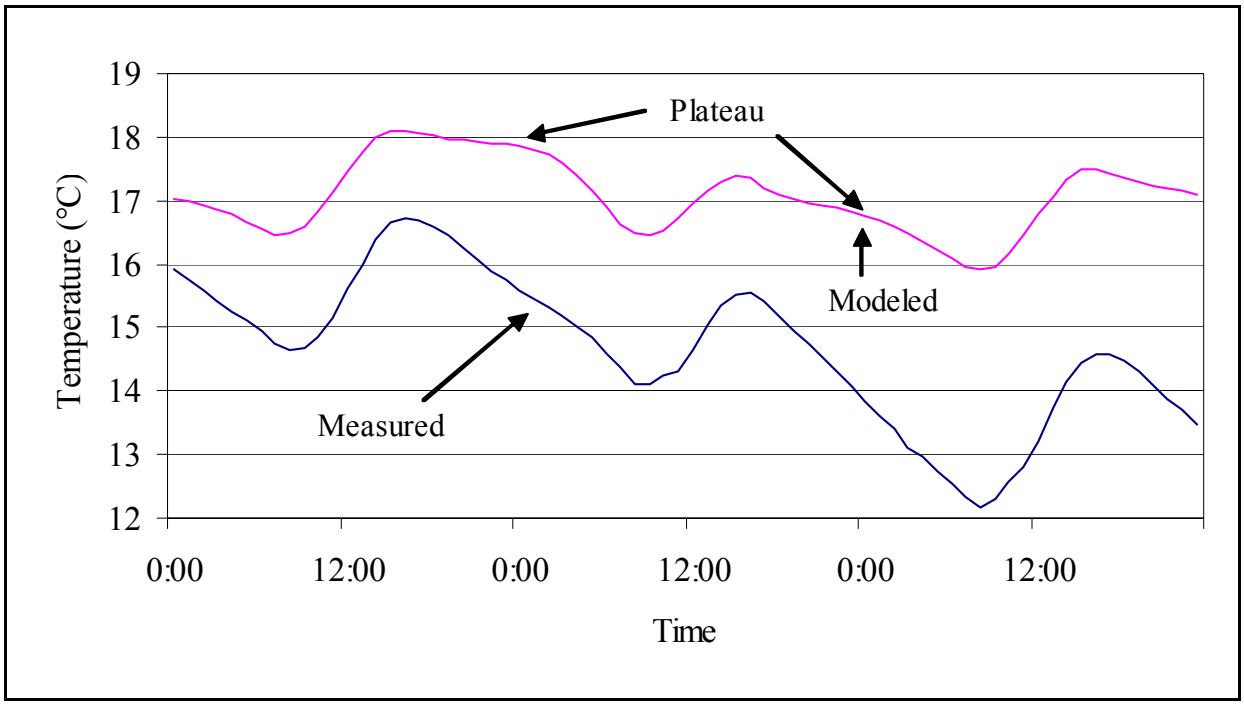

Figure 4.18: In addition to over-predicting the actual pond temperature, the modeled curve has a smaller amplitude and has plateaus. The smaller amplitude could be caused by an under-estimating the pond volume. The plateaus were caused by not properly modeling soil conduction. This is part of the first Pond 13 model run, between November 21 and 23, 2003.

Figure 4.5). Assuming that the pond was absorbing all solar radiation, PHATR would over-predict the pond temperature. Running PHATR for Pond 13 between 11/13/02 and 12/16/02 with modified solar radiation data (88% of the total measured solar radiation data) yielded better results (average bias = 0.9°C; standard deviation = 1.0°C).

In addition to the differences in bias, there were other differences between the modeled and measured results. For instance, the diurnal fluctuations in the measured data were greater than those in the modeled data. This difference, seen in Figure 4.18, was explained with the following two reasons. First, the thermal mass of Pond 13 may have been over-estimated (there may have been less water in pond than estimated). Mathematically, this makes sense. Assuming the pond temperature was a sinusoidal function of time (f(t)), the energy in the pond at any given time was (E = 0 when T = 0˚C)

$$E = \rho \forall c_p T = kf(t) \tag{4.9}$$

where E is the pond energy
f(t) is a sinusoidal function of time
ρ is the density of water
∀ is the pond volume
c_p is the specific heat of water

T is the pond temperature
k is a constant

Isolating T yielded:

$$T = \frac{k}{\rho c_p \forall} f(t) \tag{4.10}$$

where $(k/\rho c_p \forall)$ is the amplitude of f(t).

If the pond volume was overestimated, the amplitude of the modeled temperature function (f(t)) would be smaller, as was the case in Figure 4.18.

The amplitude of the measured and modeled temperature curves may also have differed because of the choice of location to measure the standard pond reference temperature. Although the reference temperature was measured 10 cm from the surface, the temperature in the bulk fluid and at the surface were visibly similar to each other (see Figure 4.19). For this reason, it was not likely that the location where the reference temperature was measured was the cause for the different amplitudes between the two curves.

The shape of the measured and modeled curves was also different. A small "plateau", not

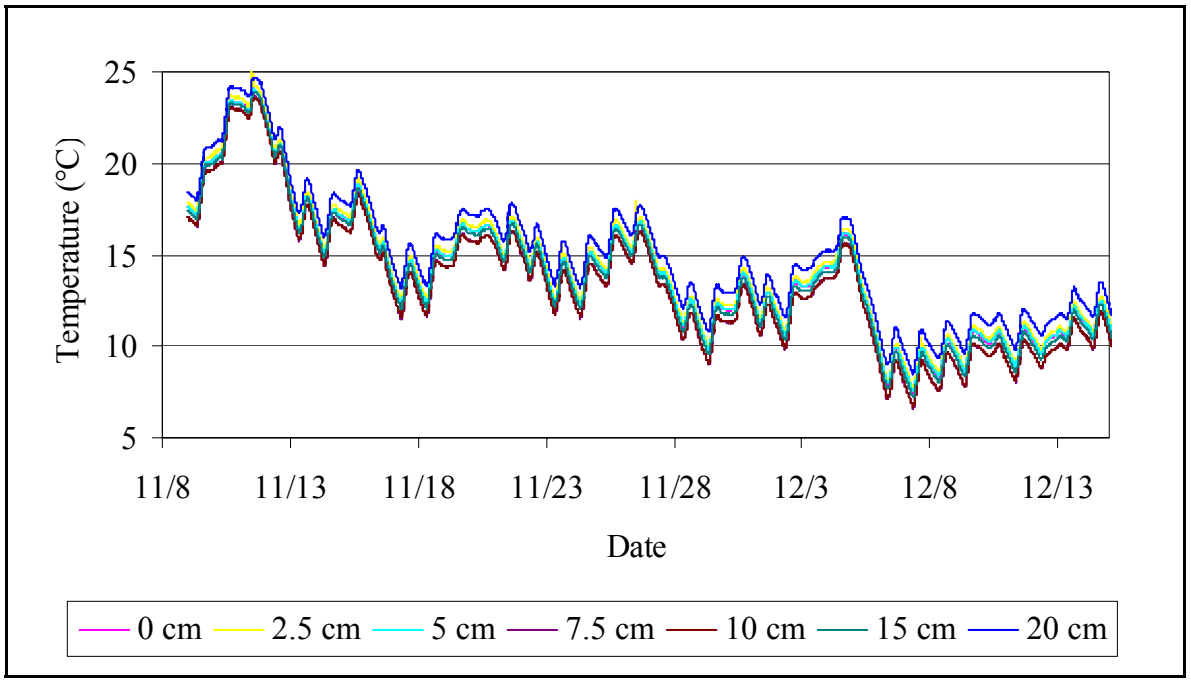

Figure 4.19: These are the measured temperatures curves for Pond 13 between November 9 and December 16, 2002. The top most curve is the pond temperature 20 cm below the water surface. Many of the curves are super-imposed over each other, meaning that the pond was well mixed. Because of this, the temperature at any depth can be used as a reference to compare model runs.

present in the measured curve, was present in the modeled curve each time the temperature decreased (see Figures 18 and 20). Closer examination revealed that these changes in slope occurred each night at the same time. This change in slope was caused by not properly modeling soil conduction. The daily phase angle (see Equation 3.41) which shifted the conduction curve in Figure 20 caused the pond temperature to decrease just as the heat transfer due to soil conduction reaches its peak. Without taking into account the effects of soil heat transfer, the average bias for Pond 13 between 11/09/02 and 12/16/02 was 1.37 °C (standard deviation = 1.0°C ; r = 0.96). Therefore, using a phase angle of $\pi/2$ was not proper. Because there was no change in slope for the measured curve while the temperature dropped (i.e. there did not seem to be a lag between the soil surface maximum temperature and the pond maximum temperature), the daily phase angle should be based on the time when the daily pond temperature maximum occurred. The maximum pond temperature normally occurred between 14:00 and 17:00. Assuming that the maximum occurs at 16:00, the daily phase angle is $-5\pi/6$ (see Appendix 5).

Energy transfer mechanisms which were important to uncontrolled ponds were dominated by radiation heat transfer mechanisms. Figures 4.5 and 4.6 reveal that the average importance of pond radiation, longwave sky radiation and solar radiation ranged between 15 and 54%, depending on the time of day and year. Solar and longwave sky radiation were therefore the two most important influxes of energy for unheated ponds while pond radiation was the greatest source of heat loss. Evaporation also seemed to be important (range: 0 to 30%) although its

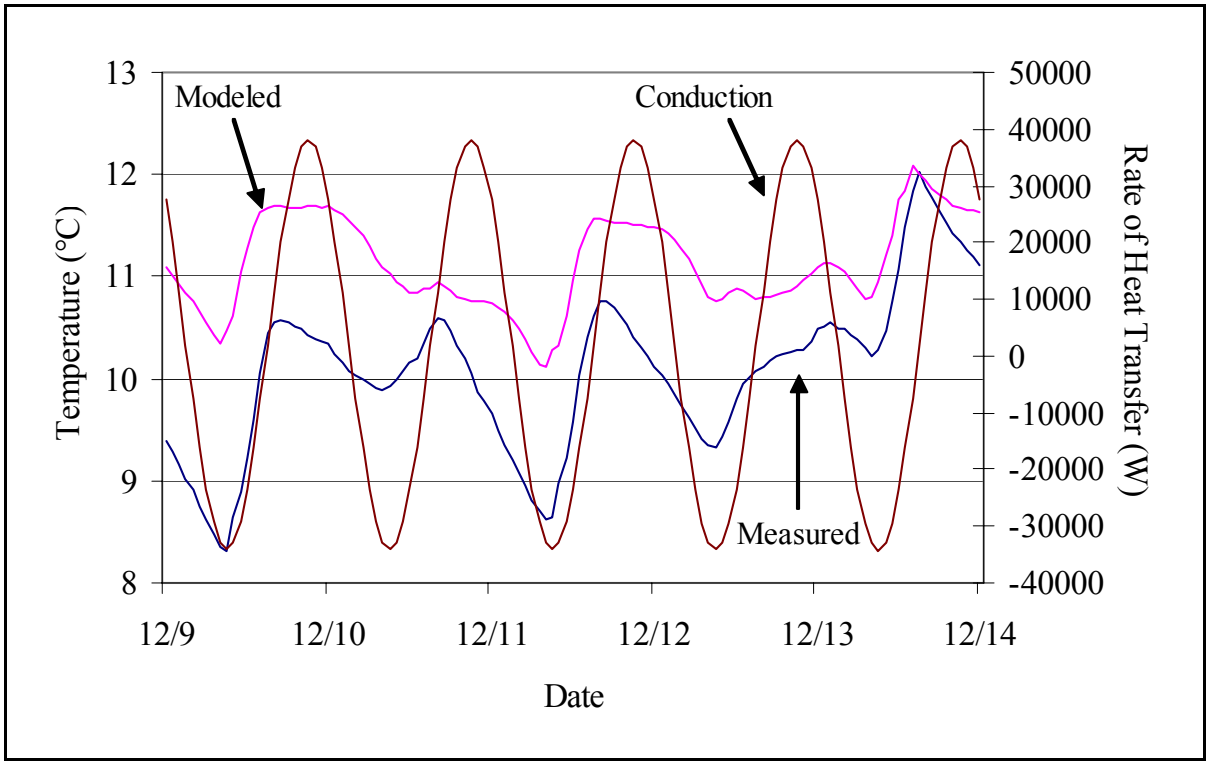

Figure 4.20: The sinusoid curve is the modeled conduction curve. As conduction begins to decrease, the modeled curve drops. There are no plateaus in the measured pond curve, which means the conduction curve is out of phase.

average importance was small (4% to 13%) compared to the radiation heat transfer mechanisms. Air convection (average importance = 4% to 6%) and soil conduction (average importance = 2% to 6%) were not as important because the temperature difference which drove these heat transfer mechanisms was relatively small.

4.5.2 Accuracy - Heated Ponds

The average bias for heated pond model runs was 2.4°C (standard deviation = 1.25°C), higher than the average bias for unheated pond model runs 0.5°C (standard deviation = 0.99°C). In particular, the average bias for the Pond 3 model run, a model run for the same time period as the heated pond model runs, was 0.2 °C (standard deviation = 2.0°C). There are four possible reasons for this:

1) The importance of surface convection and evaporation was greater for heated ponds because of the greater temperature gradient between the pond and the air. Both sets of equations used by PHATR to predict the size of both surface energy vectors were empirical and might not have been accurate when they dominated other modes of energy transfer. This happened at night or on cloudy days when there was little solar radiation and no bulk movements of energy associated with water flows. For instance, on the 22nd of February, 2003, the average importance of evaporation between 11:00 and 16:00 was 26% while the average importance of solar radiation was 16% (a cloudy day). During this period of time, the measured temperature declined at a faster rate than the modeled temperature, causing the bias to increase from 0.3°C to 1.5°C (see Figure 4.21). This might have been caused by the evaporation being under-estimated by the model.

2) The flow of water into and out of the pond varied from the estimated flows used by PHATR. The method used to measure the flow rate of warm water assumed that for a given combination of open and closed valves along the water line, a fixed flowrate would result. However, this was apparently not the case. For the evening of February 22nd, 2003, the well was turned on at 17:00 and according to the recorded data, all four valves were open. Normally, water would flow to all four controlled ponds, including pond 12. However, the rate of decline for the measured temperature curve at 17:00 did not change. Rather, the pond only began to warm at 20:00, when one of the valves at another pond closed. The bias, by this time, had increased from 1.5 to 3.8°C. Apparently, no water flowed into pond 12, despite the open valve.

3) The method used to measure the flowrate might have had a large measurement error. The flow rate was measured by timing the period it took to fill a 120-liter bucket with 100 liters of water. The measurement has an accuracy of ±1 second. When only one valve was open, measuring the flow rate took 5 seconds. This translated into a possible relative error of 17 to 24% when estimating the bulk energy flow rate (see Table 4.6).

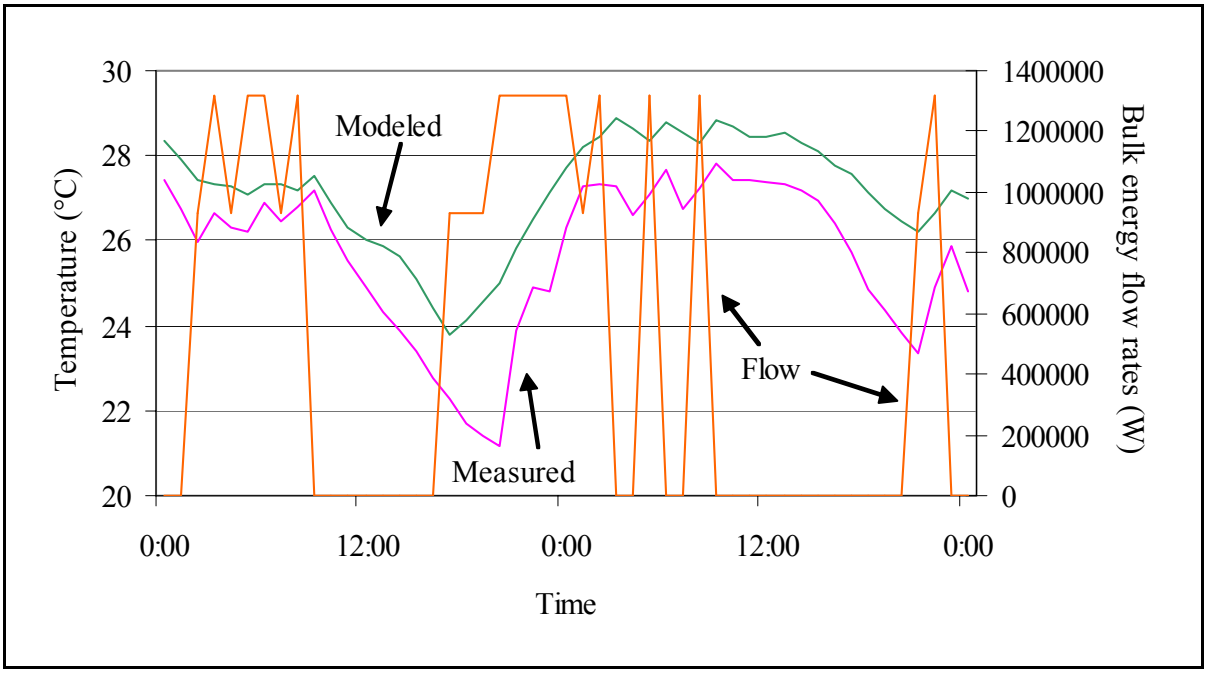

Figure 4.21: This data represents the pond temperature and warm water flow for Pond 12 on February 22 and February 23, 2003. During the first afternoon, the measured pond temperature decreased faster than the modeled pond temperature, revealing that evaporation might be underestimated. At 17:00 on the first afternoon, warm water supposedly flowed into the pond. However, the pond temperature only began to rise at 20:00, when a valve on another pond closed. This means that water only began to flow into Pond 12 at 20:00, not at 17:00. As can be seen, PHATR's accuracy is dependant on the quality of the collected data and the validity of its equations.

Table 4.6: If 5 seconds were measured to fill a 120 liter bucket when it really took 4, PHATR under-estimated the energy flow rate by 25% . If it really took 6 seconds to fill the bucket, the model over-predicted the bulk energy flow rate by 17%.

Time (s)	Flow rate (m^3/s)	Bulk Energy Flowrate (W)	Relative Error
4	0.026	988693	25%
5	0.021	790954	---
6	0.018	659128	17%

The implications of such errors in measurements can be grasped through a numerical example. Consider Pond 12 (volume = 342 m^3) at night (no solar radiation) with warm

effluent water flowing in at 36°C and flowing out at 27°C. Water losses due to evaporation were negligible so the flow rates into and out of the pond were the same. Energy losses due to surface evaporation, air convection and soil conduction were small (on average, these energy vectors together represented no more than 17% of the total energy flux in the absence of bulk fluid, and represented much less when there was warm water entering the pond). Pond radiation and sky radiation were balanced. By performing an energy balance for this example, Equation 3.4 reduces to:

$$\frac{dE}{dt} = q_{well} - q_{out} \tag{4.11}$$

or

$$\rho c_p \forall_{pond} \frac{dT}{dt} = \rho c_p \dot{\forall}_{flow} \left(T_{well} - T \right) \tag{4.12}$$

where E is the internal energy of the pond,
ρ is the density of water,
c_p is the specific heat of water,
$\forall_{pond}$ is the volume of the pond,
T is the temperature of the pond,
t is time,
$\dot{\forall}_{flow}$ is the flow rate of warm water into the pond
T_{well} is the temperature of the warm water (36°C).

For a flow rate of 0.018 m^3/s, the rate at which the pond heats up (dT/dt) is 1.7°C/hr. For a flow rate of 0.026 m^3/s, the rate at which the pond heats up is 2.5°C/hr, a difference (bias) of 0.8°C/hr. Consequently, errors in flow measurements can have an effect on the model's bias, especially if there is more water flowing than estimated.

4) The time step was too large. Unlike other energy transfer mechanisms, the flow of warm water was a discrete-event energy transfer vector (i.e. bulk energy flow rates changed within seconds). Because of this, modeling with large time steps was not appropriate. For example, if a valve were to open 50 minutes before the X:00, and PHATR was using data sampled every hour (X:00), PHATR would have ignored the effects of heating the pond 50 minutes prior to that hour reading. Similarly, if a valve were to close one minute after the hour, PHATR would wrongly have assumed that the valve was open for the next 59 minutes. This affected the bias (which can increase or decrease, depending on the situation) but more importantly, this affected the model's ability to predict change (reflected in the correlation coefficient). The correlation coefficient decreased from 0.92 (step size = 1 hour) to 0.83 (step size = 4 hours) to 0.70 (step size = 6 hours).

Because the movement of water was an important energy vector(as important as 60%), most errors in the model's output were caused by poorly estimating flow. To fully understand the importance of bulk water movements to the energy balance, consider and compare the size of these energy vectors with solar radiation. On a clear sunny day in summer, solar power may be as high as 1000 W/m^2. For Pond 12, with an area of 280 m^2, this represented a heat transfer rate of 280 kW. To produce the same net energy flux with bulk flow, the flow rate must be 451 liters per minute (119 gpm), assuming the well water is 36°C and the discharged water is 27°C. This flow rate is moderately high. So for the purposes of comparison, warm water flow can be considered as a night time substitute for sunlight. Flow is as important an energy transfer mechanism as sunlight and by failing to properly estimate flow, PHATR's accuracy suffers.

4.5.3 Stability Analysis - Unheated Ponds

The average bias for a model run using a step size of 6 hours was 1.5°C while the average bias for a model run using a step size of 10 minutes was also 1.5°C (see Figure 4.12). For a 12 hour step size, the average bias was 6.2 °C. Only when using a step size of 24 hours was the average bias negative (-2.1°C). This was because the solar radiation in the input weather data, sampled at midnight, was always 0 W/m^2. The model's ability to predict change was reflected in the correlation coefficients, ranging from 0.96 for a step size of 10 minutes to 0.92 for a step size of 6 hours (see Figure 4.13). Only for a step size of 12 hours was the correlation coefficient below 0.90 (0.62).

In spite of the presented data, using a step size of 6 hours to run PHATR was not recommended. By using a step size of 6 hours, the output lost detail. The average bias between two model runs, step sizes = 6 hours and 1 hour, is 0.7°C (standard deviation = 0.6°C). The average bias between two model runs, step size = 10 minutes and 1 hour, was 0.1°C (standard deviation = 0.1°C). Therefore, a step size of 1 hour should have been suitable in maintaining a fair amount of detail in the output.

4.5.4 Stability Analysis - Heated Ponds

Increasing the step size had no effect on decreasing the average bias. The average bias for a model run with a 10 minute step size was 2.7°C while a model run with a step size of 6 hours had a bias of 2.4°C (see Figure 4.14). However, the standard deviation never exceeded 1.2°C for step sizes 30 minutes or less. Smaller step sizes minimized the error associated with miscalculating the flow of warm water and energy entering a pond. PHATR's ability to predict change improved by using smaller step sizes ($r_{4\ hour} = 0.83$, $r_{10\ min} = 0.95$; see Figure 4.15). Therefore, because of the discrete nature of bulk energy fluxes, the model's ability to predict temperature changes in heated ponds depended on a small step size. For heated ponds, a step size of 10 or 30 minutes was appropriate.

4.5.5 Improvements to the Software

Because PHATR version 1.0 was a prototype model, certain modifications were made to the program to make it easier to use. PHATR's output had to be more user-friendly, and later versions of the model must include the following improvements:

- Using conventional methods of measuring time. Although using seconds as a time unit for numerical methods was necessary, input and output data should be labeled time, month/day/year (ex: x:xx, x/x/200x). For instance, it is difficult to compare results for the 7869600th second of the year to weather data recorded on the 2nd of April, at 2:00. PHATR should also be able to recognize the step size from these time labels in the input data.

- Calculating and printing the relative importance of each energy vector at every time step. This would save time during the analysis of results.

- Calculating and printing the 3 performance statistics, in order to save time during analysis. However, the user would be required to supply PHATR with measured pond data so that comparisons between modeled and measured data can be made.

- Separating data in the output with commas, not tabs. The current version of PHATR used spaces to separate datum on the same line. However, when converting the output ASCII file into a spreadsheet file, negative signs in the data were sometimes misplaced. For instance, two data, 5.67 and -6.32, are written to the output file as "5.67 [space] -6.23" by PHATR. The spreadsheet converts this to "5.67-" and "6.23". To solve this problem, the data should be separated with commas.

- Modeling the effects of more than one source of inlet water. This would be useful when modeling ponds using both warm and cool water during within a given time period.

- Shortening the existing programming code. There is a lot of useless programming code in this first version. A simpler code would be easier to fix and modify to suit the needs of other users.

4.6 Conclusions

An initial computer model (PHATR version1.0) using the Runge-Kutta 4th order numerical method to solve Equation 3.4 was written. Initial model runs indicated that PHATR over-predicted pond temperature. On average, for both heated and unheated ponds, the model was good a predicting temperature changes (r_{avg} = 0.94 for unheated ponds, r_{avg} = 0.87 for heated ponds) but can be improved by studying the following points and possibly correcting the model accordingly:

- the effects of light being reflected at the pond surface (when the sun is low in the sky) and the extinction of light in the pond water
- the true rate of evaporation and surface convection for this particular set of ponds
- the thermal properties of the pond soil

Major vectors of energy transfer for unheated ponds were found to be radiation heat transfer mechanisms (Figure 4.22). For heated ponds, bulk energy flow rates were also important. Surface convection and evaporation were important when there was no solar radiation or water flowing into the pond (Figure 4.23). The modeled heat conducted through the soil had a negative effect on PHATR's ability to predict change. An appropriate step size for unheated pond model runs was found to be 1 hour. An appropriate step size for heated pond model runs was found to be 10 to 30 minutes.

Improvements to the software were recommended to simplify analysis of the output data.

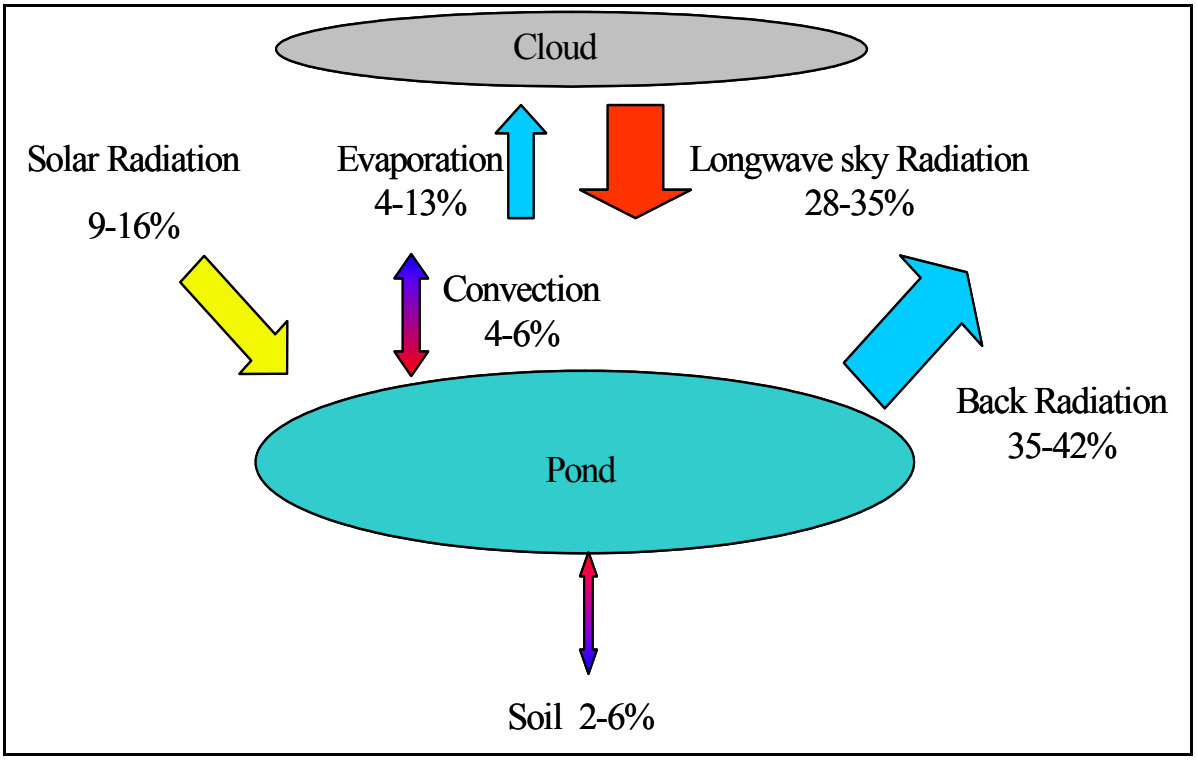

Figure 4.22: An energy balance for unheated ponds was performed during the fall of 2002 and spring 2002 - 2003 in Baton Rouge, Louisiana. The average relative importance of each energy vector is shown. For unheated ponds, longwave radiation mechanisms were more important. The importance of solar radiation during the day was found to be as high as 55%.

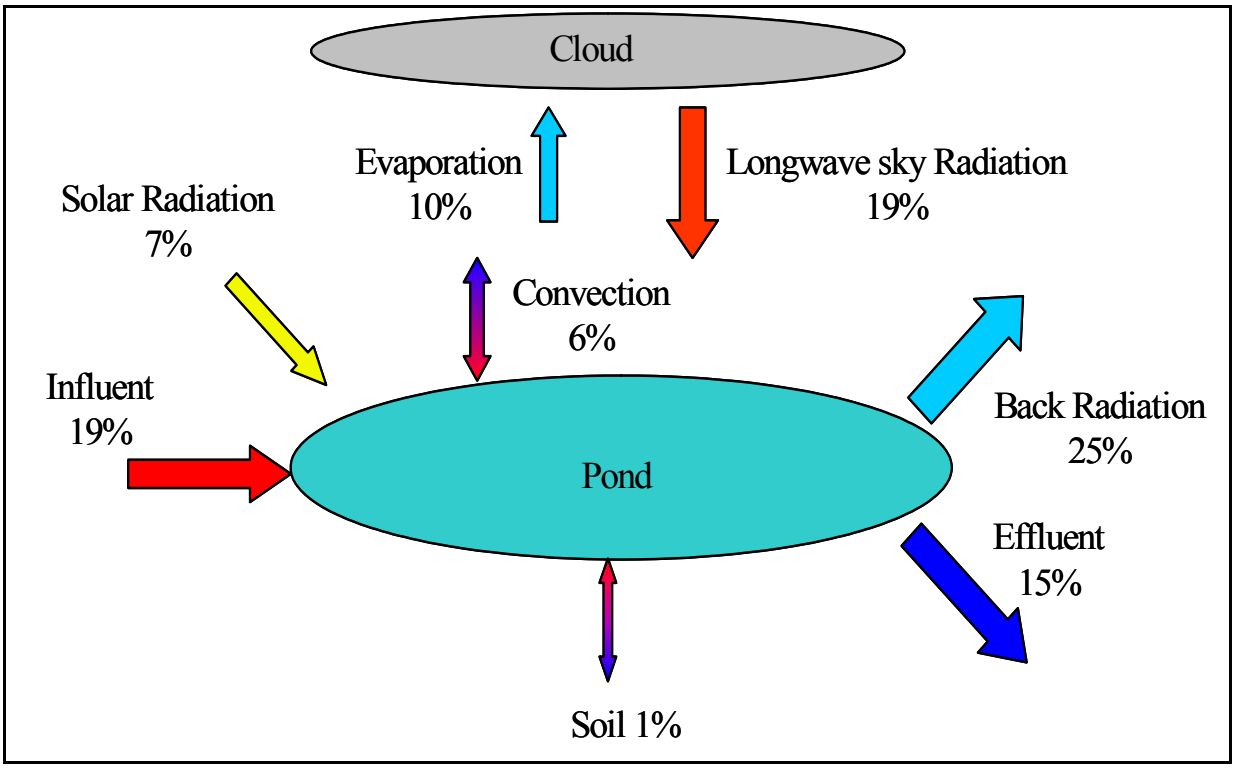

Figure 4.23: an energy balance for heated ponds was performed during the spring of 2003 in Baton Rouge, Louisiana. The average relative importance for each energy vector is shown. In addition to longwave radiation, water entering and leaving the pond represented important energy vectors. The importance of warm influent was as high as 60%. The importance of the effluent was as high as 44%. Solar radiation accounted for as much as 50% of all energy movements.

CHAPTER 5: THE EXPERIMENTAL DETERMINATION OF PARAMETERS IMPORTANT TO HEAT TRANSFER IN PONDS

5.1 Introduction

A computer model, PHATR (Pond Heating And Temperature Regulation), used to model energy balances for aquaculture ponds was developed in Chapter 4. Based on the findings from the previous chapter, parameters that could improve PHATR's accuracy were determined experimentally. These parameters were:

- the convection mass transfer (evaporation) coefficient, h_m
- the convection heat transfer coefficient at the pond surface, h
- the extinction coefficient of the pond, β
- the albedo of the pond

Because heat conducted through the soil was less important compared to other energy transfer mechanisms, soil thermal properties were not determined. Each of these parameters were determined either through field experiments or by analysis of existing data.

5.2 Theory

5.2.1 The Heat and Mass Transfer Coefficients

Two approaches were used to determine the heat and mass transfer coefficients. The first consisted of using the heat and mass transfer analogy (Incropera and De Witt, 1985) to find analytical values for the coefficients. The second consisted in comparing empirical equations found in the literature used to predict the evaporation and convection rates.

- Heat and mass transfer analogy: the heat and mass transfer analogy relies on the mathematical and physical similarities of heat and mass transfer at the pond surface. Both transport phenomena are controlled by the velocity (wind) boundary layer and both are governed by the same mathematical equation (the diffusion equation) with the same type of boundary conditions. Convection coefficients used in heat and mass transfer are determined using analogous empirical equations and, as is demonstrated in Appendix 6, can be related to one another with Equation 5.1:

$$h = h_m \rho_{air} c_{p-air} Le^{2/3} \tag{5.1}$$

where h is the convective heat transfer coefficient,
h_m is the convective mass transfer coefficient,
ρ_{air} is the density of dry air,
$c_{p\text{-}air}$ is the specific heat of air at a given moisture content and
Le is the Lewis number, a dimensionless ratio comparing the thermal diffusivity to the mass diffusivity.

•Comparison of empirical equations in the literature: The three empirical equations in the literature review used to predict evaporation (Chapter 3.5.2) were Equation 3.67 (Penman, 1948), Equation 3.70 (Piedrahita, 1991) and Equation 3.71 (Anonymous, 1952). The two empirical equations in the literature review used to predict heat convection (Chapter 3.4) were Equation 3.58 (Watmuff et al., 1977) and Equations 3.49 through 3.57 (Nusselt Number correlations; Holman, 1997). PHATR Version 1.0 used Equation 3.71 (the Lake Hefner Equation) to predict the rate of evaporation and Equation 3.58 to estimate the convection coefficient.

5.2.2 Extinction Coefficient

The extinction coefficient is the parameter that quantifies extinction of light in a medium (see Chapters 3.2.2.2 and 3.2.2.3). It can be estimated by manipulating the Bouger-Beer Law. Solving Equation 3.10 yields:

$$\ln q = \ln q_{solar} - \beta z \qquad (5.2)$$

where q is the radiation (W) at depth z (m or mm),
q_{solar} is the solar radiation (W) and
β is the extinction coefficient (m^{-1} or mm^{-1}).

By plotting the natural logarithm of solar radiation ($\ln q_{solar}$) versus the depth (z), the extinction coefficient can be determined by calculating the slope of the line of best fit.

5.2.3 Albedo

Table 3.3, based on Fresnel and Snell's Laws, shows that only a small percentage of solar radiation is reflected for angles of incidence greater than 60°(i.e. for angles of solar elevation less than 30° above the horizon). However, more solar radiation could be reflected back to the sky because of the effects of scattering. If most suspended particles are assumed to be free clay particles originally from the pond bottom, and if the size of a clay particles is defined as smaller than 2 μm in diameter, then, because visible solar radiation (poorly absorbed by pure water) have a wavelength of between 0.4 and 0.7 μm, a combination of Rayleigh scattering and "macro-scattering" (together known as Mie scattering) occur (Seigel,

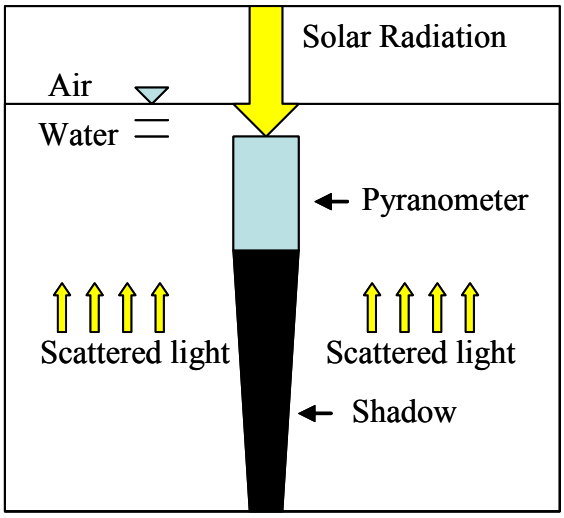

Figure 5.1: Measuring scattered radiation leaving the pond is difficult because of the shadow cast by the pyranometer (facing down in the diagram). Normally, solar radiation would contribute to the scattering. However, because the pyranometer blocking solar radiation, the solar radiation's contribution cannot be measured.

1981)**.** Mie scattering is difficult to predict and as a result, theoretical calculations can be inaccurate.

Measuring the back scattering of radiation is hampered by the shadow cast by a pyranometer (Figure 5.1). A pyranometer facing down and measuring the light traveling upwards will block the incident solar radiation traveling downward. A portion of the solar radiation would normally be reflected where the pyranometer is located. Unfortunately, this cannot happen because the pyranometer is blocking the path of solar radiation. Therefore, to estimate the albedo, it was necessary to calculate this value with an indirect method.

5.3 Materials and Methods

5.3.1 The Heat and Mass Transfer Coefficients - Heat and Mass Transfer Analogy

A modified version of PHATR (Version 1.1) was used to generate heat and mass transfer coefficients by solving for h_m, the evaporation mass transfer coefficient, in Equation 3.4:

$$h_m = \frac{\left(\frac{dE}{dt}\right)_{pond} - \left(q_{solar} - q_{back} + q_{sky} \pm q_{soil} - q_{seep} + q_{rain} + q_{well} - q_{out}\right)}{A\left(Le^{2/3}\rho_{air}c_{p-air}\left(T_{air} - T_{pond}\right) - h_{fg}\frac{MM}{R}\left(\left(\frac{P}{T}\right)_{surface} - \left(\frac{P}{T}\right)_{air}\right)\right)} \qquad (5.3)$$

Subsequently, Equation 5.1 was used to determine h, the convective heat transfer coefficient. The derivation of Equation 5.3 is provided in Appendix 7. Model runs for PHATR version 1.1 were based on input data collected at Pond 13 between November 9th and December 16th, 2002. Weather data, pond temperature data and flow rate data collected at night were used. Unlike version 1.0, Version 1.1 used the pond temperature to estimate the rate of internal energy change in the pond. By using data collected only at night in an unheated pond, the solar radiation term and the bulk energy flow rate terms in Equation 5.3 were equal to 0.

Once values for the mass transfer coefficients were generated, a relationship between both parameters and the wind speed was developed.

5.3.2 The Heat and Mass Transfer Coefficients - Comparison of Empirical Equations

An other modified version of PHATR, Version 1.2, was used to determine if certain combinations of empirical equations for evaporative and convective energy transfer could improve accuracy. Input data consisted of weather and flow rate data collected during February and March, 2003. The model output data was compared to the pond temperature data collected for Pond 3 (unheated) and Pond 12 (heated). The three criteria used in Chapter 4 (average bias between modeled and measured data, the standard deviation of the average bias and the correlation coefficient (r) between the modeled and measured data) were calculated again. Table

5.1 and Table 5.2 summarize information about each model run. Sixteen model runs were made, each using a different combination of empirical equations. Results using wind speed measurements taken at the water surface and 10 feet in the air were also compared.

5.3.3 Extinction Coefficient

A LI-COR LI-200 SZ pyranometer sensor (Lincoln, NE) was encased in a waterproof acrylic container. The container was glued to a 12 .7 mm PVC coupling (Figure 5.2). By fixing the coupling to a graduated PVC pipe, the solar radiation measurements were taken at depths of 0, 2.5, 5, 7.5, 10, 12.5, 15, 17.5, 20, 25, 30, 45, 60 and 90 cm near the aerator, in the middle of the the pond and at the standpipe (Figure 5.3). Measurements were taken from a boat to avoid suspending sediments from the pond bottom. Measurements were made on clear cloudless days as close to solar noon as possible (12:20 Central Standard Time in Baton Rouge) to minimize the effects of reflection at the water surface.

Figure 5.2: The pyranometer used to make solar radiation readings was encased in an acrylic water-tight container. It is connected to a graduated PVC pipe.

The pyranometer was connected to a Campbell 21X data logger to read the solar radiation measurements. The programming and the wiring between the data logger and the pyranometer are detailed in Appendix 8.

For each trial, the correlation coefficient was calculated to measure the strength of the linear relationship between the natural logarithm of the incident solar radiation (ln q_{sun}) and the depth at which the measurement was taken. The slope of the curve (the extinction coefficient) was calculated using linear regression models. The variability of the extinction coefficients among ponds was checked using proc Mixed in SAS.

(a) (b) (c)

Figure 5.3: Solar radiation readings were taken from a boat to avoid disturbing soil sediments (a). Solar radiation was measured above (b) and below (c) the water at different depths using a graduated PVC pipe.

Table 5.1: This is miscellanious information about the model runs used in Chapter 5 to compare empirical equations

Pond	Trials	Step size	Start time	Stop time	Notes
3	1 to 8	1 hour	2/18/03; 24:00	3/22/03; 24:00	Unheated
12	9 to 16	10 min	2/11/03; 24:00	3/22/03; 24:00	Heated

Table 5.2: Characteristics for each model run for the comparison of empirical equations are presented here.

Trial	Pond	Location of Wind	Formula		Version of PHATR
		Speed Measurement	Evaporation	Convection	
1	3	Surface	Penman (1948)	Watmuff et al. (1977)	1.2a
2	3	Surface	Peiedrahita (1991)	Watmuff et al. (1977)	1.2b
3	3	Surface	Lake Hefner (1952)	Watmuff et al. (1977)	1.2
4	3	Surface	Lake Hefner (1952)	Nusselt correlations	1.2c
5	3	3 m above the surface	Penman (1948)	Watmuff et al. (1977)	1.2a
6	3	3 m above the surface	Peiedrahita (1991)	Watmuff et al. (1977)	1.2b
7	3	3 m above the surface	Lake Hefner (1952)	Watmuff et al. (1977)	1.2
8	3	3 m above the surface	Lake Hefner (1952)	Nusselt correlations	1.2c
9	12	Surface	Penman (1948)	Watmuff et al. (1977)	1.2a
10	12	Surface	Peiedrahita (1991)	Watmuff et al. (1977)	1.2b
11	12	Surface	Lake Hefner (1952)	Watmuff et al. (1977)	1.2
12	12	Surface	Lake Hefner (1952)	Nusselt correlations	1.2c
13	12	3 m above the surface	Penman (1948)	Watmuff et al. (1977)	1.2a
14	12	3 m above the surface	Peiedrahita (1991)	Watmuff et al. (1977)	1.2b
15	12	3 m above the surface	Lake Hefner (1952)	Watmuff et al. (1977)	1.2
16	12	3 m above the surface	Lake Hefner (1952)	Nusselt correlations	1.2c

5.3.4 The Albedo

Two modified versions of PHATR (Versions 1.21 and 1.21a) were used to determine the albedo of the pond empirically. These versions prompt the user for albedo values. The model recalculates the pond temperature, taking the albedo into account. Albedos of 0%, 5%, 10%, 15%, 20% and 25% were incorporated into model runs. The three statistical criteria previously used (average bias between modeled and measured data, the standard deviation of the average bias and the correlation coefficient between the modeled and measured data) were again calculated here. The time step for model runs for Pond 3 and Pond 13 was 1 hour and for Pond 12, 10 minutes.

5.4 Results

5.4.1 Heat and Mass Transfer Coefficients - The Heat and Mass Transfer Analogy

Statistical parameters reflecting the results are shown in Table 5.3 Full model run results are presented graphically in the form of a scatter plot (wind speed vs heat/mass transfer coefficient in Figures 5.4 and 5.5).

Table 5.3: These are statistical parameters describing the accuracy of results from the heat and mass transfer analogy method. h is the heat transfer coefficient and h_m is the convective mass transfer coefficient.

Parameter	h ($W/m^2/K$)	h_m (m/s)
Average	27	0.0107
Maximum	15146	0.5959
Minimum	-12515	-1.5029
Standard deviation	597	0.0753
Standard deviation x 2	1195	0.1507
Correlation Coefficient - r	0.003	0.02934

5.4.2 Heat and Mass Transfer Coefficients - Comparison of Empirical Equations

The statistical parameters used for comparing the output from PHATR Version 1.2 trials are presented in Table 5.4. An example of the model's output is graphically presented in Figure 5.6.

5.4.3 Extinction Coefficient

Figure 5.7 is an example plot comparing the natural logarithm of incident solar radiation to the depth at which the measurement was taken. The slope of the line of best fit represents the extinction coefficient. Values for the correlation coefficient (r) and the slope of the line (the extinction coefficient) are presented in Table 5.5. The average correlation coefficient is -0.96,

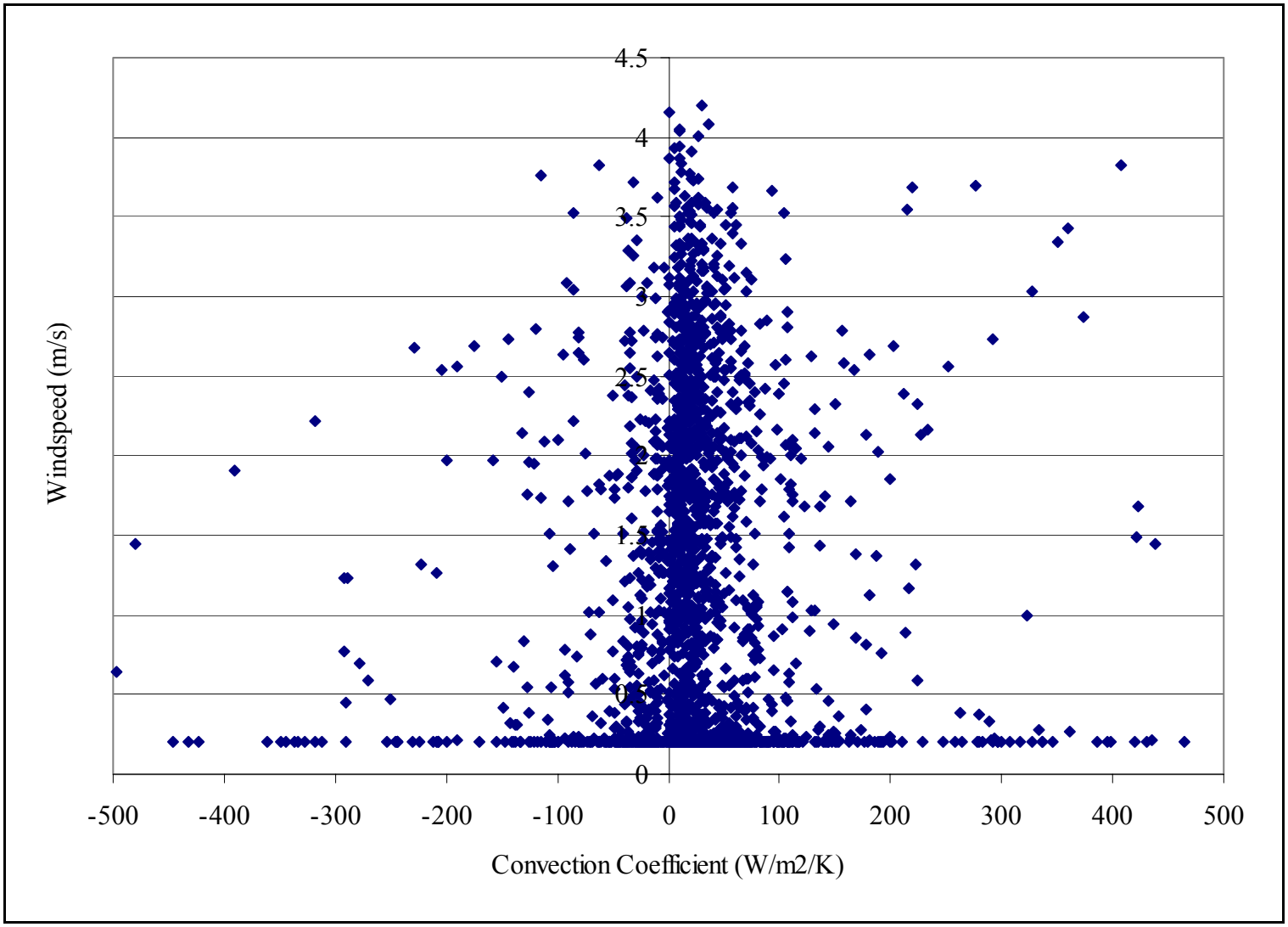

Figure 5.4: Results PHATR Version 1.1 produced negative heat transfer coefficients. The heat transfer coefficient must always be positive. Negative-valued resulted from calculations using pond temperature data, not measured accurately enough to be used for this experiment.

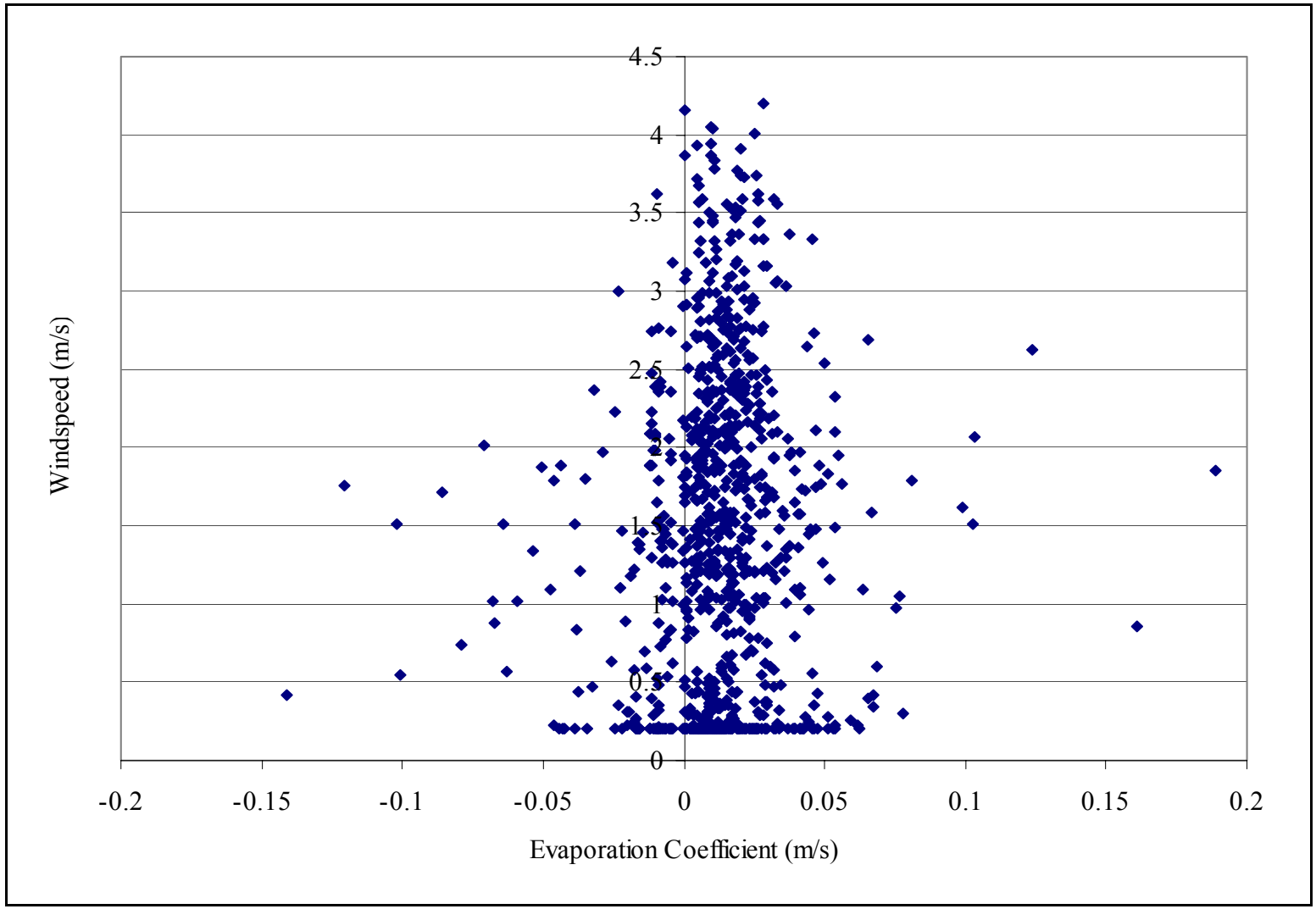

Figure 5.5 PHATR Version 1.1 produced negative evaporation coefficients. The evaporation coefficient cannot be negative. Negative-valued results resulted from calculations using pond temperature data, measured not accurately enough to be used in this experiment.

Table 5.4: These are the characteristics and results for each model run for the comparison of empirical evaporation and convection equations. The bias represents the average difference between the model and the measured data. The standard deviation (St. Dev.) and the correlation coefficient (r) between the modeled and measured data are indicators of the model's ability to predict change (see Chapter 4).

Trial	Pond Number	Pond Treatment	Location of wind speed measurment	Formula		Statistics		
				Evaporation	Convection	Bias	St. Dev.	r
1	3	Unheated	surface	Penman (1948)	Watmuff et al. (1997)	-4.5	2.2	0.85
2	3	Unheated	surface	Piedrahita (1991)	Watmuff et al. (1997)	-4.4	2.2	0.85
3	3	Unheated	surface	Lake Hefner	Watmuff et al. (1997)	-4.3	2.2	0.86
4	3	Unheated	surface	Lake Hefner	Nusselt numbers	-4.6	2.3	0.85
5	3	Unheated	3 m above the surface	Penman (1948)	Watmuff et al. (1997)	-0.7	1.8	0.96
6	3	Unheated	3 m above the surface	Piedrahita (1991)	Watmuff et al. (1997)	0.5	2.1	0.94
7	3	Unheated	3 m above the surface	Lake Hefner	Watmuff et al. (1997)	0.3	2.0	0.94
8	3	Unheated	3 m above the surface	Lake Hefner	Nusselt numbers	0.4	2.0	0.93
9	12	Heated	surface	Penman (1948)	Watmuff et al. (1997)	-5.5	2.7	0.60
10	12	Heated	surface	Piedrahita (1991)	Watmuff et al. (1997)	-5.3	2.8	0.59
11	12	Heated	surface	Lake Hefner	Watmuff et al. (1997)	-5.1	2.7	0.60
12	12	Heated	surface	Lake Hefner	Nusselt numbers	-5.1	2.7	0.61
13	12	Heated	3 m above the surface	Penman (1948)	Watmuff et al. (1997)	1.3	0.8	0.96
14	12	Heated	3 m above the surface	Piedrahita (1991)	Watmuff et al. (1997)	3.2	1.1	0.95
15	12	Heated	3 m above the surface	Lake Hefner	Watmuff et al. (1997)	2.9	1.0	0.95
16	12	Heated	3 m above the surface	Lake Hefner	Nusselt numbers	5.0	1.2	0.95

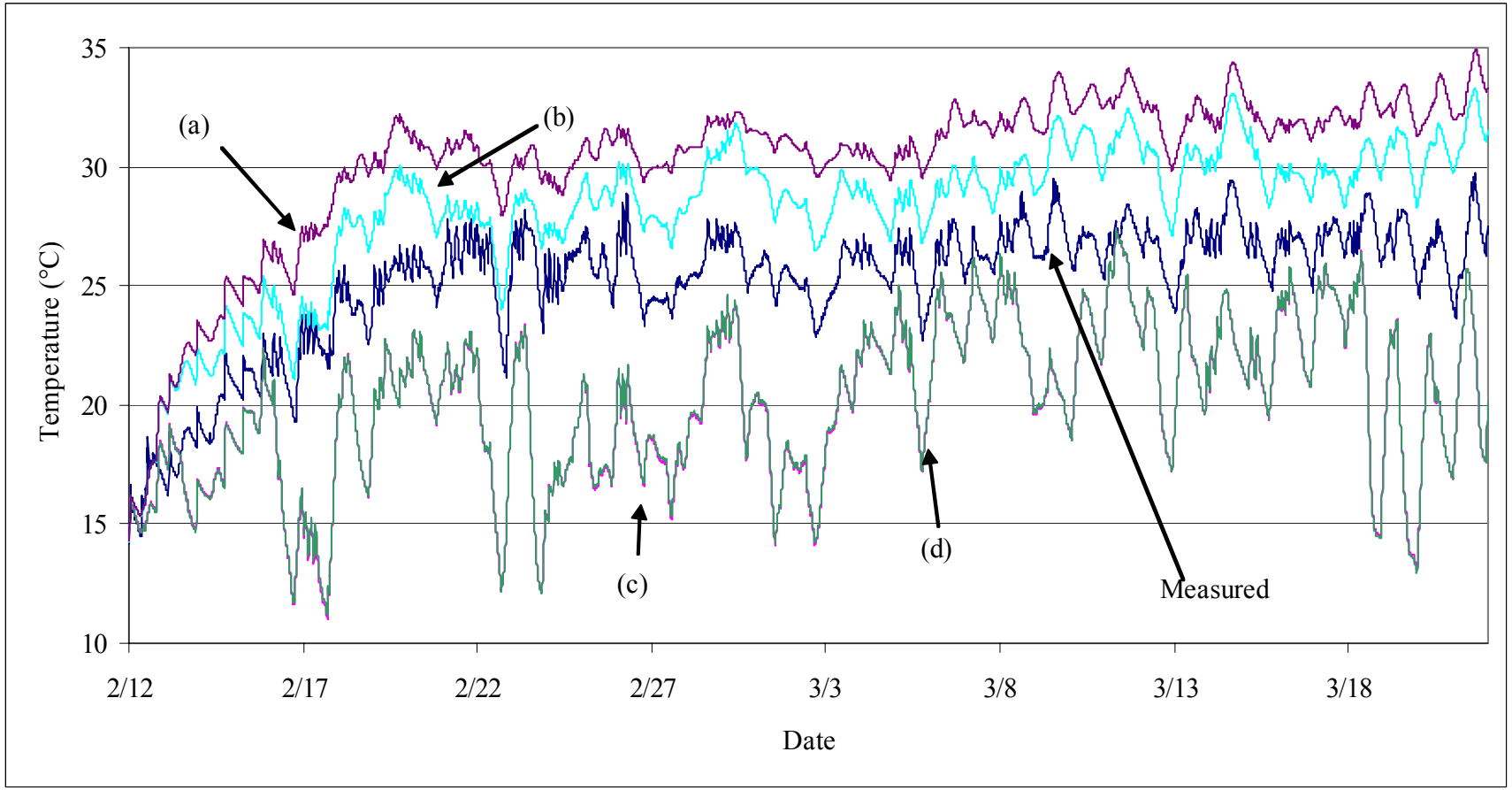

Figure 5.6: These are the temperature profiles for 4 model runs and the measured pond temperature in a heated Pond 12 between the 13th of February and the 23rd of March, 2003. The temperature curves were generated using (a) Nusselt Correlations (wind speed measured at 3 m), (b)Watmuff et al.'s (1977) Equation (wind speed measured at 10 feet), (c) Nusselt Correlation (wind speed measured at 33 cm) and (d) Watmuff et al's (1977) Equation (wind speed measured at 33 cm) for estimating convection. (Curves (c) and (d) are superimposed.) Using the wind speed measured at 33 cm caused PHATR to underestimate the pond temperature. This is because the equation used to correct the wind speed cannot be used for wind speeds at low elevations.

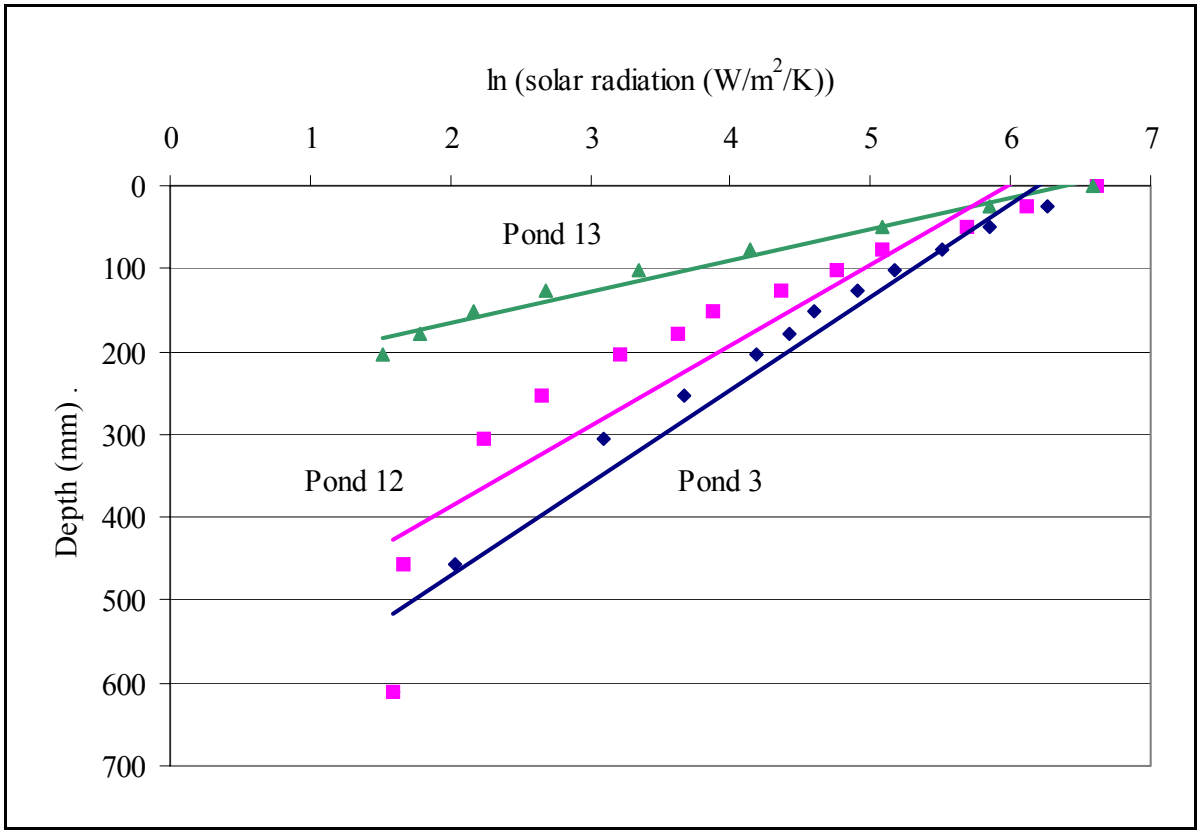

Figure 5.7: The relationship between incident solar radiation and depth was found to be linear (correlation coefficients ranging from -0.83 to -0.999; lines not shown here), which agrees with the Bouger-Beer Law. The slope of each line of best fit is the extinction coefficient. The slope for Pond 13 is greater than the slope of the other ponds. Because Pond 13 in the spring was found to be turbid when compared with the other ponds, its extinction coefficients were significantly larger ($t_{df = 26}$ = -23.66; $p < 0.0001$) than those from other ponds. Data were collected in March of 2003.

with values ranging from -0.83 to -0.999. This implies that the relationship between the natural log of light attenuation and depth is linear.

The overall average extinction coefficient was 0.013 mm^{-1} with values ranging from 0.004 to 0.031 mm^{-1}. However, there was significant variation in the results ($p = 0.0134$). Pairwise comparisons between ponds and within a pond were consequently done to determine the cause of the variations (Figure 5.8). For this analysis, Pond 13 in the fall and spring were treated as two different ponds. Results from this analysis showed that in the spring, Pond 13 had a significantly higher extinction coefficient (0.023 mm^{-1}) when compared with Ponds 3(β = 0.009 mm^{-1}), 12 (β = 0.009 mm^{-1}) and Pond 13 (β = 0.009 mm^{-1}) in the fall. There was also significant differences in the extinction coefficient ($p = 0.0268$) between locations within the pond (β = 0.014 mm^{-1} near the aerator, β = 0.010 mm^{-1} in the middle of the pond and β = 0.013 mm^{-1} near the aerator).

Table 5.5: These are the extinction coefficients and correlation coefficients for Ponds 3, 12 and 13. Reflection of sola radiation becomes important when the sun's elevation is below 30˚. Solar radiation measurements were taken near the aerator, in the middle of the pond and at the pond's discharge (outlet). The correlation coefficient r ranged from -0.83 to -0.999.)

Date	Time	Elevation (°)	Pond	Location	Extinction coefficient (mm^{-1}) from top	r
3/22/2003	13:30 - 14:00	53	3	Aerator	-0.009	-0.98
3/22/2003	13:30 - 14:00	53	3	Middle	-0.009	-0.98
3/22/2003	13:30 - 14:00	53	3	Disharge	-0.008	-0.97
3/24/2003	13:00-13:30	58	3	Aerator	-0.009	-0.94
3/24/2003	13:00-13:30	58	3	Middle	-0.009	-0.94
3/24/2003	13:00-13:30	58	3	Disharge	-0.012	-0.98
3/31/2001	12:50-13:20	60	3	Aerator	-0.008	-0.98
3/31/2001	12:50-13:20	60	3	Middle	-0.009	-0.98
3/31/2001	12:50-13:20	60	3	Disharge	-0.011	-0.99
3/22/2003	14:15-14:45	46	12	Aerator	-0.012	-0.98
3/22/2003	14:15-14:45	46	12	Middle	-0.009	-0.94
3/22/2003	14:15-14:45	46	12	Disharge	-0.008	-0.98
3/24/2003	13:45-14:15	51	12	Aerator	-0.009	-0.99
3/24/2003	13:45-14:15	51	12	Middle	-0.006	-0.92
3/24/2003	13:45-14:15	51	12	Disharge	-0.009	-0.96
10/30/2002	12:00	46	13	Aerator	-0.009	-0.997
10/30/2002	12:00	46	13	Discharge	-0.008	-0.997
10/31/2002	12:43	44	13	Aerator	-0.009	-0.997
10/31/2002	12:43	44	13	Middle	-0.008	-0.997
10/31/2002	12:43	44	13	Disharge	-0.009	-0.997
11/1/2002	12:10	45	13	Aerator	-0.011	-0.97
11/1/2002	12:10	45	13	Middle	-0.009	-0.99
11/1/2002	12:10	45	13	Disharge	-0.009	-0.999
3/27/2003	12:30-13:00	61	13	Aerator	-0.031	-0.96
3/27/2003	12:30-13:00	61	13	Middle	-0.022	-0.83
3/27/2003	12:30-13:00	61	13	Disharge	-0.027	-0.98
3/27/2003	13:00-13:30	58	13	Aerator	-0.026	-0.98
3/27/2003	13:00-13:30	58	13	Middle	-0.018	-0.97
3/27/2003	13:00-13:30	58	13	Disharge	-0.022	-0.97
3/31/2003	13:30-14:30	53	13	Aerator	-0.022	-0.92
3/31/2003	13:30-14:30	53	13	Middle	-0.012	-0.85
3/31/2003	13:30-14:30	53	13	Disharge	-0.0264	-0.91
				Average	-0.0129	-0.96

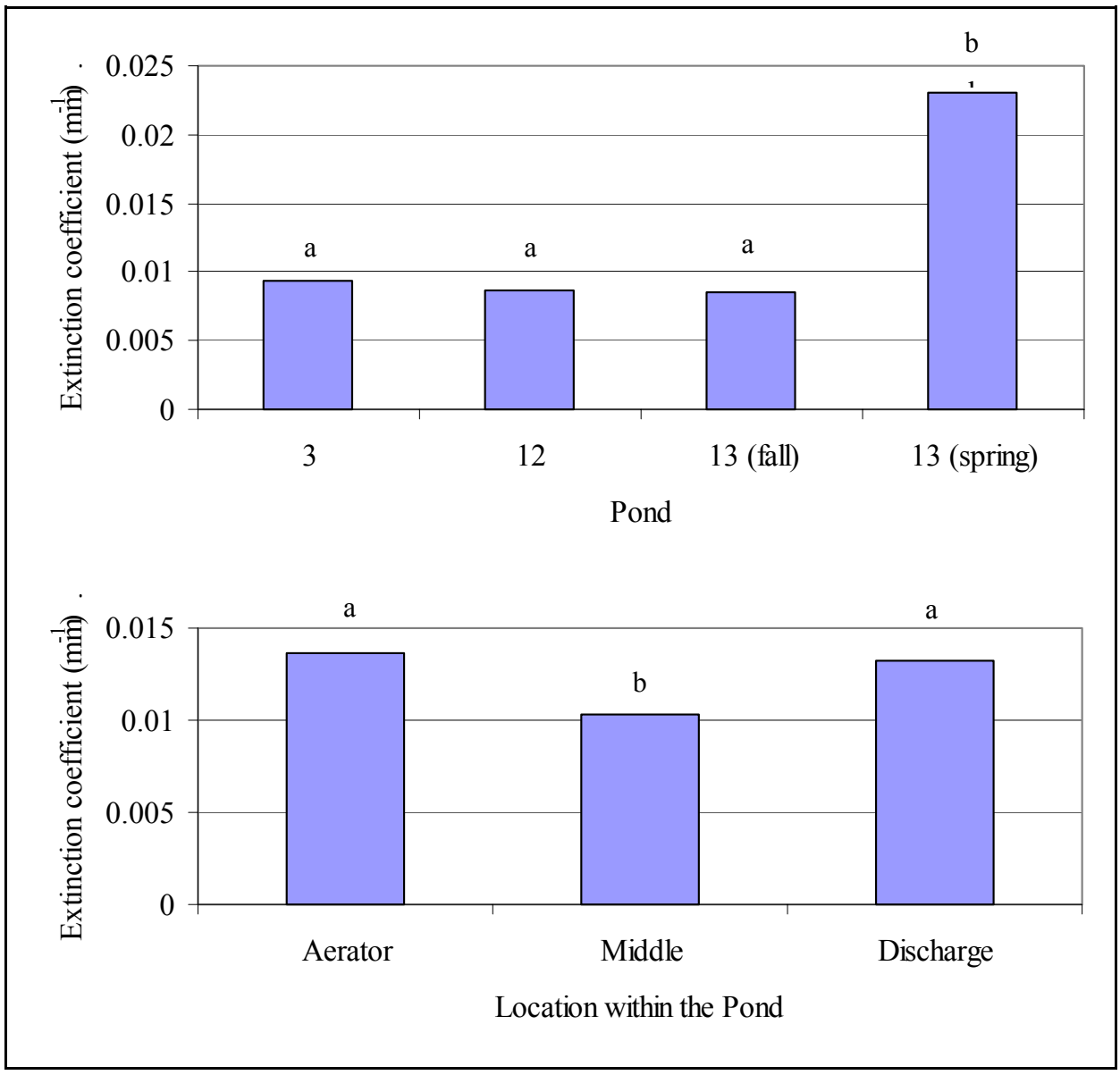

Figure 5.8: Shown here are the pairwise comparisons to determine whether there are any significant differences between extinction coefficients measured between the ponds and within the ponds. The pairwise comparison tests revealed that the extinction coefficient for Pond 13 in the spring (0.023 mm^{-1}) was significantly different to the extinction coefficient observed in all other ponds (0.009 mm^{-1}). This affected the overall results for the pairwise comparisons within a pond. Overall, the extinction coefficients within a pond were significantly different ($F_{df=2,26} = 4.17$, $p = 0.0134$) to each other. This was not the case when data from Pond 13 in the spring were not included in the statistical analysis ($F_{df=2,18} = 1.31$, $p = 0.1469$).

5.4.4 Albedo

The statistical parameters used for comparing the output from PHATR Version 1.21 and 1.21a are presented in Table 5.6. Trials when the average bias is 0 are highlighted. An example of the model's output is graphically presented in Figure 5.9

5.5 Analysis

5.5.1 Heat and Mass Transfer Coefficients - The Heat and Mass Transfer Analogy

The methodology used to determine the heat and mass transfer coefficient failed. Negative values for heat and mass transfer coefficients have no physical meaning and should always be positive (Figures 5.4 and 5.5). This was not the case, where many values were negative. Furthermore, from the scatter plots, there was no clear relationship between the two transfer coefficients and the wind speed. This was shown in Table 5.3, where r values for h vs. wind speed and h_m vs. wind speed were 0.003 and 0.030 respectively.

For both coefficients, the standard deviation (597 $W/m^2/K$ for the heat transfer coefficient; 0.0753 m/s for the mass transfer coefficient) was larger than the average mean value (27 $W/m^2/K$ for the heat transfer coefficient and 0.0107 m/s for the mass transfer coefficient). The calculated heat transfer coefficients ranged from -12515 to 15146 $W/m^2/K$. Values for convection heat transfer coefficients for air are typically between 5 and 250 $W/m^2/K$ (Incropera and De Witt, 1985). The calculated mass transfer coefficients ranged from -1.5029 to 0.5959 $W/m^2/K$..

The poor results from this model run are probably due to the measuring equipments lack of accuracy. Although thermocouple readings were made to two decimal places, type-T thermocouples are accurate up to 1.0°C (Anonymous, 2000). Therefore, small recorded changes in pond temperature (of the order of one one-hundredth of a degree) do not accurately reflect changes in the pond's internal energy. Such small changes, if accurately measured, represent relatively large changes in energy and are of the same order of magnitude as long wave radiation energy fluxes (see Appendix 9).

5.5.2 Heat and Mass Transfer Coefficients - Comparison of Empirical Equations

5.5.2.1. Evaporation

All equations predicting evaporation rates yielded similar results for given input data, especially when considering the correlation coefficient (see Table 5.4). The strong correlation coefficients (all of which are equal to or above 0.94) demonstrated that all evaporation equations used in Version 1.2 did not affect PHATR's ability to predict change.

Model runs using Equation 3.67 (Penman, 1948) had, on average, an average bias of -2.35°C (the average of the average bias was -2.35°C). Model runs using Equation 3.70 (Piedrahita, 1991) had, on average, an average bias of -1.55°C. Model runs using Equation 3.71

Table 5.9: These are the results for the model runs used to determine the albedo for Ponds 3, 12 and 13. The bias is the average difference between the model run and the measured data. The standard deviation of the bias and the correlation coefficient between the model results and the measured data are shown.

Trial	Pond	Equations for convection and evaporation	Albedo	Statistical Parameters		
				Bias	St. dev.	r
17	3	Penman (1948), Watmuff (1977)	0.00	-0.7	1.8	0.96
18	3	Penman (1948), Watmuff (1977)	0.05	-0.9	1.8	0.96
19	3	Penman (1948), Watmuff (1977)	0.10	-1.1	1.8	0.96
20	3	Penman (1948), Watmuff (1977)	0.15	-1.3	1.8	0.96
21	3	Penman (1948), Watmuff (1977)	0.20	-1.5	1.8	0.96
22	3	Penman (1948), Watmuff (1977)	0.25	-1.8	1.8	0.95
23	3	Lake Hefner (1952), Watmuff (1977)	0.00	0.3	2.0	0.94
24	3	Lake Hefner (1952), Watmuff (1977)	0.05	0.0	2.0	0.94
25	3	Lake Hefner (1952), Watmuff (1977)	0.10	-0.2	1.9	0.94
26	3	Lake Hefner (1952), Watmuff (1977)	0.15	-0.5	1.9	0.94
27	3	Lake Hefner (1952), Watmuff (1977)	0.20	-0.7	1.9	0.94
28	3	Lake Hefner (1952), Watmuff (1977)	0.25	-1.0	1.9	0.94
29	12	Penman (1948), Watmuff (1977)	0.00	1.3	0.8	0.96
30	12	Penman (1948), Watmuff (1977)	0.05	1.2	0.8	0.96
31	12	Penman (1948), Watmuff (1977)	0.10	1.2	0.8	0.96
32	12	Penman (1948), Watmuff (1977)	0.15	1.1	0.8	0.96
33	12	Penman (1948), Watmuff (1977)	0.20	1.0	0.8	0.96
34	12	Penman (1948), Watmuff (1977)	0.25	0.9	0.8	0.96
35	12	Lake Hefner (1952), Watmuff (1977)	0.00	2.9	1.0	0.95
36	12	Lake Hefner (1952), Watmuff (1977)	0.05	2.8	1.0	0.95
37	12	Lake Hefner (1952), Watmuff (1977)	0.10	2.7	1.0	0.96
38	12	Lake Hefner (1952), Watmuff (1977)	0.15	2.7	1.0	0.96
39	12	Lake Hefner (1952), Watmuff (1977)	0.20	2.6	1.0	0.96
40	12	Lake Hefner (1952), Watmuff (1977)	0.25	2.5	1.0	0.96
41	13	Penman (1948), Watmuff (1977)	0.00	0.5	0.8	0.98
42	13	Penman (1948), Watmuff (1977)	0.05	0.3	0.7	0.98
43	13	Penman (1948), Watmuff (1977)	0.10	0.0	0.7	0.98
44	13	Penman (1948), Watmuff (1977)	0.15	-0.2	0.7	0.98
45	13	Penman (1948), Watmuff (1977)	0.20	-0.4	0.6	0.98
46	13	Penman (1948), Watmuff (1977)	0.25	-0.7	0.6	0.99
47	13	Lake Hefner (1952), Watmuff (1977)	0.00	1.4	1.0	0.96
48	13	Lake Hefner (1952), Watmuff (1977)	0.05	1.1	1.0	0.96
49	13	Lake Hefner (1952), Watmuff (1977)	0.10	0.8	0.9	0.97
50	13	Lake Hefner (1952), Watmuff (1977)	0.15	0.6	0.9	0.97
51	13	Lake Hefner (1952), Watmuff (1977)	0.20	0.3	0.8	0.97
52	13	Lake Hefner (1952), Watmuff (1977)	0.25	0.0	0.8	0.98

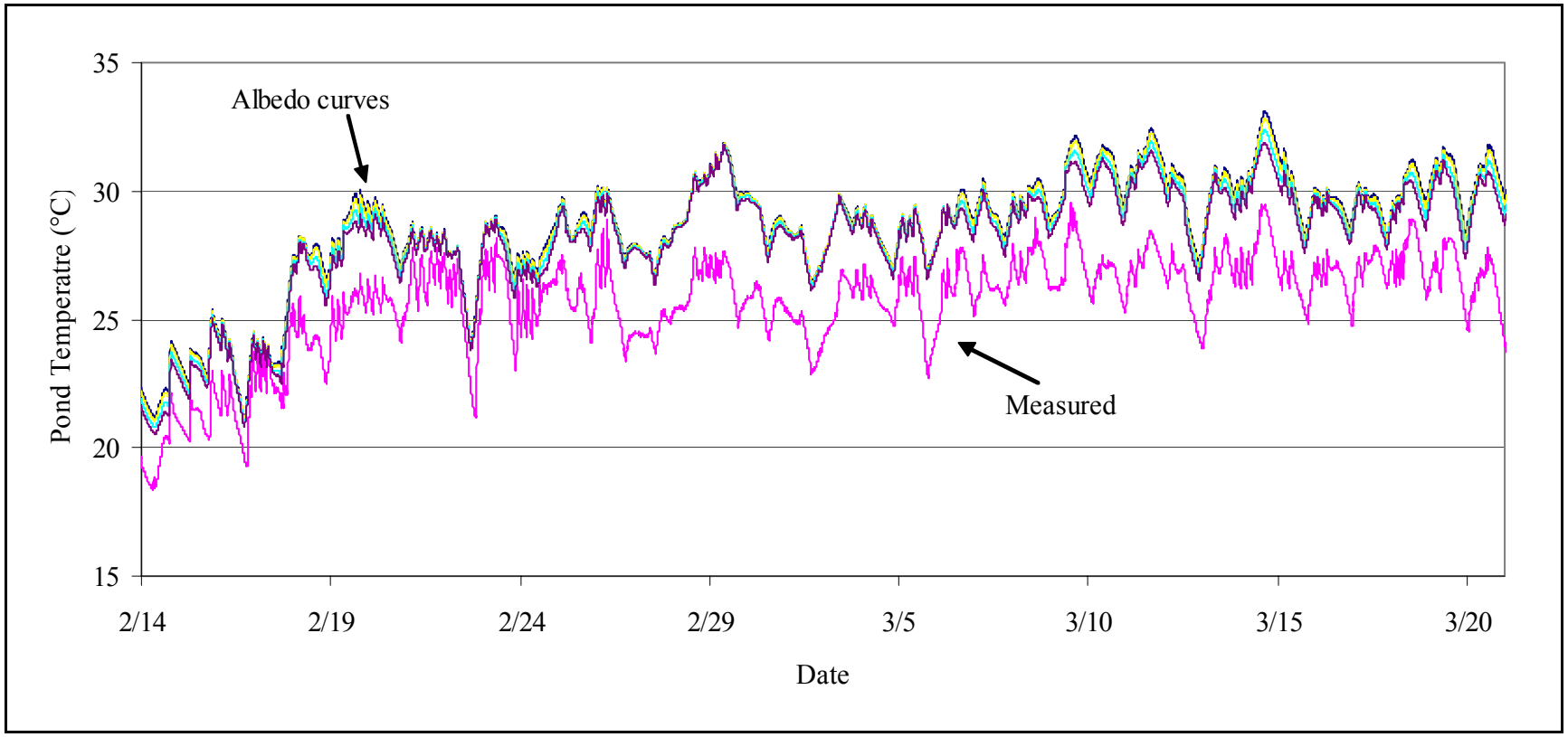

Figure 5.9: This graph shows the results from four model runs for heated Pond 12 (Trials 35, 36, 38 and 40). The model runs were done for the time period between the 13th of February and the 23rd of March, 2003. The albedos considered here are 0%, 5%, 15% and 25%. The effects of the albedo on heated ponds was small since it is difficult to visually distinguish model run curves from each other. The average bias ranged from 2.5 to 2.9°C. PHATR's ability to predict change was not hampered by including the albedo effect.

(Anonymous, 1952) had, on average, an average bias of -1.5°C Because the PHATR Version 1.0 over-predicted the pond temperature, using Penman's Equation might be more appropriate than using the Lake Hefner Equation, especially when considering heated ponds. The bias for a heated pond run, using wind speed data recorded at 3 meters and using the Penman Equation, was 1.3°C, as opposed to 2.9 for the same output data using the Lake Hefner Equation. For unheated ponds, the absolute average bias generated by the Penman Equation was greater (-0.7°C) than that generated by the Lake Hefner Equation (0.3°C). Although it might be advantageous to use Penman's Equation for heated ponds, using it for unheated ponds could cause the model to under-predict pond temperature.

The average bias for model runs for unheated ponds using wind speed at 3 meters was 0.125°C. In Chapter 4, the average bias for unheated model runs was 0.5°C. The use of different equations to estimate evaporation confirmed that PHATR was estimating the order of magnitude of evaporation energy losses properly. Consequently, if any large errors were present in the equations used by PHATR Version 1.0, it seems less likely they were caused by the Lake Hefner Equation.

5.5.2.2 Convection Coefficient

Not unlike the empirical equations used to estimate evaporation losses, the empirical equations used to estimate heat transfer losses yielded results similar to each other (see Table 5.4). This again supports the idea that PHATR Version 1.0 was properly estimating the rate of convective heat transfer to an order of magnitude.

The standard deviation for the biases and the correlation coefficient were similar between treatments. The average difference between the standard deviation for Watmuff et al.'s Equation and the standard deviation for Nusselt number correlations was 0.075°C. The average difference between the correlation coefficient for Watmuff et al.'s Equation and the correlation coefficient for Nusselt number correlations was 0.0075. This suggests that using either set of empirical equations did not affect PHATR's ability to predict change.

However, there was a pronounced difference when considering the model's bias for heated ponds. (The average difference between the average bias for Watmuff et al.'s Equation and the average bias for Nusselt number correlations was 0.83°C.) This was especially true for the model run for a heated pond (wind speed measurements taken at 3 meters), where the difference between the average biases was 2.1°C. Because the Nusselt number correlations increased PHATR's tendency to over-predict, Watmuff et al.'s Equation should be used.

Equation 3.58 (Watmuff et al., 1977) was preferred to the Nusselt number correlations for other reasons. The Nusselt number correlations represent 30 lines of computer code whereas Equation 3.58 represents only 1 line of code. Consequently, fixing and verifying PHATR's series of calculations was much simpler when using Equation 3.58. Furthermore, using the Nusselt number correlations required more input data. The additional required data sets were local atmospheric pressure (used in the ideal gas law when calculating the density of air) and

wind direction (used to determine the characteristic length of heat transfer for the correlations). The user also needed to know the orientation of his pond, which may not have been convenient. More input data meant there was a greater chance there would be more errors in the input and output data. For the user, finding more data was not convenient. Since both equations were empirical, and since both equations were roughly equivalent in predicting pond temperature (although more experimenting is required), the simpler Equation 3.58 should be used.

5.5.2.3 Effects of Height for Wind Speed Measurements

There was a difference in the bias when using wind speeds measured at different heights. The average bias for trials where the wind speed was measured at the pond surface was -4.85°C. The average bias for trials where the wind speed was measured 3 meters from the ground into the air was 1.61°C. Therefore, the using the wind speed at the surface caused the model to under-predict pond temperature.

This might be caused by Equation 3.73, the equation used to calculate an equivalent wind speed for different heights. The equation assumes that there is an exponential profile for the velocity boundary layer. However, near the surface, this is might not be true because of the roughness of the surface or because of the presence of obstacles (such as levees). By assuming that the height of the anemometer is where the wind speed is measured (33 cm or 1.1 feet), the wind speed measured at this height needs to be multiplied to a correction factor of (ln 13/ln 1.1) or 27, which is not reasonable if wind speeds measured near the pond surface ranged from 0 to 7.29 m/s (0 to 16.3 mph), as it did between February 13th and March 23st, 2003 on Pond 12. Applying the correction factor would yield wind speeds up to 196 m/s (440 mph).

An other cause for the large differences in bias might be because wind speeds at different heights poorly correlate. Upon examining the wind speed data for different heights, the correlation coefficient between these two data sets was r = 0.76. Consequently, both data sets, somewhat related, should have yielded similar results if Equation 3.73 was not used. For this reason, Equation 3.73, and not the data, was probably the cause of the error for the poor model outputs, for model runs using wind speed data collected near the water surface.

5.5.3 Extinction Coefficient

The strong negative correlation coefficients in Table 5.5 (average = -0.96, range -0.83 to -0.999) could allow for the following assumptions to be made:

- the Bouger-Beer Law, for these ponds, is valid and can be used to determine the extinction coefficient.
- the pond turbidity can be assumed to be constant with depth, probably because of the aerators, which were constantly running and continuously mixing the suspended sediments.

However, results from the pairwise comparison do not support the conclusion that the extinction coefficient is the same throughout the pond. Results showed that there were significant differences between the extinction coefficient measured at the aerator and in the middle of the pond ($p = 0.017$) and between the extinction coefficient measured at the middle and at the stand pipe ($p = 0.034$). There was no difference between the extinction coefficient measured at the aerator and at the standpipe ($p = 0.48$). This seems contradictory but might be explained with the results from the pairwise comparisons of the extinction coefficient between ponds.

Pond 13, in the spring time, had significantly different extinction coefficients from all other pond ($p < 0.001$ for all cases; see Figure 5.8). Furthermore, upon examining the data collected within Pond 13, the extinction coefficient had variations within the pond. The difference between the extinction coefficient at the aerator and the extinction coefficient at the middle of the pond was significant (difference = 0.00931 mm^{-1}, $p = 0.01735$). The difference between the extinction coefficient at the outlet and the extinction coefficient at the middle of the pond was also significant (difference = 0.007952 mm^{-1}, $p = 0.0297$). There was no significant difference between the extinction coefficient measured at the aerator or at the discharge (difference = 0.00136; $p = 0.35245$).

There were no significant differences in the extinction coefficients between the ponds ($F_{2,18} = 0.65$, $p = 0.266$) or within the ponds ($F_{2,18} = 1.31$, $p = 0.1469$) if the extinction coefficient collected from Pond 13 during the spring was excluded from the statistical analysis. Therefore, results from Pond 13 in the spring time affected the pairwise comparisons of the extinction coefficient within a pond.

Unlike the other ponds or Pond 13 in the fall, Pond 13 in the spring was noticeably more brown and muddy. This might explain the greater extinction coefficients observed in this pond.

5.5.4 Albedo

The main purpose for including the albedo in the model was to reduce the consistently over-predictive bias. This would have been especially beneficial for heated model runs, where the bias was larger. However, the albedo's effects were more pronounced in unheated ponds. Table 5.7 shows the effects of varying the bias by 25%. Although varying the albedo lowered, on average, the bias by 0.95°C, varying the albedo for heated ponds only lowered the bias by 0.45°C. Therefore, the albedo was not responsible for the large bias calculated for heated ponds.

The correlation coefficient for all runs was over 0.94. This shows that including the influence of an albedo does not affect the model's ability to predict change.

Recommending an albedo to be used in subsequent model runs might be difficult. The results in Table 5.6 make it unclear which albedo should be used. Clearly, the empirical equations used by the model to predict evaporation and surface convection had an effect on the bias. Unfortunately, this effect cannot be separated from the albedo's influence on the results.

Table 5.7: Differences in average bias between model runs with an albedo of 0 and 25% ranged from 0.4 to 1.3°C.

Pond	Treatment	Change in Bias (°C)
3	Unheated	1.0
3	Unheated	1.2
12	Heated	0.4
12	Heated	0.5
13	Unheated	1.2
13	Unheated	1.3

Therefore, an albedo will be recommended for a model using Penman's equation and an other albedo will be recommended for a model using the Lake Hefner Equation.

When considering unheated ponds, Trial 43 was the only trial using Penman's equation where the average bias was 0°C. For Trials 17 through 22, increasing the albedo increased the model's error. Therefore, because Penman's equation, when compared with the Lake Hefner equation, has a tendency to over-estimate evaporation losses, a low albedo should be used (5%).

Alternately, for a version of PHATR using the Lake Hefner equation, a higher albedo might be necessary. Trials 24 (albedo = 5%) and 52 (albedo = 25%) yielded results with an average bias of 0°C. Using an average of albedo of 15% causes the error for both ponds to be within a degree of the measured pond temperature (Trial 26, bias = -0.5°C; Trial 50, bias = 0.6°C).

5.6 Conclusions

Ways to improve PHATR Version 1.0 were explored with mixed success.

The heat and mass transfer coefficients could not be determined using the heat and mass transfer analogy. Results yielded negative heat and mass transfer coefficient values, which is physically impossible. These negative values were caused in part by the inaccuracy of thermocouples to measure the pond temperature to one one-hundredth of a degree Celsius. Accurate temperature sensing devices would be needed in order to determine both transport coefficients.

Comparisons were made between the various empirical equations used to estimate evaporation losses over bodies of water. All equations yielded similar results. Therefore, the size of evaporative energy losses was probably properly estimated. Equation 3.67 (Penman, 1948) predicted greater evaporation losses whereas equation 3.70 (Piedrahita, 1991) predicted smaller evaporation losses. Because the model already closely predicted the temperature for unheated ponds, using the Penman equation would cause the model to under-predict the pond temperature without the effects of an albedo. Therefore, the Lake Hefner equation is probably the best equation to use to estimate evaporative heat losses for heated and unheated ponds (volume = 400 m^3).

Comparisons were also made between Nusselt number correlations and Equation 3.58 (Watmuff et al, 1977). Both methods yielded similar results and therefore, the size of the convective heat transfer coefficient was probably properly estimated. However, because the Nusselt number correlations are more complex and require more input data without being more accurate, Equation 3.58 should be used.

When choosing wind speed data for PHATR's input, wind speeds recorded at 3 meters proved to yield better results. Using wind speeds recorded at the water surface caused the model to consistently under-predict the pond temperature by 4.3 to 5.5°C. This is probably because Equation 3.73 cannot be used for converting wind speeds recorded close to the water surface.

The average extinction coefficient for the warm water ponds was 0.013 mm^{-1}, with values ranging from 0.004 to 0.031 mm^{-1}. This average includes the data from the more turbid Pond 13 in the spring of 2003. The extinction coefficients for pond 13 were significantly different from the extinction coefficient measured in all other ponds. Statistically similar extinction coefficients can be explained by the aerators constantly mixing the pond water.

The albedo was estimated empirically using a modified version of PHATR. The method was partially successful although not conclusive. Because of the difficulty of either theoretically calculating or measuring this parameter, the method used was seen as the only realistic alternative. Consequently, the albedo's value is greatly affected by any inaccuracies inherent in the model, such as inaccuracies associated with empirical equations. Therefore, two albedos were calculated. An albedo of 5% is to be used in models using Equation 3.67 (Penman, 1948) to estimate evaporation energy losses, whereas an albedo of 15% is to be used in models using Equation 3.71, the Lake Hefner equation (Anonymous, 1952). Including the effects of an albedo did not impair PHATR's ability to predict changes in pond temperature. This was reflected in the high correlation coefficient values in the results.

For all the trials modeling unheated ponds, the average of the average bias was -0.88°C. For all the trials modeling heated ponds, the average of the average bias was 0.79°C. Varying the albedo, convection and evaporation did not further correct the model when predicting pond temperature for heated ponds. This supports the conclusion in Chapter 4 that the average biases for heated ponds were larger than the average biases for unheated ponds because the flow rate of warm or cool water cannot be measured accurately.

CHAPTER 6: SENSITIVITY ANALYSIS

6.1 Introduction

PHATR, a computer model used to predict the temperature for small well mixed ponds (full description of the model can be found in Chapter 4), uses data inputs of various kinds. The data describes the weather, the flow of water into the pond and the physical characteristics of the pond itself. How the data affects the model output can be studied with a sensitivity analysis.

A sensitivity analysis, defined by Saltelli (2000) is "the study of how the variation in the output of a model (numerical or otherwise) can be apportioned, qualitatively or quantitatively, to different sources of variation, and of how the given model depends upon the information fed into it." For PHATR, the sensitivity analysis revealed which changes in the input caused greater or lesser changes in the output. The sensitivity analysis also identified certain scenarios where varying a certain input variable had a counter-intuitive effect on the results.

6.2 Materials and Methods

A type sensitivity analysis was performed For such an analysis, a standard model run, with fixed input variables, is compared to trial model runs. For each trial, only one input variable in the standard model run was changed by a pre-determined increment. By comparing changes in the output to changes in the input, the model's sensitivity can be gaged.

The standard model run consisted of running PHATR Version 1.2 for 2 hypothetical days for a hypothetical pond with dimensions 1 meter x 1 meter x 1 meter (pond characteristics shown in Table 6.1).

Table 6.1: These characteristics for a hypothetical pond were used for the sensitivity analysis of PHATR, Version 1.2.

Pond Characteristic	Value
Initial Pond Temperature	20°C
Pond Volume	1 m^3
Pond Area	1 m^2
Flow rate of warm water	0 m^3/s
Time period considered for the model run	2 days (172800 seconds)

The weather during these 2 hypothetical days was clear (no clouds) with an average air temperature of 20°C. The air temperature varied sinusoidally. The daytime high, 25°C, occurred at 14:00 (2 P.M.) and the daytime low, 15°C, occurred at 2:00 (2 A.M.). Solar radiation

varied sinusoidally between 6:00 and 18:00 (6 A.M. and 6 P.M.), the maximum (1355 W/m^2) occurring at 12:00 (noon). The relative humidity was set constant at 90%. There was no wind (wind speed = 0 m/s). All weather variables for the standard are shown in Table 6.2.

There was no warm or cool water flowing in the pond for the standard model run. The pond temperature at the start of the two day period was 20°C.

Table 6.2: These weather variables described the standard weather used for the sensitivity analysis of PHATR, Version 1.2. For the equations used to describe solar radiation and air temperature, t = time in hours. Also note that between 18:00 and 6:00, solar radiation is equal to 0 W/m^2.

Weather Variable	Value
Air Temperature	$20 + 5\sin\left(\frac{\pi(t-8)}{12}\right)$
Relative Humidity	90%
Solar Radiation	$1355\sin\left(\frac{\pi(t-6)}{12}\right)$
Wind Speed	0 m/s

PHATR Version 1.2, a more "user-friendly" version of PHATR Version 1.0, was used to perform all the model runs. The time step used was 10 minutes and all model runs simulated a period of 2 days.

For each model run, one variable was changed while keeping all other weather conditions at their hypothetical standard value (see Table 6.3 for the exact nature of each variation). Four variables were changed:

- average air temperature
- solar radiation
- wind speed
- flow rate of warm water (36°C).

The average air temperature was set at either 0, 10, 15, 20, 25, 30 or 40°C. Diurnal fluctuations were modeled as a sinusoidal function with an amplitude of 5°C. The daytime high occurs at 14:00 and the night time low occurs at 2:00.

The solar radiation was varied by 0%, -25%, -50%, -75% and -100% of the standard solar radiation value predicted by the equation in Table 6.2.

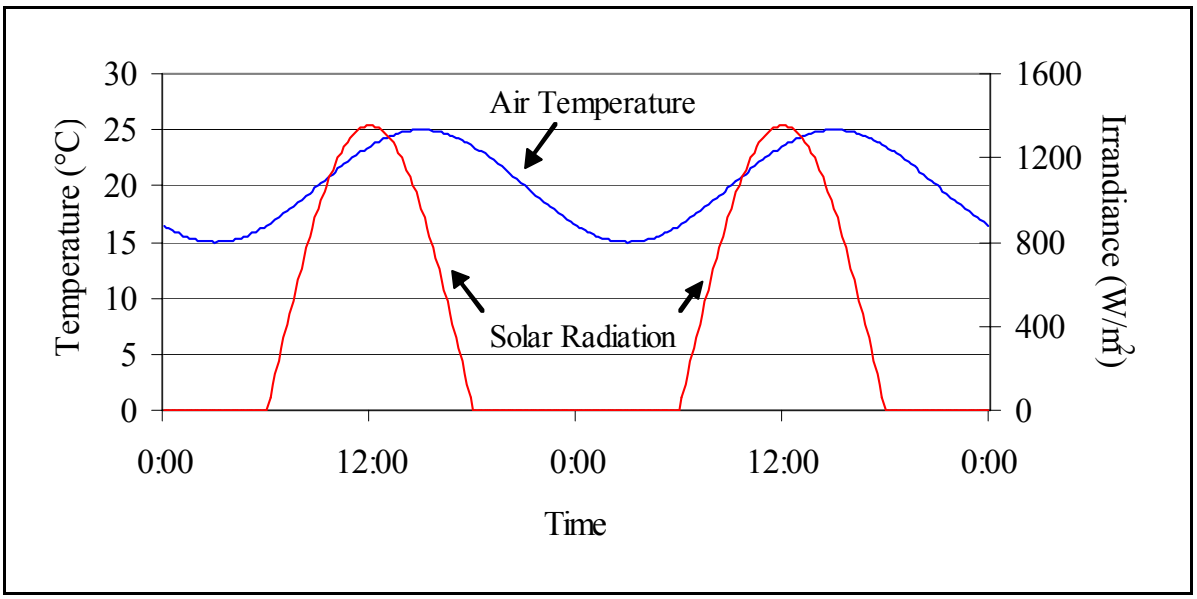

Figure 6.1: Both the air temperature and the solar radiation were modeled as sinusoidal curves, with a period of one day. At night, solar radiation was held constant at 0 W/m^2. The air temperature and the solar radiation described by these two curves were used as input data for model runs for the sensitivity analysis.

The wind speed was set at 0, 0.5, 1, 2, 5, 10, 20 and 50 m/s.

The flow rate was varied on a "per volume" scale. For instance, a flow rate of 200 liters per minute in a 400 m^3 pond (the average volume for warm water ponds 1 through 12) corresponds to a flow rate of 8.33×10^{-6} m^3/s per unit of pond volume. The flow rate was set to 2.08×10^{-6}, 4.17×10^{-6}, 8.33×10^{-6}, 1.67×10^{-5}, 2.5×10^{-5} and 3.33×10^{-5} m^3/s per unit of pond volume. In every case, the flow rate was set to 0 m^3/s during the daytime. The temperature of the inlet water was set at 36°C (warm water trials) and 15°C (cool water trials).

Model run results for the pond temperature were compared to the standard model run over the two day period. The difference in temperature between each trial and the standard at 12, 24, 36 and 48 hours was then plotted against one of the four variables of interest (average air temperature, solar radiation, wind speed or flow rate). The curves in these plots are called sensitivity curves and graphically represent relative changes in output for relative changes in input.

Quantitatively, the model's sensitivity to a given input variable (example: average air temperature, solar radiation, wind speed or flow rate) is the derivative (slope) of the sensitivity curve. To generate an equation to describe the sensitivity curve mathematically, the data points in the sensitivity curves were entered into Curve Expert (Hyams, 2001), a shareware program specifically designed for curve fitting. The derivative of the resulting equation of best fit was then calculated. Substituting statistically determined constants (determined by Curve Expert -

Hyams, 2001)) and the input variables into the derivative equation yielded numerical measurements for sensitivity.

Table 6.3: Listed here are the values of the varied parameters for each trial. Note that all other parameters were kept constant during the trial model runs.

Trial	Parameter Varied	Value
Standard	None	Hypothetical pond and weather values
1	Average air temperature	0°C
2	Average air temperature	10°C
3	Average air temperature	15°C
4	Average air temperature	20°C
5	Average air temperature	25°C
6	Average air temperature	30°C
7	Average air temperature	40°C
8	Solar Radiation	0% of standard solar radiation values
9	Solar Radiation	25% of standard solar radiation values
10	Solar Radiation	50% of standard solar radiation values
11	Solar Radiation	75% of standard solar radiation values
12	Wind Speed	0.5 m/s
13	Wind Speed	1 m/s
14	Wind Speed	2 m/s
15	Wind Speed	5 m/s
16	Wind Speed	10 m/s
17	Wind Speed	20 m/s
18	Wind Speed	50 m/s
19	Flow rate; 36°C	0 $(m^3/s)/m^3$
20	Flow rate; 36°C	2.08×10^{-6} $(m^3/s)/m^3$

Table 6.3 continued

Trial	Parameter Varied	Value
21	Flow rate; 36°C	4.17×10^{-6} $(m^3/s)/m^3$
22	Flow rate; 36°C	8.33×10^{-6} $(m^3/s)/m^3$
23	Flow rate; 36°C	1.67×10^{-5} $(m^3/s)/m^3$
24	Flow rate; 36°C	2.5×10^{-5} $(m^3/s)/m^3$
25	Flow rate; 36°C	3.33×10^{-5} $(m^3/s)/m^3$
26	Flow rate; 15°C	2.08×10^{-6} $(m^3/s)/m^3$
27	Flow rate; 15°C	4.17×10^{-6} $(m^3/s)/m^3$
28	Flow rate; 15°C	8.33×10^{-6} $(m^3/s)/m^3$
29	Flow rate; 15°C	1.67×10^{-5} $(m^3/s)/m^3$
30	Flow rate; 15°C	2.5×10^{-5} $(m^3/s)/m^3$
31	Flow rate; 15°C	3.33×10^{-5} $(m^3/s)/m^3$

6.3 Results and Analysis

6.3.1 Variations in the average air temperature

Lowering the average air temperature resulted in relatively lower pond temperatures at the end of the two day period (see Figure 6.2). For instance, the pond temperature, after being exposed to an average air temperature of 0°C for 48 hours, was 26.7°C, 6.3°C below the standard model run pond temperature. Alternately, increasing the average air temperature raised the pond temperature. As an example, the pond temperature, after being exposed to 40°C air for 48 hours, was 40.5°C, 7.5°C above the standard model run pond temperature. As time progressed, the absolute difference between the standard temperature and the resulting trial temperature increased. Therefore, the model's sensitivity to changes in air temperature were dependant on time, as shown by the different slopes for the sensitivity curves in Figure 6.2b.

A linear regression was applied to each curve in Figure 6.2b. The correlation coefficients and the slopes for each curve are shown in Table 6.4. As the time step increased from 12 to 48 hours, the slope also increased from 0.097 °C/°C to 0.48 °C/°C. Because the slope of a line is also the derivative of a line, and because the curves in Figure 6.2 were lines ($r = 0.999$ for all time steps), the slopes in Table 6.4 were measurements of the model's sensitivity.

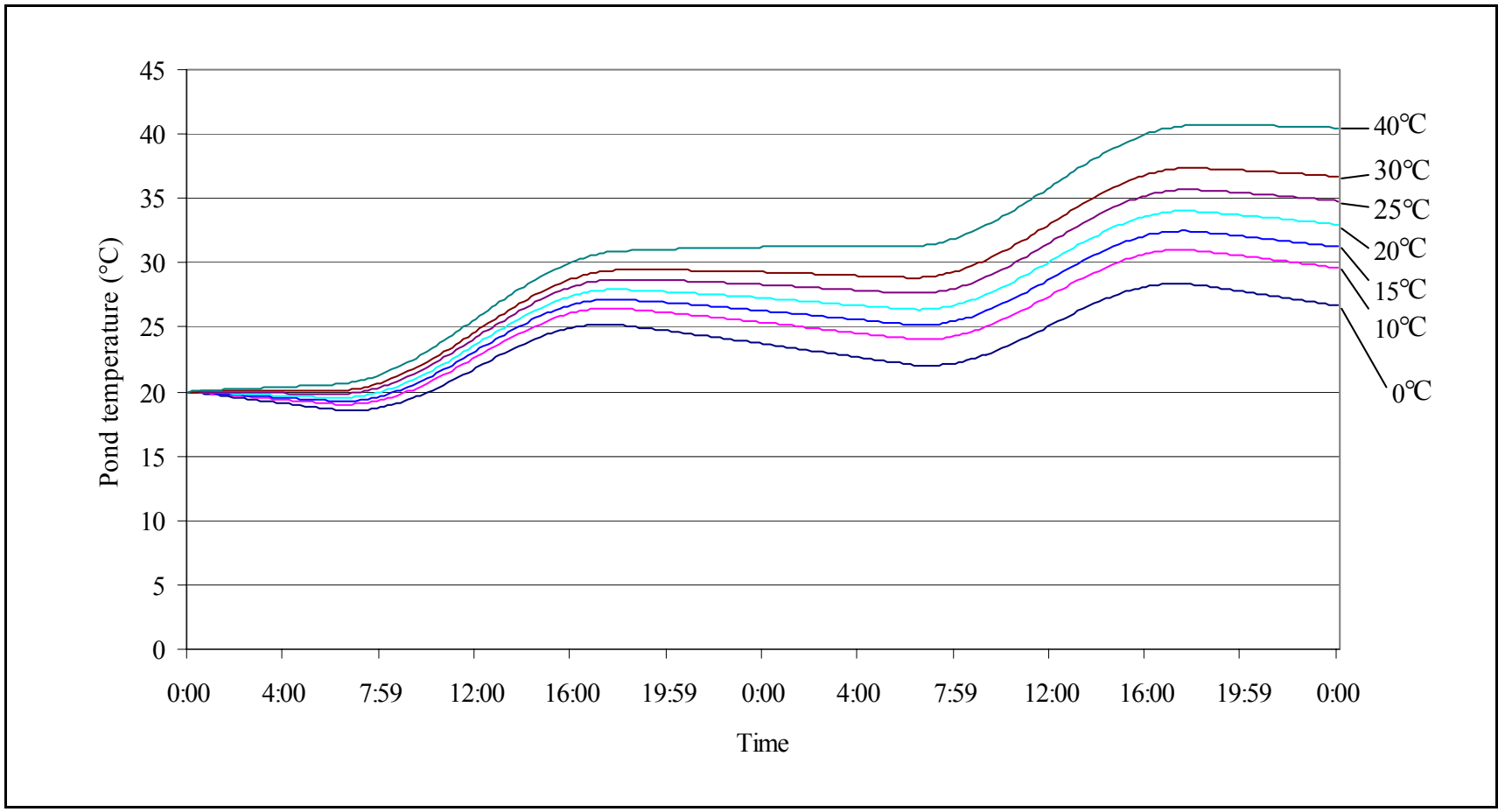

Figure 6.2a: These curves describe how the pond temperature changed over 2 days of hypothetical weather. The temperature labels on the right hand side of the graph were the average air temperature for the sensitivity analysis trials. Cooler air temperatures caused the pond temperature to decrease with respect to the standard (shown here as the 20°C curve). Warmer air temperatures caused the pond temperature to increase with respect to the standard.

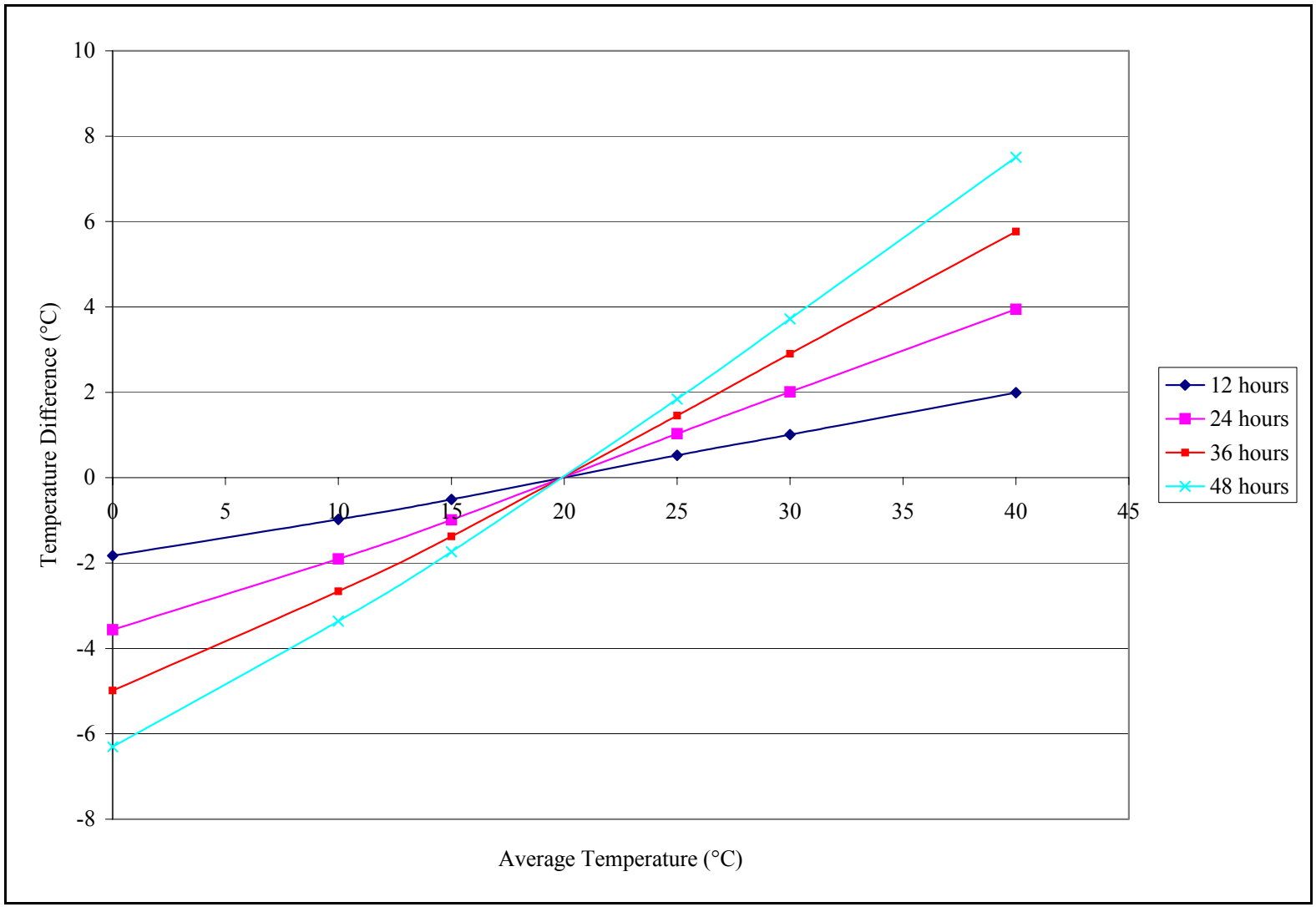

Figure 6.2b: The sensitivity curves with respect to the average air temperature are linear (for all curves, r = 0.999). The temperature difference is the difference between the standard and the trials at either 12 hours, 24 hours, 36 hours or 48 hours. The slope of each line represents the model sensitivity to changes in the average air temperature.

Table 6.4: The sensitivity curves in Figure 6.2b were statistically quantified with linear regression parameters. Note how the slope (sensitivity) increased with time.

Time (hr)	Slope ($°C_{output}/°C_{input}$)	Correlation coefficient (r)
12	0.097	0.999
24	0.190	0.999
36	0.271	0.999
48	0.348	0.999

To determine if any relationship existed between the slope of each sensitivity curve and time, the slopes were plotted against time (see Figure 6.4). The slopes were found to vary linearly with time (r = 0.999). The rate of change of the slopes was 0.00695 °C/°C/hr and the intercept for this line was 0.0178 °C/°C.

This information is useful when determining the effects of measurement errors or poor data on the model's output. For instance, suppose an error of 5°C was present in the air temperature data set. The error was present for 30 hours. What was the corresponding error in the output?

The model's sensitivity to air temperature was found to vary with time. For a 30 hour period, the sensitivity was:

$$0.00695\ {}^{0}C/_{0}C\ hr \times 30hrs + 0.0178\ {}^{0}C/_{0}C$$
$$= 0.2285\ {}^{0}C/_{0}C$$

A 5°C error in input translates into an output error of 1.1425°C.

6.3.2 Variations in Solar Radiation

Decreasing the amount of incident solar radiation decreased the pond temperature (see Figure 6.5). This made sense since solar energy was found to be the major energy transfer mechanism during the day, accounting for as much as 55% of all energy vectors (see chapter 4). After 48 hours, the pond temperature increased for all trials except for trial 8 where there was no solar radiation. In this case, the pond temperature steadily decreased almost linearly (r = -0.955) by 1.46°C.

The model's sensitivity to changes in solar radiation was quantified by calculating the slopes of the curves in Figure 6.6. All curves in Figure 6.6 had correlation coefficients above 0.999. The intercepts for each curve was also calculated (results shown in Table 6.5).

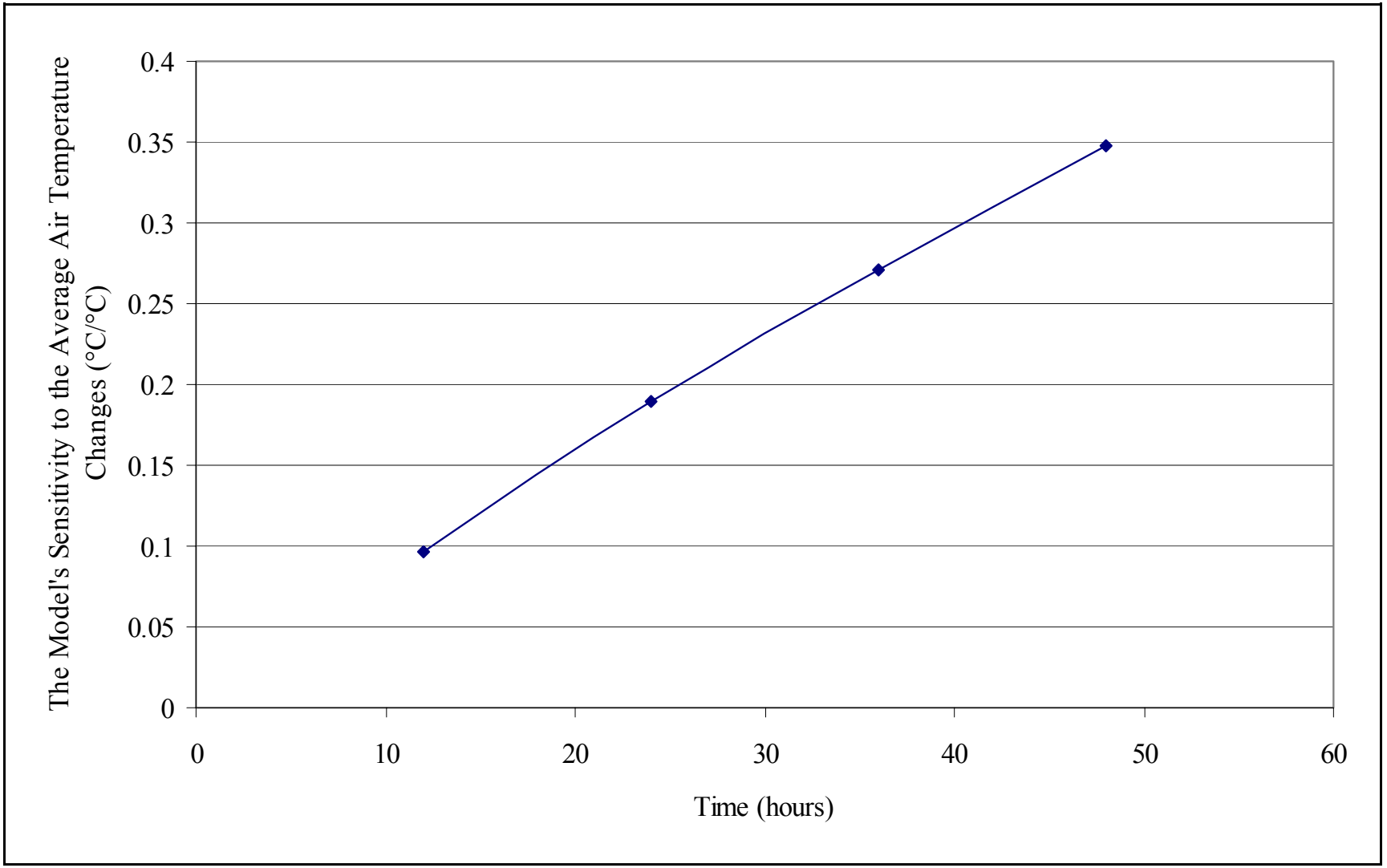

Figure 6.3: The model's sensitivity to the average air temperature increased with time at a rate of 0.00695 (°C/°C)/hr. The slope of each sensitivity curve was plotted against time to generate this graph.

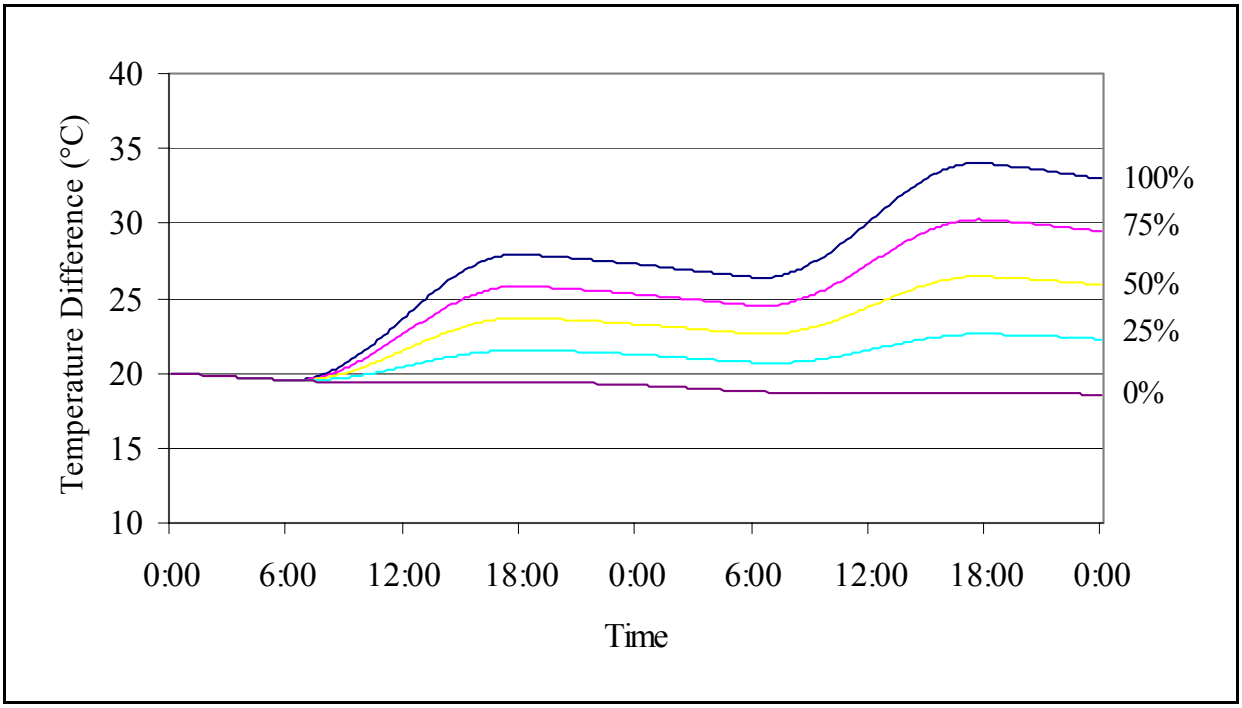

Figure 6.5: The solar radiation was varied by 0%, 25%, 50%, 75% and 100% of the "standard" solar radiation. As the amount of incident solar radiation decreased, the pond temperature also decreased. All curves were compared to the 100% curve (the "standard" curve).

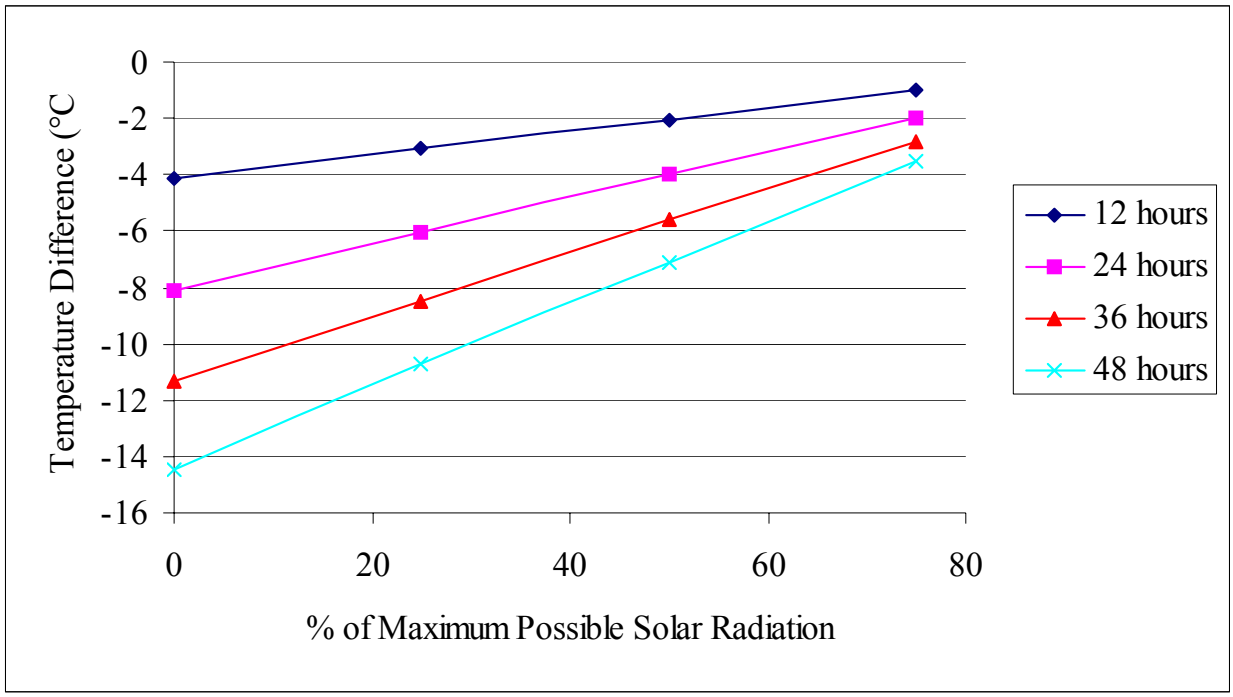

Figure 6.6: As time progresses, the output difference between the standard model and the trials where solar radiation was varied (y-axis) increased absolutely with time.

Table 6.5: These are the linear regression parameters for the sensitivity curves in Figure 6.3. Again, the slope and the intercepts varied linearly with time.

Time (hours)	Slope (°C / %)	Intercept (°C)
12	0.0413	-4.13
24	0.0812	-8.08
36	0.1138	-11.32
48	0.1455	-14.41

Again, the slope and the intercepts of each curve changed linearly with time. (The correlation coefficient for the rate of change in the slope was 0.998. The correlation coefficient for the rate of change in the intercept was -0.998.) A linear regression was applied to both the slopes and the intercepts to determine how the sensitivity changed with time. Results are shown in Figure 6.7. The equations for the slope and the intercept with respect to time are:

$$\xi_{slope} = 0.0029t + 0.0091 \tag{6.1a}$$

$$\xi_{\text{int}ercept} = -0.284t - 0.9627 \tag{6.1b}$$

$$\Delta T = \xi_{slope}\phi + \xi_{\text{int}ercept} \tag{6.1c}$$

where ϕ is the fraction of solar radiation set for the trial runs and
ΔT is the difference between the standard pond temperature and the trial pond temperature for a fixed time (°C),

The last equation, Equation 6.1c, is the equation used to determine the model's sensitivity with respect to solar radiation.

The sensitivity curves in Figures 6.3 and 6.6 were straight lines in part because of the solution to the governing differential equation but also in part because of the times chosen to examine the model's sensitivity. Consider the following simplified version of Equation 3.4, the energy balance equation, where q_{solar} is the only flux of energy present. In other words, energy transfer mechanisms associated with convection, conduction, evaporation, long wave radiation or bulk movements of mass are negligible. Equation 3.4 then simplifies to Equation 6.2:

$$\left(\frac{dE}{dt}\right)_{pond} = q_{solar} \tag{6.2}$$

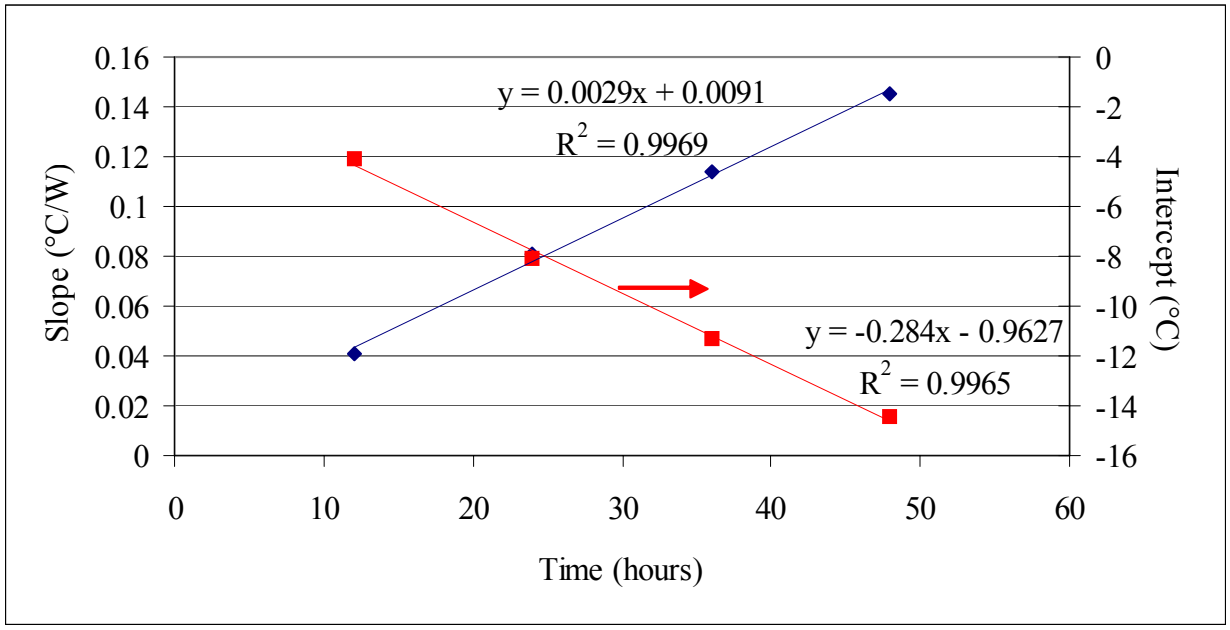

Figure 6.7: The slopes and the intercepts for the sensitivity curves varied linearly in time, as shown here. The slopes of the sensitivity curves varied according to the ascending curve with the given equation while the intercepts of the sensitivity curves along the descending curve.

where E is the internal pond energy (Joules),

q_{solar} is the solar radiation (Joules/hour)
t is time (hour).

Knowing that $(dE/dt)_{pond}$ and q_{solar} can be substituted with the following:

$$\frac{dE}{dt} = \rho c_p \forall \frac{dT}{dt} \tag{6.3a}$$

$$q_{solar} = -1355\phi\cos\left(\frac{\pi t}{12}\right) \tag{6.3b}$$

where ρ is the density of water (kg/m^3),
c_p is the specific heat of water (J/kg°C),
$\forall$ is the pond volume (m^3) and
T is the pond temperature (°C)

Equation 6.2 becomes:

$$\rho c_p \forall \frac{dT}{dt} = -1355\phi\cos\left(\frac{\pi t}{12}\right) \tag{6.4}$$

Integrating Equation 6.4 for t = 0 to some time t between 6 and 18 hours gives:

$$T = T_i - \frac{1355(12)\phi}{\pi\rho c_p}\left(\sin\frac{\pi t}{12} - 1\right) \tag{6.5}$$

Variations in ϕ caused variations in the difference between the pond temperature of the trials and the standard. If these variations became infinitely small, Equation 6.5 would become:

$$\frac{dT}{d\phi} = -\frac{1355(12)}{\pi\rho c_p}\left(\sin\frac{\pi t}{12} - 1\right) \tag{6.6}$$

If time t is held constant, dT/dϕ (the model's sensitivity with respect to radiation) is also constant. So the curve in Figure 6.6 for t = 12 hours must have a constant slope. If the time considered is 24 hours, the corresponding curve in Figure 6.6 should still have a constant slope, as is confirmed by the experimental data (r = 0.999). Using Equation 6.4 again, but this time integrating from t = 0 to t = 24 hours, yields:

$$T = T_i + \frac{1355\phi(24)}{\rho c_p \forall\, \pi} \tag{6.7}$$

Again, varying ϕ by very small increments yields:

$$\frac{dT}{d\phi} = \frac{1355 \times 24}{\rho c_p \forall\, \pi} \tag{6.8}$$

which is a constant. So the theory confirms the experimental results that sensitivity curves should be linear in Figures 6.3 and 6.6. The reason why the slopes and the intercepts of the sensitivity curves vary they themselves linearly over time is because of the chosen regular time intervals. Consider Figure 6.9, where the solar radiation is plotted against time. The area under the curve represents the energy to be gained by the pond. After 12 hours, exactly one quarter of all the available energy was absorbed. After 18 hours, exactly one half of all the energy was absorbed. After 24 hours, still, only one half of all the energy was absorbed. When considering time intervals of 12 hours, the amount of energy gained by a pond for a 12 hour period did not change; it remains constant. So if the rate of energy gained every 12 hours was constant, and if the energy gained by the pond was directly linked to the pond's temperature (as described in Equation 3.4), the rate at which the sensitivity curves changed their slopes had to also be constant, but only because 12 hour intervals were being considered. If the considered time interval was 3 hours, then the rate of change of the parameters for the sensitivity curves would not have been constant.

6.3.3 Variations in Wind Speed

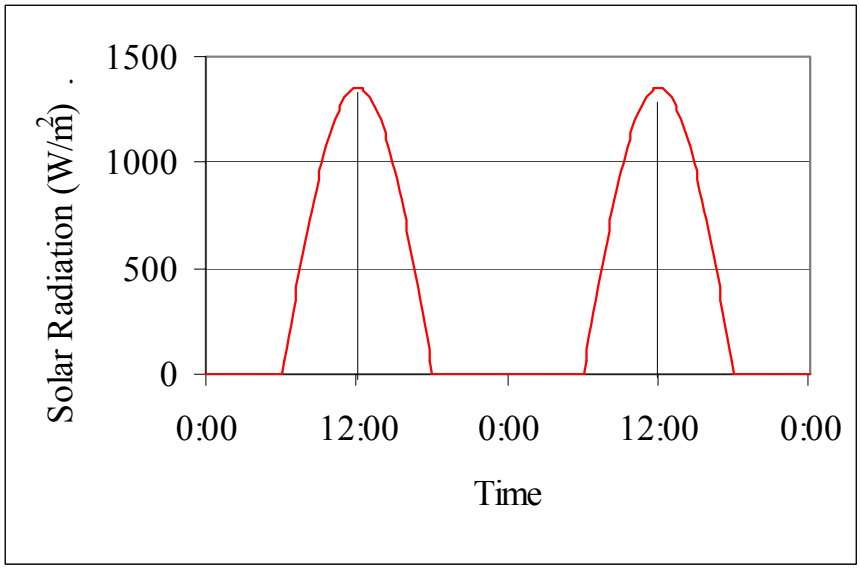

Figure 6.9: By considering the pond temperature every 12 hours, the same exact amount of solar radiation (one quarter of the two day total) was absorbed by the pond, causing the slopes and the intercepts of the sensitivity curves in Figure 6.6 to vary linearly with time.

Two energy vectors are directly affected by changes in wind speed: heat convection at the pond surface and evaporation. However, increasing the wind speed does not necessarily mean convection or evaporation are more important. Both convection and evaporation are also affected by their respective gradients, the true driving force behind these energy transfer mechanisms. In the case of convection, the temperature gradient between the air and the water surface drives this transport phenomena. In the case of evaporation, the vapor pressure gradient between the water surface and the air is the driving force. Because increasing the wind speed can change the temperature of the water, the gradients for heat and mass transfer also change and consequently, the size of the convection and evaporation vectors also change counter intuitively.

Increasing the wind speed also had different effects dependant on the time of day. At noon on day 2, increasing the wind speed from 0 to 5 m/s caused the pond temperature to decrease from 30.1°C to 25.4°C, mainly because the rate of energy lost by evaporation increased from 46 W to 110 W. However, this drop in pond temperature also decreased the vapor pressure of the water. Warmer water has more internal energy so more water vapor can evaporate from the water surface. Consequently, warmer water has a greater vapor pressure (the pressure of the water evaporating into the air) than cooler water. By cooling the pond water (and reducing the pond's vapor pressure), but keeping the air temperature constant (and keeping the air's vapor pressure constant), the pressure gradient which drives evaporation became smaller, because of the larger wind speed. Energy losses due to evaporation decreased when the wind speed was increased beyond 5 m/s. For a wind speed of 50 m/s, there was no evaporation because the water temperature was so low that the water vapor pressure (2.51 kPa) was smaller than the air vapor pressure (2.87 kPa) .

Convection only removed heat from the pond for wind speeds under 10 m/s at noon on Day 2. Because the pond temperature for a wind speed of 10 m/s, 23.3°C, was below the air temperature, 23.53°C, the air "warmed" the pond. By increasing the wind speed from 10 m/s to

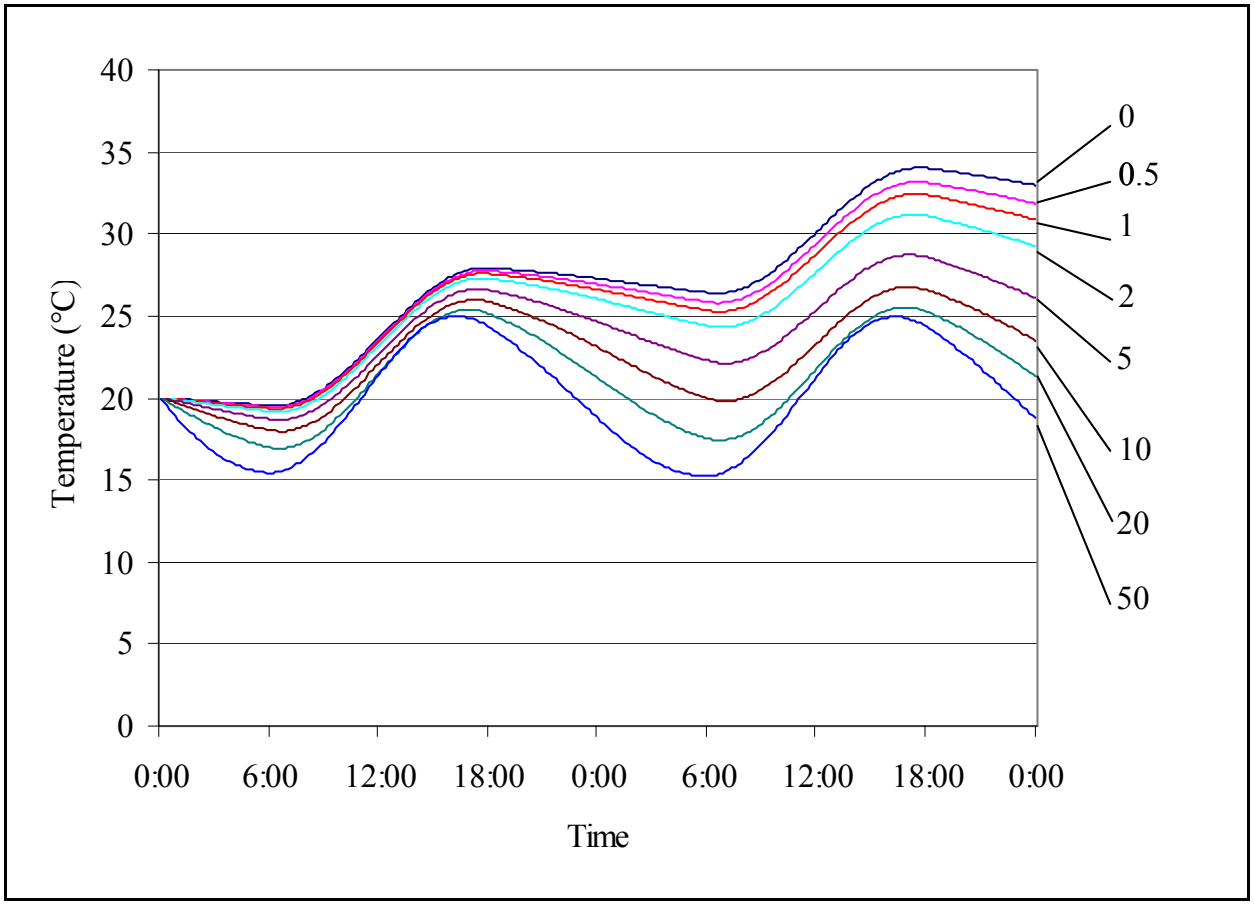

Figure 6.9: Each curve represents a model run with a different wind speed (shown on the right hand side of the graph; values in m/s). Increasing the wind speed increased night time evaporation (for instance, after 48 hours, evaporation energy losses increased from 92 W for a wind speed of 0.5m/s to 761 for wind speed of 50 m/s). This in turn reduced the pond temperature.

50 m/s, convection increased from 6 W to 336 W but the pond temperature decreased from 23.3°C to 21.3°C. This is because increasing the wind speed increased night time evaporation (from 401 W to 761 W at midnight, on Day 2) and caused the pond temperature to fall (see Figure 6.9).

Increasing the wind speed beyond 20 m/s had an additional effect: the pond temperature peaked earlier in the day. Because there was no evaporation, air convection became an un-checked heat transfer mechanism causing the pond temperature to rise more quickly. Between 8:00 and 10:00, the pond temperature changed by 1.6°C for a wind speed of 20 m/s. For the same time period but for a wind speed of 50 m/s, the pond temperature changed by 2.3°C.

The model's sensitivity to wind speed is dependant on wind speed itself and time. The model's sensitivity to wind speed cannot be quantified analytically because evaporation, which is indirectly affected by the pond temperature, does not have any temperature terms in its defining

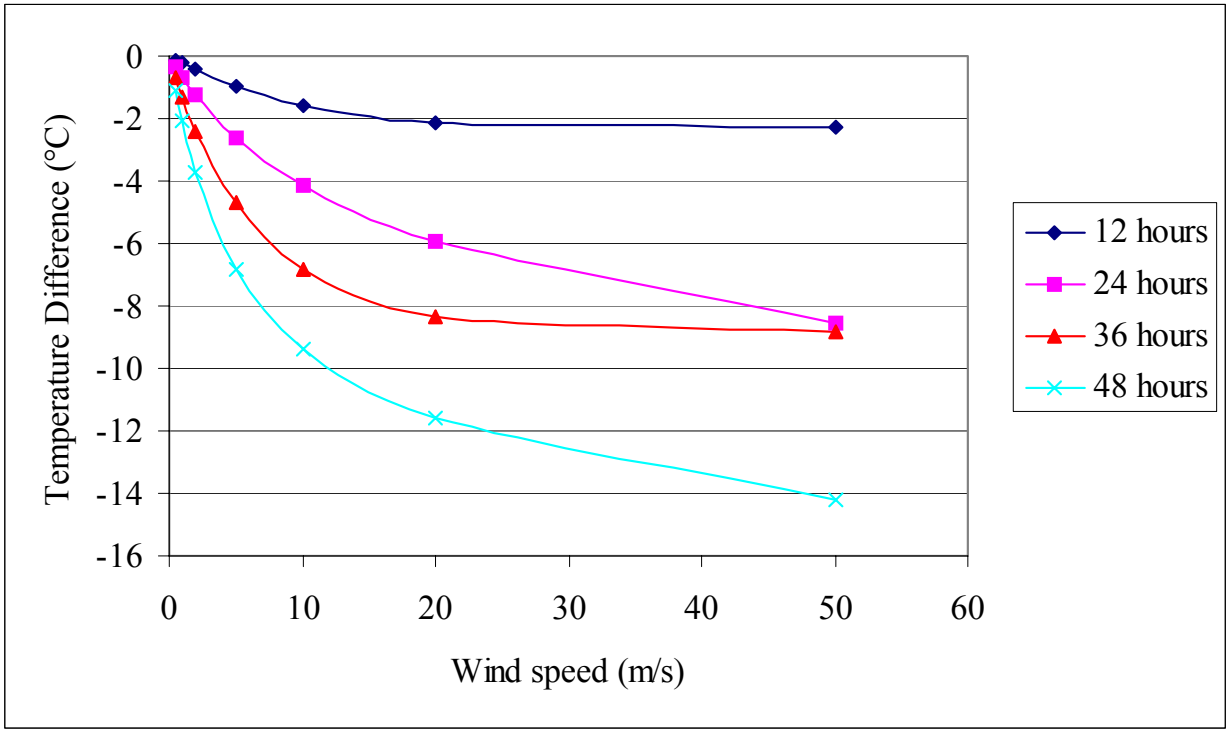

Figure 6.10: Sensitivity curves fitted as associated exponential functions decayed with time. The slopes of these curves (an exponential function with a negative exponent) were greatest for low wind speeds. Increasing the wind speed beyond 20 m/s during the day yielded little response from the model. The daytime curves are different from the night time curves because of high wind speeds during the day warm the pond.

equation. When analytically solving a simplified version of Equation 3.4, as was done for the sensitivity analysis for solar radiation, evaporation would be treated like a constant when in reality, the liquid water vapor pressure term in the Lake Hefner Equation (the equation used to predict evaporation), is dependant on temperature. Substitutions of the vapor pressure terms with pond temperature terms make the "simplified" equation too complex to solve analytically.

Curve fitting techniques were attempted using Curve Expert (Hyams, 2001) in order to get an empirical equation to describe the curves in Figure 6.10. The derivative of this equation with respect to wind speed is the model's sensitivity to wind speed. All curves were fitted to an exponential associated of the form:

$$\Delta T = a\left(1 - e^{-bv}\right) \tag{6.9}$$

where ΔT is the difference between the standard pond temperature and the trial pond temperature for a fixed time (°C),
v is the wind speed (m/s) and

a and b are arbitrary statistical constants determined by curve expert (values in Table 6.6)

The derivative of Equation 6.9 with respect to wind speed is:

$$\frac{d(\Delta T)}{dv} = abe^{-bv} \tag{6.10}$$

All parameters (a and b) for each curve in Figure 6.10 as well as the correlation coefficient r are shown in Table 6.6.

Table 6.6: The parameters for Equations 6.9 and 6.10, shown here, are used to quantify the model's sensitivity to wind speed. The correlation coefficient r represents how well the data fit equation 6.9.

Time (hr)	a	b	r
12	-2.310552	0.113607	0.999
24	-8.802606	0.062419	0.998
36	-8.763092	0.154033	0.999
48	-13.50179	0.129852	0.992

Substituting the parameters from Table 6.6 into Equation 6.10 yields the curves shown in Figure 6.11. For each time, one curve represents the model's sensitivity, calculated from Equation 6.10, as a function of wind speed. For all times considered, the model's sensitivity with respect to wind speed decreased absolutely as the wind speed increased. Increasing the wind speed for all times beyond 20 m/s yielded changes in temperature less than 0.2°C. No relationship was sought between the model's sensitivity to wind speed and time, despite the fact that time does have an impact.

6.3.4 Variations in Flow - Warm Water (36°C)

Increasing the flow of warm water increased the rate the pond temperature warmed between 0 and 6 AM on Day 1 (see Figure 6.12). The warm water was shut off for the morning and the solar radiation from that point on was responsible for warming up the ponds. In Figure 6.12, there is a discontinuity in all the curves (except for the standard curve) at 6.00 AM, reflecting the change in how the pond was being heated. During the first night, the pond temperature changed at a rate between 0.0015 °C/hr (trial 22, flow rate = 8.33×10^{-6} m^3/s) and 0.082 °C/hr (trial 20 , flow rate = 2.08×10^{-6} m^3/s). The small changes in temperature over 12 hours shows how during the first complete night (between 18:00 on Day 1 and 6:00 on Day 2), the energy gained by the pond through incoming warm water was balanced out by the energy lost through other energy

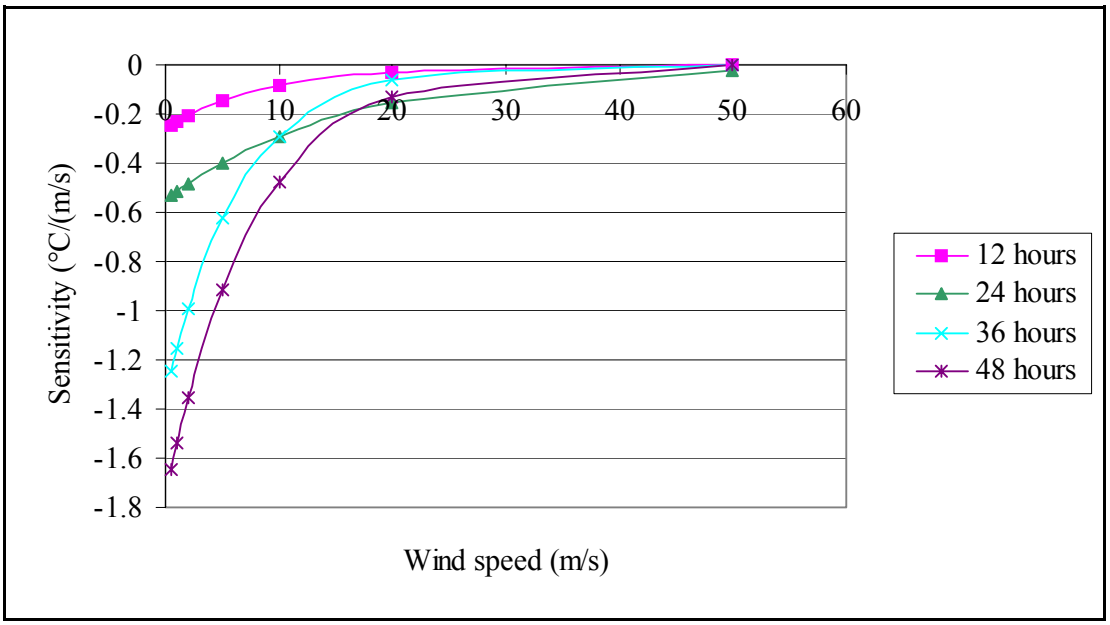

Figure 6.8: The sensitivity to wind speed was absolutely greatest for low wind speed changes. The sensitivity also increased as time progressed. As the wind speed increased beyond 20 m/s, the sensitivity was less than 0.2°C/(m/s).

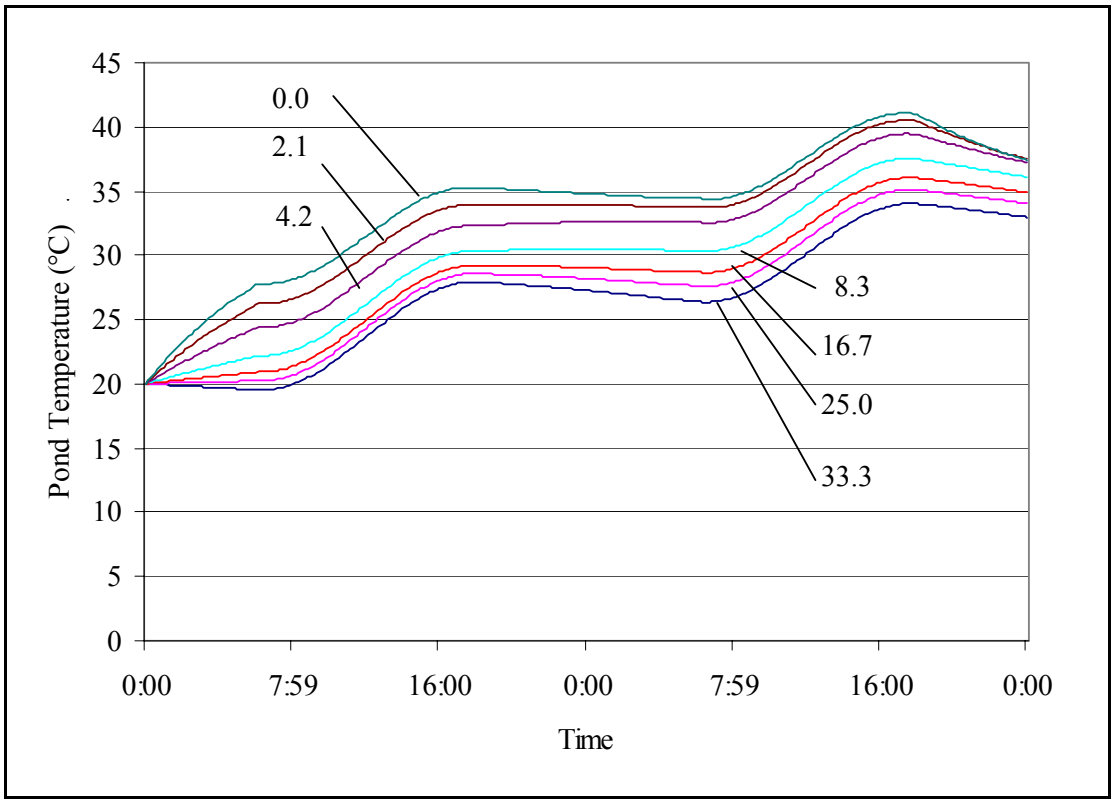

Figure 6.9a: The pond temperature increased with respect to the standard as the flow of warm water (36°) increased into the pond. The flow rates in the legend are set to 10^{-6} $(m^3/s)/m^3$ of pond volume.

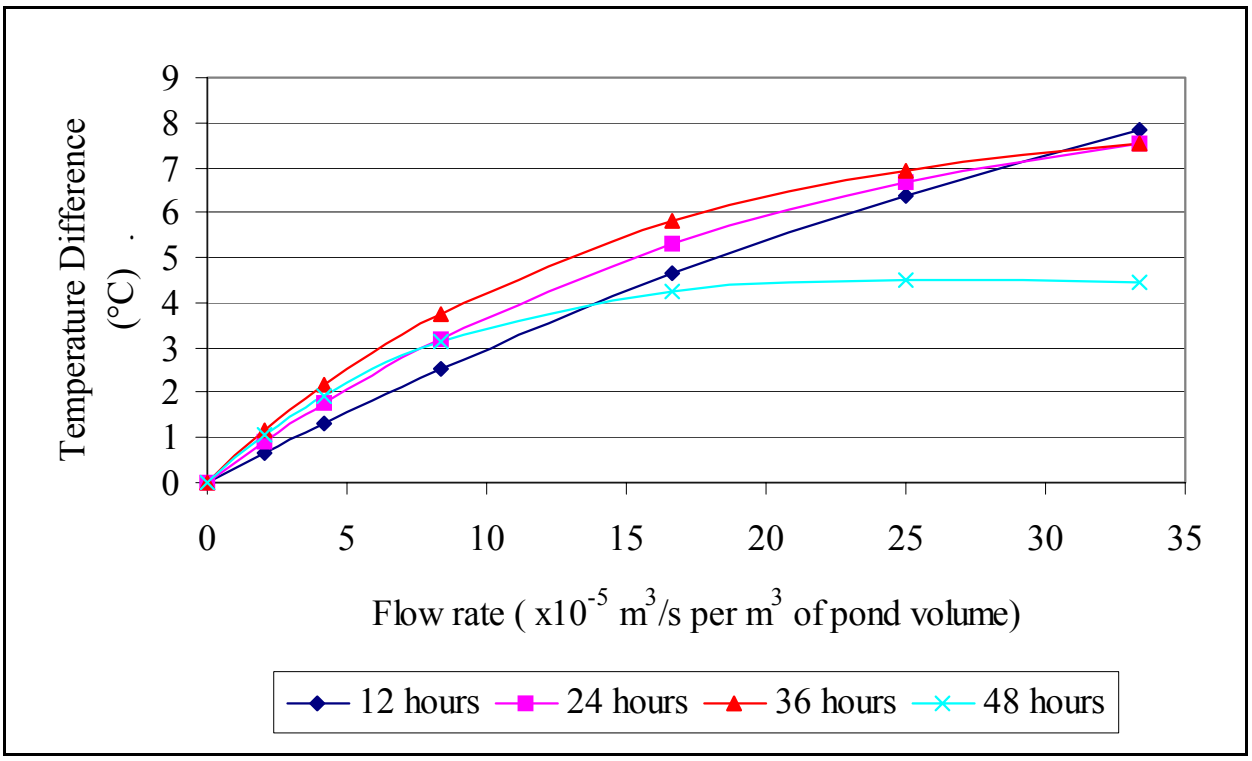

Figure 6.13: Sensitivity curves for warm water flow rates were generated by plotting the temperature difference between the standard and the trial model runs at 12, 24, 36 and 48 hours. When using Curve Expert, these curves were found to fit very well (r = 0.999) an associated exponential curve.

transfer mechanisms, as well as the energy lost to the water leaving the pond (see Figure 6.14). Therefore, increasing the flow rate of warm water, in this case, did very little in changing the temperature. The slopes of the sensitivity curves (see Figure 6.13) reflected this. Qualitatively, the slopes became smaller as the flow rate increases. Curve fitting was done to obtain an empirical equation to describe each curve. All 4 curves were described with the following general exponential association equation:

$$\Delta T = a\left(1 - e^{-b\dot{\forall}}\right) \tag{6.11}$$

where V' is the flow rate $((m^3/s)/m^3)$

Taking the derivative with respect to the flow gave the function for the model's sensitivity with respect to flow:

$$\frac{d(\Delta T)}{d\dot{\forall}} = abe^{-b\dot{\forall}} \tag{6.12}$$

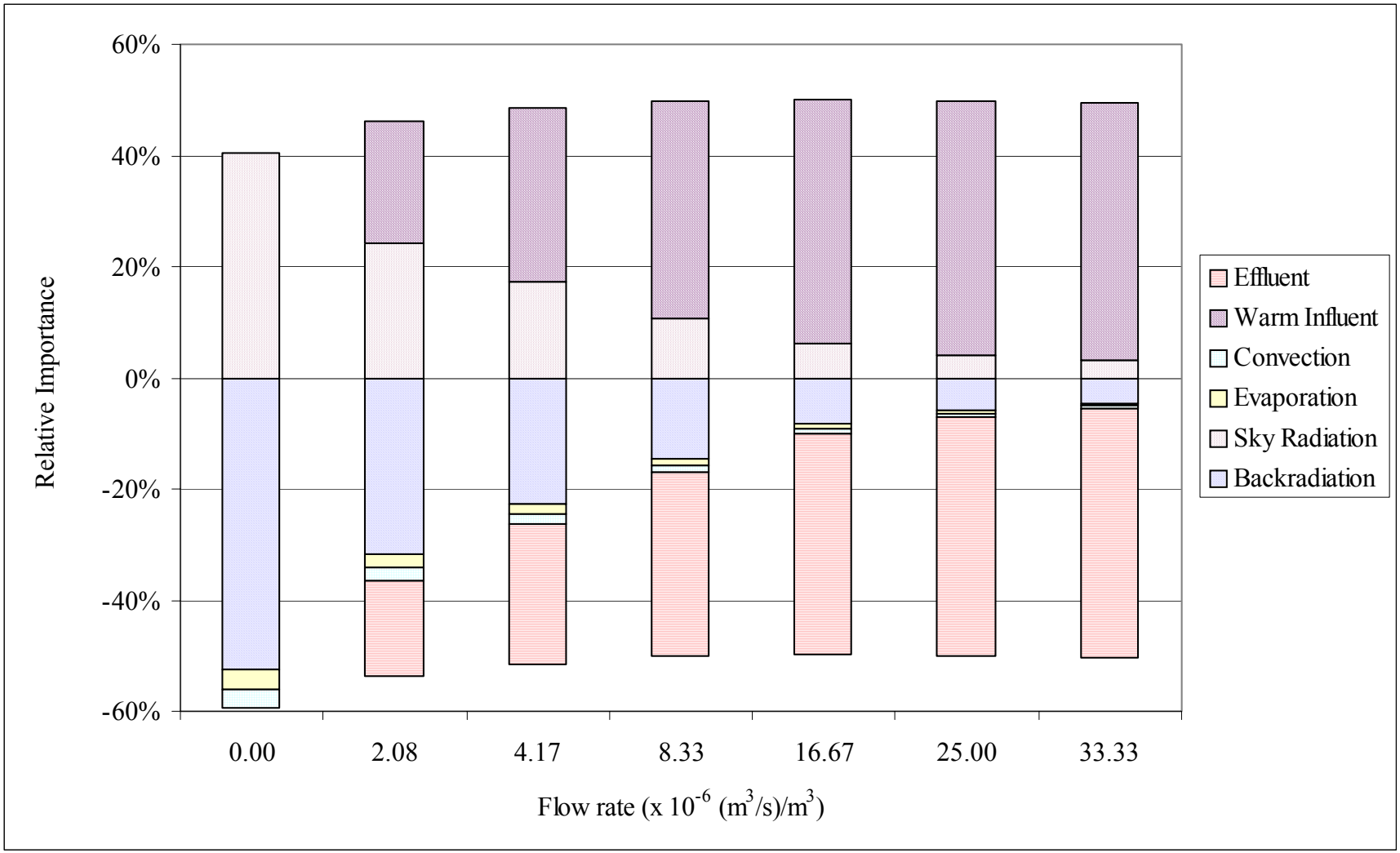

Figure 6.10: Each bar shows the relative importance of each energy transfer vector for a specific flow rate at 24:00 (midnight on Day 1. As flow increased, the relative importance of long wave radiation heat transfer diminished. The importance of evaporation and convection became negligible as the flow of warm water increased.

The value of the parameters in Equations 6.11 and 6.12 as well as the correlation coefficient were calculated with Curve Expert (Hyams, 2001) and are listed in Table 6.6.

Table 6.6: The parameters (a, b) for Equations 6.11 and 6.12, describing the model's sensitivity to warm-water flow, were determined with Curve Expert (Hyams, 2001). The correlation coefficient r represents how well the dat fit Equation 6.11.

Time (hr)	a	b	r
12	14.9	22340	0.999
24	9.2	51564	0.999
36	8.3	72658	0.999
48	4.6	13467	0.999

The basic equation used to fit the nighttime data (Equation 6.11) is somewhat consistent with the theory. Consider the simplified situation where the only energy transfer mechanisms are those associated with flow. In other words, there is no convection, no evaporation, no solar radiation, no sky radiation and no back radiation. Equation 3.4 simplifies to:

$$\rho c_p \forall \frac{dT}{dt} = \rho c_p \dot{\forall} \left(T_{in} - T \right) \tag{6.13}$$

where T_{in} is the temperature of the inlet water (°C).

Solving this differential equation yields:

$$T = T_{in} \left(1 - e^{-\dot{\forall} t / \forall} \right) + T_i e^{-\dot{\forall} t / \forall} \tag{6.14}$$

The first term in Equation 6.14 is in the exact form of Equation 6.11, the basic equation used to describe the sensitivity curves. The nature of the second term in Equation 6.14 ($T_i e^{-\forall' t/\forall}$) remains unexplained.

The model's sensitivity to flow was quantified with the use of Equation 6.12 and Table 6.6. Results are shown graphically in Figure 6.15. For all times, increasing the flow decreased the model's sensitivity. Time does have an effect on the model's sensitivity to flow but no attempt was made to relate time to sensitivity. Although the data did fit the general formula common to both Equation 6.11 and Equation 6.14, the curves in Figure 6.15 describing the model's sensitivity to flow during the daytime did not truly represent the analytical formula. This is because the main input of energy during the day was solar radiation (as much as 51% during the

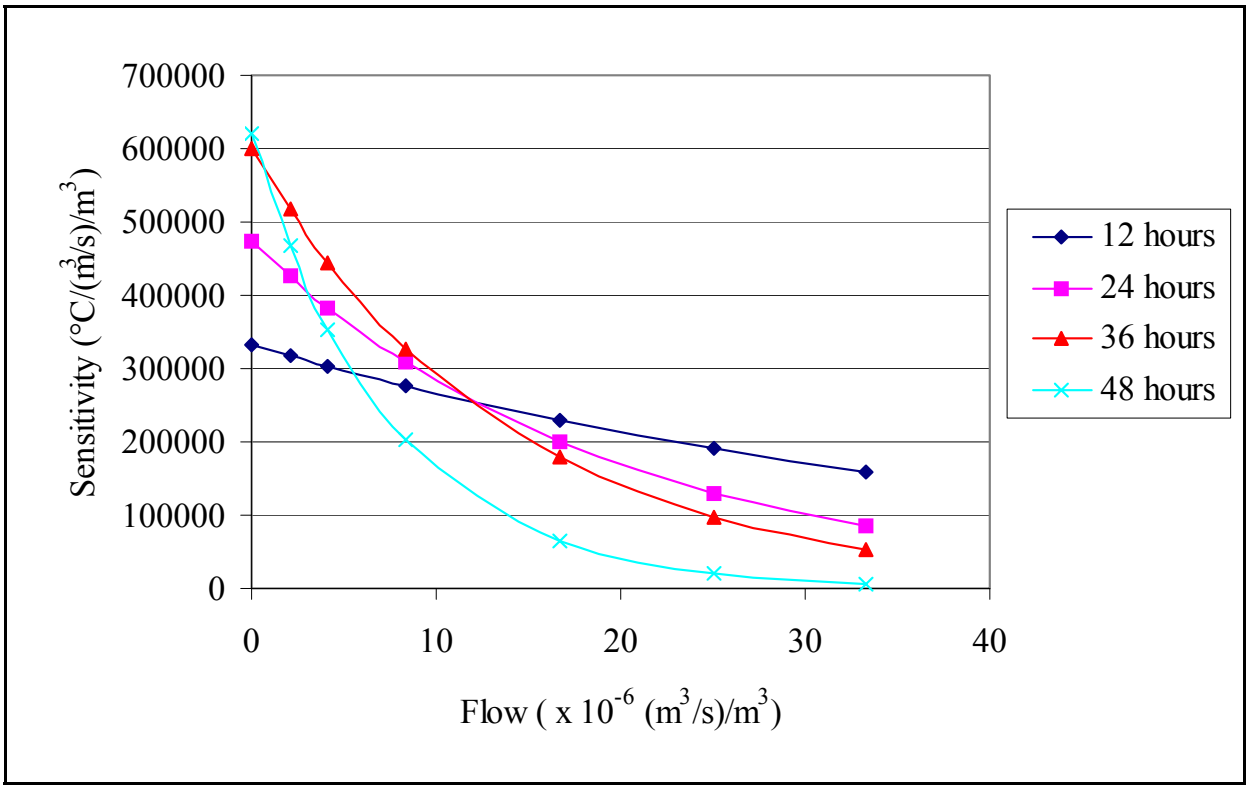

Figure 6.15: The model's sensitivity to warm water flow rates decreased exponentially as the flow increased, illustrating how the sensitivity was dependant on the flow rate.

day), not flow (0% during the day). Therefore, Equation 6.13 is not valid and its solution, Equation 6.14, did not analytically represent the daytime situation.

6.3.5 Variations in Flow - Cool Water (15°C)

Increasing the flow of cool water (15°C) to the pond decreased the pond temperature with respect to the standard model run (see Figure 6.16). The pond temperature after 48 hours for the standard was 33.0°C while the temperature of the pond after 48 hours for trial 31 (flow = 3.33 x 10^{-5} m^3/s) was 20.0°C, a difference of 13°C.

Depending on the flow rate, the cool water removed the energy gained by the pond during the day from solar radiation. The night time low for trial 31 was 17.1°C on the first night and 17.1°C on the second night. The night time low for trial 30 (flow = 2.5 x 10^{-5} m^3/s) was 17.6°C on the first night and 18.2°C on the second night an increase in 0.6°C. This increase demonstrates that the flow of cold water is barely removing all the solar energy gained during the course of the day.

The rate at which the temperature decreased in the ponds during the night was also dependant on the flow rate. For the first night, the lowest flow regime (trial 26, flow = 2.08 x 10^{-6} m^3/s) caused

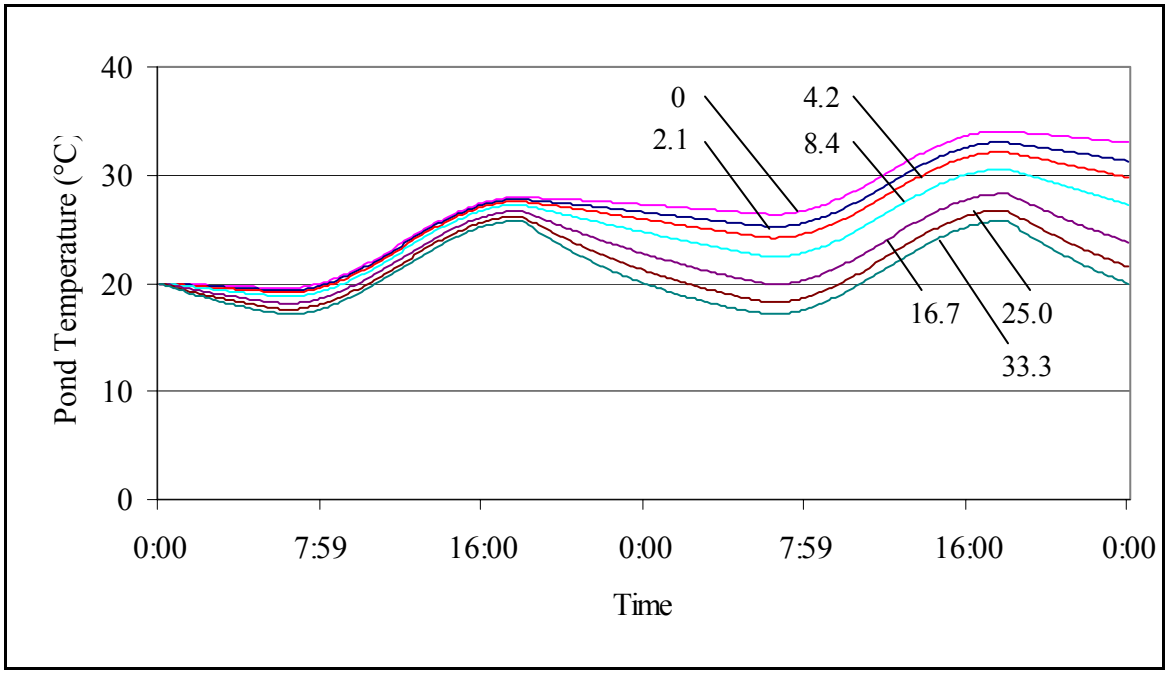

Figure 6.16: The pond temperature decreased as the flow of cool 15°C water increased. The numbers in the legend are flow readings and have the units 10^{-6} $((m^3/s)/m^3)$. Only one flow rate (flow rate = 33.3 x 10^{-6} $(m^3/s)/m^3$ was able to remove all the solar energy gained by the pond.

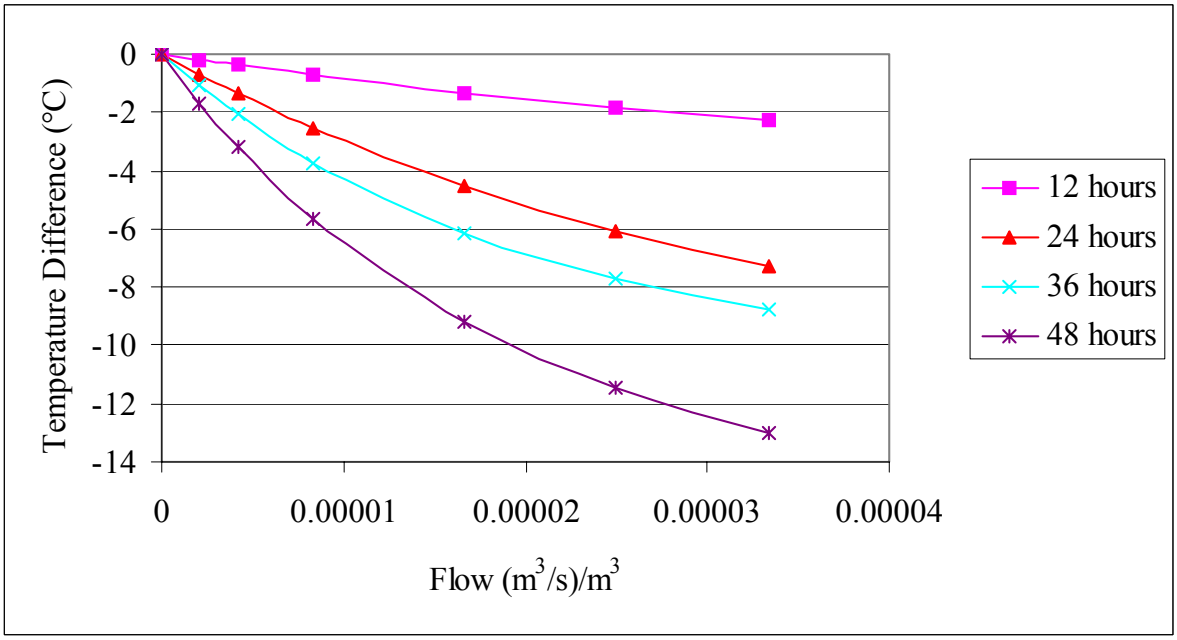

Figure 6.17: Changes in the model's output when compared with changes in cool water flow increased absolutely with flow and time. The shape of these associated exponential curves partially agrees with the theory.

the pond to cool at a rate of 0.21°C/hr whereas for the highest flow regime (trial 31), the rate the pond cooled was 0.70°C/hr. The difference between the pond temperature for the trials and the standard increased as the flow of cold water increased (see Figure 6.17). As time progressed, the temperature difference between the trials and the standard also increased. Increasing the flow from 0 m^3/s to 3.33 x 10^{-5} m^3/s increased the temperature difference between the standard and the trials by 2.3°C after 12 hours and 13.0°C after 48 hours.

Again, the model's sensitivity to flow was quantified by fitting the data in Figure 6.17 to Equation 6.11, using Curve Expert (Hyams, 2001). Parameters in Equation 6.11 for the cool water model runs as well as the correlation coefficient are shown in Table 6.7

Table 6.7: Parameters (a, b) used in Equation 6.12 determined the model's sensitivity to cold water flow. The correlation coefficient r represents how well the data fits Equation 6.11.

Time (hr)	a	b	r
12	4.4	22285	0.999
24	11.4	30615	0.999
36	10.7	51095	0.999
48	15.4	54781	0.999

The model's sensitivity to cool water flow (shown in Figure 6.18) decreased as the flow rate increased. For instance, after 24 hours, the sensitivity dropped from 348 712°C/(m^3/s)/m^3 to 125 682°C/(m^3/s)/m^3. Changes in sensitivity were greatest at 48 hours (708 805 °C/(m^3/s)/m^3) and smallest at 12 hours (51 100°C/(m^3/s)/m^3). Although this shows that time does have some impact on the model's sensitivity to flow, no relationship between time and sensitivity was sought. This is because Equation 6.11, although empirically accurate in fitting the data in Figure 6.17, is not the proper simplified solution to Equation 3.4. In other words, the curves describing the model's sensitivity to flow during the daytime do not reflect the fact that there was no flow during the daytime.

6.3.6 - Overall Conclusions from the Sensitivity Analysis

For the aquaculturist, the sensitivity analysis is as an opportunity to determine which factors have a greater effect in controlling the pond temperature. By comparing the model's sensitivity to air temperature, solar radiation, wind speed and warm or cool water flow rates, factors which are important in controlling pond temperature should become obvious. However, there are problems with direct comparisons of the numerical values for sensitivity:

- Sensitivity was a function of time. Comparisons between the sensitivity for variations of two different parameters, for example air temperature and wind speed, could only be done

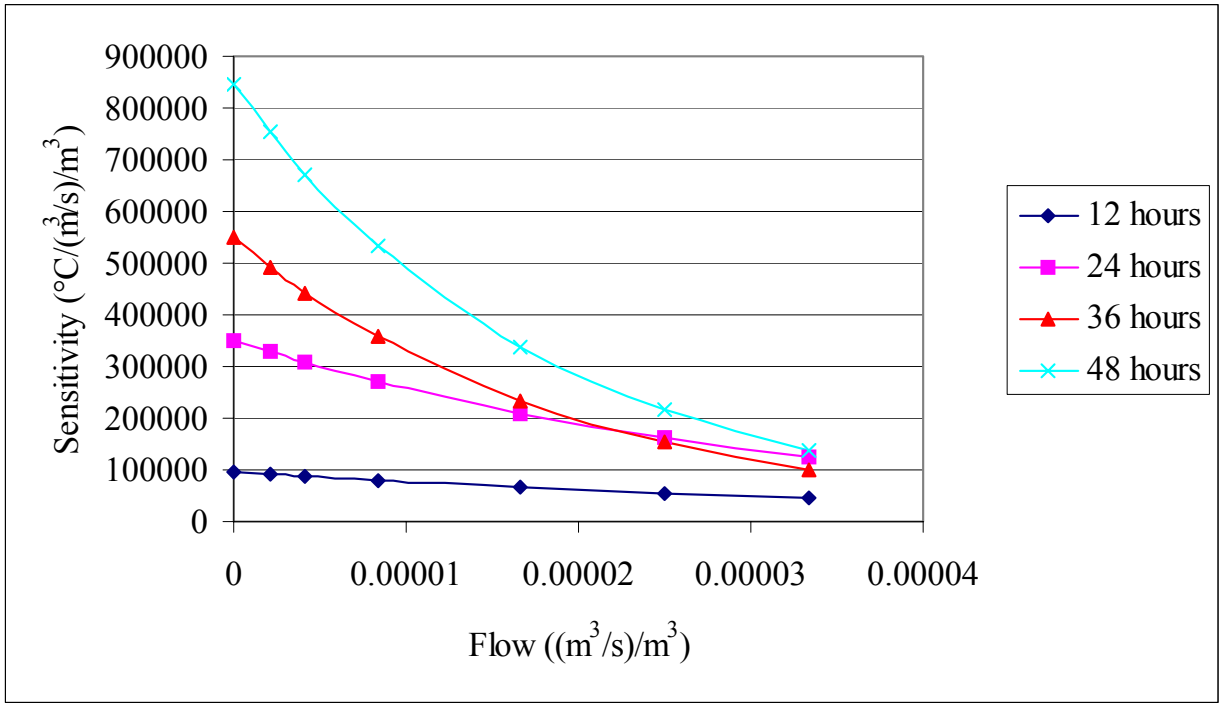

Figure 6.18: The model's sensitivity decreased exponentially as the flow rate of cool water increased. Therefore, changing the flow for low flows had a greater impact on the model's sensitivity. A relationship between the model's sensitivity to flow and time cannot be found because the 24 hour curve and the 36 hour curve crossed.

forgiven time, since for all trials, as time increased, the sensitivity also increased.

- Sensitivity, in some cases, was a function of the parameter varied. This applied to parameters where the derivative to the general equation used to fit the data in the sensitivity graphs (Figures 6.3, 6.6, 6.10, 6.13, 6.17) were dependant on the varied parameter. For variations in air temperature and solar radiation, a straight line was used to relate changes in the output to changes in the input. The derivative of a straight line (and therefore, the model's sensitivity to that particular parameter) was a constant. Therefore, for variations in air temperature and solar radiation, the model's sensitivity was not a function of these parameters. However, this was not the case for variations in wind speed and flow rates. For wind speed, the derivative of the general equation used to fit the data in Figure 6.10 (Equation 6.9 is the curve of best fit, Equation 6.10 is Equation 6.9's derivative) was still a function of wind speed. Likewise, for variations in flow rates of warm or cool water, the derivative of Equation 6.11, Equation 6.12, remained a function of the flow rate. Therefore, when comparing the model's sensitivity for different variable inputs, certain variables must be held fixed.

- The units for various sensitivity measurements were different. You cannot compare apples to oranges. Similarly, comparisons between sensitivity values with units °C/°C,

°C/Wattt, °C/(m/s) or °C/(m^3/s)/m^3 were not possible because each sensitivity value was measuring something different.

For these reasons, direct quantitative comparisons of sensitivity values were not possible. However, comparisons were possible if absolute variations in input were set at a specific value. For example, no comparison between the model's sensitivity to air temperature (0.00695°C/°C/hr) and the model's sensitivity to solar radiation (0.0029°C/Watt/hr) could be made. However, a comparison could be made between a change in air temperature of +5°C for 12 hours (absolute change in output = 0.417°C) and a reduction of 25% of the maximum solar radiation for 12 hours (absolute change in output = -1.078°C). In this case, changing the solar radiation had more of an effect in changing the pond temperature. So, in this case, the model's sensitivity to changes in solar radiation was greater than the model's sensitivity to changes in air temperature.

By doing such comparisons for specific set parameters, it becomes possible to tell which parameters have a greater effect on the model's output, especially if those set parameters are set to extreme cases.

Changing the average air temperature did relatively little affecting the pond temperature, when compared to variations in other input parameters. According to the theory, a change in the air temperature should directly affect convection because the temperature gradient between the pond and the air increases. Lowering the average air temperature to 0°C after 48 hours (absolute change in output = 6.3°C) was not as effective as increasing the wind speed from 0 to 10 m/s (or 0 to 22.4 mph) (absolute change in output = 9.4°C) or increasing the flow rate of cool 15°C water from 0 to 1.67 x 10^{-5} (m^3/s)/m^3 (absolute change in output = 9.2°C). Because the suggested variations in flow or wind speed were much more realistic than the suggested variations in air temperature for Baton Rouge, Louisiana, an aquaculturist, from that area, trying to keep the pond temperature artificially high, should be more concerned about windy nights rather than a cool nights.

Solar radiation, when left unbalanced, caused large increases in pond temperature. Over 48 hours, the difference in pond temperature for the standard model run (100% solar radiation, pond temperature = 33.0°C) and the trial run with no solar radiation (pond temperature = 18.5°C) was 14.5°C. A pond temperature of 18.5°C is more realistic than a pond temperature of 33°C. However, the scenario which made the pond temperature "realistic" was in itself unrealistic. Therefore, two observations can be drawn from this:

- Solar radiation was an important energy vector, since it can theoretically, when left unchecked, cause the pond temperature to increase by 13°C in 2 days. This increase was even more pronounced for the trial runs where the flow rate for the warm water (36°C) was varied. In this case, for a flow rate of 3.33 x 10^{-5} (m^3/s)/m^3, the pond temperature increased by 17.4°C in 48 hours.

- Solar radiation, for unheated ponds, had to be balanced, either by one or a combination of negative energy vectors. Such energy vectors included evaporation, where increasing the wind speed from 0 to 2 m/s decreased the standard pond temperature by 13.4°C to a pond temperature of 19.5°C. This underlines the importance of evaporation as a prominent energy transport mechanism.

The sensitivity analysis, although insightful, failed to determine the model's sensitivity to interacting parameters (Saltelli, 2000). This is the main drawback of the "one at a time" type of sensitivity analysis. For instance, increasing wind speed while decreasing solar radiation would have caused the model's output to change differently from the standard. Other techniques do exist and are described in detail in Saltelli, Chan and Scott (2000).

6.4 Conclusions

A sensitivity analysis was performed on PHATR Version 1.2. Four parameters were varied one at a time to determine how sensitive the model's output was to changes in the input. These four parameters were 1) average air temperature, 2) solar radiation, 3) wind speed and 4) flow rate of inlet water. Another goal of the sensitivity analysis was to determine certain counter-intuitive phenomena present under different scenarios.

The sensitivity was described as the derivative of the relationship between the output (y-axis) and the input (x-axis). In this way, the sensitivity was quantified.

For variations in the average air temperature, the pond temperature varied linearly for a fixed time (slope = derivative = sensitivity = 0.10 °C/°C at 12 hours to 0.35°C/°C at 48 hours). The sensitivity also varied linearly with time (0.00695 °C/°C/hr).

Similarly, variations in solar radiation caused the pond temperature to vary linearly as well. In this case, both the slope and the intercept for each sensitivity curve (line) was calculated. The sensitivity ranged from 0.041 °C/W (at 12 hours) to 0.154 °C/W (at 48 hours) and varied linearly with time, according to the equations presented in Figure 6.7

The sensitivity varied linearly with time only because time steps of 12 hours were chosen. Had any other time step been chose, the sensitivity would not have varied linearly.

Increasing the wind speed increased nighttime evaporation, which caused the ponds to cool down. This made the pond cooler than the air during the day. In doing so, the air vapor pressure became greater than the water vapor pressure (thus preventing evaporation from occurring). Furthermore, the air through convection warmed the pond. This explains why the pond temperature did not decrease further during the day for increased wind speeds (see Figure 6.9).

The model's sensitivity to wind speed was calculated by taking the derivative of the equation which best fit the sensitivity curves in Figure 6.10. An associated exponential function was used

to fit the data in all four cases. The model's sensitivity was again dependant on time, although no relationship between time and the parameters for the associated exponential function was sought.

Increasing the flow rate of warm water to the pond increased the pond temperature and increasing the flow rate of cool water to the pond decreased the pond temperature. An exponential association was found to be the curve of best fit between the standard trial pond temperature difference and the flow rates. An exponential association is very similar to the simplified theoretical solution of the energy balance equation (Equation 3.4). The model's sensitivity to flow was calculated by taking the derivative of the exponential association equation and substituting in the statistically determined constants.

By knowing the model's sensitivity to variations in input, the output error associated with faulty input data can be estimated using the sensitivity curves and relations presented here. Although the curves cannot directly predict errors in the model output, they can generate an idea of how the model's output will change. Furthermore, the sensitivity analysis was an other way of determining which energy transfer mechanisms were important. Because the inherent errors in the empirical equations used by PHATR cause errors in the output, the sensitivity analysis revealed how important these errors might be.

CHAPTER 7 - USING PHATR FOR DESIGN AND MANAGEMENT APPLICATIONS

7.1 Introduction

PHATR, a computer model which solves 3.4, the differential equation describing the energy balance for a small (volume = 400 m^3) well-mixed aquaculture pond (see Chapter 4), was specifically designed to determine the pond temperature for the "warm water ponds" at the Louisiana State University (LSU) Aquaculture Research Station (ARS). It was also meant to be used as a design tool for engineers or as a management tool for aquaculturists for the warm water ponds. Because the model still needs to be validated for larger ponds or ponds in different climates, PHATR should not be used by engineers or aquaculturists for the following types of ponds:

- ponds located in a climate different from that experienced in Louisiana
- ponds which are poorly mixed
- ponds which are much larger than 400 m^3
- ponds where there is little recorded information about the weather.

However, for the warm water ponds at the Louisiana State University Aquaculture Research Station (LSU ARS), PHATR has been validated and was used to answer these design and management questions:

1) What is the pond temperature throughout a year?
2) What is the energy surplus or deficit when keeping the pond temperature constant?
3) By how much does the temperature decrease in one night if there is suddenly no way to keep the pond warm?
4) What are the flow requirements for increasing the pond temperature by 2°C/day during a typical week in January?

7.2 Materials and Methods

PHATR Version 1.2 was used with these added features:

- The effects of rainfall were included as a bulk movement of energy into the pond (see Chapter 3.5.1 for theoretical explanations).
- For a given pond temperature (given in a ASCII file), PHATR could calculate the amount of cold and warm water needed to maintain the pond a that temperature. The user specified the temperature of the cold and warm water sources at the user prompt.

Weather data were compiled and generated to produce three weather input files, one for a cold year, one for an average year and one for a hot year. All the data used to create the weather files, with the exception of solar radiation, were supplied by the Southern Regional Climate Center at LSU.

The air temperature, relative humidity and wind speed data used in each file were compiled from weather data collected between 1952 and 1992 in Baton Rouge every hour, except between 1965 to 1972, where the data were collected every 3 hours. No wind speed data were collected prior to 1964. Using a FORTRAN program called "Weather_Generator(a)" (code in Appendix 13), the data were sorted to determine the following weather statistics:

- the maximum temperature of every hour of the year
- the minimum temperature of every hour of the year
- the average temperature of every hour of the year
- the average relative humidity of every hour of the year
- the average wind speed of every hour of the year

The normal rainfall data for every day of the year were converted into average hourly rainfall rates. For instance, if 24 cm of rain fell in a day, it was assumed that 1 cm of rain fell every hour during that day.

Because no solar radiation data for every hour of the year was available, the extra-terrestrial solar radiation was calculated depending on the pond's geographic location, the time of day and the time of year (Appendix 14). A "cloud" factor was multiplied by the solar radiation data to simulate the absorption of solar radiation by the atmosphere. The cloud factor was equal to 0.85 for a hot year and 0.25 for a cold year. For the average year weather data file, the average percentage of total solar radiation for a particular month was used as the cloud factor. The average percentage of total solar radiation was available through the Southern Regional Climate Center web site (http://www.srcc.lsu.edu/6190/ccd.html).

The "average year" data set consisted of :

- the average temperature of every hour of the year
- the average relative humidity of every hour of the year
- the average wind speed of every hour of the year
- the solar radiation for the average year
- the normal rainfall

The "cold year" data set consisted of:

- the minimum temperature of every hour of the year
- the average relative humidity of every hour of the year
- a constant wind speed of 10 m/s
- the calculated solar radiation with a cloud factor of 0.25
- the normal rainfall

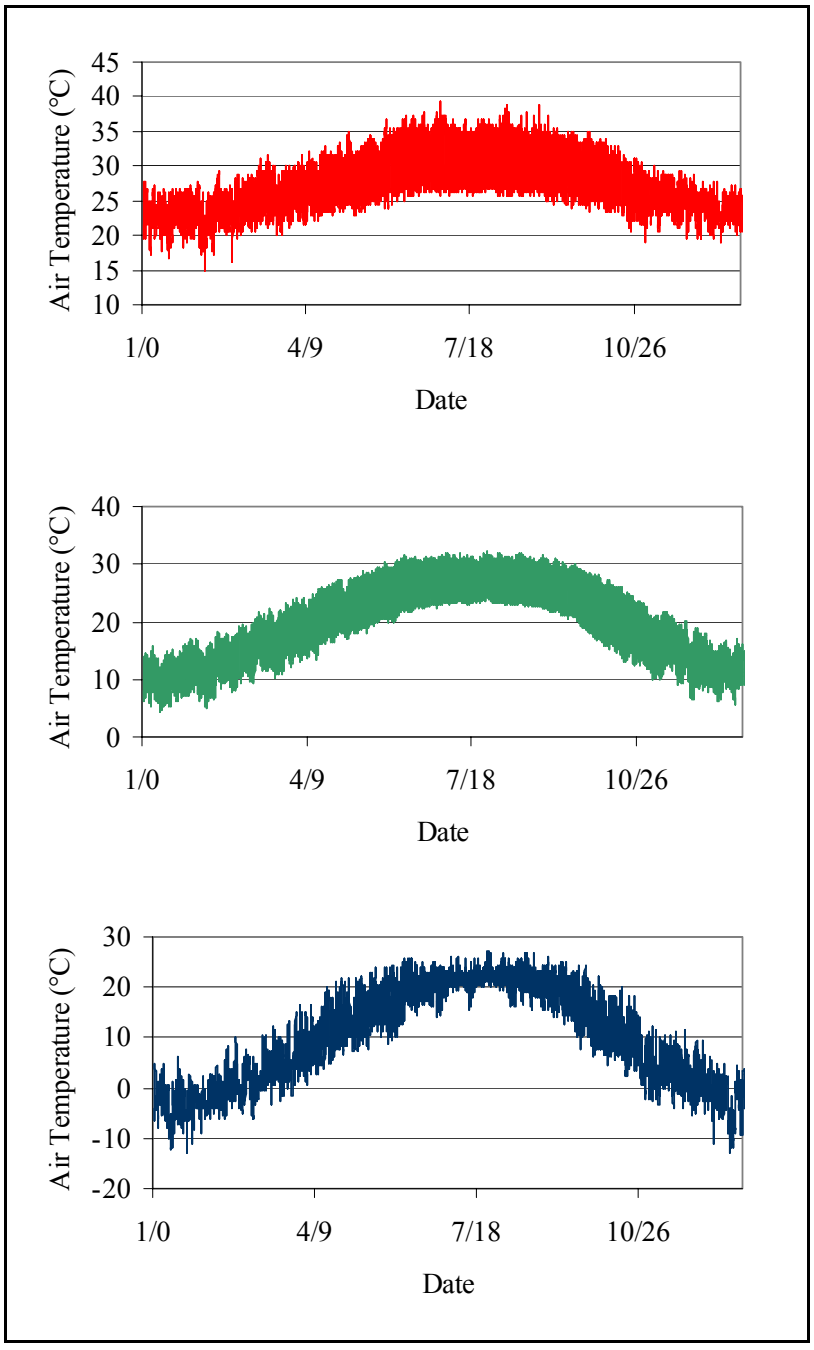

Figure 7.1: These are the maximum (top), average (middle) and minimum (bottom) air temperature compiled from hourly data collected between 1952 and 1992 for Baton Rouge, Louisiana.

The "hot year" data set consisted of:

- the maximum temperature of every hour of the year
- the average relative humidity of every hour of the year
- a constant wind speed of 0 m/s
- the calculated solar radiation with a cloud factor of 0.85
- the normal rainfall

The air temperature for all 3 model years is shown in Figure 7.1.

65 different model runs were performed in order to answer the four original questions. Trials 1, 2, and 3 were used to predict the pond temperature over an average, cold and hot year for an average warm water pond (volume = 400 m^3, area = 329 m^2). Trials 31, 32 and 33 were used to predict the pond temperature for average, cold and hot years for normalized ponds (volume = 1 m^3, area = 1 m^2). For each of these model runs, a step size of one hour was used.

Trials 4 to 30 (for 400 m^3 ponds) and trials 34 to 57 (for 1 m^3 ponds) were used to determine the surplus or deficit of energy throughout a cool, average or warm year. For these trials, the temperature of the cold inlet water was set to either 10 or 20°C. The temperature of the warm water inlet was always set to 36°C. The temperature of the pond was set to 15, 20, 25, 30 or 35°C (see Table 7.1 for details for each model run). For each trial,

Table 7.1: These are all the model runs used to determine the energy requirements for ponds kept at specific temperatures, depending on the type of year (hot, cold, average). "Natural" pond temperature listings refer to trials where the pond temperature was not controlled. For these ponds, the temperature of the hot or cold water influent was not necessary.

Trial	Pond Temperature (°C)	Year	Temperature of Inlet	
			Hot Water	Cold Water
1	Natural	Cold	---	---
2	Natural	Average	---	---
3	Natural	Hot	---	---
4	15	Cold	36	10
5	15	Average	36	10
6	15	Hot	36	10
7	20	Cold	36	10
8	20	Average	36	10
9	20	Hot	36	10
10	25	Cold	36	10
11	25	Average	36	10
12	25	Hot	36	10
13	30	Cold	36	10
14	30	Average	36	10
15	30	Hot	36	10
16	35	Cold	36	10
17	35	Average	36	10
18	35	Hot	36	10
19	20	Cold	36	20
20	20	Average	36	20
21	20	Hot	36	20
22	25	Cold	36	20

Table 7.1: continued

Trial	Pond Temperature (°C)	Year	Temperature of Inlet	
			Hot Water	Cold Water
23	25	Average	36	20
24	25	Hot	36	20
25	30	Cold	36	20
26	30	Average	36	20
27	30	Hot	36	20
28	35	Cold	36	20
29	35	Average	36	20
30	35	Hot	36	20
31	Natural	Cold	36	---
32	Natural	Average	36	---
33	Natural	Hot	36	---
34	15	Cold	36	10
35	15	Average	36	10
36	15	Hot	36	10
37	20	Cold	36	10
38	20	Average	36	10
39	20	Hot	36	10
40	25	Cold	36	10
41	25	Average	36	10
42	25	Hot	36	10
43	30	Cold	36	10
44	30	Average	36	10
45	30	Hot	36	10

Table 7.1: continued

Trial	Pond Temperature (°C)	Year	Temperature of Inlet	
			Hot Water	Cold Water
46	35	Cold	36	10
47	35	Average	36	10
48	35	Hot	36	10
49	25	Cold	36	20
50	25	Average	36	20
51	25	Hot	36	20
52	30	Cold	36	20
53	30	Average	36	20
54	30	Hot	36	20
55	35	Cold	36	20
56	35	Average	36	20
57	35	Hot	36	20

the energy surplus or deficit was calculated for every hour of the year. By knowing the energy surplus or deficit, the amount of cold or warm water needed to maintain the pond temperature constant was calculated. Trial 58 was used to find out how much warm geothermal well water would be needed on a cold January night to keep a 400 m^3 pond at 27°C. Trial 59 was used to determine how quickly a 400 m^3 pond, initially at 27°C, cools down during a cold night. Trials 58 and 59 used weather data collected during the night of the 23rd to the 24th of January, 2003, at the Ben Hur weather station. The night time low that night was -6.3°C. The air temperature profile, the relative humidity and the wind speed for the time period considered are shown in Figure 7.2. No rainfall was recorded during this time. Both model runs were done for the time period between 17:50, 01/23 (sunset), and 24:00, 01/24. The time step for both runs was 10 minutes.

Trials 61, 62, 63 and 64 were used to determined the change in pond temperature for the night of the 10th of March, 2003, under different scenarios. (That night was special because the geothermal well was only turned on at 1:00 AM on the 11th of March.) The weather conditions for that night were measured at the Ben Hur Weather Station and are presented in Figure 7.3. The trial ran for the time period 18:22, 03/10 (sunset), and 6:10, 3/11 (sunrise). The time step was 10 minutes. The initial pond temperature was measured at 28°C. Trial 61 made use of the

unmodified collected weather data. Trial 62 assumed a constant wind speed of 10 m/s after 1:00, 3/11. Trial 63 assumed a constant relative humidity of 30% after 1:00, 3/11. Trial 64 assumed a constant wind speed of 10 m/s and a constant relative humidity of 30% after 1:00, 3/11. The pond temperature throughout the night was compared to the measured temperature in pond 12. The temperature was measured 10 cm below the surface using a type T thermocouple connected to a data logger (Campbell Scientific 21X, Campbell Scientific Inc., North Logan, UT). The temperature was recorded every 10 minutes. Despite the well being turned on at 1:00, 3/11, the

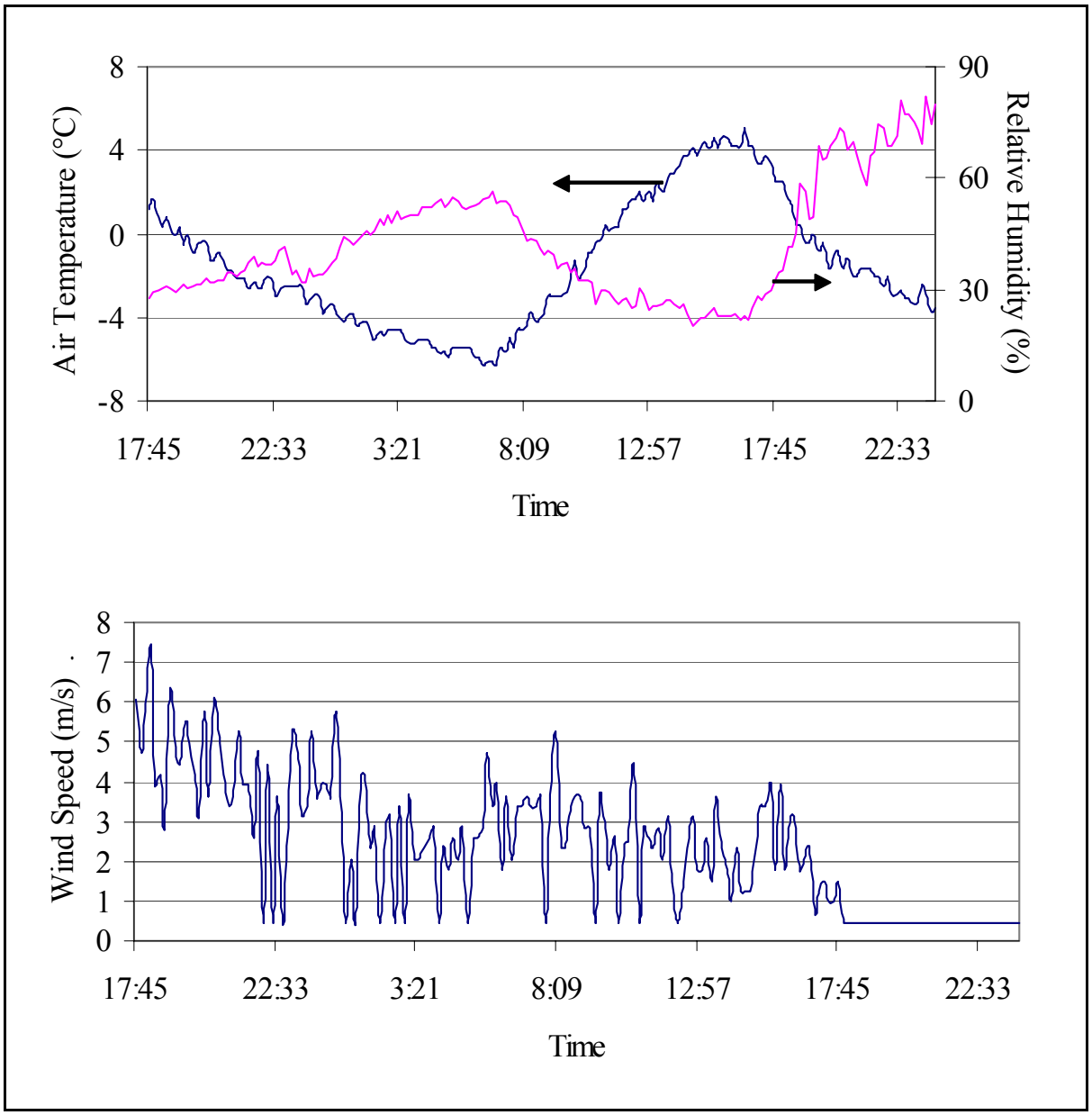

Figure 7.2: The air temperature, the relative humidity and the wind speed are shown from 17:45 on 01/23/03 to 24:00 on 01/24/03. The data, recorded at the Ben Hur Weather Station, represent weather conditions were evaporation, convection and longwave pond radiation are important.

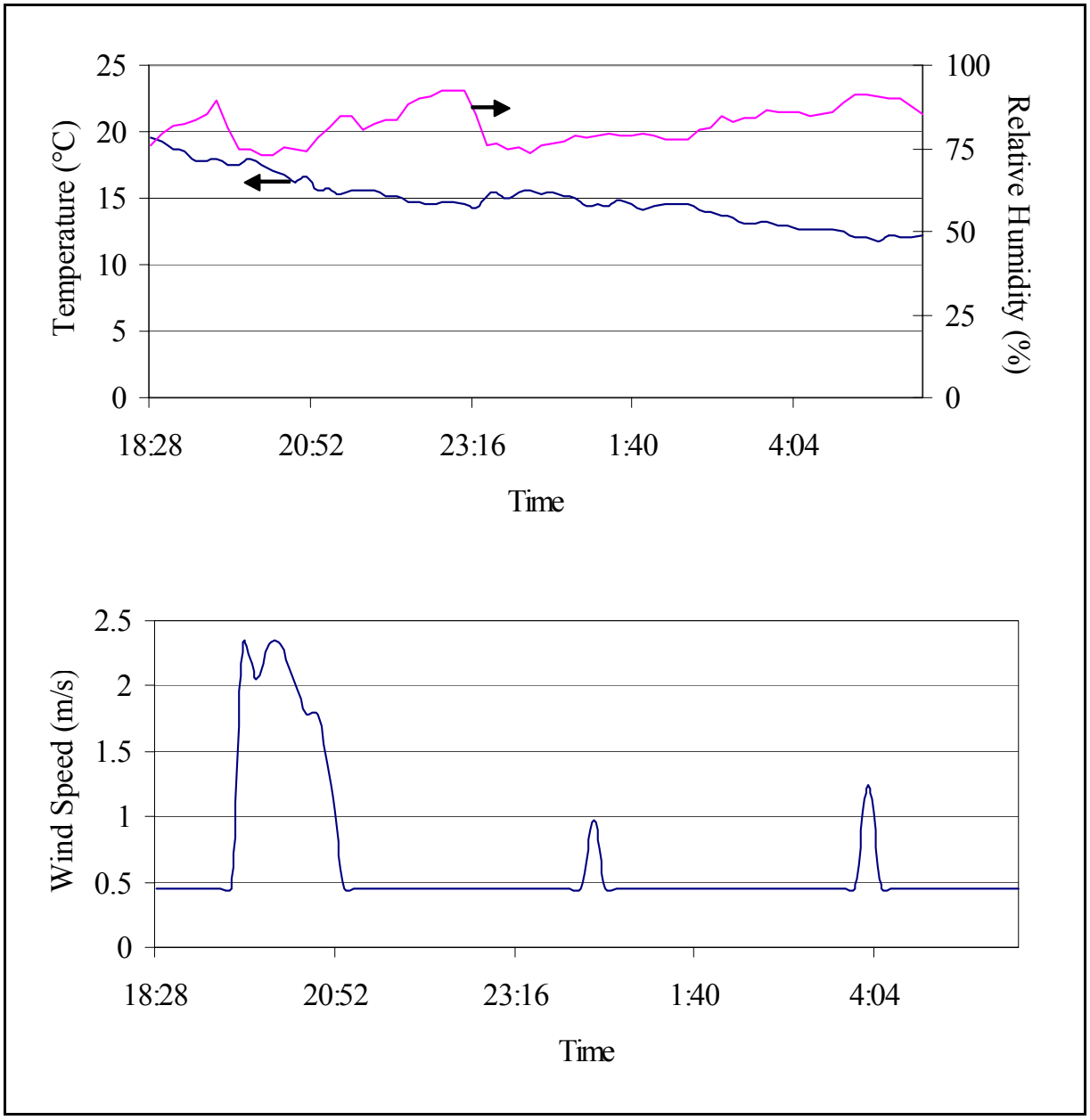

Figure 7.3: The air temperature, the relative humidity and the wind speed recorded at the Ben Hur Weather Station between 18:28, 03/10/2003 and 6:10, 03/11/2003. These data were used by PHATR to determine the pond temperature under different scenarios for that night.

model assumed that no water was added to the pond. This was done to see what would have happened if the well had remained off.

Trial 65 was done to determine the required flow rate needed to gradually increase the pond temperature from 10.5°C (the modeled pond temperature for January 15th at sundown, using the average year weather data file) to 27°C, the temperature maintained at the LSU ARS to

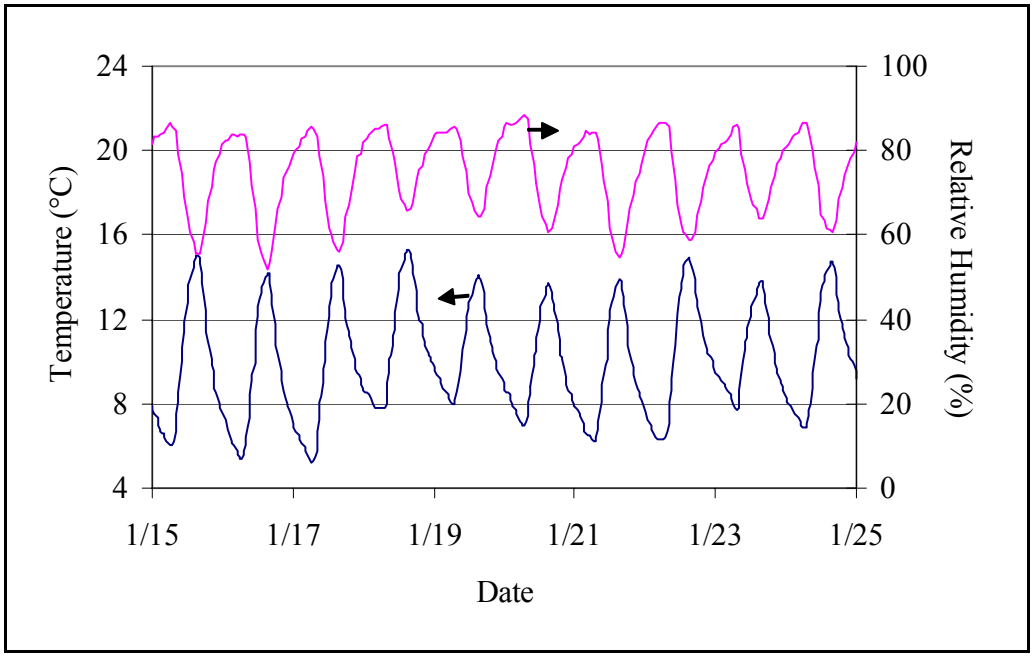

Figure 7.4: The air temperature and relative humidity data were determined for an average year. This data was used for trial 65.

artificially condition channel catfish, *Ictalurus punctatus*, to spawn out of season. The temperature was increased by 2°C every day for 8 days and 1°C on the last day. The pond volume was 400 m^3. The model ran for the time period between 17:00, 01/15, and 17:00, 01/24, for an average year. The time step was 1 hour. The weather conditions for this time period are shown in Figure 7.4.

7.3 Results: Answers to Questions 1 through 4

1) What is the pond temperature throughout a "average" year?

The pond temperature (for a 400m^3 pond) depended on the type of year. For a cold year, the pond's maximum temperature, 22.2°C, happened on 07/27 at 15:00 while the minimum pond temperature (-9.2°C) happened on 01/12 at 8:00. The average pond temperature was 9.0°C (standard deviation = 8.8°C). Although the minimum pond temperature was well below 0°C, the freezing point for pure water, it must be remembered that the minimum pond temperature was the product of a model run which used the coldest possible weather data for every hour during the year. Normally, cold spells do not last an entire year. Therefore, the purpose of this model run was not to simulate a cold year, but to provide a lower boundary for the average pond temperature.

For a hot year, the pond's maximum temperature, 54.9°C, happened on 07/02 at 17:00. The minimum temperature could not be determined because the initial pond temperature which PHATR required was also the lowest pond temperature. As a substitute to a minimum, on 01/12

at 8:00, the pond temperature was 30.0°C. The average pond temperature was 44.1°C (standard deviation = 7.9°C). Again, a pond temperature of 54.9°C is unlikely to happen in Baton Rouge, Louisiana. However, the purpose of the hot weather model run, not unlike the cold weather model run, was to provide an upper boundary for the average pond temperature.

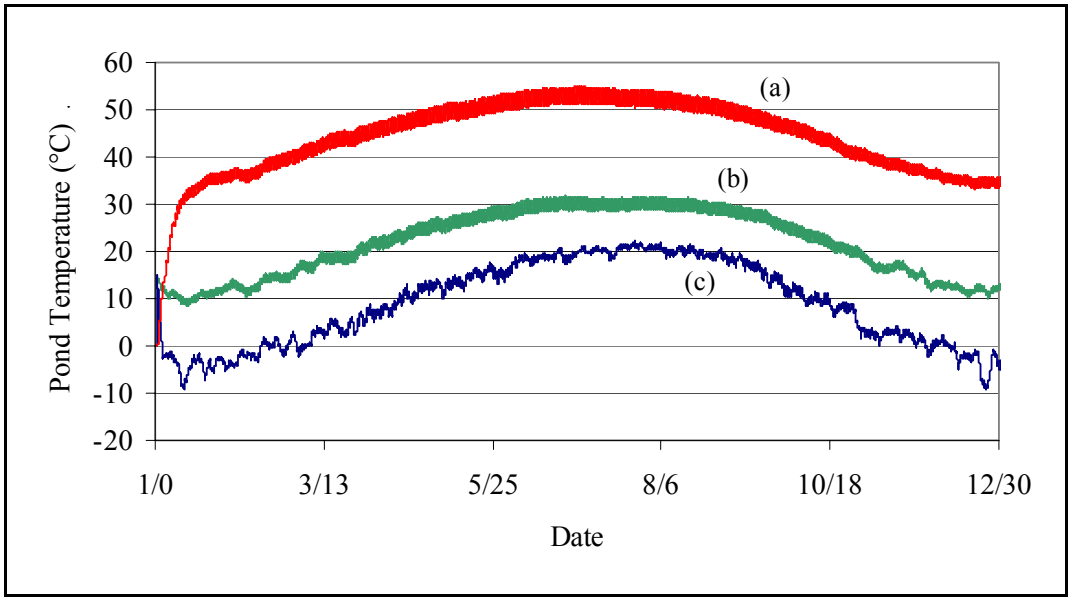

Figure 7.5: Modled pond temperature profiles for hypothetical hot (a), cold (b) and average (c) years are shown. The hot and cold years are not realistic (note the below freezing temperatures for the (c)) but they do bound the possible values for the average year.

For an average year, the pond's maximum temperature, 31.7°C, happened on 06/26 at 17:00. The minimum pond temperature, 8.5°C, happened on 01/13 at 8:00. The average pond temperature was 21.8°C (standard deviation = 7.0°C). The pond temperature for a cold, hot and average year are shown in Figure 7.5 Because the model has not yet been validated for summers or early autumn in Baton Rouge, the values generated for this time of year should be considered with caution.

2) What is the energy surplus or energy deficit when keeping the pond temperature constant?

Energy demands are dependant on the weather. A cold year was shown to have greater energy demands for keeping the pond warm. For instance, to maintain the pond temperature at 15°C for an entire year, the total energy deficit was 1.18×10^{11} J/m^3 (3 284 kWhr/m^3). To maintain the pond temperature at 35°C during the same year, the total energy deficit was 7.56×10^{11} J/m^3 (21 000 kWhr/m^3). A hot year, on the other hand, always had a yearly surplus of energy. To maintain the pond temperature at 35°C, 4.9×10^9 J/m^3 (1371 kWhr/m^3) net had to be removed.

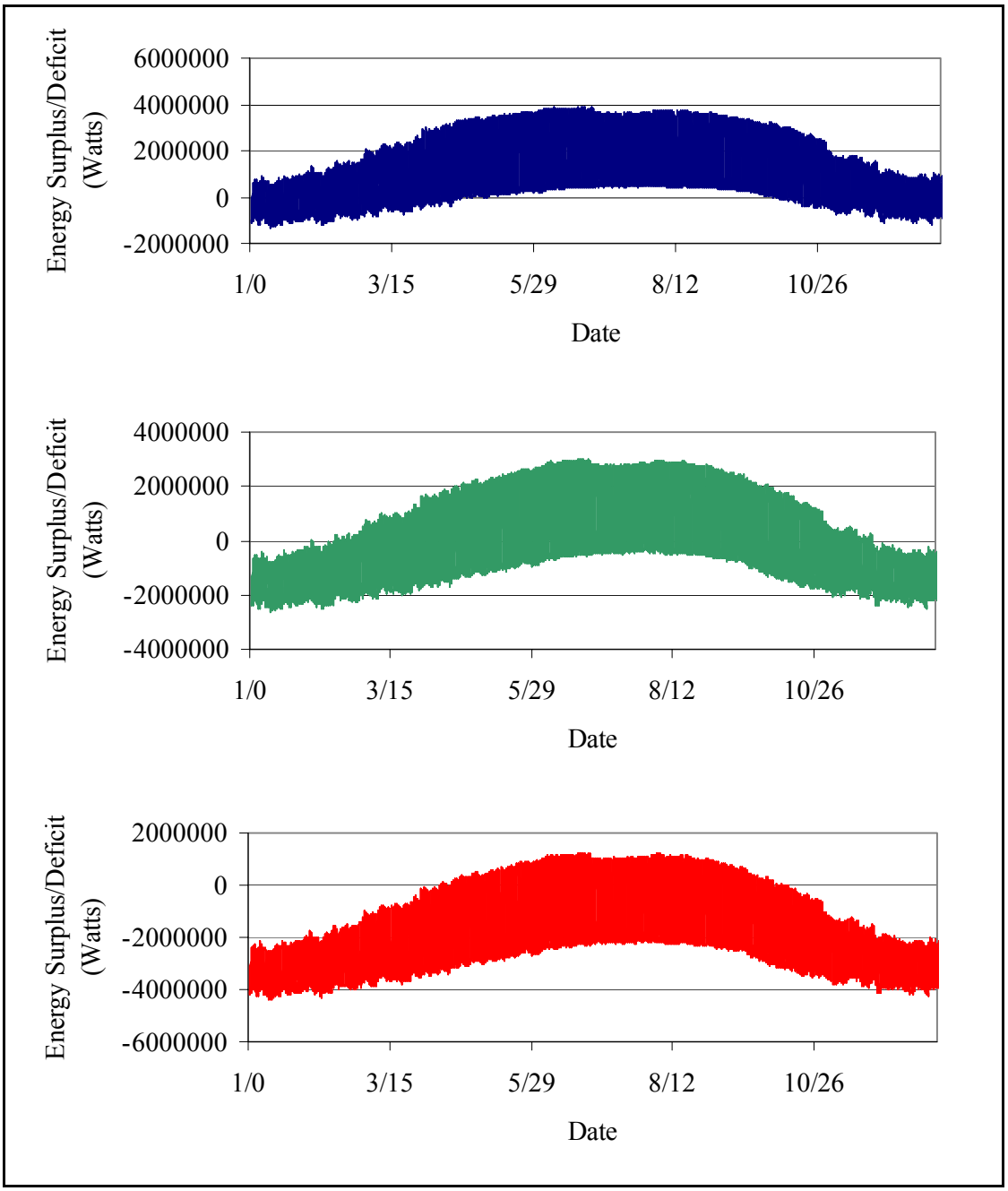

Figure 7.6: Surpluses and deficits of energy varied over the course of a day and a year. These plots show the energy requirements for a 1 m^3 pond over an average weather year. The pond temperature was maintained at 15°C (a), 25°C (b) and 35°C (c). Not shown are plots for 20 and 30°C.

To maintain the pond temperature at 15°C, 1.2 x 10^9 J/m^3 (3295 kWhr/m^3) net had to be removed (see Table 7.2 for more details on energy requirements for maintaining pond temperature).

From a design perspective, the energy requirements for an average year were more interesting because the model results were more realistic. Maintaining the pond temperature between 20°C and 25°C during an average year required no additional energy, assuming the pond energy surpluses could be stored for use when the pond had an energy deficit. The total net energy surplus when maintaining the pond temperature at 15°C during an entire average year was 6.9 x 10^9 J/m^3 (1919 kWhr/m^3). The total net energy deficit when maintaining the pond temperature at 35°C during an entire average year was 1.9 x 10^{10} J/m^3 (5175 kWhr/m^3). These numbers do not reflect, however, how the pond energy surpluses or deficits changed throughout an average year (see Figure 7.6 for variations in pond energy surpluses/deficits throughout an average year).

Table 7.2: The total energy surpluses and deficits associated with maintaining a 1 m^3 pond at a given temperature are such that the total energy surpluses are positive quantities while the total deficits are negative quantities. These values do not reflect how the energy surplus or deficit can change over a day or year.

Pond Temperature	Total Surplus/Deficit (J/m^3)		
(°C)	Cold Year	Average Year	Hot Year
15	-1.18 x 10^{10}	6.91 x 10^9	1.19 x 10^{10}
20	-2.38 x 10^{10}	2.52 x 10^9	1.05 x 10^{10}
25	-3.96 x 10^{10}	-3.24 x 10^9	8.90 x 10^9
30	-5.76 x 10^{10}	-1.03 x 10^{10}	7.03 x 10^9
35	-7.56 x 10^{10}	-1.86 x 10^{10}	4.9 x 10^9

Table 7.3: Here are estimates for the energy costs associated with maintaining the pond temperature at a set value for an average weather year. Holding the pond at 20°C was the most inexpensive pond temperature.

Pond Temperature	Energy Costs ($/m^3)		
(°C)	2¢/kWhr	7¢/kWhr	15¢/kWhr
15	56	195	418
20	54	188	403
25	61	214	460
30	80	281	602
35	111	388	831

The cost associated with heating or cooling a 1 m^3 pond was calculated every hour for an average year. The cost of heating or cooling one kilowatt-hour was assumed to be the same. The unit cost for electricity was assumed to be either \$0.02/kWh, \$0.07/kWh or \$0.15/kWh. (Based on 2003 rates, the cost for electricity for large-scale commercial operations in Baton Rouge, Louisiana, is \$0.0317 for the first 50 kWh, \$0.0297 for the next 100 kWh, \$0.02776 for the following 225 kWh and \$0.02576 kWh for any additional energy requirements.) The total cost to maintain the pond temperature constant during an average year is presented in Table 7.3. Keeping a pond at 20°C proved to be the least expensive (\$54/m^3). This is not surprising since the average temperature of an unheated pond during an average year was 21.8°C.

If geothermally enriched warm water is used to control the pond temperature, the maximum and average flow rates, used for choosing a pump, were calculated. These values are dependant on the temperature of the incoming water. For the trials used here, the "warm" water was set to 36°C while the "cool" water was set to either 10°C and 20°C. Maximum and average flow rates for an average year for each temperature setting are presented in Table 7.4. The required flow rates were smaller if the difference between the inlet water temperature and the pond temperature was small. For instance, an average flow rate of 1.99 x 10^{-6} (m^3/s)/m^3 (0.032 gpm/m^3) was required when using 10°C water to maintain the pond temperature at 25°C during an average year. When using 20°C water, the required average flow rate was 5.97 x 10^{-6} (m^3/s)/m^3 (0.095 gpm/m^3) - 3 times as much water. There are other reasons why it is desirable to increase the difference between the pond and inlet water temperature for the purposes of pond temperature control:

- to reduce the sizing of pumps. For keeping the pond temperature at 25°C using 20°C water, 3 times as much water was needed on average than if the inlet water temperature was 10°C. The peak required flow rates were also greater when using 20°C water (4 x 10^{-5} (m^3/s)/m^3 as opposed to using 10°C inlet water (1.3 x 10^{-5} (m^3/s)/m^3).

- to reduce the amount of wasted water. By adding water into a pond, assuming the pond volume was kept constant, water must be displaced out of the pond. The water was not re-used, wasted and may be considered a loss to the farm.

- to reduce pumping costs. By reducing the amount of water needed, the costs associated with pumping could also be reduced.

3) By how much does the temperature decrease in one night if there is suddenly no way to keep the pond warm?

For the night of the 23rd to the 24th of January, 2003, the average air temperature was -3.1°C and the lowest pond temperature was -6.3°C. If the pond temperature, at sunset, was 27°C, then by sunrise, the pond temperature was 19.2°C. By sunset on the 24th of January, the pond temperature had gone down to 18.1°C and by 24:00, the pond temperature was 16.8°C (see Figure 7.7). There are several reasons for the large decline in pond temperature. Because the

Table 7.4: These were the flow requirements for 10°C, 20°C and 36°C water to maintain constant pond temperature during an average weather year (pond size = $1m^3$). The standard deviation (St. Dev.) was an indicator of how the average flow rate varied over the course of a year. For design purposes, both the maximum and the average flow rate were required. The 10°C and the 20°C water were used to cool the ponds. The 36°C water was used to warm up the ponds.

Inlet water temperature = 10°C					
T_{pond}	Maximum Flow		Average Flow		St. Dev.
(°C)	$((m^3/s)/m^3)$	(gpm/m^3)	$((m^3/s)/m^3)$	(gpm/m^3)	$((m^3/s)/m^3)$
15	5.20×10^{-5}	8.25×10^{-1}	1.30×10^{-5}	2.06×10^{-1}	1.55×10^{-5}
20	2.40×10^{-5}	3.81×10^{-1}	4.67×10^{-6}	7.41×10^{-2}	6.98×10^{-6}
25	1.30×10^{-5}	2.06×10^{-1}	1.99×10^{-6}	3.16×10^{-2}	3.71×10^{-6}
30	7.00×10^{-6}	1.11×10^{-1}	7.86×10^{-7}	1.25×10^{-2}	1.80×10^{-6}
35	3.00×10^{-6}	4.76×10^{-2}	2.01×10^{-7}	3.19×10^{-3}	6.48×10^{-7}
Inlet water temperature = 20°C					
T_{pond}	Maximum Flow		Average Flow		St. Dev.
(°C)	$((m^3/s)/m^3)$	(gpm/m^3)	$((m^3/s)/m^3)$	(gpm/m^3)	$((m^3/s)/m^3)$
15	---	---	---	---	---
20	---	---	---	---	---
25	4.00×10^{-5}	6.35×10^{-1}	5.97×10^{-6}	9.48×10^{-2}	1.11×10^{-5}
30	1.50×10^{-5}	2.38×10^{-1}	1.58×10^{-6}	2.51×10^{-2}	3.59×10^{-6}
35	6.00×10^{-6}	9.52×10^{-2}	3.36×10^{-7}	5.33×10^{-3}	1.06×10^{-6}
Inlet water temperature = 36°C					
T_{pond}	Maximum Flow		Average Flow		St. Dev.
(°C)	$((m^3/s)/m^3)$	(gpm/m^3)	$((m^3/s)/m^3)$	(gpm/m^3)	$((m^3/s)/m^3)$
15	4.00×10^{-6}	6.35×10^{-2}	5.66×10^{-7}	8.98×10^{-3}	1.03×10^{-6}
20	8.00×10^{-6}	1.27×10^{-1}	1.71×10^{-6}	2.71×10^{-2}	2.35×10^{-6}
25	1.60×10^{-5}	2.54×10^{-1}	4.97×10^{-6}	7.89×10^{-2}	4.91×10^{-6}
30	3.80×10^{-5}	6.03×10^{-1}	1.46×10^{-4}	2.31	1.19×10^{-5}
35	2.94×10^{-4}	4.67	51.48×10^{-4}	2.35	8.67×10^{-5}

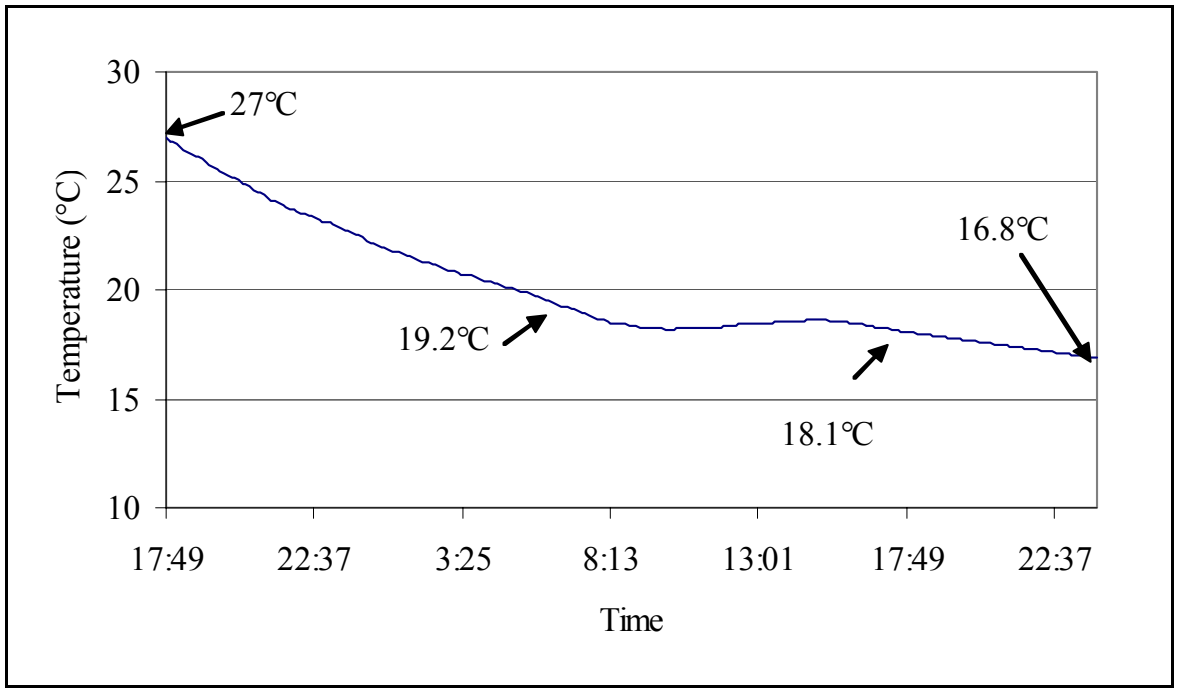

Figure 7.7: The modeled pond temperature, for the night between 01/23/03 and 01/24/03 dropped from 27°C (sunset) to 19.2°C (sunrise). During the following day (01/24), the pond temperature decreased further. The pond temperature was 18.1°C by sunset and 16.8°C by 24:00. The average air temperature during the 1st night was -3.1°C.

pond was initially very warm (27°C) with respect to its surroundings, the difference between the pond radiation and the sky radiation (-63 498 W) was greater (see Figure 7.8) than what would have been observed for an unheated pond (-38 655 W; initial pond temperature equal to 10°C). The wind driven energy transfer mechanisms (i.e. convection and evaporation) also contributed to lowering the pond temperature quickly. Energy losses due to convection on 01/23 at 24:00 represented 27% of all energy transfer mechanisms. Energy losses due to evaporation at the same time represented 25% of all energy transfer mechanisms (see Figure 7.9) Wind driven mechanisms were important in part because of the windy conditions that night (maximum wind speed = 7.38 m/s = 16.5 mph) but also because the temperature and vapor pressure gradients between the water and the air were large (maximum temperature difference between the pond and the air = 26.4°C, maximum vapor pressure difference = 3.35 kPa). When the wind speed died down an hour latter (from 5.2 to 0.4 m/s), the relative importance of evaporation and convection diminished. Energy losses due to convection on 01/24 at 1:00 represented 13% of all energy transfer mechanisms. Energy losses due to evaporation at the same time represented 9% of all energy transfer mechanisms. On average for that night, pond radiation accounted for 20% to 51% of all energy transfer mechanisms (average = 34%). Sky radiation accounted for 11% to 28% of all energy transfer mechanisms (average = 18%). Wind driven energy transfer mechanism varied in importance, depending on the wind speed. Convection represented 13% to 32% of all energy transfer mechanisms (average = 25%). Evaporation represented 8% to 38% of

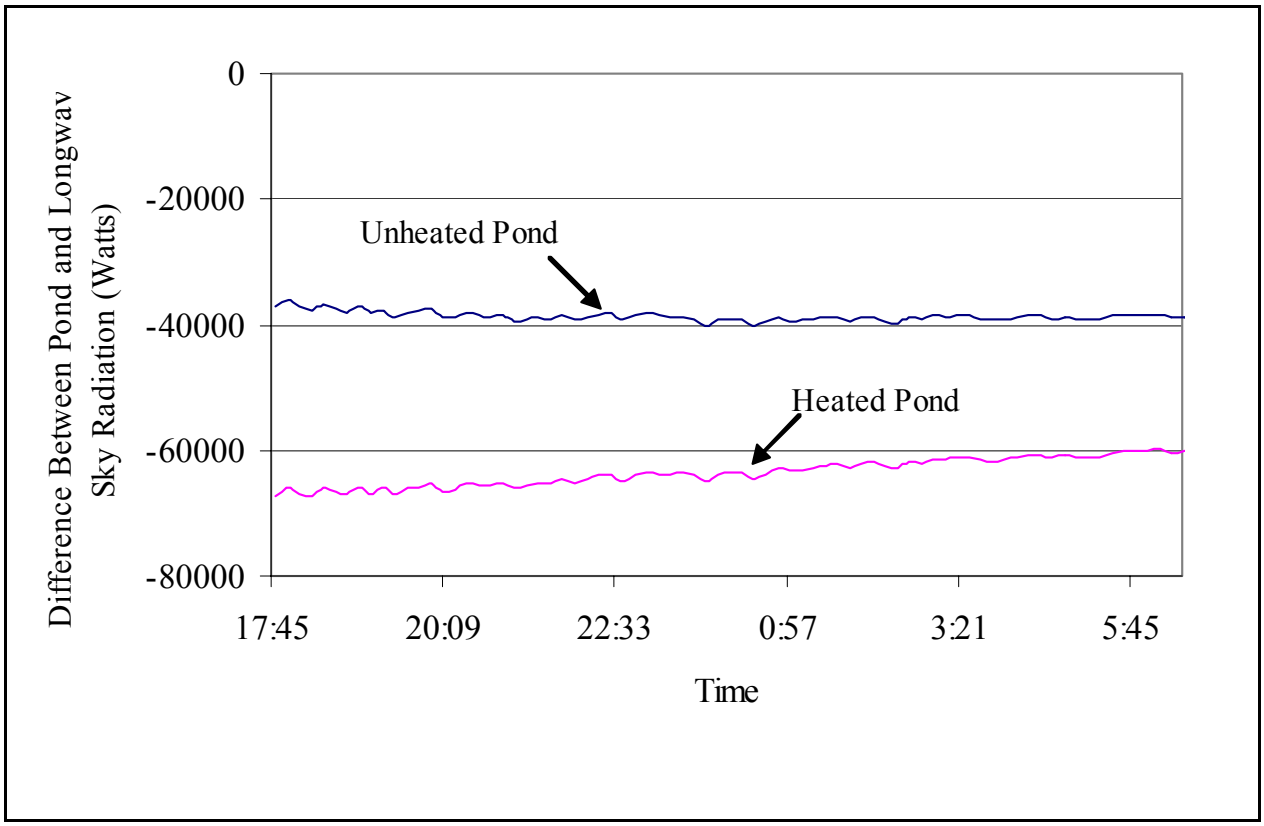

Figure 7.8: Each line represents the difference between longwave pond radiation and longwave sky radiation for a heated or unheated pond. The heated pond, maintained at 27°C, was assumed to lose its source of warm 36°C water at 17:45 (sunset) on 01/23/03, at which point, the pond cooled naturally. The unheated pond model run had an initial pond temperature of 10°C. Because the heated pond was warmer, it radiated and lost more heat than the unheated pond. The average temperature for the night was -3.1°C.

all energy transfer mechanisms (average = 23%). The amount of 36°C water required to keep a 400 m^3 pond at 27°C from sunset on 01/23 to 24:00 on 01/24, ranged from 0 to 15.1 x 10^{-3} m^3/s (0 to 240 gpm) with an average flow rate of 5.90 x 10^{-3} m^3/s (0 to 94 gpm) (see Figure 7.10 for flow demands for the model run).

For a warmer night (3/10 to 3/11, 2003, average air temperature = 14.9°C), changes in pond temperature were not as drastic. Between 18:22, 03/10 and 6:00, 03/11, the pond temperature decreased by 2.0°C. If the wind speed was 10 m/s as opposed to 0.6 m/s, the average wind speed for that night, the decrease in pond temperature would have been 5.1°C. If the relative humidity had been 30% as opposed to 82%, the average relative humidity for that night, the decrease in pond temperature would have been 2.2°C. If both the relative humidity and the wind speed were changed (relative humidity = 30% instead of 82% and wind speed = 10 m/s instead of 0.6 m/s), the change in pond temperature would have been 6.0°C.

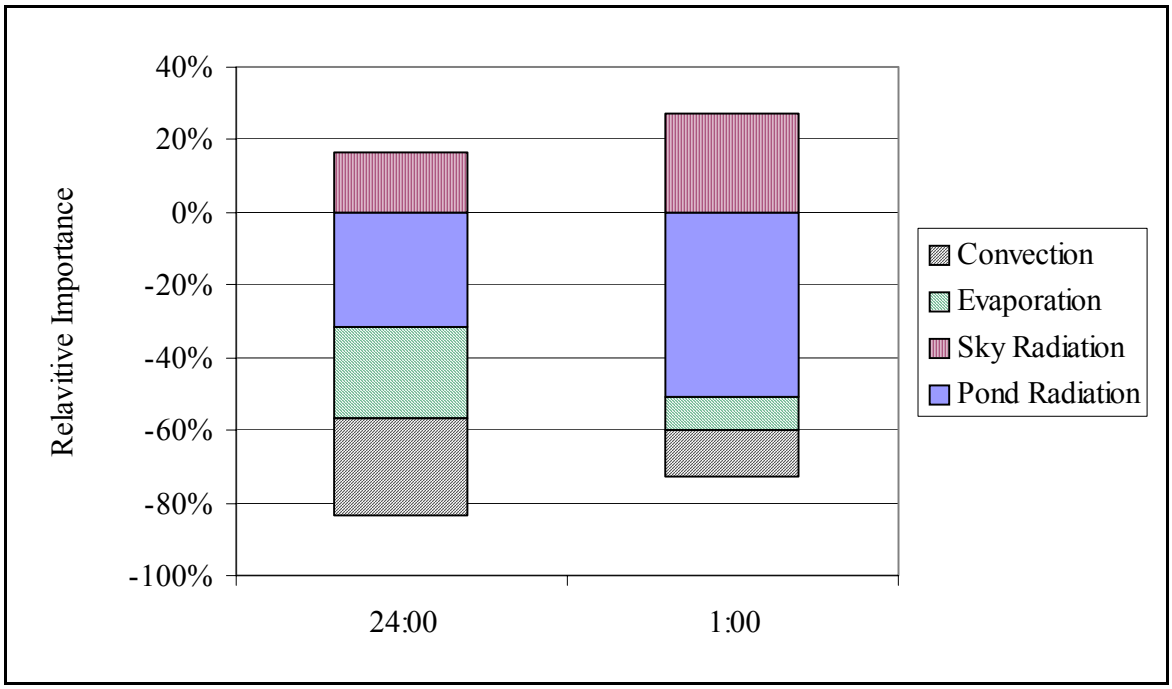

Figure 7.9: At 24:00 on 01/23/2003, the wind speed was 3.65 m/s. At this time, wind driven energy transfer mechanisms (convection: 27%, evaporation: 25%) were as importance as long wave radiation mechanisms (pond radiation: 31%, sky radiation: 17%). One hour later, at 1:00, the wind speed was 0.5 m/s. As a result, convection (13%) and evaporation (9%) were not as important as pond radiation (51%) or sky radiation (27%). The energy balance was performed for a 400 m^3 pond.

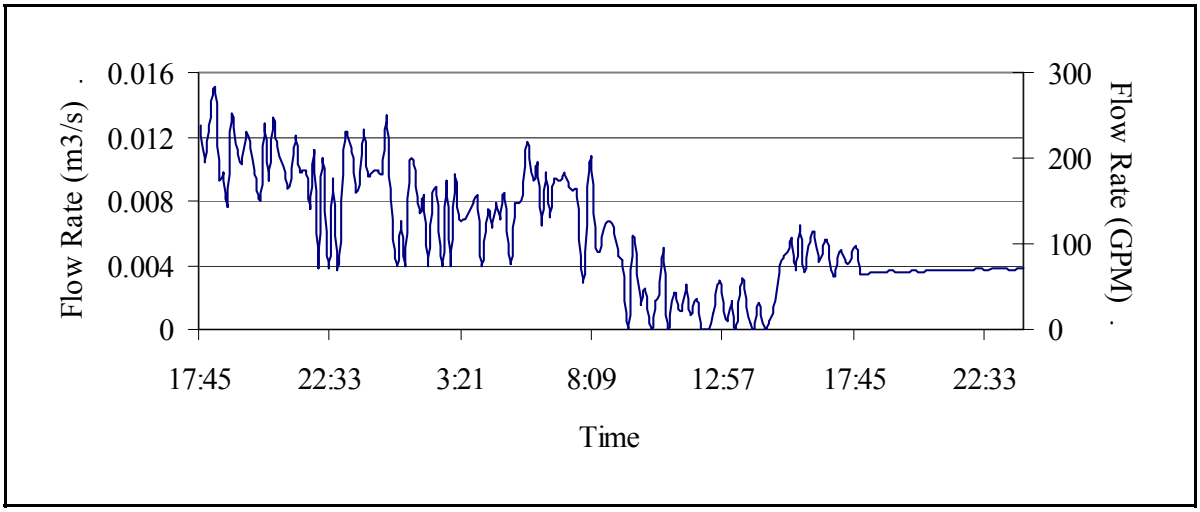

Figure 7.10: Between 17:45, 01/23/03 and 24:00, 01/24/03, the flow rate of 36°C water needed to maintain a pond temperature of 27°C was estimated. The flow rates varied between 0 and 15.1 x 10^{-3} m^3/s (0 to 240 gpm) with an average flow rate of 5.90 x 10^{-3} m^3/s (94 gpm). The pond was 400 m^3. The average night time temperature during the first night was -3.1°C.

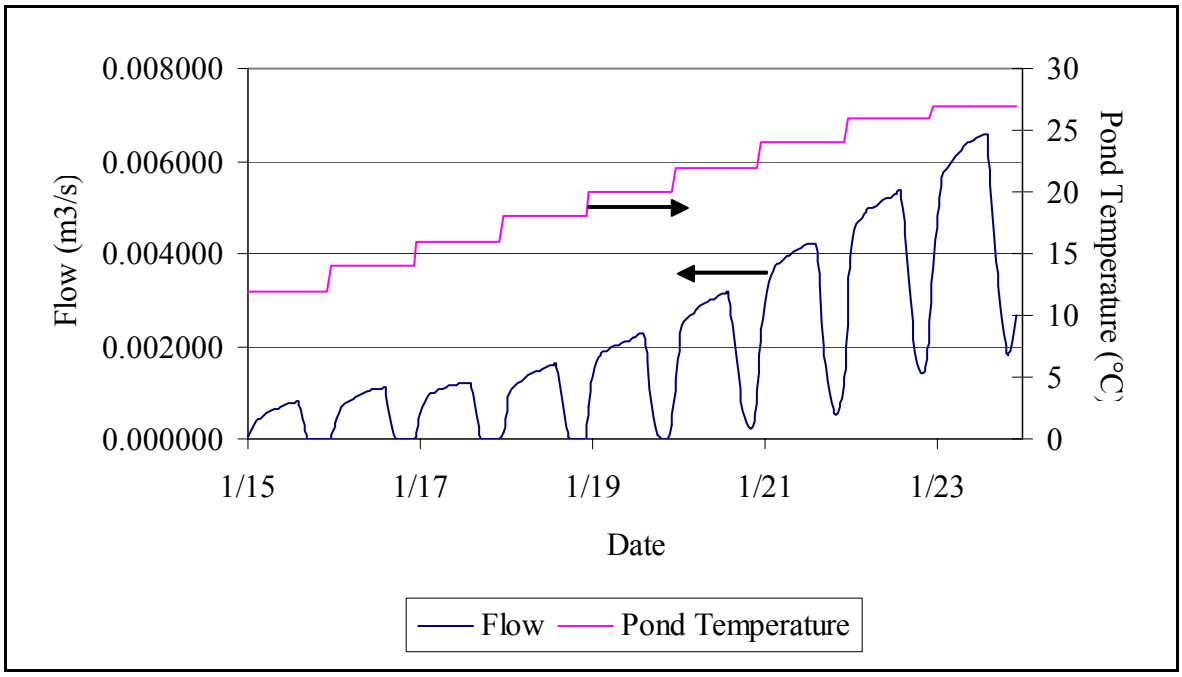

Figure 7.11: The required flow rate required to gradually increase the pond temperature from 10.5°C to 27°C at a rate of 2°C/day is shown here. The flow rates were calculated between 01/15 and 01/24 for an average year. Each tick on the date axis approximately represents sunset (16:50), when the temperature is stepped by 2°C.

Table 7.5: The maximum flow rates for a hypothetical model run are presented here. The purpose of the model run was to determine the flow rate required to warm a 400 m^3 from 10.51°C to 27°C over 9 days (2°C/day). The trial ran for the time period between 01/15 and 01/24 for an average weather year.

Night	Maximum flow rate (m^3/s)	Maximum flow rate (gpm)
1	8.19×10^{-4}	13
2	1.12×10^{-3}	18
3	1.22×10^{-3}	19
4	1.62×10^{-3}	26
5	2.28×10^{-3}	36
6	3.17×10^{-3}	50
7	4.20×10^{-3}	67
8	5.36×10^{-3}	85
9	6.59×10^{-3}	105

PHATR has a tendency of over-predicting the pond temperature so actual decreases in pond temperature were most likely greater than what was calculated here.

4) What are the flow requirements for increasing the pond temperature by 2°C/day during a typical week in January?

Because January is the coldest month of the year, warming the ponds to induce channel catfish spawning at this time of year represented the worst case scenario. For a 400 m^3 pond, with an initial pond temperature of 10.51°C, the required flow rate of 36°C water for each night is graphically shown in Figure 7.11. Each night, the peak flow rate increased as shown in Table 7.5, with the maximum flow rate happening on the last night before sunrise (6.59×10^{-3} m^3/s = 105 gpm). No warm water was needed during the daytime until the 5^{th} day (01/20). The maximum flow rate required during noon, 2.04×10^{-3} m^3/s , occurred on the 01/24. The total energy required to warm the pond over this time period was 7.64×10^{10} J (21 236 kWh).

7.4 Conclusions

The model answered four design and management questions for the warm water ponds at the LSU ARS. These results should not be seen as an exact answer but rather as an approximation of what could happen. Because Fisfhfry has a tendency of over-predicting the pond temperature, reported calculated energy deficits are smaller than those in reality and reported calculated energy surpluses were larger than those in reality. Furthermore, using the results presented in this chapter for ponds other than the LSU ARS warm water ponds should be done with great caution. In addition to assuming the ponds were well mixed, PHATR was validated only for research-sized ponds (400 m^3) in a temperate humid climate during the late fall, winter and spring. Using the model despite these warnings is left to the user's own risk.

The temperature for an unheated pond during cold, hot and average years were estimated. Results from the cold and hot years were seen as boundaries for possible pond temperatures and not as a pond temperature profile during an extreme case year. The average pond temperature for an average year was 21.8°C with a maximum temperature of 31.7°C and a minimum temperature of 8.5°C.

The net energy needed to maintain the pond temperature at 15, 20, 25, 30 and 35°C was calculated for a cold, hot and average year. For an average year, maintaining the pond temperature between 20 and 25°C required less energy. This is understandable since the average pond temperature for an average year for an unheated pond, 21.8°C, was between 20 and 25°C.

Temperature decreases for heated ponds in one night were dependant on the specific weather conditions. For instance, on a cold night, where the average night time temperature was -3.1°C and the maximum wind speed was 7.4 m/s, the modeled pond temperature decreased from 27°C to 19.2°C in one night. This was in part because of the unbalanced loss of energy through longwave pond radiation. Because the pond's surroundings were at least 20°C cooler than that

of the surroundings, back radiation was much greater than sky radiation, causing the pond to loose energy. Pond radiation accounted for 20% to 51% of all energy transfer mechanisms (average = 34%). Wind driven energy transfer mechanism varied in importance, depending on the wind speed. Convection represented 13% to 32% of all energy transfer mechanisms (average = 25%). Evaporation represented 8% to 38% of all energy transfer mechanisms (average = 23%). On a warmer night (average temperature = 14.9°C), the modeled pond temperature decreased from 27°C to 25°C. This is because there was little wind that night and the temperature difference between the pond and the surroundings was smaller than during the cold night.

The amount of energy needed to raise the pond temperature (volume = 400 m^3) from 10.5°C to 27°C at a rate of 2°C/day was modeled to be 7.64 x 10^{10} J over 9 days.. The required flow rate of warm 36°C water was calculated. On the final night, the maximum required flow rate was 2.04 x 10^{-3} m^3.

Because the model has proven itself as a good design and management tool, it could be used to address other questions about the warm water ponds. By validating PHATR for other situations, the model's applicability would become more universal.

CHAPTER 8: CONCLUSIONS

An energy balance model, called PHATR (Pond Heating And Temperature Regulation), was created, tested and validated based on the temperature in 400-m^3 earthen aquaculture ponds, given information about the weather, pond characteristics and the flow rate of warm water entering the pond. The model estimated energy surpluses and deficits which needed to be balanced to control the pond temperature. Mathematically, PHATR is a computer program which solves the following differential equation:

$$\left(\frac{dE}{dt}\right)_{pond} = q_{solar} - q_{back} + q_{sky} - q_{evap} \pm q_{conv} \pm q_{cond} - q_{seep} + q_{rain} + q_{well} - q_{out} \pm q_{other} \quad (8.1)$$

where E is the total energy at any given time (t) in the pond
q_{solar} is the rate of energy gained by the pond through solar radiation
q_{back} is the rate of heat lost through back radiation
q_{back} is the rate of heat gained by longwave sky radiation
q_{soil} is the rate of heat exchanged with the soil
q_{conv} is the rate of heat exchanged with the air by convection
q_{evap} is the rate of heat lost through the evaporation of water
q_{rain} is the rate of bulk energy gained due to rainfall
q_{well} is the rate of bulk energy gained from the warm water well
q_{out} is the rate of bulk energy lost to the overflow of water
q_{other} is the rate of energy transfer from or to other sources.

Equation 8.1 is a mathematical representation of the conceptual model presented in Figure 3.1 and again in Figure 4.1.

Model runs showed that for unheated ponds, the transport of energy through radiation dominated all energy transfer mechanisms. Solar radiation was found to account for as much as 55% of all energy transferred. Longwave pond radiation and longwave sky radiation accounted for no less than 19% and 14% respectively of all energy transfer mechanisms during the trial runs. Wind-driven energy transport mechanisms were on average less important (average importance of convection was 5%, average importance of evaporation was 6%). Although heat exchanged through the soil was equal in average importance to evaporation (2 to 6%), its importance never exceeded 13%. Because of this, and because including soil heat transfer mechanisms hindered the model's ability to estimate pond temperatures, subsequent model runs did not include the effects of soil heat transfer (see Chapter 4 for more details).

Model runs also showed that for heated ponds, the bulk transport of energy from warm well water accounted for as much as 60% of all energy transport mechanisms. However, at the same time, energy lost in the discharged water was also substantial (maximum importance was 44%). During the day, solar radiation could account for as much as 50% of all energy transport

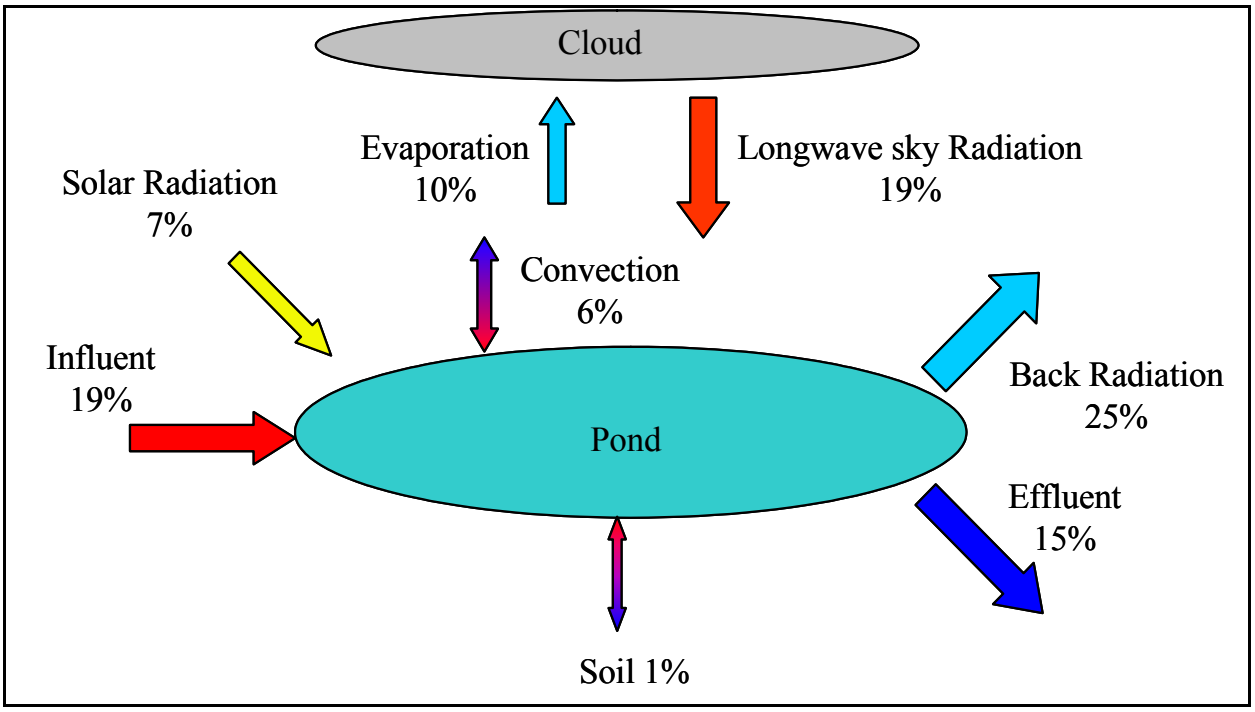

Figure 8.1: These results for the energy balance (Chapter 4) illustrate the relative average importance for each energy vector for heated ponds. This particular energy balance was developed using data from the spring of 2003.

phenomena. The average importance of longwave pond radiation was 25% and of longwave sky radiation was 19%. Heat transferred through the soil was not as important (average importance = 1%) (see Chapter 4 for more details).

PHATR had a tendency to over-estimate when predicting pond temperatures (average bias for unheated ponds was 0.5°C; average bias for heated ponds was 2.6°C). Efforts should be made to better understand evaporation and convection in future studies. Because both of these transport phenomena were determined empirically, and because both were governed by similar transport processes, understanding how the water and air boundary layers behave would be beneficial. The current version of PHATR assumes that the water is a static solid when in reality, heat must travel through a water and air boundary layer. Further study of the effects of these boundaries to develop better predictive equations are required.

The absorption of solar radiation in aquaculture ponds also needs to be studied further. This study did not quantify how much light was reflected by the suspended particles in the pond. The model also did not take into account the energy absorbed by chlorophyll, energy which is stored and not converted into thermal energy.

A sensitivity analysis was performed to determine how the model's output was influenced by average air temperature, solar radiation, wind speed and the flow of water into the pond. Variations in air temperature caused the model output to vary linearly (0.00695°C/°C/hr).

Variations in solar radiation caused the model output to vary linearly for a fixed time. Variations in wind speed and flow rates caused changes in the output to decay exponentially.

Over the course of this study, PHATR was validated during the late fall, winter and spring for well mixed earthen ponds of approximately 400 m^3 in size, located in Baton Rouge, Louisiana. The model needs to be validated for other sizes of ponds and ponds located in regions with different climates. Using PHATR for these different ponds is not recommended without proper validation.

The amount of energy to be added or removed to maintain a constant pond temperature was estimated. For Baton Rouge, Louisiana, energy requirements were smallest when the pond temperature was maintained between 20°C and 25°C. The net energy to be removed to maintain the pond temperature at 20°C during an average year was 2.52 x 10^9 J/m^3. The net energy needed to be added to maintain the pond temperature at 25°C during an average year was 3.24 x 10^9 J/m^3. Flow rate requirements for heating and cooling ponds were also generated. With this information, properly sized mechanisms can be designed to control the pond temperature as needed.

PHATR assumes fully mixed ponds. Because of thermal stratification in poorly mixed ponds, the temperature within the pond becomes dependant on location as well as on time. In order to determine the temperature within such ponds, or the energy required to control temperature, a more sophisticated numerical method (e.g.: Finite Element Methods or Finite Difference Method) would have to be used.

Despite PHATR's numerous limitations, certain general observations about energy transfer in earthen aquaculutre ponds were made:

- Evaporation and convection energy losses were more important under windy conditions. In Chapter 4, the maximum importance of evaporation for heated ponds (average importance: 10 %) was 41% and this occurred when the wind speed was 10.6 m/s. Similarly, the maximum importance of convection for heated ponds (average importance: 6%) was 21% and this occurred when the wind speed was 7.4 m/s. In Chapter 6, the sensitivity analysis demonstrated that increases in relatively low wind speeds greatly affected the output. For instance, increasing the wind speed from 0 to 1 m/s (2.2 mph) decreased the pond temperature by 2.1°C over 2 days. Increasing the wind speed from 0 to 5 m/s (11.2 mph) decreased the pond temperature by 6.8°C over 2 days. Increasing the wind speed from 0 to 10 m/s (22.4 mph) decreased the pond temperature by 9.4°C over 2 days. Finally, in Chapter 7, the answer to Question 3 revealed that on a cold night (average air temperature: -3.1°C) a 5.2 m/s wind caused the importance of convection to rise from 13 to 27% and the importance of evaporation to rise from 9 to 25%. On a warmer night (average temperature: 14.9°C, wind speed: 0.6 m/s), the pond temperature decreased by 2°C in 12 hours. If the wind speed was 10 m/s, the pond temperature would have decreased by 5°C in 12 hours.

- The effects of longwave radiation were found to be important (average importance of pond radiation: 25%, maximum importance of pond radiation: 50%, average importance of sky radiation: 19%, maximum importance of sky radiation: 43%). Longwave energy losses to the environment were greater when pond temperatures were much greater than the air (see Figure 7.8). This problem is particularly aggravated on dry nights when there is less moisture in the air. For such nights, sky radiation becomes less important and net longwave radiation losses to the surroundings therefore increase.

- Solar radiation accounted for as much as 50% of all energy transfer mechanisms in heated ponds. Solar energy was the only unbalanced energy transfer mechanism.

- Warm water used to control the pond temperature represented a major flux of energy (average relative importance: 19%, maximum relative importance: 60%). Conversely, the effluent represented a major energy loss (as much as 44%). Therefore, using warm water to control the pond temperature wasted energy in the effluent. Based on Equation 3.60 and from data in Chapter 7, using warmer water to heat or cooler water to cool a pond decreases the amount of water required and therefore decreases the flow and associated wasted energy in the effluent (i.e. if you are going heat a pond, make sure the water is as hot as possible so as to conserve water).

Based on these general observations, the following suggestions could be implemented to conserve energy:

- Building a windbreak. Because the pond temperature is sensitive to changes in wind speed, building a windbreak (walls, trees, etc) might decrease the evaporation and convection. However, such windbreaks would also block the sun, and reduce the only unbalanced energy vector. More modeling would be required to investigate the effects of windbreaks. If PHATR is used, only the solar energy and wind speed inputs in the weather file would need to be modified.

- Building a greenhouse over the pond. Doing so would:

    - reduce the amount of energy lost through evaporation and convection.
    - create extra thermal resistance between the pond and the outside environment.
    - potentially make the air above the pond humid, thus eliminating evaporation
    - trap solar energy. Glass or clear plastic is transparent to solar radiation but opaque to longwave radiation. Solar energy would warm the pond but the energy radiated back to the sky would not get past the glass or plastic. This greenhouse would get warmer and radiate energy in part back to the pond. Therefore, longwave radiation losses would be minimized. To mathematically study the effects of a greenhouse, two additional differential equations (in addition to Equation 8.1) would be required:

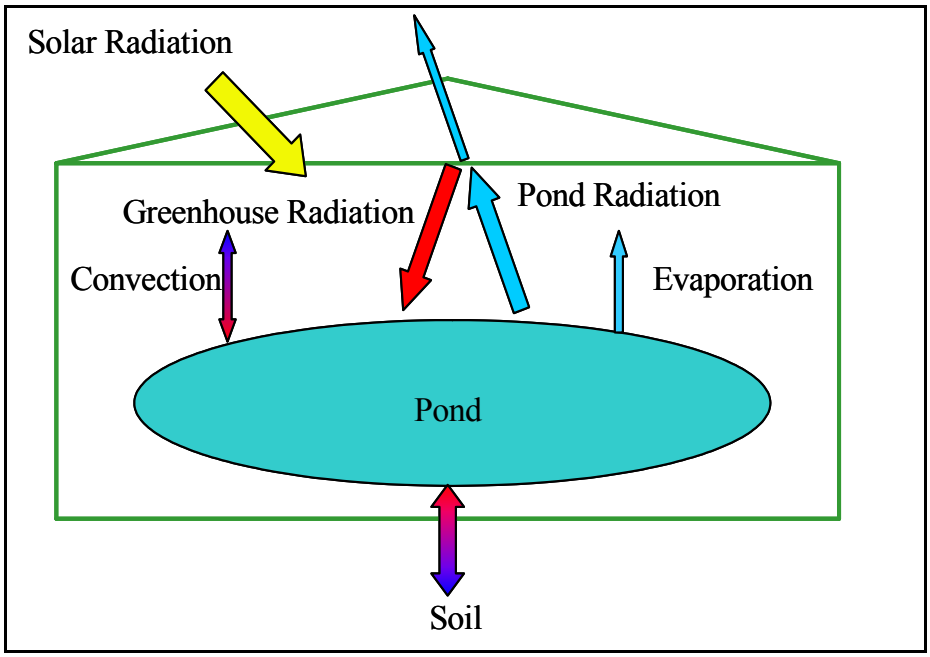

Figure 8.2: By building a greenhouse over an aquaculture pond, convection and evaporation (wind-driven energy vectors) would diminish in importance. Solar radiation would enter the greenhouse unaltered. Pond radiation, on the other hand, would not be able to escape the greenhouse because glass and plastic are opaque to longwave radiation. Instead, pond radiation would warm the air and the greenhouse structure, which in turn would further warm and insulate the pond from the cold outdoor air. Because the importance of the other vectors is diminished, the effects of soil might be more important.

$$\left(\frac{dE}{dt}\right)_{greenhouse} = \sum q_{greenhouse} \tag{8.2}$$

$$\left(\frac{dE}{dt}\right)_{air} = \sum q_{air} \tag{8.3}$$

where $dE/dt_{greenhouse}$ is the rate of energy stored in the glass/plastic cover
dE/dt_{air} is the rate of energy stored in the air inside the greenhouse
$\sum q_{greenhouse}$ is the sum of all the energy vectors for the energy balance of the greenhouse structure
$\sum q_{air}$ is the sum of all the energy vectors for the energy balance of the air

Simultaneously solving Equations 8.1, 8.2 and 8.3 would yield a model capable of predicting the pond temperature.

- Using a thermal pump. Because there are periods in the year where energy surpluses may exist in a pond, excess energy could potentially be stored in the ground. Pond water could be pumped to a buried piping network. The excess energy would be transferred to the soil. The water, now cooler, would then be returned to the pond. When energy is needed, pond water could be pumped through the same piping network, removing the stored heat. The now warm water would return to the pond, increasing the pond's internal energy. The soil's ability to diffuse and store heat would have to be investigated. The soil should allow for sufficient heat to diffuse quickly but not easily so as to avoid energy losses. To predict how well a thermal pump would work, a second differential equation, describing heat transfer in the soil would have to be solved simultaneously with Equation 8.1.

The purpose of this investigation, to perform an energy balance on an outdoor aquaculture pond, was the first step in designing systems to control pond temperature. The advantages of using such a system were reviewed in Chapter 1. It is hoped that with the data and the model presented in this report that designs for devices to control the pond temperature will be developed and sized appropriately. Additionally, the development of PHATR provided a tool for managing existing warm-water facilities, such as the ones at the Louisiana State University Aquaculture Research Station.

REFERENCES

Al-Nimir, M.A, 1998. Solar Pond Modeling. International Journal of solar Energy. 19(4):275-290.

Anderson, E E., 1983. Fundamentals of Solar Energy Conversion. Addison-Wesley Publishing Company. Reading, Mass. 636 pp.

Anonymous, 2000. The Temperature Handbook 21st century 2nd edition. Omega Engineering Inc.

Anonymous, 1992. ASAE Standards, 1992, 39th edition. American Society of Agricultural Engineers. St. Joseph, MI. 781 pp.

Anonymous, 1985. ASHRAE Handbook 1985 Fundamentals. American Society of Heating, Refrigerating and Air-Conditioning Engineers, Inc. Atlanta, GA.

Anonymous, 1952. Water-Loss Investigations: Volume1 - Lake Hefner Studies - Technical Report. U.S. Geological Survey circular 229. 151 pp.

Arnold, C.R., 1988. Controlled Year-Round Spawning of Red Drum *Sciaenops ocellatus* in Captivity. Contributions in Marine Science, Supp. to volume 30:65-70.

Avault, J.W., Jr., 1996. Fundamentals of Aquaculture. AVA Publishing Company Inc. Baton Rouge, Louisiana. 889 pp.

Avault, J.W., Jr., E.W. Shell., 1968. Preliminary Studies with Hybrid Tilapia, *Tilapia aurea x T. Mossambica.* Proceedings of the World Symposium on Warm-Water Pond Fish Culture. FAO Fisheries Report No. 44, 4:237-242.

Bliss, R. W. Jr., 1961. Atmospheric Radiation near the Surface of the Ground. Solar Energy 5:103-120.

Boyd, C.E., 1995. Bottom Soils, Sediment and Pond Aquaculture. Chapman and Hall. 350 pp.

Bye, V.J., 1984. "The Role of Environmental Factors in the Timing of Reproductive Cycles" in Fish Reproduction. p.87-205.

Cedergren, H.R., 1966. Seepage, Drainage and Flow Nets. John Wiley& sons, inc. New York. 489 pp.

Chieh, V., 1978. Two-Dimensional Numerical Model for Shallow Cooling Ponds. Proceedings of the Conference on Waste Heat Management and Utilization. pp 15-25.

Chamberlain, G.W., D.L. Hutchins, A.L. Lawrence, J.C. Parker., 1980. Winter Culture of *Penaeus vannameii* in Ponds Receiving Thermal Effluent at Different Rates. Proceedings of the World Mariculture Society. 11:30-43.

Charbeneau, R.J., 2000. Groundwater Hydraulics and Pollutant Transport. Prentice-Hall, Inc. New Jersey. 593 pp.

Davis, H.S., 1961. Culture and Diseases of Game Fishes. Berkley and Los Angeles, California: University of California Press. 332 pp.

de Vries, D.A., 1966. Thermal Properties of Soils. Found in Physics of Plant Environment, ed. Van Wijk. North Holland Publishing Company. 382 pp.

Doran, P.M., 1995. Bioprocessing Engineering Principles. Academic Press, Inc. 439 pp.

Duffie, J.A.,W.A. Beckman, 1980. Solar Engineering of Thermal Processes. John Willey and Sons. 762 pp.

Farouki, O.T., 1986. Thermal Properties of Soil. Trans Tech Publications, Germany. 136 pp.

Galtsoff, P.S., 1964. The American Oyster, *Crassostrea virginica*. Fishery Bulletin of the Fish and Wildlife Service Volume 64. Superintendent of Documents, US. Government Printing Office, Washington, D.C. 480 pp.

Guo, Q., S.J. Kleis., 1997. A Numerical Simulation of the Sea Water Solar Pond. Solar Engineering - 1997 ASME. pp. 229-235.

Hale, G.M., M.R. Querry., 1973. Optical Constants of Water in the 200 nm to 200 μm Wavelength Region. Applied Optics 12(3):555-563.

Hall, D.O., K.K. Rao., 1987. Photosynthesis, 4th edition. Edward Arnold Ltd.

Hall, S.G., J.Finney, R.P.Lang, T.R. Tiersch., 2002. Design and Development of a geothermal Temperature Control System for Broodstock Managment of Channel Catfish *Ictalurus punctatus.* Aquacultural Engineering 26:277-289.

Holman, J.P., 1997. Heat Transfer, 8th edition. McGraw-Hill. 696 pp.

Husser, R.E., Jr., 2000. Energy Analysis of a Dairy Cow Cooling Pond. Master's Thesis at Louisiana State University and Agricultural and Mechanical College. 66 pp.

Hyam, D., 2001. Curve Expert version 1.3 Shareware Software. http://www.ebicom.net/~dhyams/cvxpt.htm

Incropera, F. P., D.P. De Witt, 1985. Fundamentals of Heat and Mass Transfer, 2nd Edition. Wiley. 802 pp.

Irvine, W.M., J.B. Pollack, 1968. Infrared Optical Properties of Water and Ice Spheres. Icarus 8:324-360.

Kadlec, R.H., R.L. Knight, 1996. Treatment Wetlands. Lewis Publishers. 893 pp.

Kamal, W.A, 1991. Solar Pond Literature Analysis. Energy Conservation Management. 32:207-215.

Kildow, J. T., J.E. Huguenin., 1974. Problems and Potentials of Recycling Wastes for Aquaculture. MIT. Report number MITSG74-27.

Kimball, B.A., R.D. Jackson, J. J. Reginato, F. S. Nakayama, S. B. Idso., 1976. Comparison of Field-measured and Calculated soil-heat Fluxes. Soil Science Society of America Journal. 40:18-25.

Kirk, J.T.O., 1980. Spectral Absorption Properties of Natural Waters: Contribution of the Soluble and Particulate Fractions to Light Absorption in some Inland Waters of South-eastern Australia. Australian Journal of Marine Freswater Resources. 3:287-296.

Kondratyev, Ya K., 1969. Radiation in the Atmosphere. Academic Press. Inc. 912 pp.

Kurt, H., F.Halici, A.K.Bark., 2000. Solar Pond Conception - Experimental and Theoretical Studies. Energy Conversion and Management 41:939-951.

Lang, R.P., 2001. Induction of Early Out-of-Season Spawning in Channel Catfish (*Ictalurus Punctatus*). Master's thesis. Louisiana State University. 140 pp.

Lawson, T.B., 1995. Fundamentals of Aquacultural Engineering. Chapman and Hall. NY, NY. 355 pp.

Masser, M.P., T.R. Murphy, J.L. Shelton., 2001. Aquatic Weed Management - Herbicides. Southern Regional Aquaculture Center Publication No 361.

McAdams,W.H., 1942. Heat Transmission, 2nd edition. McGraw-Hill Book Company Inc. 459 pp.

Morrison, J. K., C.E. Smith., 1986. Altering the Spawning Cycle of Rainbow Trout by Manipulating Water Temperature. The Progressive Fish Culturist. 48:52-54.

Pawlina, A.T., H. Harding, N.B. Hanes., 1977. Estimate Cooling Pond Requirements with Surface Heat Exchange. Industrial Wastes. 23(5):22-26

Piedrahita, R.H., 1991 Engineering Aspects of Warmwater Hatchery Design. Aquaculture Systems Engineering; Proceeding of the World Aquaculture Society and the American Society of Agricultural Engineers. WAS 22nd Annual Meeting 16-20 June, 1991. pp. 85-100.

Ray, L., 1981. Channel Catfish Production in Geothermal Water. In: Alen, L., E. Kinney, Editors. Bioengineering Symposium for Fish Culture. American Fisheries Society, Bethsheda, Maryland. pp 192-195.

Rabl, A., C.E. Nielsen, 1975. Solar Ponds for Space Heating. Solar Energy. 17:1-12.

Randall, C.M., R. Bird, 1989. Insolation Models and Algorithms in R.L.Hulstrom (editor) Solar Resources. pp 61-143.

Romaire, R., 2002. Personal communication.

Saltelli, A., 2000. What is Sensitivity Analysis? in Sensitivity Analysis. Edited by A. Saltelli, K. Chan and E. M. Scott. Wiley. 475 pp.

Sezai, I. And E. Tasdemiroglu., 1995. Effect of Bottom Reflectivity on Ground Heat Losses for Solar Ponds. Solar Energy. 55(4):311-319

Siegel, R. and J.R. Howell., 1981. Thermal Radiation Heat Transfer, 2nd edition. McGraw-Hill Book Company. 862 pp.

Singh, T.P., A,K, Singh, N.D. Kaushika., 1994. Investigations of Thermohydrodynamic Instabilities and Ground Storage in a Solar Pond by Simulation Model. Heat Recovery Systems CHP 14(4):401-407.

Smith, A.W., J.N. Cooper, 1957. The Elements of Physics. 6th edition. McGraw Hill.

Sodha, M.S., U. Singh, G.N. Tiwari, 1982. A Thermal Model of a Roof Pond System with Moveable Insulation for Heating a Building. Building and Environment. 17(2):135-144.

Subhakar, D., S.S. Murthy, 1993. Saturated Solar Ponds: 1. Simulation Procedure. Solar Energy 50(3):275-282.

Swinbank, W.C., 1963 Long-Wave Radiation from Clear Skies. Royal Meteorological Society, Quarterly Journal. 89:339-348

Threlkeled, J.L., R.C. Jordan, 1958. Direct Solar Radiation Available on Clear Days. American Society of Heating and air-Conditioning Engineers - Transactions. 46:45-56.

Tsilingiris, P.T., 1991. The Radiation Transmission across a Salinity Gradient. Energy Conversion Management 32(4):333-343.

Van Wijk, W.R., D.A. de Vries, 1966. Periodic Temperature Variations in a Homogeneous Soil. in Van Wijk, W.R. (editor) Physics of Plant Environment, North Holland Publishing Company. pp. 102-140.

Wang, J, J. Seyed-Yaggobi, 1994. Effect of Water Turbidity and Salt Concentration Levels on Penetration of Solar Radiation Under Water. Solar Energy 5:429-438.

Watmuff J.H., W.W.S. Charters, D. Proctor, 1977. Solar and Wind Induced External Coefficients for Solar Collectors. Technical Note. Comples, 2:56.

APPENDIX 1: EXPERIMENTAL EVIDENCE SHOWING THE ARS WARM-WATER PONDS ARE WELL MIXED

The aerators located approximately 2 m from the inlet were continuously operating, ensuring that the temperature within the pond was uniform. The assumption that the geothermal ponds were well mixed is a necessary condition for using Equation 3.4 and Fishfry. Between 2002 and 2003, the pond temperature was measured at various locations and depths. The temperature, measured with type T thermocouples and recorded with a 21X Campbell Scientific data logger, varied little with respect to position or depth within the pond. For instance, between 04/07/02 and 04/14/02, the temperature in Pond 8 was measured at the aerator, at the discharge pipe and midway between the aerator and the discharge pipe. The temperature, at these locations, was measured 1 foot above the pond bottom and 1 foot below the water surface. The greatest temperature difference measured between any 2 of the 6 thermocouples was 1.6°C. The greatest average temperature difference between any 2 of the 6 thermocouples for the one week period was 0.3°C.

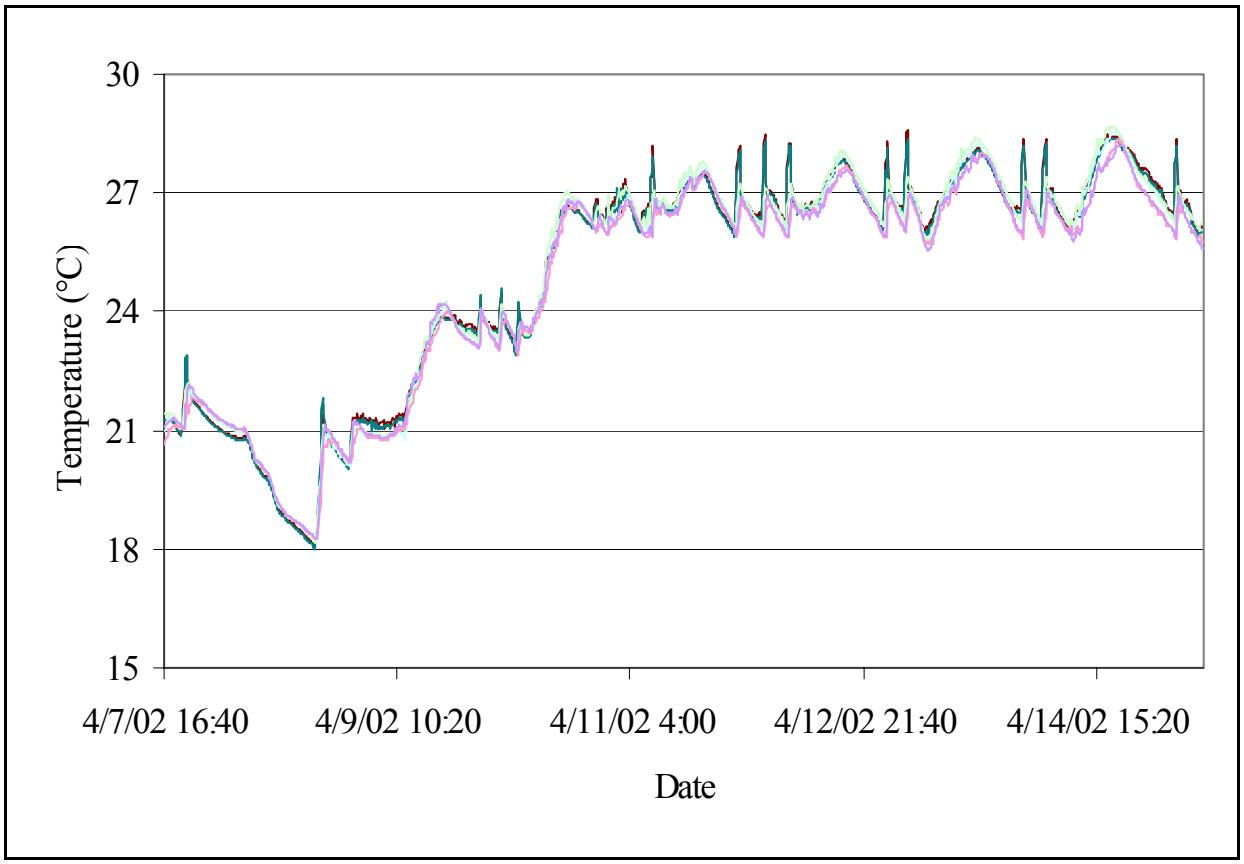

Figure A1.1: The pond temperature was recorded between April 7 and April 14, 2002 in Pond 8. Temperature was measured at the aerator, 13 meters from the aerator and at the pond discharge. At each of location, measurements were taken at 1 foot above the soil surface - pond bottom and 1 foot below the water surface. A total of 6 temperature profiles are shown here. Before April 9, Pond 8 was unheated. The maximum recorded difference between two curves for this time period was 1.6 °C. The maximum average difference between two curves was 0.3°C.

APPENDIX 2: CALCULATING THE SOLAR ZENITH (EXAMPLE)

Example: Determine the solar zenith on the 14th of July at 10:30 A.M. for Baton Rouge, LA (30.53˚N, 91.15˚W).

The 14th of July is 195th day of the year. Therefore, the solar declination is:

$$\delta = 23.45 \sin\left[\frac{360}{365}(284 + 195)\right] \quad \text{(A2.1)}$$

$$\delta = 21.67° \quad \text{(A2.2)}$$

Baton Rouge is in the Central Time Zone, where the standard median is at 90˚ W. If the standard time is 9:30 (remember, 10:30 in July is actually 9:30 standard time), then

$$\omega_{time} = 9.5 + (90 - 91.15) \div 15 \quad \text{(A2.3)}$$

$$\omega_{time} = 9.42 = 9{:}25 \text{ A.M.} \quad \text{(A2.4)}$$

from which

$$\omega = (12 - 9.42) \times 15° \quad \text{(A2.5)}$$

$$\omega = 38.7° \quad \text{(A2.6)}$$

and

$$\cos\theta_z = \sin 30.52° \sin 21.67° + \cos 30.52° \cos 21.67° \cos 38.7° \quad \text{(A2.7)}$$

$$\cos\theta_z = 0.8123 \quad \text{(A2.8)}$$

$$\theta_z = 35.7° \quad \text{(A2.9)}$$

APPENDIX 3: CALCULATING THE EMISSIVE WAVELENGTH SPECTRUM OF WATER AT 300 K

The emissive power of a black body is the sum of all the power carried by all radiation emissions at all wavelengths. The emissive power for a given wavelength can be calculated using Planck's Distributive Equation:

$$\frac{E_{b\lambda}}{T^5} = \frac{C_1}{(\lambda T)^5\left(e^{\left(C_2/\lambda T\right)-1}\right)} \tag{A3.1}$$

where $E_{b\lambda}$ is the emissive power of a black body for a specific wavelength($W/m^2/\mu m$)
T is the temperature of the black body (Kelvin)
λ is the wavelength (μm)
$C_1 = 3.743 \times 10^8$ W • $\mu m^4/m^2$
$C_2 = 1.4387 \times 10^4$ μm • K

Integrating this equation for all wavelengths, one obtains the familiar:

$$E_b = \frac{q}{A} = \sigma T^4 \tag{A3.2}$$

which represents the total emitted radiation from a black body.

The Planck distributive equation is a function of the λT term and its solution for different λT is presented in tabulated form (Holman, 1997). The table also shows, for given λT terms, the percentage of the total black body emitted radiation found within that bandwidth. For 1%, λT = 1444 μm • K. For 99%, λT = 22 222 μm • K. If the temperature of the pond is 27°C, or 300 K, then $\lambda_{1\%} = 4.8$ μm and $\lambda_{99\%} = 74$ μm, the bandwidth of the radiation emitted by a black body at 300 K.

APPENDIX 4: JUSTIFYING THE USE OF CONSTANT SURFACE TEMPERATURE AS AN APPROPRIATE BOUNDARY CONDITION IN DETERMINING THE SOIL HEAT TRANSFER RATE

The soil was treated as a semi-infinite homogenous material when solving the heat diffusion equation:

$$\frac{\partial T}{\partial t} = \alpha \frac{\partial^2 T}{\partial z^2} \tag{A4.1}$$

where T is the temperature at any time and at any position within the soil,
α is the soil's thermal diffusivity (a property of the soil) and
z is depth below the soil surface.

One initial and two boundary conditions were required in solving the heat diffusion equation. They were:

$$T_{soil}(z,t) = T_{initial} \tag{A4.2}$$

(initial condition)

$$\lim_{z\to\infty} T_{soil}(z,t) = T_{z=\infty} \tag{A4.3}$$

(first boundary condition)

$$-k_{soil} A \left.\frac{\partial T}{\partial z}\right|_{z=0} = -hA\left(T_{soil} - T_{pond}\right) \tag{A4.4}$$

(second boundary condition)

where k is the soil's thermal conductivity,
A is the area of the soil surface and
h is the convective heat transfer coefficient.

However, the second boundary condition required the heat transfer coefficient (h) to be known. Because of this, it was desirable to replace the second boundary condition with the following boundary condition:

$$T(z = 0, t) \approx T_{pond} \tag{A4.5}$$

(alternate second boundary condition)

This approximation could be made if the heat transfer rate between the pond and the soil was mainly a function of the thermal properties of the soil. The Biot number (Bi) is a convenient dimensionless number which compares the resistance to conduction and the resistance to convection for the soil.

$$Bi = \frac{R_{cond}}{R_{conv}} = \frac{hL_{char}}{k_{soil}} \tag{A4.6}$$

where R_{cond} is the thermal resistance to conduction
R_{conv} is the thermal resistance to convection
h is the heat transfer coefficient of the water ($W/m^2/K$)
L_{char} is the characteristic length of the soil (m)
k_{soil} is the thermal conductivity of the soil (W/m/K)

The characteristic length of the soil was chosen to be the dampening depth (D) with $\omega = 1.157 \times 10^{-5}\ s^{-1}$ (equation 3.39). The dampening depth for clay is 0.122 m (Van Wijk and De Vries, 1966). From Table 3.7, the thermal conductivity of the soil was estimated as 2.92 W/m/K. If the source of resistance to heat transfer is the soil's conductance, the Biot number will be large (30). So the heat transfer coefficient is:

$$h = \frac{100 \times (2.92W/m/K)}{0.122m} = 2393W/m^2/K \tag{A4.7}$$

To relate this heat transfer coefficient as a velocity, Nusselt, Prandtl and Reynolds numbers were used. The Nusselt number (Nu) is (equation 3.48):

$$Nu = \frac{hL_{char}}{k_{water}} = \frac{(2393W/m^2/K)(3.75m)}{0.614W/m/K} = 14615 \tag{A4.8}$$

Note here that the characteristic length (L_{char}) is different, and was calculated from Equation 3.49. Assuming mixed laminar and turbulent conditions were present, Equation 3.54 was used to determine the Reynolds number (Re) (the Prandlt number (Pr) is 5.85 when the water temperature is at 26°C; Holman, 1997):

$$\mathrm{Re} = \left(\frac{\frac{Nu}{\mathrm{Pr}^{1/3}} + 871}{0.037} \right)^{5/4} = 5388535 \tag{A4.9}$$

Finding the velocity using Equation 3.55 yielded:

$$V = \frac{\mathrm{Re}\,\mu}{\rho L_{char}} = \frac{5388535\left(8.6 \times 10^{-4} kg/m/s\right)}{\left(995.8kg/m^3\right)(3.75m)} = 1.24m/s \tag{A4.10}$$

If the velocity of the water at the soil surface is faster than 0.36 m/s, then the Biot number is large enough to assume that resistance to conduction is limiting the overall heat transfer rate.

APPENDIX 5: DETERMINING THE DAILY PHASE ANGLE AT THE SOIL SURFACE

The second boundary condition in Equation 3.37 gives the soil temperature profile at the surface with respect to time. Daily variations in soil temperature were represented by the second term:

$$T_{amp-day} \sin\left(\omega_{day} t\right) \tag{A5.1}$$

which can be rewritten as

$$T_{amp-day} \sin\left(2\pi \frac{t}{86400}\right) \tag{A5.2}$$

where $T_{amp\text{-}day}$ is the amplitude of the sinusoidal curve describing soil temperature at the surface (°C),
t is time in seconds.

The more general form of this equation is:

$$T_{amp-day} \sin\left(2\pi \frac{t}{86400} + \phi\right) \tag{A5.3}$$

where ϕ is the daily phase angle.

Equation 3.37 assumed that the phase angle is 0 and Fishfry assumes the phase angle is $\pi/2$, both of which are not true for the case of a soil surface submerged under 1.2 meters of water. Assuming that the maximum daily pond temperature occurred at t = 16:00 (t = 57600 seconds), and that the angle inside the sine function must be $\pi/2$ at 16:00, then the daily phase angle must be $-5\pi/6$.

APPENDIX 6: THEORY BEHIND THE DETERMINATION OF TRANSPORT COEFFICIENTS - ANALYTICAL METHOD

(Source: Incropera and De Witt, 1985. Fundamentals of Heat and Mass Transfer 2nd edition , page 284.)

The theory relating the convective heat transfer coefficient (h) and the convective mass transfer coefficient (h_m) relies on boundary layer theory. Both the concentration and thermal boundary layers are similar in shape and are determined by the velocity boundary layer. Both use the diffusion equation and both can be calculated using analogous empirical equations.

$$Nu = f_1(\mathrm{Re}, \mathrm{Pr}) \tag{A6.1a}$$
$$Sh = f_2(\mathrm{Re}, Sc) \tag{A6.1b}$$

Normally, Pr and Sc are related to Nu and Sh by powers of some quantity n.

$$Nu = f_1(\mathrm{Re})\,\mathrm{Pr}^n \tag{A6.2a}$$
$$Sh = f_2(\mathrm{Re})\,Sc^n \tag{A6.2b}$$

The Reynolds number (Re) is the same for both functions because both functions are subjected to the same geometry,

$$f_1(\mathrm{Re}) = f_2(\mathrm{Re}) \tag{A6.3}$$

so...

$$\frac{Nu}{\mathrm{Pr}^n} = \frac{Sh}{Sc^n} \Rightarrow \frac{Nu}{Sh} = \frac{\mathrm{Pr}^n}{Sc^n} = Le^{-n} \tag{A6.4}$$

and...

$$\frac{Nu}{Sh} = \frac{\dfrac{hL_c}{k_{fluid}}}{\dfrac{h_m L_c}{D_{AB}}} = \frac{h}{h_m}\frac{D_{AB}}{k_{fluid}} = Le^{-n} \tag{A6.5}$$

By definition, the Lewis number is thermal diffusivity divided by the mass diffusivity.

$$Le = \frac{\alpha}{D_{AB}} = \frac{k_{fluid}}{\rho_{fluid} c_{p-fluid} D_{AB}} \tag{A6.6}$$

Rearranging the terms gives:

$$\frac{D_{AB}}{k_{fluid}} = \left(\rho_{fluid} c_{p-fluid} Le\right)^{-1} \tag{A6.7}$$

$$h = h_m \left(\rho c_p\right) Le^{1-n}$$

Substituting A6.7 into equation A6.5, and isolating for h_m gives Equation 5.1:

(A6.8)

APPENDIX 7: DERIVATION OF EQUATION 5.3

Given Equation 3.4:

$$\left(\frac{dE}{dt}\right)_{pond} = q_{solar} - q_{back} + q_{sky} \pm q_{conv} - q_{evap} \pm q_{soil} + q_{rain} - q_{seep} + q_{well} - q_{out} \quad \text{(A7.1)}$$

and given Equation 5.1

$$h = h_m\left(\rho c_p\right)Le^{1-n} \quad \text{(A7.2)}$$

one can solve for h_m. Consider Fick's law of diffusion:

$$\dot{m}_{water} = h_m A\left(C_{water} - C_{air}\right) \quad \text{(A7.3)}$$

where m'_{water} is the evaporation rate,
h_m is the convective mass transfer coefficient,
A is the area,
C_{water} is the concentration of water vapour at the pond surface and
C_{air} is the concentration of water vapour in the air.

Using the perfect gas law, Equation A7.3 can be rewritten as

$$\dot{m}_{water} = h_m A\left(\frac{MM}{R}\right)\left(\left(\frac{P}{T}\right)_{water} - \left(\frac{P}{T}\right)_{air}\right) \quad \text{(A7.4)}$$

where MM is the molar mass of water,
R is the universal gas constant,
P is the pressure of the water vapour and
T is the absolute temperature.

The energy lost to evaporation is:

$$q_{evap} = h_{fg}\dot{m} = h_{fg}h_m A\left(\frac{MM}{R}\right)\left(\left(\frac{P}{T}\right)_{water} - \left(\frac{P}{T}\right)_{air}\right) \quad \text{(A7.5)}$$

Newton's law of cooling is used to predict the heat lost by convection.

$$q_{conv} = hA\left(T_{air} - T_{pond}\right) \quad \text{(A7.6)}$$

Using Equation A7.2, Equation A.6 becomes

$$q_{conv} = h_m \left(\rho c_p\right)_{air} Le^{1-n} A\left(T_{air} - T_{water}\right) \tag{A7.7}$$

Substituting A7.5 and A7.7 into A7.1, and then isolating h_m, one gets Equation 5.3

$$h_m = \frac{\left(\frac{dE}{dt}\right)_{pond} - \left(q_{solar} - q_{back} + q_{sky} \pm q_{soil} - q_{seep} + q_{rain} + q_{well} - q_{out}\right)}{A\left(Le^{2/3}\rho_{air} c_{p-air}\left(T_{air} - T_{pond}\right) - h_{fg}\frac{MM}{R}\left(\left(\frac{P}{T}\right)_{surface} - \left(\frac{P}{T}\right)_{air}\right)\right)} \tag{A7.8}$$

APPENDIX 8: PYRANOMETER INFORMATION

A pyranometer sensor (LI-COR LI-200SZ) was used to measure the solar radiation below the water surface. The sensor, shown below, had a coaxial cable with the inner cable being the positive lead and the outer cable being the negative lead. Because the pyranometer produced a current signal, it was necessary to use a 147-Ohm resistor to convert this signal into a voltage signal (schematic in Figure A8.2).

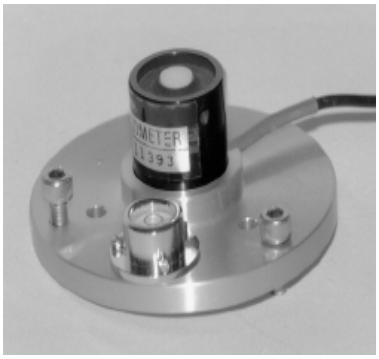

Figure A8.1: A pyranometer, similar to this one, was used to measure solar radiation under water.

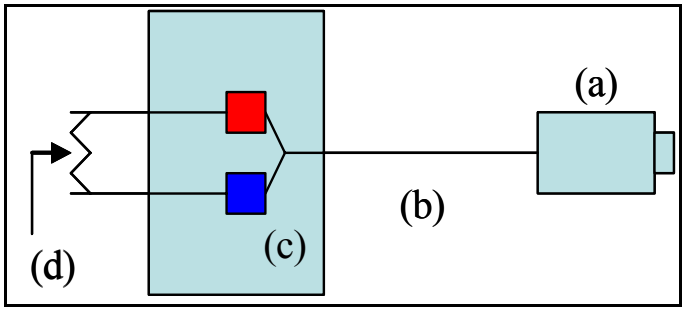

Figure A8.2: The pyranometer (a) was connected to the data logger (c) with the use of a coaxial wire (b). The inner wire was connected to the high lead while the outer shield was connected to the low lead. A 147 Ohm resistor (d) was also connected across the data logger terminal.

A data logger (Campbell Scientific 21X, Campbell Scientific Inc., North Logan, UT) was used as an output device so that measurements could be read. The following program was entered into the data logger. Measurements were recorded so that the LI-COR pyranometer could be calibrated to an Eppley Radiometer (model PSP).

```
;{21X}
;
*Table 1 Program
  01: 1        Execution Interval (seconds)

1:  Volt (Diff) (P2)
 1: 1        Reps
 2: 3        50 mV Slow Range
 3: 2        DIFF Channel
 4: 1        Loc [ small     ]
 5: 99.8     Mult
 6: 0.0      Offset
```

```
2:  Volt (Diff) (P2)
 1: 1        Reps
 2: 3        50 mV Slow Range
 3: 3        DIFF Channel
 4: 2        Loc [ big       ]
 5: 115.7    Mult
 6: 0.0      Offset


3:  If time is (P92)
 1: 0        Minutes into a
 2: 1        Minute Interval
 3: 10       Set Output Flag High


4:  Real Time (P77)
 1: 1220     Year,Day,Hour/Minute (midnight = 2400)

5:  Sample (P70)
 1: 2        Reps
 2: 1        Loc [ small     ]

6:  Batt Voltage (P10)
 1: 3        Loc [ batery    ]

*Table 2 Program
  02: 0         Execution Interval (seconds)

*Table 3 Subroutines

End Program
```

APPENDIX 9: EXAMPLE CALCULATIONS SHOWING THE NEED FOR SENSITIVE TEMPERATURE SENSING DEVICES IN CHAPTER 5.5.1

Consider a pond 400 m^3 in volume, subjected to a temperature change of 0.01°C over 10 minutes (600 seconds). Such a change in temperature represents a change in energy of

$$\left(\frac{\Delta E}{\Delta t}\right)_{pond} = \rho \forall c_p \frac{\Delta T}{\Delta t}$$

$$= \left(990 kg/m^3\right)\left(400 m^3\right)\left(4180 J/kg/K\right)\left(\frac{0.01^o C}{600 s}\right)$$

$$= 27588 W$$

The average long wave sky radiation between the 13th of February and the 23rd of March, 2003 for unheated Pond 3 was 110 000W. Therefore, an error of 0.04°C for a difference of two successive pond temperature readings is equivalent in magnitude to long wave sky radiation.

APPENDIX 10: DATA LOGGER PROGRAMS

The following basic program was used to measure the pond temperature a data logger (Campbell Scientific 21X, Campbell Scientific Inc., North Logan, UT). The multiplier in Instruction P:14(7) and the offset in Instruction P:14(8) were used to calibrate the thermocouple readings, so as to avoid additional manipulations during the analysis of data.

```
;{21X}
;
*Table 1 Program
  01: 60       Execution Interval (seconds)
1:  Internal Temperature (P17)
 1: 1        Loc [ ref_temp  ]

2:  Thermocouple Temp (DIFF) (P14)
 1: 1        Reps
 2: 1        5 mV Slow Range
 3: 1        DIFF Channel
 4: 1        Type T (Copper-Constantan)
 5: 1        Ref Temp (Deg. C) Loc [ ref_temp  ]
 6: 2        Loc [ soil_far  ]
 7: 1.008    Mult
 8: -.016    Offset

3:  Thermocouple Temp (DIFF) (P14)
 1: 1        Reps
 2: 1        5 mV Slow Range
 3: 2        DIFF Channel
 4: 1        Type T (Copper-Constantan)
 5: 1        Ref Temp (Deg. C) Loc [ ref_temp  ]
 6: 3        Loc [ bot_far   ]
 7: 1.008    Mult
 8: -.016    Offset

4:  Thermocouple Temp (DIFF) (P14)
 1: 1        Reps
 2: 1        5 mV Slow Range
 3: 3        DIFF Channel
 4: 1        Type T (Copper-Constantan)
 5: 1        Ref Temp (Deg. C) Loc [ ref_temp  ]
 6: 4        Loc [ high_far  ]
 7: 1.020    Mult
 8: -.136    Offset
```

5: Thermocouple Temp (DIFF) (P14)
 1: 1 Reps
 2: 1 5 mV Slow Range
 3: 4 DIFF Channel
 4: 1 Type T (Copper-Constantan)
 5: 1 Ref Temp (Deg. C) Loc [ref_temp]
 6: 5 Loc [sur_far]
 7: 1.008 Mult
 8: -.016 Offset

6: Thermocouple Temp (DIFF) (P14)
 1: 1 Reps
 2: 1 5 mV Slow Range
 3: 5 DIFF Channel
 4: 1 Type T (Copper-Constantan)
 5: 1 Ref Temp (Deg. C) Loc [ref_temp]
 6: 6 Loc [soil_near]
 7: 1.005 Mult
 8: .034 Offset

7: Thermocouple Temp (DIFF) (P14)
 1: 1 Reps
 2: 1 5 mV Slow Range
 3: 6 DIFF Channel
 4: 1 Type T (Copper-Constantan)
 5: 1 Ref Temp (Deg. C) Loc [ref_temp]
 6: 7 Loc [bot_near]
 7: 1.010 Mult
 8: 0 Offset

8: Thermocouple Temp (DIFF) (P14)
 1: 1 Reps
 2: 1 5 mV Slow Range
 3: 7 DIFF Channel
 4: 1 Type T (Copper-Constantan)
 5: 1 Ref Temp (Deg. C) Loc [ref_temp]
 6: 8 Loc [high_near]
 7: 1.008 Mult
 8: 0.017 Offset

9: Thermocouple Temp (DIFF) (P14)
 1: 1 Reps
 2: 1 5 mV Slow Range
 3: 8 DIFF Channel

```
 4: 1        Type T (Copper-Constantan)
 5: 1        Ref Temp (Deg. C) Loc [ ref_temp  ]
 6: 9        Loc [ sur_near  ]

 7: 1.005    Mult
 8: 0.101    Offset

10:  Batt Voltage (P10)
 1: 10       Loc [ battery   ]

11:  If time is (P92)
 1: 0        Minutes into a
 2: 10       Minute Interval
 3: 10       Set Output Flag High

12:  Real Time (P77)
 1: 1220     Year,Day,Hour/Minute (midnight = 2400)

13:  Sample (P70)
 1: 10       Reps
 2: 1        Loc [ ref_temp  ]

*Table 2 Program
  02: 0.0000    Execution Interval (seconds)

*Table 3 Subroutines

End Program
```

If in addition to 8 thermocouples an anemometer is being used, the following program should be entered into the data logger.

```
*Table 1 Program
  01: 60        Execution Interval (seconds)
1:  Internal Temperature (P17)
 1: 1        Loc [ ref_temp  ]

2:  Thermocouple Temp (DIFF) (P14)
 1: 1        Reps
 2: 1        5 mV Slow Range
 3: 1        DIFF Channel
 4: 1        Type T (Copper-Constantan)
 5: 1        Ref Temp (Deg. C) Loc [ ref_temp  ]
```

6: 2 Loc [soil_far]
7: 0.988 Mult
8: .544 Offset

3: Thermocouple Temp (DIFF) (P14)
1: 1 Reps
2: 1 5 mV Slow Range
3: 2 DIFF Channel
4: 1 Type T (Copper-Constantan)
5: 1 Ref Temp (Deg. C) Loc [ref_temp]
6: 3 Loc [bot_far]
7: 1.002 Mult
8: .154 Offset

4: Thermocouple Temp (DIFF) (P14)
1: 1 Reps
2: 1 5 mV Slow Range
3: 3 DIFF Channel
4: 1 Type T (Copper-Constantan)
5: 1 Ref Temp (Deg. C) Loc [ref_temp]
6: 4 Loc [high_far]
7: 1.004 Mult
8: .385 Offset

5: Thermocouple Temp (DIFF) (P14)
1: 1 Reps
2: 1 5 mV Slow Range
3: 4 DIFF Channel
4: 1 Type T (Copper-Constantan)
5: 1 Ref Temp (Deg. C) Loc [ref_temp]
6: 5 Loc [sur_far]
7: .997 Mult
8: .25 Offset

6: Thermocouple Temp (DIFF) (P14)
1: 1 Reps
2: 1 5 mV Slow Range
3: 5 DIFF Channel
4: 1 Type T (Copper-Constantan)
5: 1 Ref Temp (Deg. C) Loc [ref_temp]
6: 6 Loc [soil_near]
7: 1.033 Mult
8: -.905 Offset

```
7:  Thermocouple Temp (DIFF) (P14)
 1: 1        Reps
 2: 1        5 mV Slow Range
 3: 6        DIFF Channel
 4: 1        Type T (Copper-Constantan)
 5: 1        Ref Temp (Deg. C) Loc [ ref_temp  ]
 6: 7        Loc [ bot_near  ]

 7: 1.028    Mult
 8: -.834    Offset

8:  Thermocouple Temp (DIFF) (P14)
 1: 1        Reps
 2: 1        5 mV Slow Range
 3: 7        DIFF Channel
 4: 1        Type T (Copper-Constantan)
 5: 1        Ref Temp (Deg. C) Loc [ ref_temp  ]
 6: 8        Loc [ high_near ]
 7: 1.013    Mult
 8: -.218    Offset

9:  Thermocouple Temp (DIFF) (P14)
 1: 1        Reps
 2: 1        5 mV Slow Range
 3: 8        DIFF Channel
 4: 1        Type T (Copper-Constantan)
 5: 1        Ref Temp (Deg. C) Loc [ ref_temp  ]
 6: 9        Loc [ sur_near  ]
 7: .988     Mult
 8: 1.265    Offset

10:  Batt Voltage (P10)
 1: 10       Loc [ battery   ]

11:  Pulse (P3)
 1: 1        Reps
 2: 2        Pulse Input Channel
 3: 21       Low Level AC, Output Hz
 4: 11       Loc [ wind      ]
 5: 0.75     Mult
 6: .2       Offset

12:  If time is (P92)
 1: 0        Minutes into a
```

```
 2: 10       Minute Interval
 3: 10       Set Output Flag High

13:  Real Time (P77)
 1: 1220     Year,Day,Hour/Minute (midnight = 2400)

14:  Sample (P70)
 1: 10       Reps
 2: 1        Loc [ ref_temp  ]

15:  Average (P71)
 1: 1        Reps
 2: 11       Loc [ wind      ]

*Table 2 Program
  02: 0.0000    Execution Interval (seconds)

*Table 3 Subroutines

End Program
```

If, in addition to 8 thermocouples a weather vane is being use, the following program should be entered into the datalogger:

```
;{21X}
;
*Table 1 Program
  01: 60       Execution Interval (seconds)
1:  Internal Temperature (P17)
 1: 1        Loc [ ref_temp  ]

2:  Thermocouple Temp (DIFF) (P14)
 1: 1        Reps
 2: 1        5 mV Slow Range
 3: 1        DIFF Channel
 4: 1        Type T (Copper-Constantan)
 5: 1        Ref Temp (Deg. C) Loc [ ref_temp  ]
 6: 2        Loc [ soil_far  ]
 7: 1.01     Mult
 8: -.269    Offset

3:  Thermocouple Temp (DIFF) (P14)
 1: 1        Reps
 2: 1        5 mV Slow Range
```

```
 3: 2       DIFF Channel
 4: 1       Type T (Copper-Constantan)
 5: 1       Ref Temp (Deg. C) Loc [ ref_temp  ]
 6: 3       Loc [ bot_far   ]
 7: 1.008   Mult
 8: -.185   Offset

4:  Thermocouple Temp (DIFF) (P14)
 1: 1       Reps
 2: 1       5 mV Slow Range
 3: 3       DIFF Channel
 4: 1       Type T (Copper-Constantan)
 5: 1       Ref Temp (Deg. C) Loc [ ref_temp  ]
 6: 4       Loc [ high_far  ]
 7: 1.027   Mult
 8: -.635   Offset

5:  Thermocouple Temp (DIFF) (P14)
 1: 1       Reps
 2: 1       5 mV Slow Range
 3: 4       DIFF Channel
 4: 1       Type T (Copper-Constantan)
 5: 1       Ref Temp (Deg. C) Loc [ ref_temp  ]
 6: 5       Loc [ sur_far   ]
 7: 1.01    Mult
 8: -.236   Offset

6:  Thermocouple Temp (DIFF) (P14)
 1: 1       Reps
 2: 1       5 mV Slow Range
 3: 5       DIFF Channel
 4: 1       Type T (Copper-Constantan)
 5: 1       Ref Temp (Deg. C) Loc [ ref_temp  ]
 6: 6       Loc [ soil_near ]
 7: 1.01    Mult
 8: -.202   Offset

7:  Thermocouple Temp (DIFF) (P14)
 1: 1       Reps
 2: 1       5 mV Slow Range
 3: 6       DIFF Channel
 4: 1       Type T (Copper-Constantan)
 5: 1       Ref Temp (Deg. C) Loc [ ref_temp  ]
 6: 7       Loc [ bot_near  ]
```

7: 1.013 Mult
8: -.219 Offset

8: Thermocouple Temp (DIFF) (P14)
1: 1 Reps
2: 1 5 mV Slow Range
3: 7 DIFF Channel
4: 1 Type T (Copper-Constantan)
5: 1 Ref Temp (Deg. C) Loc [ref_temp]
6: 8 Loc [high_near]
7: 1.01 Mult
8: -.202 Offset

9: Thermocouple Temp (DIFF) (P14)
1: 1 Reps
2: 1 5 mV Slow Range
3: 8 DIFF Channel
4: 1 Type T (Copper-Constantan)
5: 1 Ref Temp (Deg. C) Loc [ref_temp]
6: 9 Loc [sur_near]
7: 1.046 Mult
8: -.508 Offset

10: Batt Voltage (P10)
1: 10 Loc [battery]

11: Excite Delay Volt (SE) (P4)
1: 1 Reps
2: 5 5000 mV Slow Range
3: 1 SE Channel
4: 1 Excite all reps w/Exchan 1
5: 2 Delay (units 0.01 sec)
6: 5000 mV Excitation
7: 11 Loc [winddir]
8: 0.071 Mult
9: 0.0 Offset

12: If time is (P92)
1: 0 Minutes into a
2: 10 Minute Interval
3: 10 Set Output Flag High

13: Real Time (P77)

```
 1: 1220     Year,Day,Hour/Minute (midnight = 2400)

14:  Sample (P70)
 1: 10       Reps
 2: 1        Loc [ ref_temp  ]

15:  Average (P71)
 1: 1        Reps
 2: 11       Loc [ winddir   ]

*Table 2 Program
  02: 0.0000    Execution Interval (seconds)

*Table 3 Subroutines

End Program
```

APPENDIX 11: HOW TO USE FISHFRY

To use Fishfry, the following 4 ASCII data files must be available to the executive program in the same directory:

- information.dat: lists all the soil and pond parameters as well as the initial conditions. The file must have the following layout, although the numeric values can change.

3600.0000000000	step size (s)
31104000.0000000000	Initial time (s)
17.0000000000	Pond temperature (˚C)
33609600.0000000000	Upper time limit (s)
480.0000000000	Pond Volume (m^3)
394.0000000000	Pond area (m^2)
990.0000000000	Water density (kg/m^3)
4180.0000000000	Specific heat of water (J/kg˚C)
0.9599999785	Water emissivity (decimal)
0.0000005500	thermal diffusivity (m^2/s)
1.0000000000	soil density (kg/m^3)
2900000.0953674316	specific heat (J/kg˚C)
5.6999998093	soiltempamp_year (˚C)
5.0000000000	soiltempamp_day (˚C)
1.5707963705	phase_year (radians)
1.5707963705	phase_day (radians)

Figure A11.1: The required layout for the information.dat file.

- weather.dat: lists all the weather data for a certain time step specified in information.dat. This ASCII file contains 8 columns. The first 3 are arbitrary numbers (usually the year, day of the year and time). The forth column is for the air temperature (°C), the fifth is for relative humidity (a number between 1 and 100), the sixth is for solar radiation (kW/m^2), the seventh is for wind speed (m/s), the eight is for rainfall (inches/hr).

- flow.dat: this is a 5 column ASCII file. The first 3 are arbitrary numbers (usually the year, day of the year and time). The forth column lists the flow rate of warm water into the pond. The fifth column lists the flow rate of cold water into the pond.

- temp.dat: this is a 1 column ASCII file which lists the pond temperature (°C). This is for cases when the user is interested in knowing the flow rate of water

needed to maintain his pond temperature at a certain value (used only for option 1).

Once these files are available in the home directory, the user can run Fishfry.exe. After starting the program, the following prompt will appear:

```
Welcome to FISHFRY, the easy way to know how much heat you
need to supply to the pond so that your fish won't freeze or cook.

Please remember to include the following files in the FISHFRY
directory/folder before running the program:

                    - information.dat
                    - weather.dat
                    - flow.dat
                    - temp.dat

The output file will be called output.dat, where columns are space
seperated, and easily viewed in your favorite spreadsheet.

Press any number to continue

What do you want FISHFRY to do?
Please enter the appropriate number.

(1) Determine the flow rate of water into the pond to maintain
    a desired pond temperature.

(2) Determine the temperature of a pond given the flow rate
    and weather.

(0) End FISHFRY, the best program in the whole wide world.
```

Figure A11.2: The Fishfry User Prompt is accessed from DOS.

Once the user has selected one of these choice, the model will prompt the user for a name for the output file, the initial pond temperature (°C), the temperature of the warm water at the inlet (°C), the temperature of the cold water at the inlet (°C), the name of the weather file and the name of the pond temperature file. If no warm or cold water is being used, enter 0 when asked for the temperature.

Fishfry will then compile results. Sometimes, Fishfry will give out an error statement at the end of a model run. This happened because there was not enough input information for the defined

time period (defined in information.dat). The user must make sure the number of input data in a file is equal to the number of time steps.

Once the program is finished, the user can open the output file in a spreadsheet program as a ASCII file with comma separated variables.

APPENDIX 12: PROGRAM CODE FOR FISHFRY

```
PROGRAM fishfry
IMPLICIT NONE

!=====================================================================
! INTRODUCTION
!---------------------------------------------------------------------
!
!      Fishfry v 1.2 is the master version of Fishfry which includes some
!      some of the suggested modifications made in chapter 4.  Although
!      equations for the effects of soil heat transfer are present, they
!      have been made idle due to their small contribution to the overall
!      pond energy balance.
!
!      This version of Fishfry has two modes.  The first is more practicle
!      for managing the supply of cool and warm water.  For a given pond
!      temperature, which can be made to varry in the temp.dat input file,
!      Fishfry will calculate the amount of cold and warm water required to
!      keep the pond at that given temperature.
!
!      The second Fishfry mode is more useful for validating the model,
!      although it can be used as a management tool.  Fishfry, in mode 2,
!      will solve for the pond temperature given all the energy fluxes.
!
!=====================================================================
! FUNCTIONS
!---------------------------------------------------------------------
!      dTemp - Differential Equation
!
!      The following interface evaluates dTemp for a given temp and time, using
!         the 4th order Runge Kutta numerical method

Interface
FUNCTION dTemp(Temp,time,coefficient,thermal_mass, airtemp) !step)
IMPLICIT NONE
      REAL (8), INTENT (IN):: Temp, time, thermal_mass, airtemp !, step
      REAL (8), dimension (10), INTENT (IN):: coefficient
      REAL (8):: dTemp
END function dTemp
END interface

!---------------------------------------------------------------------
!      emissivity_sky
```

```
!
!       The following interface evaluates the emissivity of a clear sky.

Interface
Function emissivity_sky(airtemp,rh)
Implicit NONE

REAL (8), INTENT(IN):: airtemp, rh
rEAL (8):: emissivity_sky

END function emissivity_sky
end interface

!-------------------------------------------------------------------------
!       vapour pressure
!
!       The following interface is for a function which evaluates the vapour
!       pressure in Pascals.
!

Interface
FUNCTION vp(T, rh)
IMPLICIT NONe
REAL (8), INTENT (IN):: T, rh
REAL (8):: vp
eND function vp
end Interface

!-------------------------------------------------------------------------
!       Wind speed correction function - REQUIRES AN INPUT!
!
!       The following interface is for a function which corrects wind speed for
!       the Lake Hefner equation.  It also converts units from m/s to mph.
!

Interface
function ws(windspeed)
implicit none
REAL (8), INTENT (IN):: windspeed
REAL (8):: ws
end function ws
END interface

!
```

```
!=====================================================================
! VARIABLE DECLARATIONS
!---------------------------------------------------------------------
!         Runge Kutta variables

REAL (8)::  F1, F2, F3, F4
REAL (8)::  Temp, time, step, timemax

!       Temp: pond temperature (C)
!       time: time (sec)
!       step: time step (sec)
!       timemax: upper integration limit (sec)
!       F1, F2, F3, F4: integration formulae for Runge-Kutta
!
!---------------------------------------------------------------------
!       Pond parameters

REAL(8):: volume, area, density, specheat, Thermal_mass, emissivity_water

!       Volume: pond volume (m^3)
!       Area: pond surface area (m^2)
!       density: density of pond water (kg/m^3)
!       specheat: specific heat of water (J/kg/C)
!       Thermal_mass: Volume*density*specfic heat (J/C)
!       emissivity_water: emissivity of the water
!
!---------------------------------------------------------------------
!      Flux parameters

REAL(8):: latent_energy
REAL(8):: flow_rate_hot, flow_rate_cold, gpm_hot, gpm_cold, hot, cold

!       latent_energy: energy for the vapourization of water
!       hot: the temperature of the warm influent  (C)
!       cold: the temperature of the cold influent (C)
!       flow_rate_hot: the flow rate of the warm effluent (m^3/s)
!       flow_rate_cold: the flow rate of the cold effluent (m^3/s)
!       gpm_hot:: the flow rate of the warm effluent (gpm)
!       gpm_cold: the flow rate of the cold effluent (gpm)
!
!---------------------------------------------------------------------
!       Atmospheric parameters
```

```
REAL (8):: airtemp, rh, windspeed, solar_radiation, x, rain!, winddirection

!       emissivity_sky: emissivity in the sky (decimal)
!       airtemp: air temperature (C)
!       rh: relative humidity (demical)
!       solar_radiation: solar_radiation (J/m^2/s)
!       windspeed: wind speed (mph)

!       wind direction: degrees, 0 = North
!       x: relative humidity of 100% (1)
!
!-------------------------------------------------------------------------
!       Soil parameters
!
!Real(8):: thermal_conductivity, thermal_diffusivity, soil_density
!REAL(8):: cp_soil, Dday, Dyear, temp_initial, PI
!REAL(8):: Soiltempamp_year, Soiltempamp_day, phase_year, phase_day

!
!       thermal conductivity: J/m/C/s (Fourier's heat conduction law)
!       thermal diffusivity: m^2/s    (Heat diffusion equation)
!       Soil_density: kg/m^3
!       cp_soil: Soil specific heat (J/kg˚C)
!       Dday: dampening depth for daily variations (m)
!       Dyear: dampening depth for yearly variations (m)
!       temp_initial: initial soil temperature (˚C)
!          Soiltempamp_year: The yearly amplitude for soil temperature (˚C)
!          Soiltempamp_day: The daily amplitude for soil temperature (˚C)
!          phase_year: phase angle for the year
!          phase_day:  phase angle for the day
!       PI
!
!-------------------------------------------------------------------------
!          Coefficient arrays
!

REAL(8), dimension (10):: coefficient, vector

!       Coefficient (1): coefficient for pond longwave radiation
!       Coefficient (2): coefficient for atmospheric longwave radiation
!       Coefficient (3): coefficient for soil heat exchange
!       Coefficient (4): coefficient for surface evaporation
!       Coefficient (5): coefficient for surface convection
!       Coefficient (6): coefficient for penetrated solar radiation
```

```
!      Coefficient (7): coefficient for warm water inlet

!      Coefficient (8): coefficient for cold water inlet
!      Coefficient (9): coefficient for discharge
!
!      Vector (1): Power due to pond longwave radiation
!      Vector (2): Power due to atmospheric longwave radiation
!      Vector (3): Power due to soil heat exchange
!      Vector (4): Power due to surface evaporation
!      Vector (5): Power due to surface convection
!      Vector (6): Power due to solar radiation
!      Vector (7): Energy flow in the hot water
!      Vector (8): Energy flow in the cold water
!      Vector (9): Energy flow in the discharge
!
!      All vector terms are in Joules/second (Watts)
!
!-------------------------------------------------------------------------
!         Other parameters
!

integer:: choice
CHARACTER(LEN=12):: weather_file, temp_file, pond
!
!=========================================================================
! FILES AND FORMAT
!-------------------------------------------------------------------------

OPEN (99, FILE="information.dat")    ! Information input data file
!OPEN (100, FILE="output.dat")       ! Output data file
!OPEN (200, FILE="weather.dat")      ! Input air temperature data file
OPEN (300, FILE="flow.dat")         ! Flow input
!OPEN (400, FILE="temp.dat")         ! Pond Temperature input

10     FORMAT (20(f30.6, ","), f30.6)
20     FORMAT (20(a30, ","), a30)


!=========================================================================
! SETTING OF PARAMETERS (USER REQUIRED INPUT HERE)
!-------------------------------------------------------------------------
!      Initial conditions
```

```
READ (99,*) step           ! Step size (s)
Read (99,*) time           ! Initial time(s)
Read (99,*) temp           ! Initial pond water temperature (C)
Read (99,*) timemax        ! Upper limit for time (s)

!
!-------------------------------------------------------------------------
!       Properties of the pond


Read (99,*) Volume          ! in m^3
Read (99,*) Area            ! in m^2

Read (99,*) Density         ! in kg/m^3
Read (99,*) Specheat        ! in J/kg/C

Thermal_mass = Volume*Density*Specheat

Read (99,*) Emissivity_water     ! decimal
x = 1.0                          ! constant (no input here)
!PI=ACOS(-1.0)                   ! the value of pi
!-------------------------------------------------------------------------
!       Properties of the liner (soil)
!


!read (99,*) thermal_diffusivity   ! soil thermal diffusivity (m^2/s)
!read (99,*) soil_density          ! bulk soil density (kg/m^3)
!read (99,*) cp_soil               ! soil specific heat (J/kg˚C)
!read (99,*) Soiltempamp_year      ! Yearly soil amplitude (˚C)
!read (99,*) Soiltempamp_day       ! Daily soil amplitude (˚C)
!read (99,*) phase_year            ! Phase angle, year (radians)
!read (99,*) phase_day             ! Phase angle, day (radians)


!temp_initial=temp
!Thermal_conductivity=thermal_diffusivity*(soil_density*cp_soil)
!Dday=SQRT(2.0*thermal_conductivity/soil_density/cp_soil*86400.0/2/PI)
!Dyear=SQRT(2.0*thermal_conductivity/soil_density/cp_soil*31536000.0/2/PI)


!
!=========================================================================
!         User prompt to determine if the pond is at steady state or transient.
```

```
!
write (*,*) "Welcome to FISHFRY, the easy way to know how much heat you need"
write (*,*) "to supply to the pond so that your fish won't freeze or cook."
write (*,*) " "
write (*,*) "Please remember to include the following files in the FISHFRY"
write (*,*) "directory/folder before running the program: "
write (*,*) " "
write (*,*) "               - information.dat "
write (*,*) "               - weather.dat"
write (*,*) "               - flow.dat"
write (*,*) "               - temp.dat"
write (*,*) " "
write (*,*) "The output file will be called output.dat, where columns are space"
write (*,*) "seperated, and easily viewed in your favorite spreadsheet."
write (*,*) " "
write (*,*) "Press any number to continue"
write (*,*) " "
READ (*,*) choice

111 write (*,*) "What do you want FISHFRY to do?"
write (*,*) "Please enter the appropriate number."
write (*,*) " "
write (*,*) " (1) Determine the flow rate of water into the pond to maintain"
write (*,*) "     a desired pond temperature."
write (*,*) " "
write (*,*) " (2) Determine the temperature of a pond given the flow rate"
write (*,*) "     and weather."
write (*,*) " "
write (*,*) " (0) End FISHFRY, the best program in the whole wide world."
write (*,*) " "
read (*,*) choice

IF (choice>2) THEN
write (*,*) "You have made an invalid choice."
GO TO 111
END IF

!=====================================================================
!      SETTING INITIAL OR BOUNDARY CONDITIONS
!

write (*,*) "Which pond is being considered?"
write (*,*) " "
read (*,*) pond
```

```
write (*,*) "What is the temperature of the warm influent? (C)"
write (*,*) " "
read (*,*) hot

write (*,*) "What is the temperature of the cool influent? (C)"
write (*,*) " "
read (*,*) cold

IF (choice==2) THEN

write (*,*) "What is the initial pond temperature?"
write (*,*) " "
read (*,*) temp

END IF

IF (choice==0) GO TO 9

WRITE (*,*) "What is the name of the weather file? "
READ (*,*) weather_file
WRITE (*,*) "What is the name of the temp file? "
READ (*,*) temp_file


OPEN (200, FILE=weather_file)       ! Input air temperature data file
OPEN (400, FILE=temp_file)          ! Flow input
open (100, FILE=pond)


!=====================================================================
! HEADINGS FOR OUTPUT FILES
!
!
WRITE (100, *) "Results from Fishfry; OUTPUT.DAT"
WRITE (100, *) " "
WRITE (100, *) "Pond number: ", pond
WRITE (100, *) " "
WRITE (100, *) "Initial day of trial: ", time/24/3600+1
WRITE (100, *) "Final day of trial: ", timemax/24/3600+1
WRITE (100, *) " "

WRITE (100,*) "Influent hot temperature (C): ", hot , "Type of year:", weather_file
WRITE (100,*) "Influent cold temperature (C): ", cold, "Pond Temperature:", temp_file
WRITE (100,*) " "
```

```
!
! Case 1: Determination of flowrates
!

IF (choice==1) THEN

WRITE (100,20) "Time", " ", "Pond Radiation", "Sky Radiation", "Soil Conduction", &
        & "Evaporation", "Convection", "Solar Radiation", "Rain", "Rain out",&
        & "Surplus/deficit", "Warm Water Flow", "Warm Water Flow",&
        & "Cool Water Flow","Cool Water Flow"

WRITE (100,20) "(seconds)","(days)", "(Watts)", "(Watts)", "(Watts)", "(Watts)", "(Watts)",&
        & "(Watts)", "(Watts)", "(Watts)", "(Whr)", "(m^3/s)", "(GPM)",&
        & "(m^3/s)", "(GPM)"


        END IF

! Case 2: Determination of pond temperature

IF (choice==2) THEN

WRITE (100,20) "Time", " ", "Pond Radiation", "Sky Radiation", "Soil Conduction", &
        & "Evaporation", "Convection", "Solar Radiation", &
        & "Warm inlet", "Cold inlet", "Discharge", "Rain", "Pond Temperature"

WRITE (100,20) "(seconds)", "(days)", "(Watts)", "(Watts)", "(Watts)", "(Watts)", &
        & "(Watts)", "(Watts)", "(Watts)", "(Watts)", "(Watts)", "(Watts)","(˚C)"

        END IF

!=======================================================================
! CALCULATIONS AND INTEGRATION

DO

!-----------------------------------------------------------------------
!       Determination of the atmospheric variables
!
!       Because the user may wish to either use recorded data or generated
!       weather data, all atmospheric variables will be called up from *.dat
!       files.  The user, however, must make sure the time steps in the data
!       file corresponds to the time step in this program.  For instance, if the
!       model is to simulate pond heat transfer as of March 10th, every 10
```

```
!         minutes, then data for every 10 minutes as of March 10th are to be in
!      the respective *.dat file.
!
!      In the absence of real data, the user may generate his/her own data
!      with the use of sinusoidal functions.  For temperature approximations for
!      Baton Rouge, LA, the program temperature.exe, generated from the
!         temperature.f90 code, can be used.
!
!      Also, MAKE SURE THAT THE DATA FILES ARE IN THE SAME DIRECTORY AS
! FISHFRY!
!

read (200, *) airtemp, airtemp, airtemp, airtemp, rh, solar_radiation, windspeed, rain

!     Conversions

rh=rh*0.01
solar_radiation=solar_radiation*1000.0
windspeed=windspeed*3600.0/1609.0 ! converts m/s to mph
rain=rain/3600.0 ! converts m/hr into m/s

if (choice==1) read (400,*) temp
if (choice==2) read (300,*) flow_rate_hot, flow_rate_hot, flow_rate_hot,&
                      & flow_rate_hot, flow_rate_cold
!
!      From these variables, all other atmospheric variables can be determined.
!
!      Energy of vaporization

latent_energy= 2502535.259 -212.56384*temp ! J/kg

!-------------------------------------------------------------------------
!
!      Determination of the coefficients
!
coefficient(1)=emissivity_water*area*5.67*(10.0**(-8))
coefficient(2)=emissivity_sky(airtemp, rh)*area*5.67*(10.0**(-8))*(airtemp+273)**4


!if (choice==3) then
               ! For the case when the temperature is the driving force

!coefficient(3)   = -thermal_conductivity * Area&
 !              & * (-soiltempamp_year/Dyear&
```

```
  !             & *(sin(2*acos(-1.0)/31536000.0*time+phase_year)&
   !            & +cos(2*acos(-1.0)/31536000.0*time+phase_year))&
    !           & -soiltempamp_day/Dday&
     !          & *(sin(2*acos(-1.0)/86400.0*time+phase_day)&
      !         & +cos(2*acos(-1.0)/86400.0*time+phase_day)))
!
!
!
!else            ! Steady state constant temperature conditions

!coefficient(3)=thermal_conductivity*area/sqrt(PI*thermal_diffusivity)
!END if
!
!
!

coefficient(3)=0.0
coefficient(4)=(0.068+0.059*ws(windspeed))*(vp(Temp, x)-vp(airtemp,rh))&
            & *area*density/24.0/3600.0*0.0254& ! rate of evaporation (kg/s)
            & *latent_energy

coefficient(5)=(2.8+3.0*windspeed*1609.0/3600.0)*area
coefficient(6)=solar_radiation*area
coefficient(7)=density*specheat*hot*flow_rate_hot
coefficient(8)=density*specheat*cold*flow_rate_cold
coefficient(9)=density*specheat*airtemp*area*rain

if (choice==1) then
coefficient(10)=density*specheat*(area*rain)
else
coefficient(10)=density*specheat*(flow_rate_hot+flow_rate_cold+area*rain)
end if


!
! "If" statements to make sure no evaporation occurs when the air is saturated.
!
if (rh>=1.0) coefficient(4)=0
if (vp(airtemp,rh)>vp(Temp,x)) coefficient(4) =0
!
!=========================================================================
!      DETERMINATION OF VECTORS
!
```

```
vector(1)= - coefficient(1)*(273.0+temp)**4  ! Pond radiation (J/s)
vector(2)= coefficient(2)                    ! Sky radiation

!if (choice==3) then                ! Soil conduction (weather forcing)
 !     vector(3)= coefficient(3)
!ELSE                               ! Soil conduction (temperature constant)

 !     vector(3)=coefficient(3)*(Temp_initial-temp)/SQRT(time)
!end if
vector(3)=0.0
vector(4)= - coefficient(4)                 ! Evaporation
vector(5)= coefficient(5)*(airtemp - temp)   ! Surface convection
vector(6)= coefficient(6)                   ! Solar Radiation
vector(9)= coefficient(9)                   ! Rain
vector(10)=-coefficient(10)*temp

if (choice==1) THEN

      vector(7)=0.0
      vector(8)=0.0

      if (SUM(vector)<0) then
       flow_rate_hot=SUM(vector)/(specheat*density*(temp-hot))
       gpm_hot=flow_rate_hot*1000*60/3.78
       flow_rate_cold=0.0
       gpm_cold=0.0
      end if

      if (SUM(vector)>0) then
       flow_rate_cold=SUM(vector)/(specheat*density*(temp-cold))
       gpm_cold=flow_rate_cold*1000*60/3.78
       flow_rate_hot=0.0
       gpm_hot=0.0
      end if
END if



if (choice==2) then

       vector(7)= coefficient(7)
       vector(8)= coefficient(8)
       vector(9)= coefficient(9)
       vector(10)= -coefficient(10)*temp
```

```
end if

!=====================================================================
!      Output of results
!
!      Case 1

IF (choice==1) THEN

vector(7)=0
vector(8)=0

        write (100,10) Time, time/3600.0/24.0 + 1, vector(1), vector(2), &
                & vector(3), vector(4), vector(5), vector(6), vector(9),&
                & vector(10), SUM(vector), flow_rate_hot, gpm_hot, &
                & flow_rate_cold, gpm_cold
END IF

!
!      Case 2
!

IF (choice==2) THEN

        write (100,10) Time, time/3600.0/24.0+1, vector, temp
END IF
!
!=====================================================================
!      Runge-Kutta Formulae
!
!      Remember, the Runge-Kutta method predicts the temperature for the
!      following step.
!

F1=step*dTemp(Temp,time,coefficient,thermal_mass, airtemp)!step)
F2=step*dtemp(Temp+0.5*F1, time+0.5*step,coefficient,thermal_mass, airtemp)!step)
F3=step*dTemp(Temp+0.5*F2, time+0.5*step,coefficient,thermal_mass, airtemp)!step)
F4=step*dTemp(Temp+F3, time+step,coefficient,thermal_mass, airtemp)!step)

time=time+step
Temp=temp+(F1+2*F2+2*F3+F4)/6

IF (time>timemax) GO TO 9
```

```
END do

9 write (*,*) "Thank you for using FISHFRY, the best program in the whole,"
write (*,*) "wide world.  (Quite frankly, I don't know why you would want to"
write (*,*) "end your session.  I mean, do you really have anything better"
WRITE (*,*) "to do?)"
WRITE (*,*) " "
WRITE (*,*) "Results are in the output.dat file."
write (*,*) " "

stop
end program fishfry


!=======================================================================
!      FUNCTIONS
!=======================================================================

!-----------------------------------------------------------------------
!      Function to evaluate dtemp
!-----------------------------------------------------------------------

Function dtemp (temp, time,coefficient,thermal_mass, airtemp)
IMPLICIT NONE
        REAL (8), INTENT (IN):: temp, time, thermal_mass, airtemp
        REAL (8), dimension (10), INTENT (IN):: coefficient
        REAL (8):: dtemp

dtemp= (&
       & - coefficient(1) * ((Temp+273.0)**4)&          ! Backradiation
       & + coefficient(2) &                             ! Sky longwave rad
       & + coefficient(3) &
!       & + coefficient(3)*(Tsoil-temp)/SQRT(timereset)& ! Soil heat exchange
       & - coefficient(4)&                              ! Evaporation
       & + coefficient(5)*(airtemp-temp)&               ! Convection
       & + coefficient(6)&                              ! Solar radiation
       & + coefficient(7)&
       & + coefficient(8)+coefficient(9) &
       & - coefficient(10)*temp&
       & )/thermal_mass - time+ time                    ! Thermal mass


Return
END function dtemp
```

```
!-------------------------------------------------------------------------
!      Function to evaluate emissivity_sky
!-------------------------------------------------------------------------


Function emissivity_sky(airtemp,rh)
IMPLICIT NONE

!      This function calculates the emissivity of the sky based on a graph
!      produced by Bliss,1961, Atmospheric Radiation Near the Surface of
!         the Ground: a Summary for Engineers.  Solar Energy 5:103-120
!

REAL (8), INTENT(IN):: airtemp, rh
REAL (8):: emissivity_sky, dewT

dewT = 1/((1/(airtemp+273))-1.846*(10.0**(-4))*LOG(rh)) - 273
emissivity_sky = 1/(1.2488219 -0.0060896701*dewT+4.8502935e-005*dewT**2)

! dewT = dew temperature (C)
! emissivity_sky = the sky's emissivity (decimal)

Return
END function emissivity_sky

!-------------------------------------------------------------------------
!      Function to evaluate the vapour pressure
!-------------------------------------------------------------------------
!
!      This function was taken from ASHRAE Fundamentals Handbook, 1985, SI
!         edition. All temperatures must be in Kelvin and all pressures are in
!      Pascals.

FUNCTION vp(t, rh)
IMPLICIT NONE
REAL (8), INTENT (IN):: T, rh
REAL (8):: vp_saturated, vp

vp_saturated= exp ( -5800.2206/(t+273) &
              & +1.3914993 &
              & -0.04860239 * (t+273) &
              & +0.41764768 * (10.0**(-4)) * ((t+273)**2)&
              & -0.14452093 * (10.0**(-7)) * ((t+273)**3)&
              & +6.5459673 * log(t+273))
```

```
vp=rh*vp_saturated

vp=vp/3387 ! conversion from Pascals to inches of mercury (I HATE IMPIRIAL UNITS!!)

return
END function vp

!-------------------------------------------------------------------------------
!      Function to evaluate the corrected wind speed (REQUIRES INPUT!)
!-------------------------------------------------------------------------------

function ws(windspeed)
implicit none
REAL (8), INTENT (IN):: windspeed
REAL (8):: ws, height_anemometer

!          This function corrects the windspeed for a height of 13 feet above
!          the ground.  The height of the anemometer is in feet and the windspeed
!      in m/s.  The function then converts from m/s to mph.
!

height_anemometer=10.0

ws=windspeed*LOG(13.0)/LOG(height_anemometer)! conversion due to anemometer height
!ws=ws*3600.0/1609.0                    ! converts m/s to mph

return
end function ws
```

APPENDIX 13: PROGRAM CODE FOR WEATHER GENERATOR(A)

```
program weather_generator
implicit none

interface
function solar(i, month, x)
implicit none

INTEGER, INTENT (IN):: i, month, x
REAL:: solar
END function solar
END interface

CHARACTER (LEN=20):: filename, garbage
REAL, dimension (8760):: airtemp, rh, windspeed
REAL, DIMENSION (8760):: airtemp_max, airtemp_min, airtemp_avg
REAL, DIMENSION (8760):: rh_avg, windspeed_avg
REAL, DIMENSION (8760):: solar_radiation_max, solar_radiation_min
REAL, DIMENSION (8760):: solar_radiation_avg

INTEGER:: i, year, month, day, hour, j, n, choice, x


88 FORMAT (f5.1, ",", f5.0, ",", f10.5, ",", f5.1 )

!=====================================================================
open (300, FILE="hot.dat")
open (301, FILE="cold.dat")
open (302, FILE="avg.dat")

!=====================================================================
airtemp_max=-1000.0
airtemp_min=1000.0

n=0

!=====================================================================

1 n=n+1

write (*,*) "What is the name of the file?"
read (*,*) filename
open (10, FILE=filename)
```

```
read (10,*) garbage
read (10,*) garbage
open (20, file = "garbage")
write (20, *) garbage

Do i=1,8760

! years before 1964 do not have wind speed data

if (year<1964) then

        read (10, *) year, month, day, hour, airtemp(i), rh(i)

        if (month==2.and.day==29) then
           Do j=1,24
           read (10,*) year, month, day, hour, airtemp(i), rh(i)
           END do
        end if

        if (airtemp_max(i)<airtemp(i)) airtemp_max(i)=airtemp(i)
        if (airtemp_min(i)>airtemp(i)) airtemp_min(i)=airtemp(i)
        airtemp_avg(i)=(airtemp_avg(i)*(n-1.0)+airtemp(i))/n
        rh_avg(i)=(rh_avg(i)*(n-1.0)+rh(i))/n
        windspeed_avg(i)=(windspeed_avg(i)*(n-1.0)+windspeed(i))/n

            else ! ALTERNATE CASES

        ! First alternate case: between years 1965 and 1972, the records are
        ! every 3 hours

        IF (year>=1965.and.year<=1972) THEN

        if (MOD(i, 3)==1) then

        read (10, *) year, month, day, hour, airtemp(i), rh(i), windspeed(i)

        if (month==2.and.day==29) then
           Do j=1,23
           read (10,*) year
           END do
        read (10, *) year, month, day, hour, airtemp(i), rh(i), windspeed(i)
        end if
```

```
         if (airtemp_max(i)<airtemp(i)) airtemp_max(i)=airtemp(i)
        if (airtemp_min(i)>airtemp(i)) airtemp_min(i)=airtemp(i)
        airtemp_avg(i)=(airtemp_avg(i)*(n-1.0)+airtemp(i))/n
        rh_avg(i)=(rh_avg(i)*(n-1.0)+rh(i))/n
        windspeed_avg(i)=(windspeed_avg(i)*(n-1.0)+windspeed(i))/n

        else
           read (10,*) year, month, day, hour
           airtemp(i)=airtemp(i-1)
           rh(i)  =rh(i-1)
           windspeed(i) = windspeed(i-1)
           if (airtemp_max(i)<airtemp(i)) airtemp_max(i)=airtemp(i)
           if (airtemp_min(i)>airtemp(i)) airtemp_min(i)=airtemp(i)
        airtemp_avg(i)=(airtemp_avg(i)*(n-1.0)+airtemp(i))/n
        rh_avg(i)=(rh_avg(i)*(n-1.0)+rh(i))/n
        windspeed_avg(i)=(windspeed_avg(i)*(n-1.0)+windspeed(i))/n

        END if

        ! Second alternate case: 1964, and 1973 onward

            Else

        read (10, *) year, month, day, hour, airtemp(i), rh(i), windspeed(i)

        if (month==2.and.day==29) then
           Do j=1,24
           read (10,*) year, month, day, hour, airtemp(i), rh(i), windspeed(i)
           END do
        end if

        if (airtemp_max(i)<airtemp(i)) airtemp_max(i)=airtemp(i)
        if (airtemp_min(i)>airtemp(i)) airtemp_min(i)=airtemp(i)
        airtemp_avg(i)=(airtemp_avg(i)*(n-1.0)+airtemp(i))/n
        rh_avg(i)=(rh_avg(i)*(n-1.0)+rh(i))/n
        windspeed_avg(i)=(windspeed_avg(i)*(n-1.0)+windspeed(i))/n

        END IF
END if

airtemp(i) = (airtemp(i)-32)*5.0/9.0
airtemp_max(i) = (airtemp_max(i)-32)*5.0/9.0
airtemp_min(i) = (airtemp_min(i)-32)*5.0/9.0
```

```
airtemp_avg(i) = (airtemp_avg(i)-32)*5.0/9.0
windspeed_avg(i) = windspeed_avg(i) * 0.51444

! Solar radiation calculations

x=0
solar_radiation_avg(i)=solar(i, month, x)

x=1
solar_radiation_max(i)=solar(i, month, x)

x=2
solar_radiation_min(i)=solar(i, month, x)

END do

WRITE (*,*) "Do you want to run an other year? (1 for yes, 2 for no) "
read (*,*) choice
if (choice==1) GO TO 1

!=====================================================================

DO i=1,8760
        write (300,88) airtemp_max(i), rh_avg(i), solar_radiation_max(i), windspeed_avg(i)
        write (301,88) airtemp_min(i), rh_avg(i), solar_radiation_min(i), windspeed_avg(i)
        write (302,88) airtemp_avg(i), rh_avg(i), solar_radiation_avg(i), windspeed_avg(i)

END DO

stop
end program weather_generator

!
=====================================================================

function solar(i, month, x)
implicit none

INTEGER, INTENT (IN):: i, month, x

REAL:: solar

REAL:: dy, a, pi
REAL:: ET, decl, rr
```

```
REAL:: TST, LST, Lnt, Lng, Lat
REAL:: HR, Elev, Directsun, etr, PETR
REAL:: sunup, sundown

Lat =  30.32
Lng =  91.15
Lnt =  90.00
pi=ACOS(-1.0)

Dy=i/24
LST=1.0*MOD(i,24)

! Position of the sun

a=2*pi*dy/365.0
rr=1.000110+0.034221*COS(a)+0.001280*SIN(a)+&       ! ratio
        & 0.000719*COS(2*a)+0.000077*SIN(2*a)

ET= 0.0172+0.4281*COS(a)-7.3515*SIN(a)&             ! time (min)
      & -3.3495*COS(2*a)-9.3619*sin(2*a)

Decl= 0.39637 -22.91326*COS(a)+4.02543*SIN(a)&      ! degrees
          & -0.38720*COS(2*a)+0.05197*SIN(2*a)&
          & -0.15453*COS(3*a)+0.08479*SIN(3*a)

TST = LST +(Lnt-Lng)/15.0+ET/60.0

HR = (12.0-tst)*15                                  ! degrees

Elev = ASIN(SIN(pi/180*lat)*SIN(pi/180*Decl)&               ! radians
    & +COS(pi/180*lat)*COS(pi/180*decl)*COS(pi/180*HR))

! Daylength

sundown=((180/PI*ACOS(-TAN(Lat*Pi/180)*TAN(decl*pi/180)))/15+12)-(lnt-lng)/15-et/60
sunup  =(12-(180/PI*ACOS(-TAN(Lat*Pi/180)*TAN(decl*pi/180)))/15)-(lnt-lng)/15-et/60
!      \----------hour angle-----------------------/
!      \---------------------true solar time----------------/
!      \---------------------------------local standard time-------------------/


! Extra-terrestrial solar radiation
```

```
Directsun=1377 * rr              ! Solar constant taken as 1377 W/m^2
etr=Directsun/1000*COS(pi/2-elev)      ! kW/m^2

if (LST<sunup.or.lst>sundown) etr=0

if (month==1) petr= 0.46
if (month==2) petr= 0.50
if (month==3) petr= 0.56
if (month==4) petr= 0.62
if (month==5) petr= 0.62
if (month==6) petr= 0.63
if (month==7) petr= 0.58
if (month==8) petr= 0.61
if (month==9) petr= 0.61
if (month==10) petr= 0.64
if (month==11) petr= 0.54
if (month==12) petr= 0.48
if (x==1) petr=0.85
if (x==2) petr=0.25

solar=petr*etr

Return
END function solar
```

Vita

Jonathan Lamoureux was born in Montreal, Quebec, Canada, on September 28, 1978. His love for the outdoors, creativity and problem solving prompted him to become an agricultural engineer. In 1997, he enrolled in the Department of Biosystems and Agricultural Engineering at Macdonald Campus, McGill University in Ste. Anne-de-Bellevue, Quebec. Four years later, he earned his Bachelor of Science degree in agricultural engineering with a minor in agricultural production and made the Dean's Honor Roll. In August 2001, the promise of French-speaking Cajuns, financial security and a chance to learn more about aquaculture caused him to move to Baton Rouge, Louisiana, where he enrolled in Louisiana State University's Department of Biological and Agricultural Engineering. He will graduate from this department in August 2003 with a Master of Science in Biological and Agricultural Engineering.